MODELLING BIOLOGICAL SULPHATE REDUCTION IN ANAEROBIC DIGESTION USING WEST®

Shailendra Rajkumar

BScEng (Chem) Natal

Submitted in fulfilment of the academic
requirements for the degree of
MScEng
in the
School of Chemical Engineering
University of KwaZulu-Natal, Durban

June 2009

DECLARATION

I..... declare that

(i) The research reported in this thesis, except where otherwise indicated, is my original work.

(ii) This thesis has not been submitted for any degree or examination at any other university.

(iii) This thesis does not contain other persons' data, pictures, graphs or other information, unless, specifically acknowledged as being sourced from other persons.

(iv) This thesis does not contain other persons' writing, unless specifically acknowledged as being sourced from other researchers. Where other written sources have been quoted, then:

a) their words have been re-written but the general information attributed to them has been referenced;

b) where their exact words have been used, their writing has been placed inside quotation marks, and referenced.

(v) Where I have reproduced a publication of which I am an author, co-author or editor, I have indicated in detail which part of the publication was actually written by myself alone and have fully referenced such publications.

(vi) This thesis does not contain text, graphics or tables copied and pasted from the Internet, unless specifically acknowledged, and the source being detailed in the thesis and in the References sections.

Signed: _____

Date: _____

As the candidate’s supervisor I agree/do not agree to the submission of this thesis

Name: _____

Signed: _____

Date: _____

ACKNOWLEDGEMENTS

I would like to acknowledge the following people and organisations for their contribution to this study:

Prof C.A. Buckley	Thank you for having confidence and providing me with the opportunity to undertake this study.
Mr C.J. Brouckaert	It was through your guidance, advice and technical insight that this work was able to reach fruition. This has proved invaluable within this study and beyond.
Family	To my parents, sister, wife Marsh and son Shrey…thank you for your continued support and encouragement throughout the duration of this study.
University of Gent (Department of Applied Mathematics Biometrics and Process Control)	It was a rare privilege to have worked with exceptional people of Biomath, especially Prof. P.A Vanrolleghem, Dr G. Sin and Dr U. Zaher. I am extremely grateful for your insights and influence on my work.
Mr P. Gounder	Thank you for your friendship, encouragement and experiences we shared over the years.
God	For inspiration and courage in the face of adversity.
Water Research Commission (WRC)	Funding this study.
National Research Foundation (NRF)	Funding the Flemish/South Africa Scientific Exchange.

ABSTRACT

Researchers at Rhodes University conducted investigations into the anaerobic co-disposal of primary sewage sludge (PSS) and high sulphate acid mine drainage (AMD) resulting in the development of the Rhodes BioSURE Process® which forms the basis for the operation of a pilot recycling sludge bed reactor (RSBR). Further research has been conducted by researchers at the University of Cape Town (UCT), with the principle aim of determining the rate of hydrolysis of PSS under methanogenic, acidogenic and sulphate reducing conditions in laboratory-scale anaerobic digesters.

The University of Cape Town's Anaerobic Digestion Model No.1 (UCTADM1) which integrates various biological anaerobic processes for the production of methane was extended with the development of a mathematical model incorporating the processes of biosulphidogenic reduction and the biology of sulphate reducing bacteria (SRB). Kinetic parameters used in the model were obtained from Sötemann et al. (2005b) and Kalyuzhnyi et al. (1998).

The WEST® software was used as a platform in translation of the basic UCTADM1 from AQUASIM, and subsequently applied to data sets from UCT laboratory experiments. Incomplete closure of mass balances was attributed to incorrect reaction stoichiometry inherited through translation of the AQUASIM model into WEST®. The WEST® implementation of the model to the experimental methanogenic systems gave fairly close correlations between predicted and measured data for a single set of stoichiometric and kinetic constants, with regressed hydrolysis rate constants. Application of the extended UCTADM1 to experimental sulphidogenic systems demonstrated simulation results reasonably close to measured data, with the exception of effluent soluble COD and sulphate concentrations. Except for a single system with a high COD:SO_4 ratio, sulphidogens are out competed for substrate by methanogens within the model. Therefore the model does not properly represent the competition between methanogenic and sulphidogenic organism groups.

Trends observed in application of the model to available pilot plant RSBR data were similar to those observed in sulphidogenic systems, resulting in methanogens out-competing sulphidogens. The model was used as a tool to explore various scenarios regarding operation of the pilot plant. Based on the work conducted in this study, various areas for further information and research were highlighted and recommended.

GLOSSARY

Anaerobic digestion	Anaerobic digestion is a biological process in which volatile organic materials are broken down in the absence of oxygen resulting in the production of a gas, referred to as biogas.
Acetoclastic methanogenic bacteria	Organisms responsible for the conversion of acetic acid to methane and carbon dioxide.
Acetoclastic sulphate reducing bacteria	Acetate degrading bacteria use acetic acid and sulphate as substrates to produce hydrogen sulphide, carbon dioxide and hydrogen.
Acetogenic methanogenic bacteria	Organisms that convert propionic acid generated by acidogenesis to acetic acid, carbon dioxide and water.
Acetogenic sulphate reducing bacteria	Propionate degrading bacteria that convert propionic acid and sulphate to acetic acid, sulphide, carbon dioxide and water.
Acid mine drainage	Drainage/run-off from coal mines containing a large concentration of acidic sulphates
Acidogenic bacteria	Fermentative organisms that produce propionic acid, acetic acid, hydrogen, carbon dioxide from glucose.
Bacteria	Single-cell, prokaryotic micro organisms.
Biodegradable	A property which allows the microbial decomposition of an organic compound to inorganic molecules.
Biological wastewater	A process that modifies wastewater characteristics such as its

treatment	chemical oxygen demand (COD), pH, ammonia, etc., to enable it to meet discharge/reuse standards.
Chemical oxygen demand	The amount of oxygen required organic compounds present in wastewater
Dissociation	Dissociation in chemistry and biochemistry is a general process in which ionic compounds separate or split into smaller molecules, ions, or radicals, usually in a reversible manner.
Effluent	An outflow from a system, sewage system or discharge of liquid waste from an industry.
Experiment	Research method for testing different hypotheses under conditions constructed and controlled by the researcher. During the experiment, one or more conditions are allowed to change in an organized manner and the effects of these changes on associated conditions is measured, recorded, validated, and analysed for arriving at a conclusion.
Hydrogenotrophic methanogenic bacteria	Organisms that use hydrogen and carbon dioxide to produce methane and water.
Hydrogenotrophic sulphate reducing bacteria	Organisms using hydrogen and sulphate as substrates to form hydrogen sulphide and water.
Hydrolysis	The first step in the anaerobic degradation of complex polymeric organics required for microbial utilisation whereby fermentative bacteria colonise the surface of particles, secreting hydrolytic enzymes, which are responsible for the extracellular breakdown of complex organic materials.

Influent	The feed or inflow to a system
Inhibition	The condition in which or the process by which a reaction/enzyme is inhibited.
Kinetics	The branch of chemistry that is concerned with the rates of change in the concentration of reactants in a chemical reaction.
Liquid effluent	Liquid waste flowing out of an industry, farm, commercial establishment, or a household into a water body such as a river, lake, or lagoon, or a sewer system or reservoir.
Mathematical model	A mathematical representation of a process, device, or concept by means of a number of variables which are defined to represent the inputs, outputs, and internal states of the device or process, and a set of equations and inequalities describing the interaction of these variables.
Primary sewage sludge	Sludge that originates from the solid component of raw sewage settled prior to any biological treatment.
Seeding	The use of an actively digesting sludge to aid the start-up of a digester by supplying a quantity of the preferred types of organisms. This usually reduces the time taken for a digester to become active.
Sludge	The general term applied to the accumulated solids separated from wastewater. A large portion of the sludge material in a digester consists of bacteria which are responsible for its decomposition.

Stoichiometry	Determination of the proportions (by weight or number of molecules) in which elements or compounds react with one another.
Wastewater	Spent or used water containing contaminants that is discharged from an industry, farm, commercial establishment or a household.

LIST OF ABBREVIATIONS AND SYMBOLS

ABBREVIATIONS

Name	Description	Unit
AMD	Acid mine drainage	-
COD	Chemical oxygen demand in effluent	mg COD/ℓ
CSTR	Continuously stirred tank reactor	-
ERWAT	East Rand Water Care Company	-
FSA	Free and saline ammonia in effluent	mg N/ℓ
HGE	Hierarchical graphical editor	-
HRT	Hydraulic retention time	d
LCFA	Long-chain fatty acid	-
PSS	Primary sewage sludge	-
RSBR	Recycling sludge bed reactor	-
SCFA	Short-chain fatty acid	-
SRB	Sulphate reducing bacteria	-
TKN	Total Kjeldahl nitrogen in effluent	mg N/ℓ
UASB	Upflow anaerobic sludge blanket	-
UCTADM1	University of Cape Town Anaerobic Digestion Model No.1	-
VFA	Volatile fatty acid in effluent	mg HAc/ℓ
WEST®	Wastewater Treatment Plant Engine for Simulation and Training	-

SYMBOLS

Symbol	Description	Unit
μmax_a	Acidogenic biomass maximum specific growth rate constant	d^{-1}
μmax_{ae}	Acetogenic biomass maximum specific growth rate constant	d^{-1}
μmax_{am}	Acetoclastic methanogen biomass maximum specific growth rate constant	d^{-1}
μmax_{as}	Acetoclastic sulphidogen biomass maximum specific growth rate constant	d^{-1}
μmax_{hm}	Hydrogenotrophic methanogen biomass maximum specific growth rate constant	d^{-1}
μmax_{hs}	Hydrogenotrophic sulphidogen biomass maximum specific growth rate constant	d^{-1}
μmax_{ps}	Acetogenic sulphidogen biomass maximum specific growth rate constant	d^{-1}
AW_C	Atomic weight of carbon	g/mol
AW_H	Atomic weight of hydrogen	g/mol
AW_N	Atomic weight of nitrogen	g/mol
AW_O	Atomic weight of oxygen	g/mol
AW_P	Atomic weight of phosphorous	g/mol
AW_S	Atomic weight of sulphur	g/mol
b_a	Acidogenic biomass decay constant	d^{-1}
b_{ae}	Acetogenic biomass decay constant	d^{-1}
b_{am}	Acetoclastic methanogen biomass decay constant	d^{-1}
b_{as}	Acetoclastic sulphidogen biomass decay constant	d^{-1}

b_{hm}	Hydrogenotrophic methanogen biomass decay constant	d^{-1}
b_{hs}	Hydrogenotrophic sulphidogen biomass decay constant	d^{-1}
b_{ps}	Acetogenic sulphidogen biomass decay constant	d^{-1}
C_T	Total concentration of dissolved carbon species in digester	-
f_$C_5H_7O_2$NCOD	COD/biomass ratio	-
f_d	Divalent activity coefficient	-
f_m	Trivalent activity coefficient	-
f_t	Trivalent activity coefficient	-
HydKmax	Hydrolysis maximum specific rate constant	g S_{bp}/mol Z_{ai}. d
in_f_GlucCOD	Influent COD/Glucose Ratio	-
in_f_HAcCOD	Influent COD/HAc Ratio	-
in_f_HPrCOD	Influent COD/HPr Ratio	-
in_f_N_bp	Fraction of influent Nitrogen content in biodegradable particulate COD	g N/g COD
in_f_N_up	Fraction of influent Nitrogen content in unbiodegradable particulate COD	g N/g COD
in_f_N_Xi	Fraction of influent Nitrogen content in Biomass	-
in_f_P_bp	Fraction of influent Phosphorous content in biodegradable particulate COD	g P/g COD
in_f_P_up	Fraction of influent Phosphorous content in unbiodegradable particulate COD	g P/g COD
inSC	Conductivity of the influent	mS/m
K_a	Equilibrium constant for HAc/Ac system	-
K_{c1}	Equilibrium constant for H_2CO_3/HCO_3 system	-

K_{c2}	Equilibrium constant for HCO_3/CO_3 system	-
k_{CO2}	Henry's law coefficient for CO_2	-
Kf_a	Forward dissociation constant for $HAc \leftrightarrow Ac^- + H^+$	-
Kf_{c1}	Forward dissociation constant for $H_2CO_3 \leftrightarrow HCO_3^- + H^+$	-
Kf_{c2}	Forward dissociation constant for $HCO_3^- \leftrightarrow CO_3^{2-} + H^+$	-
Kf_{HS}	Forward dissociation constant for $H_2S \leftrightarrow HS^- + H^+$	-
Kf_n	Forward dissociation constant for $NH_4^+ \leftrightarrow NH_3 + H^+$	-
Kf_{p1}	Forward dissociation constant for $H_3PO_4 \leftrightarrow H_2PO_4^- + H^+$	-
Kf_{p2}	Forward dissociation constant for $H_2PO_4^- \leftrightarrow HPO_4^{2-} + H^+$	-
Kf_{p3}	Forward dissociation constant for $HPO_4^{2-} \leftrightarrow PO_4^{3-} + H^+$	-
Kf_{Pr}	Forward dissociation constant for $HPr \leftrightarrow Pr^- + H^+$	-
Kf_S	Forward dissociation constant for $HS^- \leftrightarrow S^{2-} + H^+$	-
Kf_W	Forward dissociation constant for $H_2O \leftrightarrow OH^- + H^+$	-
K_{H2}	Hydrogen inhibition coefficient for high pH_2	mol H_2/ℓ
k_{H2S}	Henry's law coefficient for H_2S	-

KH_{CO2}	Henry's Law constant for CO_2	-
KH_{H2S}	Henry's Law constant for H_2S	-
Ki_{aes}	Acetogenic biomass hydrogen sulphide inhibition constant	mol/ℓ
Ki_{ais}	Acidogenic biomass hydrogen sulphide inhibition constant	mol/ℓ
Ki_{am}	Acetoclastic methanogen biomass hydrogen ion inhibition constant	mol/ℓ
Ki_{ams}	Acetoclastic methanogen biomass hydrogen sulphide inhibition constant	mol/ℓ
Ki_{as}	Acetoclastic sulphidogen biomass hydrogen sulphide inhibition constant	mol/ℓ
Ki_{hm}	Hydrogenotrophic methanogen biomass hydrogen ion inhibition constant	mol/ℓ
Ki_{hms}	Hydrogenotrophic methanogen biomass hydrogen sulphide inhibition constant	mol/ℓ
Ki_{hs}	Hydrogenotrophic sulphidogen biomass hydrogen sulphide inhibition constant	mol/ℓ
Ki_{ps}	Acetogenic sulphidogen biomass hydrogen sulphide inhibition constant	mol/ℓ
K_n	Equilibrium constant for NH_3/NH_4 system	-
Kn_{as}	Acetoclastic sulphidogen biomass half saturation constant for sulphate	mol/ℓ
Kn_{hs}	Hydrogenotrophic sulphidogen biomass half saturation constant for sulphate	mol/ℓ
Kn_{ps}	Acetogenic sulphidogen biomass half saturation constant for sulphate	mol/ℓ
K_p	Equilibrium constant for HPr/Pr system	-

Kr_a	Reverse dissociation constant for $HAc \leftrightarrow Ac^- + H^+$	-
Kr_{c1}	Reverse dissociation constant for $H_2CO_3 \leftrightarrow HCO_3^- + H^+$	-
Kr_{c2}	Reverse dissociation constant for $HCO_3^- \leftrightarrow CO_3^{2-} + H^+$	-
Kr_{CO2}	Reverse dissociation constant for CO2 expulsion	-
Kr_{H2S}	Reverse dissociation constant for H2S expulsion	-
Kr_{HS}	Reverse dissociation constant for $H_2S \leftrightarrow HS^- + H^+$	-
Kr_n	Reverse dissociation constant for $NH_4^+ \leftrightarrow NH_3 + H^+$	-
Kr_{p1}	Reverse dissociation constant for $H_3PO_4 \leftrightarrow H_2PO_4^- + H^+$	-
Kr_{p2}	Reverse dissociation constant for $H_2PO_4\text{-} \leftrightarrow HPO_4^{2-} + H^+$	-
Kr_{p3}	Reverse dissociation constant for $HPO_4^{2-} \leftrightarrow PO_4^{3-} + H^+$	-
Kr_{Pr}	Reverse dissociation constant for $HPr \leftrightarrow Pr^- + H^+$	-
Kr_S	Reverse dissociation constant for $HS^- \leftrightarrow S^{2-} + H^+$	-
Kr_W	Reverse dissociation constant for $H_2O \leftrightarrow OH^- + H^+$	-
Ks_a	Acidogenic biomass half saturation constant	mol/ℓ
Ks_{ae}	Acetogenic biomass half saturation constant	mol/ℓ

Ks_{am}	Acetoclastic methanogen biomass half saturation constant	mol/ℓ
Ks_{as}	Acetoclastic sulphidogen biomass half saturation constant	mol/ℓ
Ks_{hm}	Hydrogenotrophic methanogen biomass half saturation constant	mol/ℓ
Ks_{hs}	Hydrogenotrophic sulphidogen biomass half saturation constant	mol/ℓ
Ks_{Hyd}	Hydrolysis half saturation constant	g S_{bp}/mol Z_{ai}
Ks_{ps}	Acetogenic sulphidogen biomass half saturation constant	mol/ℓ
K_W	Equilibrium constant for water system	-
MW_{Ac}	Molecular weight of Ac^-	g/mol
$MW_{C5H7O2N}$	Molecular weight of biomass	g/mol
$MW_{C6H12O6}$	Molecular weight of $C_6H_{12}O_6$	g/mol
MW_{CaCO3}	Molecular weight of $CaCO_3$	g/mol
MW_{CH4}	Molecular weight of CH_4	g/mol
MW_{CO2}	Molecular weight of CO_2	g/mol
MW_{CO3}	Molecular weight of CO_3	g/mol
MW_{H}	Molecular weight of H^+	g/mol
MW_{H2}	Molecular weight of H_2	g/mol
MW_{H2CO3}	Molecular weight of H_2CO_3	g/mol
MW_{H2O}	Molecular weight of H_2O	g/mol
MW_{H2PO4}	Molecular weight of H_2PO_4	g/mol
MW_{H2S}	Molecular weight of H_2S	g/mol
MW_{H3PO4}	Molecular weight of H_3PO_4	g/mol
MW_{HAc}	Molecular weight of HAc	g/mol

MW_{HCO3}	Molecular weight of HCO_3^-	g/mol
MW_{HPO4}	Molecular weight of HPO_4^{2-}	g/mol
MW_{HPr}	Molecular weight of HPr	g/mol
MW_{HS}	Molecular weight of HS^-	g/mol
MW_{NH3}	Molecular weight of NH_3	g/mol
MW_{NH4}	Molecular weight of NH_4	g/mol
MW_{OH}	Molecular weight of OH^-	g/mol
MW_{PO4}	Molecular weight of PO_4^{3-}	g/mol
MW_{Pr}	Molecular weight of Pr^-	g/mol
MW_S	Molecular weight of S^{2-}	g/mol
MW_{SO4}	Molecular weight of SO_4^{2-}	g/mol
Patm	Atmospheric pressure	atm
pCH_4	Partial pressure of CH_4 gas	-
pCO_2	Partial pressure of CO_2 gas	-
pH_2S	Partial pressure of H_2S gas	-
pK_a	pK constant for $HAc \leftrightarrow Ac^- + H^+$	-
pK_{c1}	pK constant for $H_2CO_3 \leftrightarrow HCO_3^- + H^+$	-
pK_{c2}	pK constant for $HCO_3^- \leftrightarrow CO_3^{2-} + H^+$	-
pKH_{CO2}	pK constant for the dissolution of CO_2	-
pKH_{H2S}	pK constant for the dissolution of H_2S	-
pKH_{HS}	pK constant for $H_2S \leftrightarrow HS^- + H^+$	-
pKH_{Pr}	pK constant for $HPr \leftrightarrow Pr^- + H^+$	-
pK_n	pK constant for $NH_4^+ \leftrightarrow NH_3 + H^+$	-
pK_{p1}	pK constant for $H_3PO_4 \leftrightarrow H_2PO_4^- + H^+$	-
pK_{p2}	pK constant for $H_2PO_4^- \leftrightarrow HPO_4^{2-} + H^+$	-
pK_{p3}	pK constant for $HPO_4^{2-} \leftrightarrow PO_4^{3-} + H^+$	-

pK_S	pK constant for $HS^- \leftrightarrow S^{2-} + H^+$	-
pK_W	pK constant for dissociation of H_2O	-
PsC	Relative proportion of carbon in feed material	-
PsH	Relative proportion of hydrogen in feed material	-
PsN	Relative proportion of nitrogen in feed material	-
PsO	Relative proportion of oxygen in feed material	-
Q_i	Influent flowrate	ℓ/d
R	Universal gas constant	ℓ.atm/mol.K
R_s	Reactor retention time	d
S_{bpi}	Biodegradable particulate COD in feed	g COD/d
S_{bsi}	Biodegradable soluble COD in feed	g/d
SC	Specific conductivity	mS/m
S_{si}	Total soluble COD in feed	g COD/d
S_{ti}	Total feed COD	g COD/d
S_{upi}	Unbiodegradable particulate COD in feed	g COD/d
S_{us}	Unbiodegradable soluble COD in effluent	g COD/d
S_{usi}	Unbiodegradable soluble COD in feed	g COD/d
S_{VFAi}	Volatile fatty acids in effluent	g COD/d
T_c	Temperature in degrees Celsius	^oC
T_k	Temperature in degrees Kelvin	K
V_r	Reactor volume	ℓ
Y_{ae}	Acetogenic biomass yield coefficient	mol VSS/mol COD
Y_{ai}	Acidogenic biomass yield coefficient	mol VSS/mol COD
Y_{am}	Acetoclastic methanogen biomass yield coefficient	mol VSS/mol COD
Y_{as}	Acetoclastic sulphidogen biomass yield coefficient	mol VSS/mol COD

Y_{hm}	Hydrogenotrophic methanogen biomass yield coefficient	mol VSS/mol COD
Y_{hs}	Hydrogenotrophic sulphidogen biomass yield coefficient	mol VSS/mol COD
Y_{ps}	Acetogenic sulphidogen biomass yield coefficient	mol VSS/mol COD
Z_{ae}	Acetogenic organism concentration	g/m^3
Z_{ai}	Acidogen active biomass concentration	g/m^3
Z_{am}	Acetoclastic methanogen organism concentration	g/m^3
Z_{as}	Acetoclastic sulphidogen organism concentration	g/m^3
Z_{hm}	Hydrogenotrophic methanogen organism concentration	g/m^3
Z_{hs}	Hydrogenotrophic sulphidogen organism concentration	g/m^3
Z_{ps}	Acetogenic sulphidogen organism concentration	g/m^3

CONTENTS

LIST OF TABLES

LIST OF FIGURES

CHAPTER 1

INTRODUCTION

1.1 Background

The South African mining industry has been one of the primary contributors to the economic upliftment and development of the country for more than a century (Pulles, 2003, WRC, 2005). Exploitation of the national mineral resource has resulted in employment, foreign currency earnings, national tax revenues and national infrastructure development (Pulles, 2003). However, these benefits have come with a consequence of environmental risk associated with obsolete and abandoned mines, current operational mines and the future closure of mines. Post-mining wastes emanating from sulphidic mine activities undergoes chemical and biological oxidation processes when exposed to water and air resulting in a highly acidic leachate characterised by low pH and high concentrations of sulphate and heavy metal ions (Christensen, et al., 1996, Gibert, et al., 2004). These effluents are known as acid mine drainage (AMD).

Anaerobic waste treatment is one of the major biological waste treatment processes in use today. It has been employed for many years in the stabilisation of municipal sewage sludges (primary and waste activated), and more recently, in the treatment of high and medium strength industrial wastes. Over the past two decades anaerobic biological sulphate reduction has received increasing attention as an accepted technology suited to the treatment of sulphate-rich waste streams such as AMD (Knobel and Lewis, 2002). During this process sulphate reducing bacteria (SRB) use the sulphate as an electron acceptor directly reducing salinity and protons, generating alkalinity and sulphide which results in an increase in the pH and the precipitation of many heavy metals as sulphides, carbonates or hydroxides (Knobel and Lewis, 2002, Ristow, et al., 2002). Sources of carbon or simple electron donors, including methanol and ethanol, are fairly expensive and are therefore not suitable for use in developing countries such as South Africa (Molwantwa, et al., 2004). The use of primary sewage sludge (PSS) has been identified as a practically feasible carbon source or electron donor and an attractive economic alternative for the treatment of AMD (Ristow, et al., 2004). Primary sludge originates from the solid component of raw sewage settled prior to any biological treatment (Hansford, 2004). The complex particulate sewage sludge would need to be degraded anaerobically to produce simple soluble organic substrates for SRB in order to achieve successful sulphate reduction (Hansford, 2004, Ristow, et al., 2005).

Researchers in the Environmental Biotechnology Research Unit and Department of Biochemistry, Microbiology and Biotechnology at Rhodes University (RU) have been undertaking investigations into the anaerobic co-disposal of PSS and high sulphate AMD. The use of organic carbon in the form of PSS as an electron donor source for sulphate reduction in low-cost bioreactor applications has resulted in the development of the Rhodes BioSURE Process®. This process forms the basis for the operation of a pilot recycling sludge bed reactor (RSBR) responsible for the treatment of AMD on-site at the East Rand Watercare Company's (ERWAT) Ancor Works at the Grootvlei Mine.

Further research has been conducted by researchers in the Water Research Group, Department of Civil Engineering at the University of Cape Town (UCT). The principle aim of this research was to determine the rate of hydrolysis of PSS under methanogenic, acidogenic and sulphate reducing conditions, and the influence of the system physical constraints on the rate which will enable a direct comparison of the rate under each of the three conditions and possible influences thereof (Ristow, et al., 2005, Ristow, et al., 2004). The experimental investigation involved the operation of a series of laboratory-scale completely mixed anaerobic digesters fed with PSS as influent. The behaviour of these systems were monitored under a range of feed COD concentrations, retention times, pH and influent sulphate concentrations under methanogenic, acidogenic and sulphate-reducing conditions (Ristow, et al., 2005).

The design, operation and control of anaerobic digesters treating sewage sludges is mainly based on experience or empirical guidelines despite its widespread application, and therefore a mathematical model would prove to be an invaluable tool into the research of the above (Sötemann, et al., 2005b, van Rensburg, et al., 2001). The purpose of a mathematical model is to provide quantitative expression to behavioural patterns of interest in a treatment system (Sam-Soon, et al., 1991). This enables the identification of parameters that significantly influence the system response, and provides guidance for the establishment of design, operational and control criteria resulting in overall system optimisation. Sötemann et al., (2005b) developed and validated a two phase (aqueous-gas) integrated mixed weak acid/base chemical, physical and biological processes kinetic model for the anaerobic digestion of sewage sludges. The development of this mathematical model has led to what is known as the University of Cape Town Anaerobic Digestion Model No.1 (UCTADM1).

The UCTADM1 formed the basis of this research project. The biological processes (for the production of methane) in the model are mediated by four anaerobic digestion organism groups, viz. acidogenic, acetogenic, acetoclastic methanogenic and hydrogenotrophic

methanogenic bacteria. However the UCTADM1 does not account for the processes of biological sulphate reduction and does not apply to the anaerobic degradation processes that take place in the treatment of sulphate-rich wastewaters such as AMD. The UCTADM1 needed to be extended to incorporate the processes of biosulphidogenic reduction and the biology of SRB.

This dissertation details the implementation, extension (to incorporate biosulphidogenic reduction), calibration and application of the UCTADM1 to a range of operating scenarios using the WEST® (**W**astewater Treatment Plant **E**ngine for **S**imulation and **T**raining) modelling platform. WEST® is a modelling and simulation environment and can, together with a model base, be used in the design, operation and optimisation of a wastewater treatment system.

1.2 Research Objectives

The principal aim of this research is to model biological sulphate reduction in anaerobic digestion using WEST®. The experimental results of researchers together with a new mathematical representation of anaerobic digestion developed at UCT and previously modelled in AQUASIM (simulation software of aquatic systems) will be used to model the combined process including the RSBR in WEST®. The main objectives of this study were:

i. Translation and coding of the basic UCTADM1 (without sulphate reduction) from AQUASIM to WEST®.

ii. Extension of the model to include reactions for sulphate reducing processes.

iii. Calibration of the model using data sets from the UCT laboratory experiments carried out in completely mixed reactors.

iv. Adaptation of the model to represent the Rhodes BioSURE pilot plant's RSBR configuration and its calibration using available operating data.

v. Highlight requirements for further information and research.

CHAPTER 2

LITERATURE REVIEW

2.1 Acid Mine Drainage

"The greatest challenge for the mine, for which we are actively searching for a solution, is to find a sustainable treatment technology that will be able to improve the quality of the mine water and to be operational even after the mine closes," reported Grootvlei Mine environmental manager Irene Lea (WRC, 2005).

Acidic wastewaters characterised by high sulphate concentrations and usually high concentrations of dissolved metals originate from mining, mineral and chemical processing, electricity generation and other industrial activities (Hansford, 2004). The post-mining wastes emanating from these activities undergo chemical and biological oxidation processes when exposed to water and air resulting in a highly acidic leachate known as AMD (Gibert, et al., 2004). AMD generation in South Africa is a significant problem as South Africa is a semi-arid to arid country with a large number of mines either still in operation or abandoned (Knobel and Lewis, 2002).

According to Petrik, and co-workers, the sources of mine water pollution include (Petrik, et al., 2005):

- Underground workings and open cast mining
- Metallurgical plants
- Mining infrastructure and mine residue deposits
- Tailings impoundments
- Ore stockpiles and abandoned heap leach piles

It is possible for the pH of AMD wastewaters to drop below 2 (Burgess and Stuetz, 2002) and have TDS concentrations in the range of 4000-5000 mg/ℓ (Petrik, et al., 2005). Table 2-1 shows

a typical composition of an AMD waste stream from a coal mine.

Table 2-1: Typical composition of an AMD wastewater from a coal mine (Burgess and Stuetz, 2002)

Constituent	Concentration	Unit
pH	3.0-5.5	-
Mg^{2+}	80	mg/ℓ
Ca^{2+}	200	mg/ℓ
Al_{total}	50	mg/ℓ
Fe_{total}	50-300	mg/ℓ
Mn^{2+}	20-300	mg/ℓ
$SO4^{2-}$	20-2000	mg/ℓ

Other than sulphuric acid (formed as a result of pyrite oxidation), AMD contains high concentrations of heavy metals, as is evident from Table 2-1, which are released due to direct solubilisation of metal sulphides by acidic extraction of metals adsorbed on mineral surfaces (Burgess and Stuetz, 2002).

It is clearly evident from Table 2-1 that sulphate is the most significant constituent having the highest concentration. According to Toerien and Maree (1987), sulphate is directly responsible for the salination or mineralisation of receiving waters in excessive amounts but constitutes greater indirect problems including corrosion, imparting of tastes to drinking water, scaling of pipes, boilers and heat exchangers, and facilitating biocorrosion.

2.1.1 Formation and Chemistry of Acid Mine Drainage

The Pennsylvania Department of Environmental Protection (DEP, 1999), states that the formation of AMD is primarily a function of the geology, hydrology and mining technology employed for the mine site and is formed by a series of complex geochemical and microbial reactions that occur when water comes in contact with pyrite in coal or overburden of a mining operation. The result is a wastewater typically high in acidity and dissolved metals that remain dissolved in solution until the pH is raised to a level where precipitation occurs.

DEP (1999) and Ford (2003) provide a comprehensive description of basic acid mine drainage chemistry as follows:

The overall summary equation for AMD formation is as follows:

$$4FeS_2 + 15O_2 + 14H_2O \rightarrow 4Fe(OH)_3 + 8H_2SO_4 \quad (2\text{-}1)$$

The transformation of pyrite to form AMD is represented by four commonly accepted chemical reactions. The first reaction represents the oxidation of pyrite by oxygen whereby sulphur is oxidised to sulphate and ferrous iron is released resulting in the generation of two moles of acidity for each mole of pyrite oxidised.

$$2FeS_2 + 7O_2 + 2H_2O \rightarrow 2Fe^{2+} + 4SO_4^{2-} + 4H^+ \quad (2\text{-}2)$$

The second reaction involves the conversion of ferrous iron to ferric iron, consuming one mole of acidity. This pH dependent reaction proceeds slowly under acidic conditions (pH = 2-3) with no bacteria present and several orders of magnitude faster at pH values close to 5. It is therefore the rate limiting step in the overall acid-generating sequence.

$$4Fe^{2+} + O_2 + 4H^+ \rightarrow 4Fe^{3+} + 2H_2O \quad (2\text{-}3)$$

The third reaction represents the hydrolysis of iron which splits the water molecule, generating three moles of acidity as a byproduct. The formation of a solid ferric hydroxide precipitate is pH dependent whereby solids precipitate at a pH greater than 3.5 as opposed to little or no precipitation at a pH below 3.5.

$$4Fe^{3+} + 12H_2O \rightarrow 4Fe(OH)_3 + 12H^+ \quad (2\text{-}4)$$

The fourth reaction is the oxidation of additional pyrite by ferric iron generated in reaction steps 1 and 2. This is the cyclic and self-propagating part of the overall reaction and occurs very rapidly and proceeds until either ferric iron or pyrite is depleted. In this reaction iron is the oxidising agent as opposed to oxygen.

$$FeS_2 + 14Fe^{3+} + 8H_2O \rightarrow 15Fe^{2+} + 2SO_4^{2-} + 16H^+ \quad (2\text{-}5)$$

2.1.2 Impacts of Acid Mine Drainage

Murphy, et al. (1999) describe the negative impacts of AMD on the ecology of streams, affecting the beneficial use of waterways downstream of mining activities as the following:

- Leaching of high levels of heavy metals into groundwater that become harmful to aquatic ecosystems and human health.
- Limiting of downstream beneficial uses of receiving waters to stock, recreation, fishing, aquaculture and irrigation.
- Altering important life supporting balances in water chemistry such as the bicarbonate buffering system.
- Result in the development of harmful chemical precipitates such as ferric hydroxide and aluminium hydroxide that smother the aquatic habitat and reduce light penetration.
- Impact groundwater quality.
- Lead to installation of expensive control, treatment and rehabilitation processes.
- Limitation of mine water reuse and aggravation of corrosion to site infrastructure and equipment.
- The creation of long-term environmental liabilities.

2.1.3 Treatment and Remediation of Acid Mine Drainage

AMD control and treatment techniques can be broadly classified into chemical, biological, and those using a combination of the two. AMD remediation is aimed at increasing the pH of the wastewater as well as the reduction of heavy metals and salts to acceptable concentration levels.

2.1.3.1 Chemical Treatment

The chemical remediation of AMD may involve the use of active or passive treatment technologies. Active treatment involves the addition of alkaline reagents, like CaO, $Ca(OH)_2$, $CaCO_3$, NaOH, NH_3 and Na_2CO_3, resulting in acid water neutralisation and the precipitation of heavy metals (Ledin and Pedersen, 1996, Petrik, et al., 2005). Reagents are relatively cost

effective (Murphy, et al., 1999), but the maintenance requirements of this technique are high (Ledin and Pedersen, 1996).

Passive treatment systems use naturally occurring processes or consist of large drains packed with crushed limestone through which the AMD flows prior to its release into a constructed wetland system (Petrik, et al., 2005). Heavy metals are removed via the precipitation of hydroxides, oxyhydroxides and sulphides (Petrik, et al., 2005). The absence or strict control of dissolved oxygen, ferric iron and aluminium to control metal hydroxide precipitation determines the success of these passive systems (Murphy, et al., 1999). These tend to coat the limestone preventing further neutralisation reactions taking place (Gazea, et al., 1996).

2.1.3.2 Bioremediation of AMD using SRB

Biological or microbial treatment systems require the establishment and maintenance of anaerobic conditions allowing the growth of SRB, which reduce sulphate to sulphide by oxidising an organic carbon source (Gibert, et al., 2004). In this process SRB use the sulphate as an electron acceptor directly reducing salinity and protons, generating alkalinity in the form of sulphide which results in an increase in the pH and the precipitation of many heavy metals as sulphides, carbonates or hydroxides (Knobel and Lewis, 2002, Ristow, et al., 2002).

Dvorak, et al., (1992) illustrates with the following reactions, how SRB oxidises a simple organic compound such as lactic acid with sulphate, thereby generating hydrogen sulphide and bicarbonate ions:

$$3SO_4^{2-} + 2CH_3CHOHCOOH\left(lactic\ acid\right) \rightarrow 3H_2S + 6HCO_3^- \qquad (2\text{-}6)$$

Hydrogen sulphide reacts with many heavy metals to remove them from solution as insoluble metal sulphides:

$$H_2S + M^{2+} \rightarrow MS\left(s\right) + 2H^+ \qquad (2\text{-}7)$$

where M includes metals such as Cd, Fe, Pd, Ni and Zn. The bicarbonate ion reacts with protons to form CO_2 and water, and removes acidity from solution as CO_2 gas:

$$HCO_3^- + H^+ \rightarrow CO_2\left(g\right) + H_2O \qquad (2\text{-}8)$$

The H_2S and HCO_3^- formed during sulphate reduction equilibrate into a mixture of H_2S, HS^-, S^{2-} CO_2, HCO_3^-, and CO_3^{2-}, which will buffer the solution pH to a value typically in the range of 6-7 provided sufficient sulphate reduction takes place and the specific quantities and types of end-products are formed.

Sources of carbon or simple electron donors, including methanol and ethanol, are fairly expensive and are therefore not suitable for use in developing countries such as South Africa (Molwantwa, et al., 2004). Alternative relatively inexpensive soluble carbon sources that have been evaluated for active bacterial sulphate reduction include producer gas (Du Preez, et al., 1992), molasses (Maree and Hill, 1989), lactate and cheese whey (Oleszkiewicz and Hilton, 1986), cattle waste (Ueki, et al., 1988) and sewage sludge (Burgess and Wood, 1961).

The use of sewage sludge as an organic electron donor for the bioremediation of AMD in developing countries such as South Africa is possibly the most cost-effective option as costs associated with chemical reagents, labour and sludge removal are negligible (Molwantwa, et al., 2004). The additional advantage of treating AMD in conjunction with sewage sludge is that there is no longer a need to treat sewage sludge independently (Ristow, 1999).

2.2 Mechanisms and Kinetics of Anaerobic Digestion and Sulphate Reduction with regard to the UCTADM1

2.2.1 Overview of Anaerobic Digestion

Anaerobic digestion is a natural biological process in which an interdependent community of bacteria work together to form a stable, autonomous fermentation that converts organic material into a mixture of inorganic end-products including methane, carbon dioxide and sulphide, in the absence of oxygen.

Biological treatment of sewage and industrial wastewaters such as aerobic treatment generates additional sludge which must be disposed of in a method which is deemed to be acceptable to any community owing to environmental concern (Roberts, et al., 1999). The synthesis of biological cells during anaerobic treatment is significantly lower than with aerobic processes, tending to minimise waste sludge disposal problems and nutrient requirements (McCarty, 1974). Due to anaerobic treatment not requiring oxygen, treatment rates are not limited by oxygen transfer and the non-requirement for oxygen reduces power requirements (Sacks and Buckley, 2004). An additional advantage of anaerobic digestion is the production

of methane gas which is a useable source of fuel energy (McCarty, 1974).

The process of anaerobic biological sulphate reduction involves the use of sulphate in wastewaters, such as AMD, as a terminal electron acceptor for the degradation of organic compounds, resulting in the reduction of sulphate concentration, increased pH due to the consumption of protons, production of alkalinity and the precipitation of heavy metals as metal sulphides. A suitable cost-effective organic electron donor is sewage sludge. The particulate sewage sludge would need to be degraded anaerobically to produce simple soluble organic substrates for SRB in order to achieve successful sulphate reduction (Hansford, 2004, Ristow, 1999).

Anaerobic degradation of complex, particulate organic materials can be described as a multistage biochemical process consisting of series and parallel reactions. From a kinetic viewpoint, anaerobic digestion (including sulphate reduction) can be described by the following process steps as explained by Hansford (2004) and illustrated in Figure 2-1:

- Hydrolysis of particulate organic material to simple soluble organic compounds by extracellular enzymatic action. Carbohydrates are broken down to sugars, proteins to amino acids, and lipids to long-chain fatty acids (LCFAs) and polyols such as glycerol

- Acidogenesis or acid fermentation of sugars and amino acids to hydrogen, carbon dioxide and short-chain fatty acids (SCFAs)

- Anaerobic or beta oxidation of LCFAs to yield acetate, propionate and hydrogen

- Acetogenesis of propionate and other SCFAs to acetate, hydrogen and carbon dioxide

- Methanogenesis (methane production) utilising hydrogen and acetate as substrate

- Sulphidogenesis utilising hydrogen, acetate, propionate and potentially other intermediate SCFAs as substrates

- Homoacetogenesis resulting in the production of acetate from hydrogen and carbon dioxide

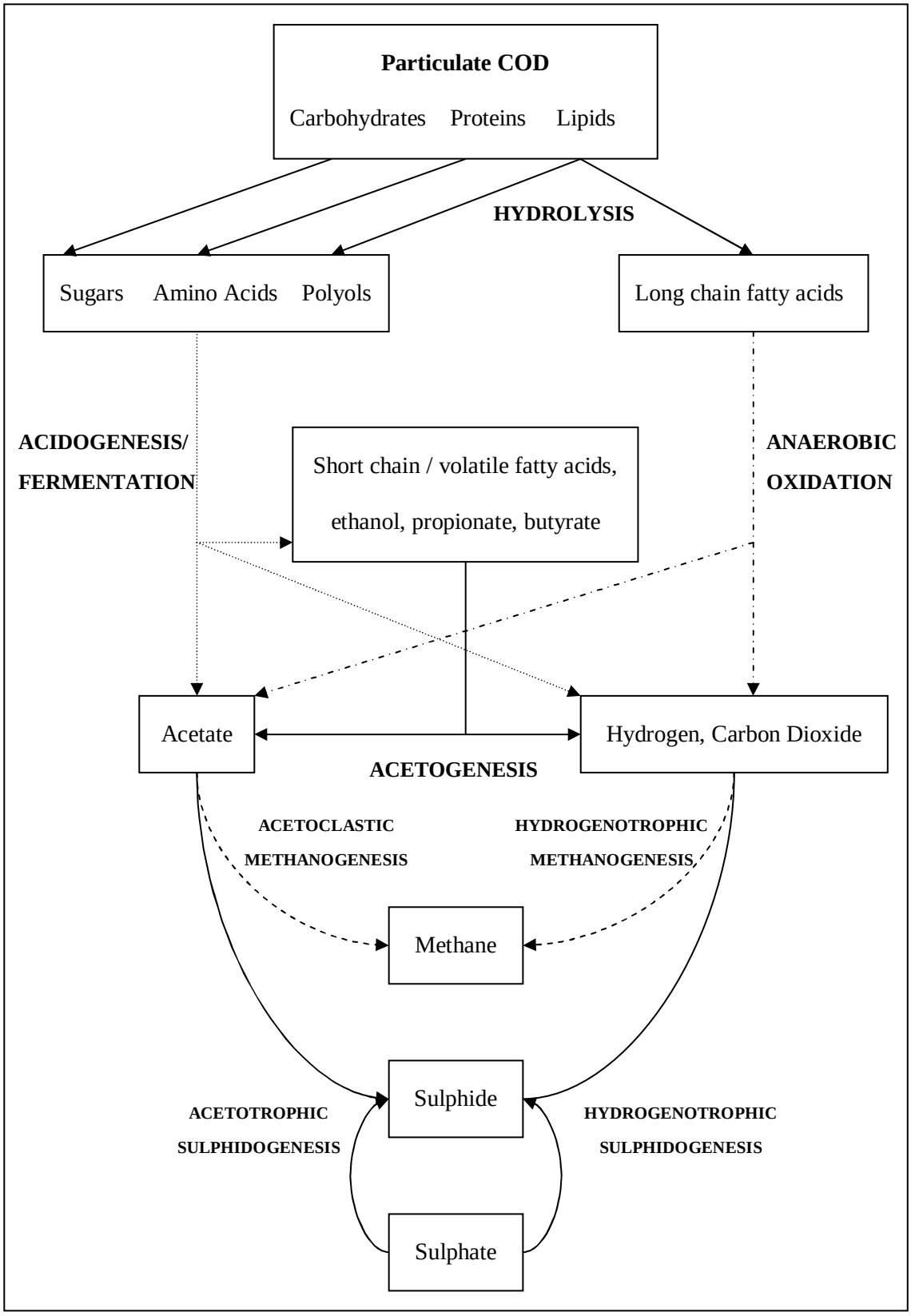

Figure 2-1: Reaction scheme showing the interacting flows of substrates between each biological process of anaerobic digestion including sulphate reduction. (From Hansford (2004) and Ristow (1999) who modified the original reaction scheme proposed by Gujer and Zehnder (1983))

The University of Cape Town Anaerobic Digestion Model No.1 (UCTADM1) is a two phase (aqueous-gas) integrated mixed weak acid/base chemical, physical and biological processes kinetic model for the anaerobic digestion of sewage sludges. This model was developed and validated by Sötemann et al. (2005b), and is based on the anaerobic digestion processes scheme of Gujer and Zehnder (1983), which consists of ten biological processes (Table 2-2) that are mediated by four anaerobic digestion organism groups.

Table 2-2: Biological processes included in the two phase UCTADM1 (Sötemann, et al., 2005b)

Process	**Specific biological process**	**Organism group**
Hydrolysis	1. Hydrolysis of $C_XH_YO_ZN_A$ to glucose	Acidogens
Growth	2. Acidogens on glucose under low pH_2	Acidogens
	3. Acidogens on glucose under high pH_2	Acidogens
	4. Acetogens on propionic acid	Acetogens
	5. Acetoclastic methanogens on acetic acid	Acetoclastic methanogens
	6. Hydrogenotrophic methanogens on H_2	Hydrogenotrophic methanogens
Death/	7. Acidogens	Acidogens
Endogenous	8. Acetogens	Acetogens
decay	9. Acetoclastic methanogens	Acetoclastic methanogens
	10. Hydrogenotrophic methanogens	Hydrogenotrophic methanogens

The biological kinetic processes for anaerobic digestion are integrated in a two phase subset of the three phase mixed weak acid/base chemistry kinetic model of Musvoto et al. (1997, 2000a,b,c). Sewage sludge is characterised with the COD, carbon, hydrogen, oxygen and nitrogen (CHON) composition. The model is formulated in mole units and is based on the conservation of these components.

The 10 biological processes act on 14 components in the model. The biological processes, model components, biochemical rate coefficients and kinetic process rates of the UCTADM1 are shown in a Petersen matrix format in Appendix A, Table A-1. Included in the anaerobic digestion model are 18 chemical equilibrium dissociation processes (j = 11-28) of ammonia, carbonate, phosphate, acetate, propionate and water acid/base systems and their 15 associated components (i = 2-7, 9-17). Four gases were considered when integrating the biological

processes of anaerobic digestion into the two phase (aqueous-gas) mixed weak acid/base chemistry model of Musvoto et al. (2000a), viz. CO_2, CH_4, H_2 and NH_3. Only the physical processes for carbon dioxide gas exchange with the atmosphere were included (i = 27, j = 29-30). CO_2 was modelled with both expulsion and dissolution due to its significantly soluble nature.

Sötemann et al. (2005b) obtained the rate equations for the ten biological processes (Table 2-2) in the UCTADM1 from various literature sources and modified them, where possible to best describe the reactions as realistically and accurately as possible. The kinetic model was extended to include to the condition of digester failure due to hydrogen ion activity (pH) and hydrogen partial pressure (pH_2), to which certain organisms are most sensitive to. The experimental data set of Izzett et al. (1992) was used for the successful calibration and validation of the UCTADM1 in the AQUASIM modelling and simulation platform. It must be noted that the basic UCTADM1 does not include the processes of biological sulphate reduction and would therefore need to be extended to incorporate this. The kinetic rate equations chosen for the biological processes in the anaerobic digestion model are described below:

2.2.2 Hydrolysis

Bacteria are unable to take up polymeric material unless it is broken down to soluble compounds such as soluble polymers, monomers or dimers, and therefore hydrolysis is the first step in the anaerobic degradation of complex polymeric organics required for microbial utilisation (Gujer and Zehnder, 1983, Pavlostathis and Giraldo-Gomez, 1991). During hydrolysis fermentative bacteria colonise the surface of particles, secreting hydrolytic enzymes, which are responsible for the extracellular hydrolysis of complex organic materials such as PSS. According to Hansford (2004), the following reactions are expected to occur:

- Hydrolysis of amide bonds of proteins to yield amino acids;
- Hydrolysis of ester bonds of lipids to yield LCFAs, glycerol (and other polyols) and alcohols;
- Hydrolysis of glucoside bonds of polysaccharides to yield dimeric and monomeric sugars.

Further, the rate of hydrolysis has been shown to be dependent on a large number of factors and is generally the rate-limiting step in the anaerobic digestion of particulate matter.

These factors include:

- Temperature: exponential increase in reaction rate with increasing temperature (Gujer and Zehnder, 1983);

- pH: approximately neutral condition result in faster hydrolysis than acidogenesis (Eastman and Ferguson, 1981, Ristow, et al., 2005);

- Microbial biomass and hence the level of hydrolytic enzymes;

- Particle geometry;

- Different rates of hydrolysis for the lipid, carbohydrate and protein fractions;

- Various components being intimately bound.

The approach of characterising sewage sludge into carbohydrates, lipids and proteins, as is done in the International Water Association (IWA) Anaerobic Digestion Model No.1 (ADM1) (Batstone, et al., 2002) requires measurements that are not readily available. Due to this, the hydrolysis of these organics was modified to a single hydrolysis process acting on a generic organic material representing biodegradable sewage sludge i.e. $C_XH_YO_ZN_A$ (McCarty, 1974). This simplification is reasonable as the end-products of hydrolysis, followed by acidogenesis are SCFAs which are essentially the same. However, the relative proportions of C, H, O and N in sewage sludge need to be determined i.e. the X, Y, Z and A values in $C_XH_YO_ZN_A$. This approach was adopted by Sötemann, et al. (2005b) in the development of the UCTAMD1. A sludge composition formula of $C_{3.5}H_7O_2N_{0.196}$ was obtained interactively through analysis of and model application to the experimental data set of Izzett et al. (1992). Further, the stoichiometric formulation for all organism groups was accepted as $C_5H_7O_2N$. The end-product of this single hydrolysis process was chosen to be the idealised carbohydrate, glucose, for the following reasons as explained by Sötemann, et al. (2005b):

- Subsequent biological processes on glucose are well established and the acidogenic process acting on glucose to convert it to SCFAs is unlikely ever to be rate-limiting with particulate particulate biodegradable organics in sewage sludge.

- In model application accumulation of glucose will not occur, even under digester failure conditions.

- Glucose acts merely as an intermediate compound, which is acidified to SCFAs as soon as it is produced.

- Irrespective of the hydrolysis formulation used, no acidogen biomass growth takes place and 1 g COD biodegradable sewage sludge forms 1 g COD glucose intermediate.

Various kinetic formulations for the hydrolysis process were investigated:

2.2.2.1 First Order Kinetics

Although the rate of hydrolysis is affected by all of the above-mentioned factors, the most common rate equation with respect to the total biodegradable particulate COD (S_p) concentration (Eastman and Ferguson, 1981, Gujer and Zehnder, 1983, Henze and Harremöes, 1983, Pavlostathis and Giraldo-Gomez, 1991):

$$r_{HYD} = K_h \left[S_p \right] \tag{2-9}$$

where:

r_{HYD} = hydrolysis rate (mol S_{bp}/ℓ.d)

K_h = first order hydrolysis rate constant (d^{-1})

$[S_p]$ = sum of biodegradable (S_{bp}) and unbiodegradable (S_{up}) particulate fractions (mol/ℓ)

The hydrolysis rate constant is a function of the conditions used, with substrates used ranging from primary domestic sludge (Eastman and Ferguson, 1981), to organic solids (Gujer and Zehnder, 1983), to wastewater (Henze and Harremöes, 1983).

Ristow, et al. (2005) and Ristow (1999) stated that in all applications of the first order rate equation above, the hydrolysis rate was formulated with respect to the total particulate COD (S_p) and no differentiation was made between the biodegradable (S_{bp}) and unbiodegradable (S_{up}) fractions. Further, for pure substrates this omission is reasonable as the substrate is known and defined, but for waste sludges such as PSS, the S_{up} fraction would need to be considered, since

by definition, this fraction would not participate in the hydrolysis reaction. Shimizu, et al. (1993) proposed an expression similar to Equation 2-9, but in which the rate of hydrolysis is dependent on the S_{bp} organic fraction only, with the S_{up} fraction being subtracted from S_p:

$$r_{HYD} = K_h \left[S_p - S_{up} \right] = K_h . S_{bp} \tag{2-10}$$

Ristow, et al. (2005) went further to state that in all of the above models, the rate equation used suggests that the rate of hydrolysis would increase linearly to infinity as the concentration of the total or biodegradable particulate organics respectively increase to infinity. The hydrolysis process is mediated by acidogenic biomass and the limitation on the maximum hydrolysis rate should be linked to the concentration of this biomass in the same manner.

The acidogen organism concentration plays an important role in regulating the rate of hydrolysis and should therefore be included in the kinetic rate expression (Ristow, et al., 2005, Sötemann, et al., 2005b) as proposed by Eliosov and Argaman (1995):

$$r_{HYD} = K_H \left[S_{bp} \right] \left[Z_{ai} \right] \tag{2-11}$$

where:

K_H = first order specific hydrolysis kinetic rate constant (ℓ/mol Z_{ai}.d)

$[Z_{ai}]$ = acidogen active biomass concentration (mol/ℓ)

2.2.2.2 Monod Kinetics

The use of Monod kinetics in the modelling of biological wastewater treatment processes is a common practice as in (Batstone, et al., 2002, Henze, et al., 1987, McCarty, 1974).

$$r_{HYD} = \left[\frac{\mu_{\max,HYD} \left[S_{bp} \right]}{K_{SM,HYD} + \left[S_{bp} \right]} \right] \left[Z_{ai} \right] \tag{2-12}$$

where:

$\mu_{max,HYD}$ = maximum specific hydrolysis rate constant (mol S_{bp}/mol Z_{ai}.d)

$K_{SM,HYD}$ = Monod half saturation constant for hydrolysis (mol S_{bp}/ℓ)

2.2.2.3 Surface mediated reaction (or Contois) kinetics

Sötemann, et al., (2005b) investigated the use of surface mediated reaction kinetics for their anaerobic digestion model and implemented the approach of Levenspiel (1972), used by Dold et al. (1980) to model the hydrolysis of particulate slowly biodegradable COD in activated sludge systems. Using a single set of constants, these kinetics gave reasonable predictions over a wide range of activated sludge system conditions and is therefore feasible to use this approach as the hydrolysis processes in activated sludge and anaerobic digestion can be regarded as similar and operate on the same organics present in raw sludge (Sötemann, et al., 2005b):

$$r_{HYD} = \left[\frac{k_{\max,HYD} \frac{[S_{bp}]}{[Z_{ai}]}}{K_{SS,HYD} + \frac{[S_{bp}]}{[Z_{ai}]}} \right] [Z_{ai}] \qquad (2\text{-}13)$$

where:

$k_{max,HYD}$ = maximum specific hydrolysis rate constant (mol S_{bp}/mol Z_{ai}.d)

$K_{SS,HYD}$ = Half saturation constant for hydrolysis (mol S_{bp}/mol Z_{AD})

The data set of Izzett et al. (1992) was used to calibrate the constants for the four variations in hydrolysis kinetics. It was difficult to decide which rate expression was best and each yielded a slightly different unbiodegradable particulate COD fraction on the sewage sludge between 0.33 and 0.36. It was decided by Sötemann et al. (2005b) that since this process is mediated by the acidogens, the surface reaction mediated kinetics which includes this organism group would naturally be more reasonable, and was therefore accepted for incorporation with the UCTADM1.

2.2.3 Acidogenesis

Acidogenesis refers to the use of the model intermediate, glucose (S_{bs}), by acidogenic or fermentative organisms, producing propionic acid, acetic acid, hydrogen, carbon dioxide and protons.

Acidogenic organisms produce acetic acid, propionic acid, hydrogen and carbon dioxide according to the following reactions (Hansford, 2004, Mosey, 1983):

$$C_6H_{12}O_6 + 2H_2O \rightarrow 2CH_3COOH\,(acetic\ acid) + 2CO_2 + 4H_2 \qquad (2\text{-}14)$$

$$C_6H_{12}O_6 + 2H_2 \rightarrow 2CH_3CH_2COOH\,(propionic\ acid) + 2H_2O \qquad (2\text{-}15)$$

Under conditions of low hydrogen partial pressure (pH_2), glucose is catabolised to acetic acid, hydrogen and carbon dioxide (Sam-Soon, et al., 1991). This process is formulated in terms of the acidogen growth rate (r_{Zai}), which is modelled with a Monod equation (Gujer and Zehnder, 1983, Pavlostathis and Giraldo-Gomez, 1991) as follows:

$$r_{Z_{ai}} = \frac{\mu_{\max,ai}\left[S_{bsf}\right]}{K_{S,ai} + \left[S_{bsf}\right]}\left\{1 - \frac{\left[H_2\right]}{k_{H_2} + \left[H_2\right]}\right\}\left[Z_{ai}\right] \qquad (2\text{-}16)$$

where:

$\mu_{max,ai}$ = maximum specific growth rate constant for acidogens (d^{-1})

$K_{S,ai}$ = half saturation concentration for acidogens (mol/ℓ)

$[S_{bsf}]$ = biodegradable soluble (glucose) substrate concentration (mol/ℓ)

$[H_2]$ = hydrogen concentration (mol/ℓ)

k_{H2} = hydrogen inhibition constant for high pH_2 (mol/ℓ)

The non-competitive inhibition function accounts for the reduction in rate when the pH_2 is high, i.e. the term in { } brackets. When the pH_2 is high, in addition to acetic acid, hydrogen and carbon dioxide, propionic acid is also produced from glucose (Sam-Soon, et al., 1991). The production of propionic acid is also based on the same Monod equation (Equation 2-16) as for low pH_2:

$$r_{Z_{ai}} = \frac{\mu_{\max,ai}\left[S_{bsf}\right]}{K_{S,ai} + \left[S_{bsf}\right]}\left\{\frac{\left[H_2\right]}{k_{H_2} + \left[H_2\right]}\right\}\left[Z_{ai}\right] \qquad (2\text{-}17)$$

A switching function is used to switch from one process to the other based on the concentration of hydrogen (Sam-Soon, et al., 1991). To ensure that this process only operates when the pH_2 is high, the non-competitive inhibition function in { } brackets switches the process "on" under conditions of high pH_2 and "off" under conditions of low pH_2. To ensure that the rate of glucose utilisation is the same under both conditions and in the intermediate condition, the rate of acetate production (Equation 2-16) is reduced by subtracting the inhibition function value

from 1.

2.2.4 Acetogenesis

Acetogenesis is the process whereby under low hydrogen partial pressure acetogenic organisms convert propionic acid generated by acidogenesis under high hydrogen partial pressure to acetic acid. McCarty and Mosey (1991) describe the anaerobic oxidation of propionate:

$$CH_3CH_2COOH + 2H_2O \rightarrow CH_3COOH + CO_2 + 3H_2 \qquad (2\text{-}18)$$

The rate of acetogenesis was modelled in terms of acetogen growth rate (r_{Zae}) and with a Monod equation for the specific growth rate:

$$r_{Z_{ae}} = \frac{\mu_{\max,ae}[H\,\mathrm{Pr}]}{K_{S,ae} + [H\,\mathrm{Pr}]}\left\{1 - \frac{[H_2]}{k_{H_2} + [H_2]}\right\}[Z_{ae}] \qquad (2\text{-}19)$$

where:

$\mu_{max,ae}$ = maximum specific growth rate constant for acetogens (d^{-1})

$K_{S,ae}$ = half saturation concentration for acetogens growth on propionic acid (mol/ℓ)

[HPr] = undissociated propionic acid concentration (mol/ℓ)

$[Z_{ae}]$ = acetogenic organism concentration (mol/ℓ)

The non-competitive inhibition function in the { } brackets is also present as in Equation 2-16 due to the acetogenesis process being sensitive to pH_2, the rate decreases as pH_2 increases. As pH_2 increases, acidogens begin to produce propionic acid and the rate of propionic acid utilisation by acetogens decreases resulting in a build-up of propionic acid which contributes to a drop in the pH.

2.2.5 Acetoclastic Methanogenesis

Acetoclastic methanogenesis, or acetate cleavage, is the process whereby acetic acid is converted to methane and carbon dioxide. The overall reaction for the biological production of methane from acetic acid is given by:

$$CH_3COOH \rightarrow CH_4 + CO_2 \qquad (2\text{-}20)$$

The rate of acetoclastic methanogenesis (r_{Zam}) was again modelled with a Monod equation:

$$r_{Z_{am}} = \frac{\mu_{\max,am}[HAc]}{\left(K_{S,am} + [HAc]\right)\left\{1 + \frac{[H^+]}{K_{i,am}}\right\}}[Z_{am}] \qquad (2\text{-}21)$$

where:

$\mu_{max,am}$ = maximum specific growth rate constant for acetoclastic methanogens (d^{-1})

$K_{S,am}$ = half saturation concentration of acetoclastic methanogens growth on acetic acid (mol/ℓ)

$Ki_{,am}$ = inhibition constant (mol/ℓ) i.e. the hydrogen ion concentration at which the growth of acetoclastic methanogens is half the maximum rate

[HAc] = undissociated acetic acid concentration (mol/ℓ)

$[H^+]$ = hydrogen ion concentration (mol/ℓ) from which pH = -log [H+]

$[Z_{am}]$ = acetoclastic methanogen organism concentration (mol/ℓ)

Acetoclastic methanogens are probably the most sensitive organisms in anaerobic digesters (Gujer and Zehnder, 1983). Digester failure usually starts with inhibition of acetoclastic methanogens caused by a sudden drop in temperature, a toxin in the influent, or a shock load, which slows down its growth rate resulting in an increase in digester acetic acid concentration (Sötemann, et al., 2005b). This causes a decrease in the pH which slows down their growth rates resulting in a further increase in acetic acid concentration as well as hydrogen partial pressure which has an impact on the acetogenesis process as mentioned above. A first order inhibition term in { } was used in the growth rate equation to represent inhibition by hydrogen ion activity or pH.

2.2.6 Hydrogenotrophic Methanogenesis

Hydrogenotrophic methanogenic organisms use hydrogen and carbon dioxide to produce methane and water according to the following reaction:

$$CO_2 + 4H_2 \rightarrow CH_4 + 2H_2O \qquad (2\text{-}22)$$

This process is also modelled in terms of the growth rate of hydrogenotrophic methanogens (r_{Zhm}), using a Monod equation:

$$r_{Z_{hm}} = \frac{\mu_{\max,hm}[H_2]}{K_{S,hm} + [H_2]\left\{1 + \frac{[H^+]}{K_{i,hm}}\right\}}[Z_{hm}] \qquad (2\text{-}23)$$

where:

$\mu_{max,hm}$ = maximum specific growth rate constant for hydrogenotrophic methanogens (d^{-1})

$K_{S,hm}$ = half saturation concentration of hydrogenotrophic methanogens growth on hydrogen (mol/ℓ)

$Ki_{,hm}$ = inhibition constant (mol/ℓ) i.e. the hydrogen ion concentration at which the growth of hydrogenotrophic methanogens is half the maximum rate

$[H_2]$ = molecular hydrogen concentration (mol/ℓ)

$[Z_{hm}]$ = hydrogenotrophic methanogen organism concentration (mol/ℓ)

The effect of hydrogenotrophic methanogens is to keep the hydrogen partial pressure low and like acetoclastic methanogens, they are sensitive to a pH decrease within in anaerobic digesters. A first order inhibition term for hydrogen ion or pH inhibition was again included in the growth rate equation.

2.2.7 Sulphate Reduction

SRB are capable of growing on more varied substrates than methane producing bacteria (Oude Elferink, et al., 1994). Both sulphate reduction and methanogenesis can be the final step in the degradation process of sulphate fed anaerobic reactors, due to SRB being capable of utilising many of the intermediates formed during methanogenesis (Kalyuzhnyi, et al., 1998). This is illustrated in Figure 2-2.

Competition for substrate in such systems is possible on two levels: competition between SRB and acetogenic bacteria for VFA and a carbon source, and competition between SRB and methanogenic bacteria for acetate and hydrogen.

During the process of biological sulphate reduction, sulphate is reduced to the main product of this process viz. sulphide, which is a strong toxicant for most anaerobic organisms including acetogens, methanogens and SRB. Sulphide inhibition is related with the undissociated form which can permeate the cell membrane, affecting the activity of the organism. Small variations in pH can also result in significant changes in the degree of inhibition.

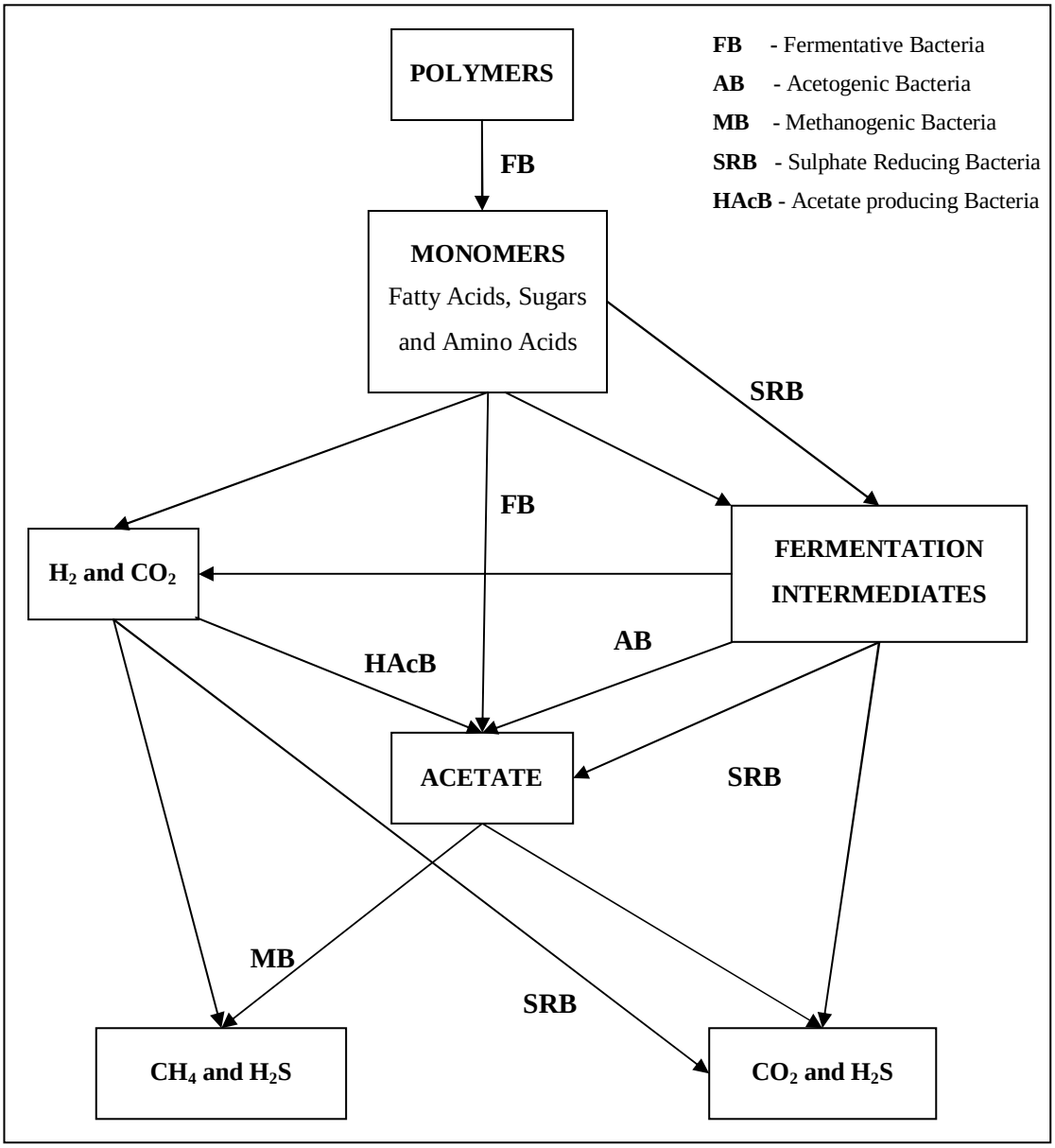

Figure 2-2: Pathways of competition between acetogenic, methanogenic and sulphate reducing bacteria during anaerobic digestion of organic matter (From Kalyuzhnyi et al., 1998)

To date, few models of sulphate fed anaerobic digesters have been investigated. Kalyuzhnyi et al. (1998) initially reviewed the existing mathematical models of sulphate fed anaerobic digesters developed by Gupta et al. (1994), Kalyuzhnyi and Fedorovich (1997 and 1998), and Vavilin et al. (1994). These models are useful in studying population dynamics such as mutualism and competition between methanogenic bacteria and SRB and existence of trigger and feed-back loop mechanisms. They are also helpful in studying operational performance and stability of sulphate fed anaerobic digesters. However, in the model of Gupta et al. (1994), the biological subsystem was represented in a simplified way, using the Monod equation for organism groups without pH modulation and without taking into account sulphide inhibition.

The model proposed by Vavilin et al. (1994) did not address the competition between sulphate reduction and methanogenesis. All the above-mentioned models, including that of Kalyuzhnyi and Fedorovich (1997 and 1998), were developed mainly for continuously stirred tank reactors (CSTR's).

Kalyuzhnyi et al. (1998) developed a new integrated mathematical model of the functioning of a sulphate fed granular sludge reactor which takes into account concentration gradients on substrates, intermediates, products and organisms inside the digester. The proposed model was developed for the degradation of a mixture of sucrose, propionate, acetate and sulphate. Multiple-reaction stoichiometry and kinetics have also been developed and verified for this dispersed plug-flow model of upflow anaerobic sludge blanket (UASB) reactors.

2.2.7.1 Acetogenic Sulphidogenesis

Acetogenic sulphidogenesis is the process whereby propionate degrading SRB convert propionic acid and sulphate to acetic acid, sulphide, carbon dioxide and water. Kalyuzhnyi et al. (1998) presented the reaction sequence for substrate utilisation of propionate to produce acetate as follows:

$$CH_3CH_2COOH + \frac{3}{4}SO_4^{2-} + \frac{3}{2}H^+ \rightarrow CH_3COOH + \frac{3}{4}H_2S + CO_2 + H_2O \qquad (2\text{-}24)$$

This process was formulated in terms of the acetogenic sulphidogen growth rate (r_{Zps}), which is modelled with a Monod equation including a sulphide inhibition term in { }:

$$r_{Z_{ps}} = \frac{\mu_{\max,ps}\left[H\,\mathrm{Pr}\right]}{K_{S,ps} + \left[H\,\mathrm{Pr}\right]}\left\{1 - \frac{\left[H_2S\right]}{Ki_{ps}}\right\}\left(\frac{\left[SO_4^{2-}\right]}{Kn_{ps} + \left[SO_4^{2-}\right]}\right)\left[Z_{ps}\right] \qquad (2\text{-}25)$$

where:

$\mu_{max,ps}$ = maximum specific growth rate constant for acetogenic sulphidogens (d^{-1})

$K_{S,ps}$ = half saturation concentration for acetogenic sulphidogen growth on propionic acid (g COD/ℓ)

$Ki_{,ps}$ = inhibition constant i.e. the hydrogen sulphide concentration at which the growth of acetogenic sulphidogens is half the maximum rate (g S/ℓ)

$Kn_{,ps}$ = half saturation concentration for acetogenic sulphidogen growth on sulphate (g/ℓ)

[HPr] = total propionic acid concentration (g COD/ℓ)

$[H_2S]$ = undissociated hydrogen sulphide concentration (g S/ℓ)

$[SO_4^{2-}]$ = total sulphate concentration (g/ℓ)

$[Z_{ps}]$ = acetogenic sulphidogen organism concentration (g/ℓ)

2.2.7.2 Acetoclastic Sulphidogenesis

Acetoclastic sulphidogenic bacteria or acetate degrading bacteria use acetic acid and sulphate as substrates to produce hydrogen sulphide, carbon dioxide and hydrogen according to the following reaction from Kalyuzhnyi et al. (1998):

$$CH_3COOH + SO_4^{2-} + 2H^+ \rightarrow H_2S + 2CO_2 + 2H_2O \qquad (2\text{-}26)$$

The rate of acetoclastic sulphidogenesis (z_{Zas}) was again modelled with a Monod equation including a sulphide inhibition term in { }:

$$r_{Z_{as}} = \frac{\mu_{\max,as}[HAc]}{K_{S,as}+[HAc]}\left\{1-\frac{[H_2S]}{Ki_{as}}\right\}\left(\frac{[SO_4^{2-}]}{Kn_{as}+[SO_4^{2-}]}\right)[Z_{as}] \qquad (2\text{-}27)$$

where:

$\mu_{max,as}$ = maximum specific growth rate constant for acetoclastic sulphidogens (d^{-1})

$K_{S,as}$ = half saturation concentration for acetoclastic sulphidogen growth on acetic acid (g COD/ℓ)

$Ki_{,as}$ = inhibition constant i.e. the hydrogen sulphide concentration at which the growth of acetoclastic sulphidogens is half the maximum rate (g S/ℓ)

$Kn_{,as}$ = half saturation concentration for acetoclastic sulphidogen growth on sulphate (g/ℓ)

[HAc] = total acetic acid concentration (g COD/ℓ)

$[Z_{as}]$ = acetoclastic sulphidogen organism concentration (g/ℓ)

2.2.7.3 Hydrogenotrophic Sulphidogenesis

The use of hydrogen and sulphate as substrates by hydrogenotrophic sulphidogens to form hydrogen sulphide and water is shown by the following reaction (Kalyuzhnyi, et al., 1998):

$$4H_2 + SO_4^{2-} + 2H^+ \rightarrow H_2S + 4H_2O \qquad (2\text{-}28)$$

This process is also modelled in terms of the growth rate of hydrogenotrophic methanogens (r_{Zhm}), using a Monod equation with a sulphide inhibition term in { }:

$$r_{Z_{hs}} = \frac{\mu_{\max,hs}[H_2]}{K_{S,hs}+[H_2]}\left\{1-\frac{[H_2S]}{Ki_{hs}}\right\}\left(\frac{[SO_4^{2-}]}{Kn_{hs}+[SO_4^{2-}]}\right)[Z_{hs}] \qquad (2\text{-}29)$$

where:

$\mu_{max,hs}$ = maximum specific growth rate constant for hydrogenotrophic sulphidogens (d^{-1})

$K_{S,hs}$ = half saturation concentration for hydrogenotrophic sulphidogen growth on hydrogen (g COD/ℓ)

$Ki_{,hs}$ = inhibition constant i.e. the hydrogen sulphide concentration at which the growth of hydrogenotrophic sulphidogens is half the maximum rate (g S/ℓ)

$Kn_{,hs}$ = half saturation concentration for hydrogenotrophic sulphidogen growth on sulphate (g/ℓ)

$[H_2]$ = total hydrogen concentration (g COD/ℓ)

$[Z_{hs}]$ = hydrogenotrophic sulphidogen organism concentration (g/ℓ)

2.2.8 Death/Endogenous Respiration of organisms

Organism death in anaerobic digestion is associated with endogenous respiration only, as predation apparently does not occur. The organism death rate for each organism group was modelled with first order kinetics:

$$-r_Z = b_Z[Z] \qquad (2\text{-}30)$$

where:

b_Z = death/endogenous respiration rate for a specific organism group (d^{-1})

[Z] = specific organism group concentration (mol/ℓ)

2.2.9 Kinetic and Stoichiometric Parameters

The kinetic and stoichiometric parameters shown in Table 2-3 were used by Sötemann et al. (2005b) in the calibration and verification of the UCTADM1 and were obtained from Sam-Soon et al. (1991) at 37 ^{o}C. The data set of Izzett et al. (1992) was used to calibrate constants for hydrolysis kinetics i.e. $K_{max,HYD}$ and $K_{s,HYD}$.

Table 2-3: Kinetic and stoichiometric constants used in the UCTADM1 (From Sötemann et al., 2005b)

Organism group	Y (mol organism/mol substrate)	μ_{max} (d^{-1})	K_s (mol/ℓ)	b (d^{-1})
Acidogens	0.1074	0.8	7.8E-04	0.041
Acetogens	0.0278	1.15	8.9E-05	0.015
Acetoclastic methanogens	0.0157	4.39	1.3E-05	0.037
Hydrogenotrophic methanogens	0.004	1.2	1.56E-04	0.01
Hydrogen inhibition coefficient for high pH_2 (mol H_2/ℓ)			6.25E-4	
Acidogenic hydrolysis of biodegradable particulate organics				
First order:	K_h (d^{-1})		0.381	
First order specific:	K_H (ℓ/mol Z_{ai}.d)		40	
Monod:	$\mu_{max,HYD}$ (mol S_{bp}/mol Z_{ai}.d)		4.529	
	$K_{SM,HYD}$ (mol S_{bp}/ℓ)		0.0486	
Surface mediated reaction (Contois):	$k_{max,HYD}$ (mol S_{bp}/mol Z_{ai}.d)		6.797	
	$K_{SS,HYD}$ (mol S_{bp}/mol Z_{ai})		10.829	

.

Kalyuzhnyi and co-workers (1998) obtained kinetic and stoichiometric parameters directly from literature at 30 ^{o}C. Various preliminary simulations were undertaken to determine the most appropriate set of kinetic model parameters that best fit the experimental data used to calibrate and verify the model for a sulphate fed reactor. Table 2-4 gives the complete set of kinetic parameters for seven organism groups (Kalyuzhnyi, et al., 1998)

Table 2-4: Kinetic parameters used in the sulphate reduction model (From Kalyuzhnyi et al., 1998)

Organism Group	μ_{max} (d^{-1})	K_s (g COD/ℓ)	K_n (g/ℓ)	K_i (g S/ℓ)	Y (g VSS/g COD)	b (d^{-1})
Acidogens	4	0.028	-	0.55	0.034	0.09
Acetogens	0.16	0.247	-	0.19	0.016	0.014
Acetogenic sulphidogens	0.583	0.295	0.0074	0.185	0.027	0.0185
Acetoclastic methanogens	0.264	0.12	-	0.185	0.0215	0.02
Acetoclastic sulphidogens	0.612	0.024	0.0192	0.164	0.033	0.0275
Hydrogenotrophic methanogens	1	1.2E-04	-	0.165	0.015	0.04
Hydrogenotrophic sulphidogens	2.8	7E-05	0.0192	0.55	0.05	0.06

2.3 The Rhodes BioSURE Process®

Researchers in the Environmental Biotechnology Research Unit and Department of Biochemistry, Microbiology and Biotechnology at Rhodes University studied the use of PSS for sulphate reduction. This research resulted in the development of the Rhodes BioSURE Process® which links AMD bioremediation and sewage sludge disposal. The Rhodes BioSURE Process® has been developed as a low-cost active treatment method for AMD wastewaters, where the process development was based on prior studies in the microbial ecology of sulphidogenic ponding environments (Rose, et al., 2002, Whittington-Jones, et al., 2002).

The Rhodes BioSURE Process® was claimed to be more economic than any other biological treatment option presently available, reducing costs from approximately R5/kℓ to R1/kℓ in operating expenditure (WISA, 2005).

The benefits of the Rhodes BioSURE Process® as reported by WISA (2005) include:

- Removal of metals and radioactive elements.
- Aromatic pollutants are degraded.
- Pathogens are destroyed.
- Provides an unusually robust biotechnological solution.
- The waste effluent is a safe humus compost material.
- The process can be customised to suit any requirements.
- Relatively low capital and operational costs.
- The process has the lowest cost solution for AMD remediation.

2.3.1 The Rhodes BioSURE Process® Configuration

The heart of the Rhodes BioSURE Process® is a unit operation called the recycling sludge bed reactor (RSBR). The result of studies undertaken by the Environmental Research Unit on a 10 ℓ and 1 m^3 lab-scale RSBR led to the concept of a dual-stage sulphate reduction operation and the development of the Rhodes BioSURE Process® (Rose, et al., 2002). The process flow diagram (Figure 2-3) consists of a series of interconnected biological and chemical unit operations in which sulphate-rich AMD wastewater is treated by the process of biological sulphate reduction using PSS as a carbon source and electron donor.

The process of biological sulphate reduction is separated in two stages for increased optimisation of the overall process. The first stage takes place in a RSBR where PSS is hydrolysed to soluble organic material. In this unit the solids are drawn down into the reactor bed and sludge is continuously settled and recycled to blend with the incoming AMD feed resulting in the enhancement of the hydrolysis and initial sulphate reduction reactions. It has been shown that in this unit, PSS as a carbon source and electron donor may be solubilised biosulphidogenically to yield a hydrolysed product of over 30% volatile fatty acid equivalents (Rose, 2002).

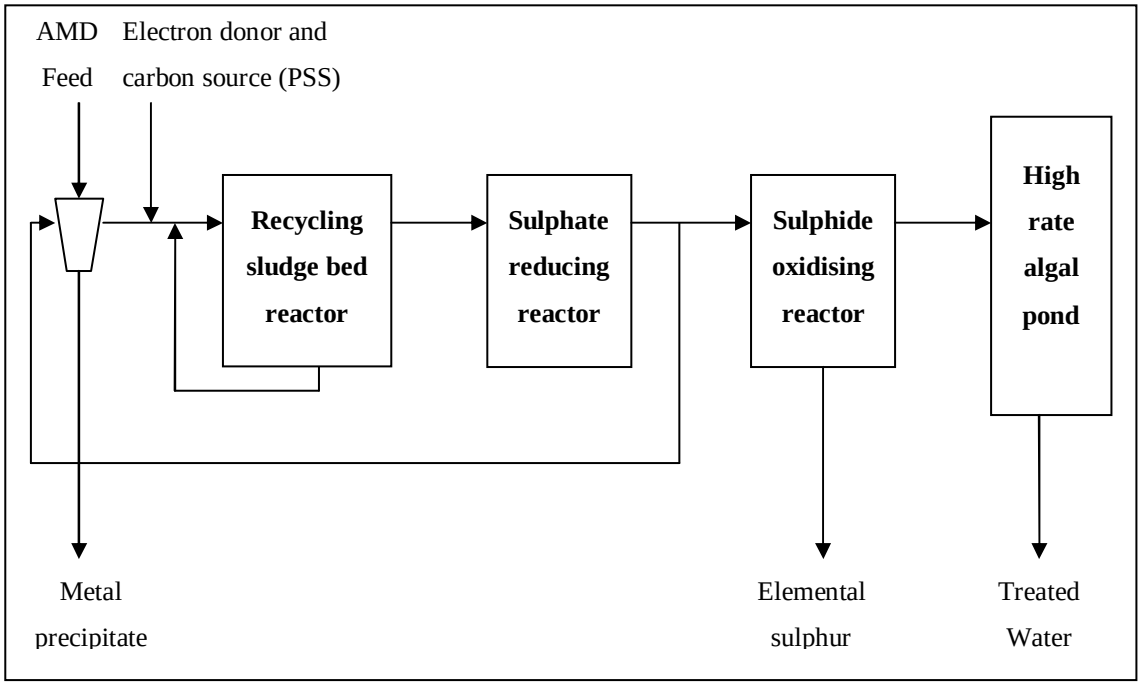

Figure 2-3: Process flow diagram of the Rhodes BioSURE Process ® applied to the treatment of acid mine drainage (From Rose et al., 2002)

The products from the RSBR are then used by SRB in the sulphate reducing digester. The configuration selected for the sulphate reducing digester is that of an anaerobic baffled reactor (ABR). Sulphate reduction is optimised further by the recycling of sulphide and carbonate alkalinity which comes into contact with the feed AMD, neutralising the pH and precipitating the feed heavy metals as metal sulphides, carbonates and hydroxides (Ristow, et al., 2005). The fraction of the sulphide-rich stream that is not recycled is passed to a sulphide oxidising reactor where it is reduced to elemental sulphur and removed from the process. The final unit operation in the process is a high rate algal pond, where the neutralised stream from the sulphide oxidising reactor is polished and disinfected prior to discharge of treated water.

2.4 Closure

In summary, Sötemann et al., (2005b) developed the UCTADM1 which integrates various biological anaerobic processes for the production of methane. This methanogenic model forms the basis to be extended with the development of a mathematical model incorporating the processes of biosulphidogenic reduction and the biology of SRB. Kinetic parameters of Sötemann et al. (2005b) and Kalyuzhnyi et al. (1998) will be further investigated in this work for application within the model.

This work will also investigate application of the extended UCTADM1 to the pilot RSBR which is based on the Rhodes BioSURE Process®.

CHAPTER 3

EXPERIMENTAL AND PILOT PLANT STUDIES

3.1 The UCT Experimental Investigation

The main reaction in the Rhodes BioSURE Process® is biosulphidogenic reduction of AMD with PSS, and therefore the design, operation and control of this process is dependent on the rate at which PSS is used (Ristow, et al., 2005). The Water Research Group at the University of Cape Town (UCT) have conducted an experimental investigation into, as well as the mathematical modelling of the rate of PSS hydrolysis under methanogenic, acidogenic and sulphate reducing conditions.

According to Ristow et al., (2005), the principle aim of this research was to determine the rate of hydrolysis of PSS under methanogenic, acidogenic and sulphate reducing conditions, and the influence of the system physical constraints on the rate which will enable a direct comparison of the rate under each of the three conditions and possible influences thereof. The experimental investigation undertaken by Ristow and co-workers (2005) is summarised as follows:

3.1.1 Feed collection and storage

PSS was collected from the Athlone Wastewater Treatment Works in Cape Town and stored in a cold room at a temperature of 4 ^{o}C for the duration of a digester steady state. The PSS was passed through a mesh sieve to remove large particles such as rags, cigarette butts, seeds and other debris, but without changing the nature of the feed by removing a significant fraction of the feed.

3.1.2 Feed preparation

The feed was prepared by weighing a mass of PSS and then adding warm or hot water to a temperature of 35 ^{o}C, until a desired final mass of diluted sludge was obtained. This would minimise the temperature shock load to the system as the digester operating temperature is 35 ^{o}C before feeding the headspace of the digester was purged with nitrogen to remove any oxygen from the system and capture any H_2S formed in and $FeCl_3$ solution and after feeding was resealed. After sealing it was again purged with N_2. This enabled a completely anaerobic environment to be maintained.

3.1.3 Feed characterisation

The PSS was analysed on a regular basis for total and soluble COD, TKN, FSA, total and soluble phosphorous, total VFA, H_2CO_3 alkalinity and pH. An elemental analysis was also performed on each feed batch to determine the relative proportions of carbon (X), hydrogen (Y), oxygen (Z) and nitrogen (A) in the $C_XH_YO_ZN_A$ stoichiometric formulation of PSS, but however not given by Ristow et al. (2005). For the purpose of mass balances in order to determine the rate of hydrolysis under various conditions, Ristow, et al. (2005) utilised the generic particulate organic and biomass molecular formulae of $C_{3.5}H_7O_2N_{0.196}$ and $C_5H_7O_2N$ respectively which were taken from Sötemann, et al. (2005b). In addition the soluble fermentable biodegradable COD was given the formula of the idealised organic glucose. The approach of Ristow, et al. (2005) was adopted for the purpose of modelling and characterising the influent in this work.

3.1.4 Digester Operation and Control

Six parallel laboratory-scale completely mixed anaerobic digesters were used in this study, two of which had a working volume of 16 ℓ, and the other four had a working volume of 20 ℓ. The digesters were operated at a temperature of 35 ^oC and were fed with PSS as the influent once or twice daily, depending on the volume of feed or retention time, in order to stimulate continuous feeding, however eliminating problems associated with the pumping of PSS in a laboratory-scale experiment.

These systems were monitored and analysed daily for pH, gas volume produced, VFA, alkalinity and sulphate concentrations where applicable, until a steady state operation was observed. Total COD, soluble COD, aqueous sulphide, gas composition and suspended solids were thereafter measured on a daily basis. A pH controller was implemented in systems where the digester pH was maintained at a certain value, and could be selected to add either acid or base from a 1M HCl or 1M NaOH solution respectively.

3.1.5 Methanogenic Systems

Steady state methanogenic anaerobic digesters were operated at hydraulic retention times from 5-60 days, with the feed COD concentrations of 2-40 g COD/ℓ at a controlled temperature of 35 ^oC (Table 3-1). For each COD concentration, the system hydraulic retention time was decreased until methanogenic process became unstable resulting in an increase in VFA and soluble COD concentrations, a decrease in the pH, alkalinity and gas production, and overall system failure. These systems were monitored daily and measurements made for the parameters

mentioned above.

Table 3-1: Steady states measured for varying hydraulic retention times and feed COD concentrations, where numbers indicate steady state period number for methanogenic systems (From Ristow et al., 2005)

Feed COD Concentration	**Hydraulic Retention Time (d)**							
(g COD/ℓ)	**60**	**20**	**15**	**10**	**8**	**6.67**	**5.71**	**5**
40			10, 11	12	21	23	28	
25		3	4	1	2	7	8	9
13			5	13	14	24	31	
9	17							
2				25	18, 19, 26, 27			

3.1.6 Acidogenic Systems

Steady state acidogenic digesters were operated under hydraulic retention times from 3.33-10 days and feed COD concentrations 2-40 g COD/ℓ at a constant temperature of 35 ^{o}C (Table 3-2).

Table 3-2: Steady states measured for varying hydraulic retention times and feed COD concentrations, where numbers indicate steady state period numbers for acidogenic systems (From Ristow et al., 2005)

Feed COD Concentration	**Hydraulic Retention Time (d)**		
(g COD/ℓ)	**10**	**5**	**3.33**
40		30	29
13	38	33	32
2	39	35	34

As mentioned above, the reduction in hydraulic retention times for each feed concentration in methanogenic systems resulted in the methanogenic biomass becoming unstable and

reflected by a change in the measured values of VFA concentration, pH, alkalinity and gas production. Once this instability was observed, the retention times in these systems were reduced to 3.33 days to ensure that all the methanogenic biomass was washed out and therefore acidogenic conditions were established. Each digester was allowed to reach steady state at these reduced retention times before the system was analysed in detail. Daily steady state parameter measurements were taken as mentioned above.

3.1.7 Sulphidogenic Systems

Sulphate reducing digesters were operated in parallel to methanogenic digesters to make the direct comparison of the two systems and to quantify the rate of PSS hydrolysis. Comparison of these systems was made possible with a single parameter change in a single experiment. The aims were achieved by conducting a series of experiments under sulphate reducing conditions, in which the systems were operated with excess sulphate. For steady state 15, the feed was supplemented with Fe with the aim of precipitating FeS and thereby eliminate sulphide toxicity. Steady state numbers for the sulphate reducing experiments are listed in Table 3-3 as well as the corresponding methanogenic system with which it is compared.

Table 3-3: Sulphate reducing steady states and corresponding methanogenic systems at various operating conditions (From Ristow et al., 2005)

Steady state number	HRT (d)	Feed COD (g COD/ℓ)	Feed SO_4^{2-} (g/ℓ)	Additional factors	Comparative steady state number
6	10	26	1	Excess COD	1
15	8	13	9.6	All S_{total} as FeS	14
16	8	13	9.6	No Fe addition	14 and 15
20	8	2	2	pH ~ 7.5	18 and 37
22	8	2	2	pH ~ 7	19
36	8	2	2	pH ~ 6.5	27
41	16	2	2		
42	13.3	2	2		
46	10	1	1		
47	8	2	2	pH ~ 8.3	

3.2 The Pilot Plant

One of the areas in South Africa where AMD and decanting mine water is becoming a significant issue is the Witwatersrand Basin. According to WRC (2005), the gold mines in the basin contribute as much as 35 % of the salt load entering the Vaal Barrage by way of their point source discharges. Mines are required to pump water from underground to dewater areas for development or to prevent flooding of existing works. The closure of mines through the years has resulted in the Grootvlei Mine taking on the responsibility of pumping most of the water from the Eastern Basin (WRC, 2005).

The Environmental Biotechnology Research Unit was invited toward the end of 1997 to participate in the Grootvlei desalination technology evaluation exercise and since 1998 have proceeded to design, construct and implement the Rhodes BioSURE® pilot plant on-site at the East Rand Watercare Company's (ERWAT) Ancor Works at the Grootvlei Mine. Hydrolysis of PSS, a by-product from ERWAT, together with AMD provides the primary reaction in the Rhodes BioSURE Process® and takes place in the pilot RSBR.

The existing design and configuration of the pilot RSBR, illustrated in Figure 3-2, has been revised to that of an upflow anaerobic sludge blanket (UASB) with recycle of the clarified liquid and wasting of the sludge. The most significant characteristic of this configuration is the improved separation of particulates from the overflow effluent and their retention time in the reactor. The UASB vessel has three outlets viz. overflow, recycle and gas streams.

At the time of this study, the pilot plant had only been in operation for a short period due to equipment teething problems and therefore the available operating data is minimal. Figure 3-1 contains all the information available at the time (Ristow, 2005), including estimated values and qualitative statements. The recycle stream was removed from 1 m below the liquid level at a flowrate of 5 m^3/h. The sludge bed was maintained at ± 0.5 m below the liquid level by a sludge withdrawal rate of ± 1 m^3/h. The overflow was practically free of suspended solids.

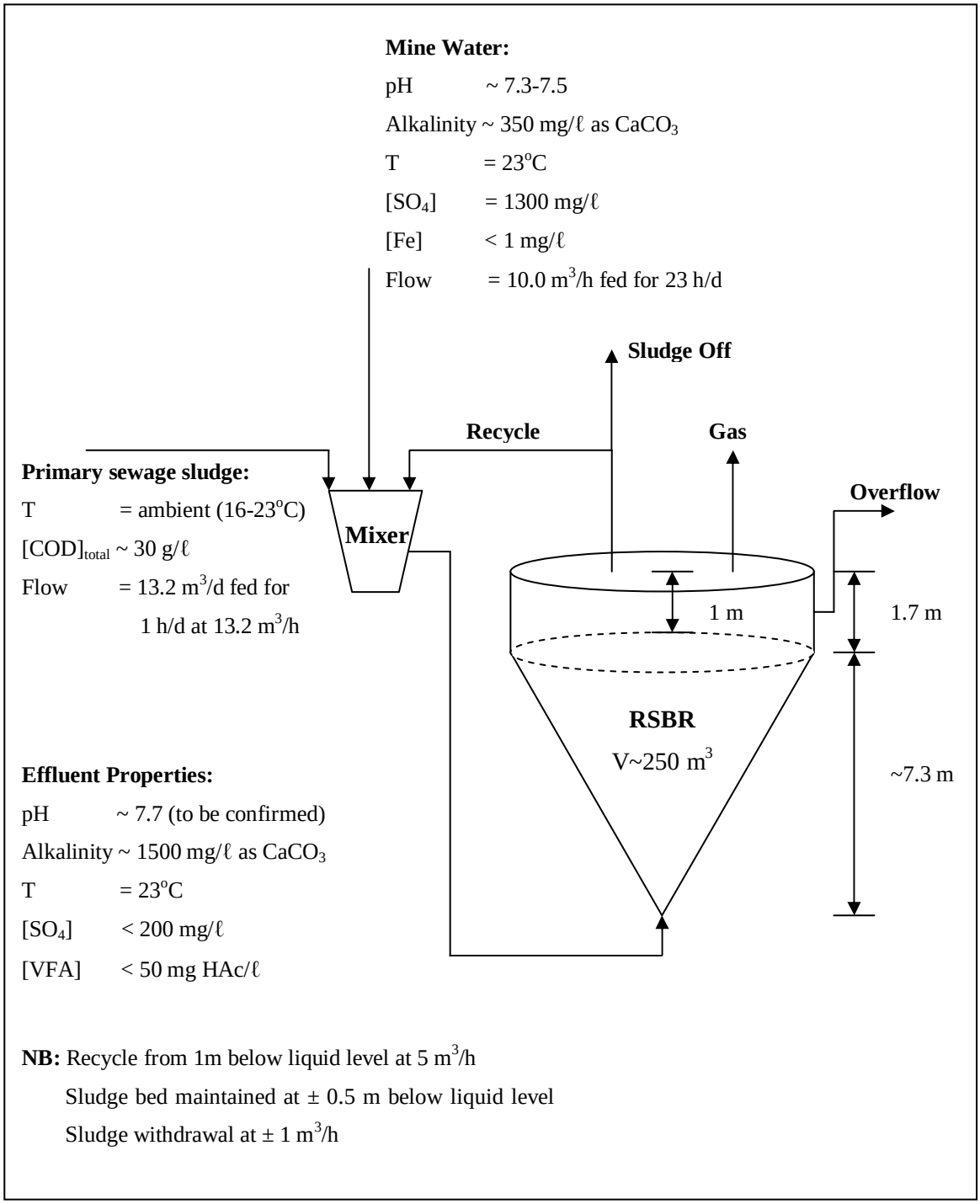

Figure 3-1: Revised design of the recycling sludge bed reactor (RSBR) showing its upflow anaerobic sludge blanket (UASB) configuration with recycle of clarified liquid and sludge wasting, and available operating data (Ristow, 2005)

CHAPTER 4

WEST®: A PLATFORM FOR MODELLING AND SIMULATION

4.1 Introduction to Modelling

Modelling is an important tool and forms an inherent part in the comprehensive study of microbial ecology, process design and the determination of optimal operating conditions in biological wastewater treatment plants. It allows the evaluation of key hypotheses and predicting the effects of a perturbation on the system without actually disturbing it. Attention is drawn to deficiencies in the conceptual structure by the comparison of simulated and experimental responses which allows potentially feasible solutions to be explored without pilot-scale or experimental studies, thereby aiding the selection of more promising ones for testing (Kalyuzhnyi, et al., 1998).

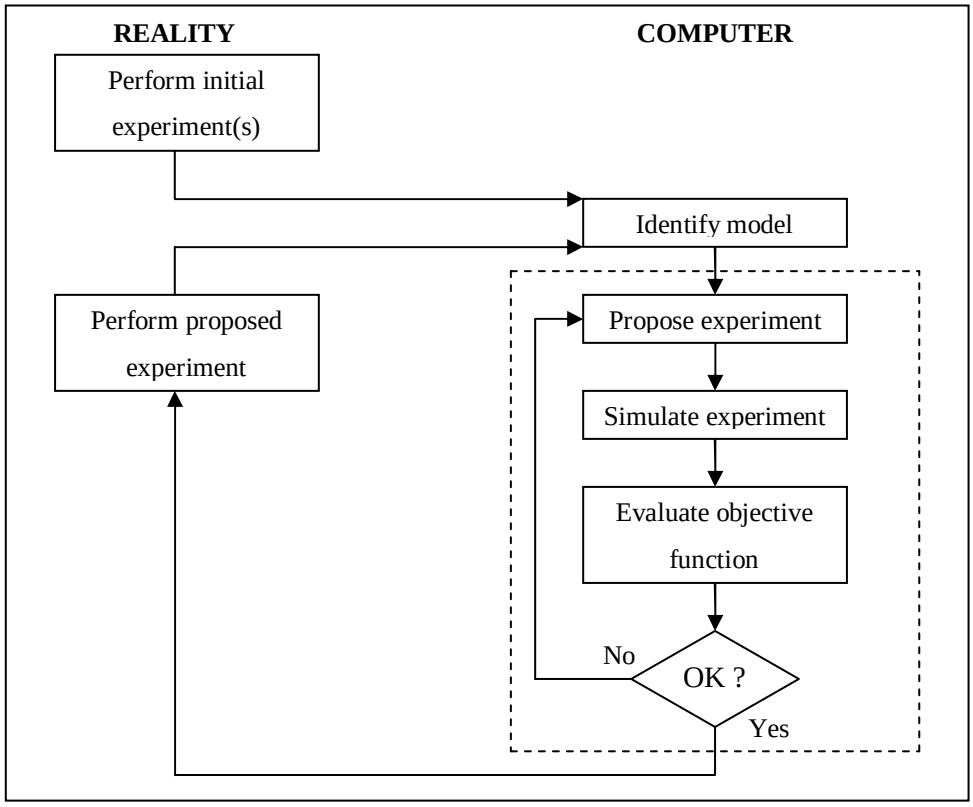

Figure 4-1: General procedure for optimal experimental design (From Dochain and Vanrolleghem, 2001)

The procedure for optimal experimental design with respect to a defined objective function, proposed by Dochain and Vanrolleghem (2001) and shown in Figure 4-1, can be implemented to calibrate an existing model on lab-scale and pilot-scale studies.

Prior to starting the experimental design, it is essential that a preliminary model is available, usually based on data that is available from the plant, laboratory investigations or a proper set of default values if no data is available. Simulated experiments are performed by the algorithm performing the design to measure the possible effect of proposed experimental conditions on the objective function. A non-linear optimisation algorithm is used to propose different experiments to find an optimal experiment or calibrated model that maximises the parameter estimation accuracy, which is then applied in reality to laboratory experiments, pilot-scale or a full-scale process.

4.2 The WEST® Modelling and Simulation Software

4.2.1 Introduction to WEST®

The ability to use empirical or mechanistic mathematical models is dependent on an efficient software tool to implement these models. The modelling and simulation package WEST® (**W**astewater Treatment Plant **E**ngine for **S**imulation and **T**raining) provides the modeller with a platform to use existing models or to implement and test new models. WEST® is a modelling environment that can be applied to any type of process that can be described as a structured collection of Differential Algebraic Equations (DAEs). WEST® was developed at BIOMATH, the Department of Applied Mathematics, Biometrics and Process Control of Ghent University in conjunction with HEMMIS, a Belgium based software company.

The methodology outlined in subsequent sections was used initially in the translation and coding of the basic UCTADM1 (without sulphate reduction) from AQUASIM to WEST®. This model was subsequently extended to incorporate the processes of biological sulphate reduction and used in the calibration of data sets from the UCT laboratory experiments and available operating data from the Rhodes BioSURE pilot plant's RSBR. This will be discussed further in successive chapters.

4.2.2 WEST® Software Architecture

The functional architecture of WEST® and the different steps that need to be followed to build a model and perform experiments with it, as explained by Vanhooren and co-workers (2003), is graphically represented in Figure 4-2.

The model base is the core of WEST® whereby models are described in MSL-USER (MSL stands for model specification language), a high level object-oriented declarative language specifically developed to incorporate models. Figure 4-3 represents a model base in the WEST® MSL Editor. The purpose of the model base is to maximise the reuse of existing knowledge such as mass balances, physical units, default parameter values and applicable ranges, and is therefore structured hierarchically.

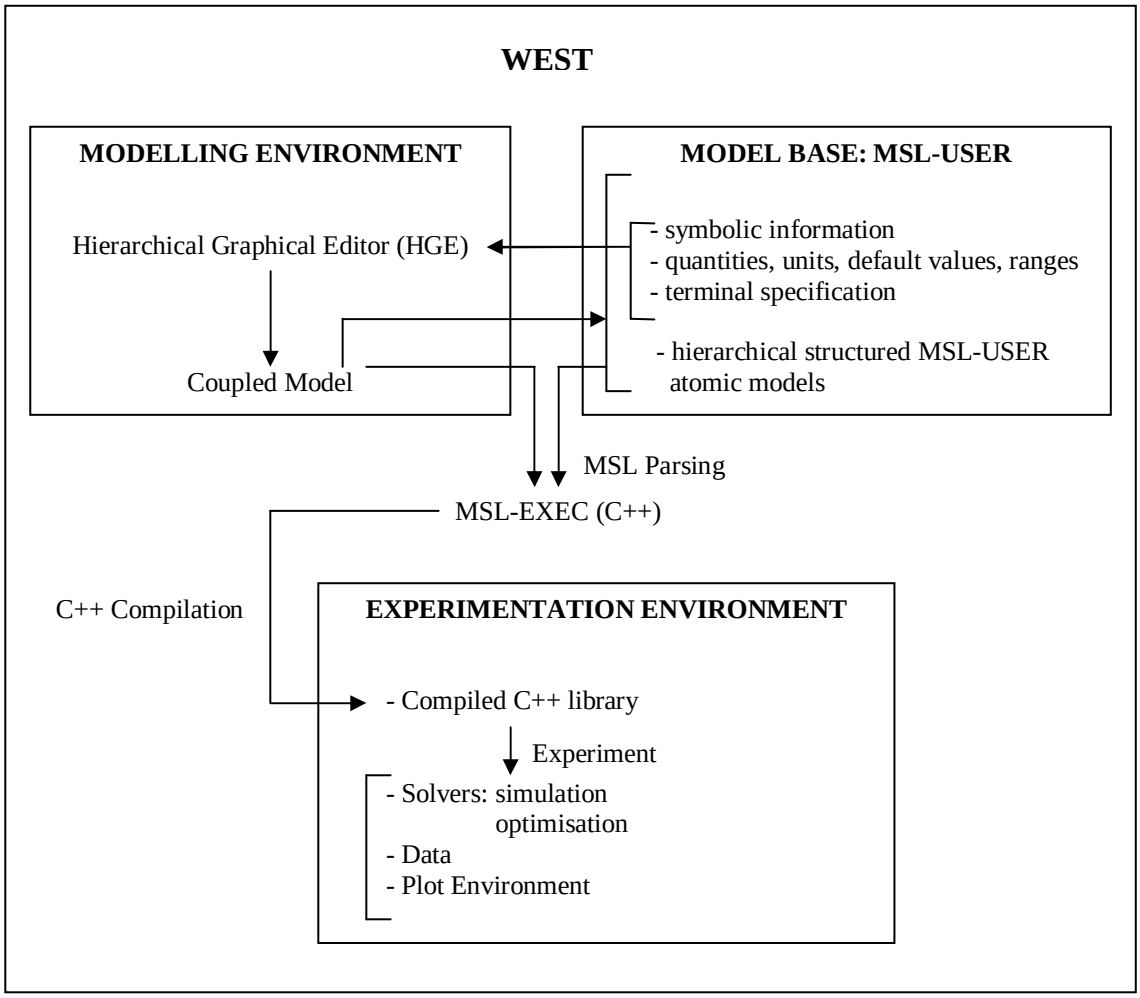

Figure 4-2: Functional architecture of WEST® (From Vanhooren et al., 2003)

This reusable knowledge is defined centrally and can be used by an expert to build new models. WEST® therefore has an open structure which allows the user to make changes to existing models and define new ones as required.

Once the modelling environment is started, the model base is loaded and all relevant information for the user is extracted from it. By using the symbolic information such as model structure and listings of parameters and variables in the model base, the 'atomic' models (Figure 4-3) available in the model base are linked to a graphical representation. A hierarchical

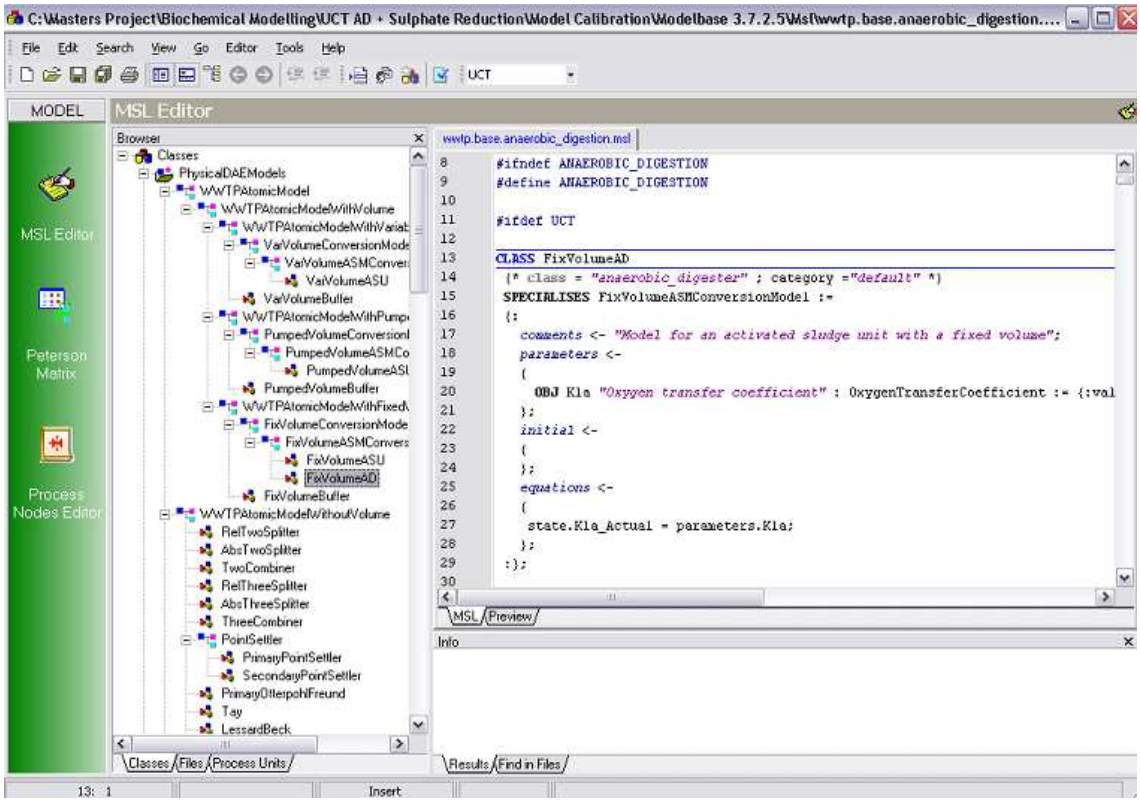

Figure 4-3: Representation of a model base in the WEST® MSL Editor

graphical editor (HGE) allows for an interactive composition of complex configurations from these graphical building blocks. An example of a HGE in the WEST® configuration builder is shown in Figure 4-4. Input and output terminals of the models are also extracted from the model base to decide whether or not two models can be linked together in the HGE.

Once a configuration is built, the HGE begins from the information extracted from the model base and creates and outputs a coupled model in MSL-USER, which is automatically added to the model base for further use in new modelling exercises.

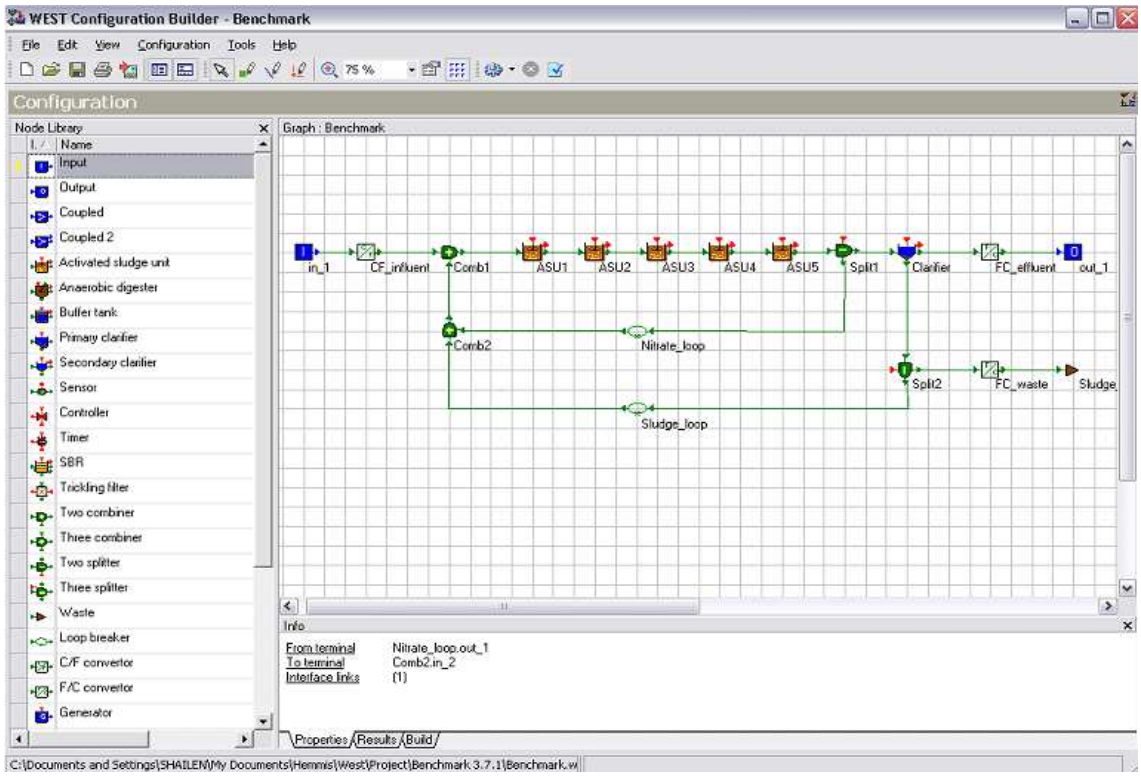

Figure 4-4: Depiction of a wastewater treatment plant model in the Hierarchical Graphical Editor (HGE) of the configuration builder

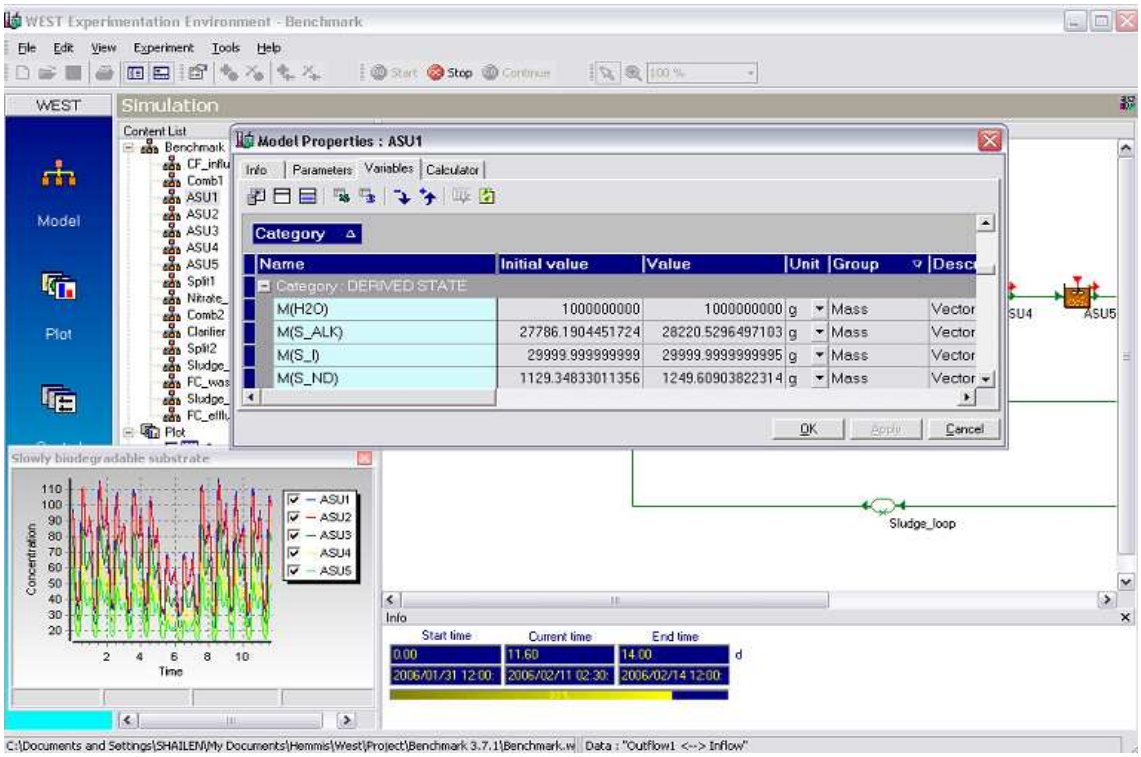

Figure 4-5: The WEST® experimentation environment, showing a plot and a variable listing

The model parser is used in the following step to generate low-level MSL-EXEC (C++) code, from the MSL-USER model and the atomic model representations in the model base. After the C++ compilation step, a model library is formed which can be used for execution within the experimentation environment (Figure 4-5).

The compiled model in the experimentation environment is loaded and symbolic information (model structures, listings of parameters and variables) is retrieved from the library. Once the model library is loaded, several virtual experiments can be performed. Experiment types include simulation, sensitivity analysis, scenario analysis, Monte-Carlo experiments, optimal experimental design and process optimisation (parameter estimation). Solvers within the experimentation environment are able to generate data that is used for plotting (as shown in Figure 4-5) and outputs to file.

4.2.3 Modelling Biochemical Conversion: The Petersen Matrix

Modelling of biochemical conversions in a wastewater treatment plant is essential to realistically and appropriately describe inter-component biochemical reactions, which represent the most important fundamental processes occurring within the system (Vanhooren, et al., 2003). Further, the model should quantify both the kinetics and the biochemical rate coefficients (stoichiometry) of each process. Process identification and the selection of appropriate kinetic and stoichiometric expressions for each process are the major conceptual tasks in the development of a mathematical conversion model.

The International Water Association task group (Batstone, et al., 2002, Henze, et al., 1987) chose the matrix format proposed by Petersen (1965) for representation of its models. Identification of relevant components in the model is the first step in developing the matrix, followed by the identification of biological process occurring within the system. The key features that constitute the Petersen matrix are shown in Table 4-1.

The dynamics of the i-th component in the matrix is shown by the following differential equation:

$$\forall\ Component: \quad \frac{d}{dt} C_i = \sum_{i=1}^{m} \upsilon_{i,j} . \rho_j \tag{4-1}$$

Table 4-1: Petersen matrix representation of biochemical rate coefficients $\upsilon_{i,j}$ and kinetic process rate equations ρ_j for components (i = 1-m, j = 1-n)

Component	**C_1**	**C_2**			**C_i**			**C_m**	**Rates**
Process 1	$\upsilon_{1,1}$	$\upsilon_{2,1}$			$\upsilon_{i,1}$				ρ_1
Process j					$\upsilon_{i,j}$				ρ_j
Process n								υ_{mn}	ρ_n

Once biological processes, model components, biochemical rate coefficients and kinetic process rates are implemented in the WEST® Petersen matrix of the model editor, the MSL-USER compiler generates the simulation code.

The matrix representation is not only limited to already built-in models such as ASM1 or ADM1, but allows the modeller to implement mass balance models himself using only the component vector, the reaction vector and the stoichiometric and kinetic coefficients that need to be specified, as in the case of the UCTADM1. The Petersen matrix or table format offers the best opportunity for overcoming the difficulty of tracing all the interactions of the system components, while conveying the maximum amount of information.

CHAPTER 5

MODEL FORMULATION AND DEVELOPMENT FOR SULPHATE REDUCTION

The formulation and development of a mathematical model for the biology of SRB was based on the method of approach discussed by Kalyuzhnyi et al., (1998). This model was integrated with the UCTADM1.

Since sulphate reduction was integrated with the existing UCTADM1, only three of the nine bacterial groups presented by Kalyuzhnyi et al. (1998) were of interest viz. acetogenic (propionate degrading) SRB, acetoclastic (acetate degrading) SRB and hydrogenotrophic (hydrogen degrading) SRB.

5.1 Stoichiometry

Researchers at the Water Research Group, UCT, used the general reaction sequence of Kalyuzhnyi et al., (1998), where the influent substrates were transformed by the different groups of SRB, and presented (on a molar basis) the derived stoichiometry in relation to the UCTADM1. This work (Ristow, et al., 2006) was submitted as part of a research report to the Water Research Commission for publication in 2006.

5.1.1 Acetogenic Sulphidogenesis

Kalyuzhnyi et al. (1998) presented the reaction sequence for producing acetate from propionate as follows:

$$CH_3CH_2COOH + \frac{3}{4}SO_4^{2-} + \frac{3}{2}H^+ \rightarrow CH_3COOH + \frac{3}{4}H_2S + CO_2 + H_2O \qquad (5\text{-}1)$$

Accepting an organism stoichiometric formulation of $C_5H_7O_2N$ (Sötemann, et al., 2005b) and assuming that the growth process of the SRB is identical to that of the biomass in the UCTADM1, the reaction for acetogenic bacteria is shown as follows:

$$3CH_3CH_2COOH + CO_2 + 2NH_4^+ \rightarrow 2C_5H_7O_2N + 4H_2O + H_2 + 2H^+ \qquad (5\text{-}2)$$

Multiplying Equation 5-2 by the anabolic yield (Y'_{ps}) of acetogenic bacteria and adding the associated Equation 5-1 to it:

$$\begin{aligned}&\left(1+3Y'_{ps}\right)CH_3CH_2COOH+\frac{3}{4}SO_4^{2-}+Y'_{ps}\,CO_2+2Y'_{ps}\,NH_4^{+}+\frac{3}{2}H^{+}\\&\rightarrow 2Y'_{ps}\,C_5H_7O_2N+CH_3COOH+\frac{3}{4}H_2S+CO_2+Y'_{ps}\,H_2+2Y'_{ps}\,H^{+}\\&+\left(1+4Y'_{ps}\right)H_2O\end{aligned}\qquad (5\text{-}3)$$

Dividing Equation 5-3 by $2Y'_{ps}$ for 1 mole biomass generation and simplifying:

$$\begin{aligned}&\left(\frac{1+3Y'_{ps}}{2Y'_{ps}}\right)CH_3CH_2COOH+\frac{3}{8Y'_{ps}}SO_4^{2-}+NH_4^{+}\rightarrow C_5H_7O_2N+\frac{1}{2Y'_{ps}}CH_3COOH\\&+\frac{3}{8Y'_{ps}}H_2S+\left(\frac{1}{2Y'_{ps}}-\frac{1}{2}\right)CO_2+\frac{1}{2}H_2+\left(1-\frac{3}{4Y'_{ps}}\right)H^{+}+\left(\frac{1+4Y'_{ps}}{2Y'_{ps}}\right)H_2O\end{aligned}\qquad (5\text{-}4)$$

The stoichiometry in terms of the anabolic organism yield Y'_{ps} for the growth process of acetogenic SRB is taken directly from Equation 5-4 and listed in Table 5-1. It must be noted that the anabolic organism yield Y'_{ps} is not the true yield as it excludes the catabolic propionate requirement of the organisms. The metabolic (anabolic + catabolic) yield is a true yield in terms of propionate utilisation and since it is more conventional to express yields as true yields, this approach is also adopted here. The metabolic yield is obtained from Equation 5-4.

Let Y_{ps} = metabolic yield.

1 mol biomass (160 g COD) grows from $\frac{1+3Y'_{ps}}{2Y'_{ps}}$ mol propionate. The true yield Y_{ps} (mol/mol) is expressed as:

$$Y_{ps}=\frac{2Y'_{ps}}{1+3Y'_{ps}}\qquad (5\text{-}5)$$

Making Y'_{ps} the subject of Equation 5-5:

$$Y'_{ps} = \frac{Y_{ps}}{2 - 3Y_{ps}} \tag{5-6}$$

Table 5-1: Stoichiometry for acetogenic SRB in terms of the anabolic organism yield

Component	Unit	Stoichiometric coefficient
HPr	mol	$-\left(\frac{1+3Y'_{ps}}{2Y'_{ps}}\right)$
SO_4^{2-}	mol	$-\left(\frac{3}{8Y'_{ps}}\right)$
H_2CO_3	mol	$\frac{1}{2Y'_{ps}} - \frac{1}{2}$
NH_4^+	mol	-1
Z_{ps}	mol	1
HAc	mol	$\frac{1}{2Y'_{ps}}$
H_2S	mol	$\frac{3}{8Y'_{ps}}$
H_2	mol	$\frac{1}{2}$
H^+	mol	$1 - \frac{3}{4Y'_{ps}}$
H_2O	mol	$\frac{1+4Y'_{ps}}{2Y'_{ps}}$

The negative terms are the reactants and the positive terms are the products of the biological process. This is also the case in Tables 5.2 to 5.6. Substituting Equation 5-6 into the stoichiometric terms shown in Table 5-1 results in the stoichiometry for acetogenic SRB in

terms of the true metabolic organism yield, shown in Table 5-2.

Table 5-2: Stoichiometry for acetogenic SRB in terms of the true organism yield

Component	Unit	Stoichiometric coefficient
HPr	mol	$-\left(\frac{1}{Y_{ps}}\right)$
SO_4^{2-}	mol	$-\left(\frac{3}{4Y_{ps}}-\frac{9}{8}\right)$
H_2CO_3	mol	$\frac{1}{Y_{ps}}-2$
NH_4^+	mol	-1
Z_{ps}	mol	1
HAc	mol	$\frac{1}{Y_{ps}}-\frac{3}{2}$
H_2S	mol	$\frac{3}{4Y_{ps}}-\frac{9}{8}$
H_2	mol	$\frac{1}{2}$
H^+	mol	$\frac{13}{4}-\frac{3}{2Y_{ps}}$
H_2O	mol	$\frac{1}{Y_{ps}}+\frac{1}{2}$

5.1.2 Acetoclastic Sulphidogenesis

The same methodology applied for acetogenic sulphidogenesis was used for the growth of acetoclastic SRB. The reaction sequence (Kalyuzhnyi, et al., 1998) for use of acetate as a substrate is as follows:

$$CH_3COOH + SO_4^{2-} + 2H^+ \rightarrow H_2S + 2CO_2 + 2H_2O \quad (5\text{-}7)$$

As for the growth of acetoclastic methanogens in the UCTADM1 (Sötemann, et al., 2005b), the reaction is as follows:

$$5CH_3COOH + 2NH_4^+ \rightarrow 2C_5H_7O_2N + 6H_2O + 2H^+ \quad (5\text{-}8)$$

Multiplying Equation 5-8 by the anabolic organism yield (Y'_{as}) and adding Equation 5-7 to Equation 5-8:

$$\begin{aligned}&\left(1+5Y'_{as}\right)CH_3COOH + SO_4^{2-} + 2Y'_{as}\,NH_4^+ + 2H^+ \\ &\rightarrow 2Y'_{as}\,C_5H_7O_2N + H_2S + 2CO_2 + 2Y'_{as}\,H^+ + \left(2+6Y'_{as}\right)H_2O\end{aligned} \quad (5\text{-}9)$$

Dividing Equation 5-9 by $2Y'_{as}$ and simplifying:

$$\begin{aligned}&\left(\frac{1+5Y'_{as}}{2Y'_{as}}\right)CH_3COOH + \frac{1}{2Y'_{as}}SO_4^{2-} + NH_4^+ \\ &\rightarrow C_5H_7O_2N + \frac{1}{2Y'_{as}}H_2S + \frac{1}{Y'_{as}}CO_2 + \left(1-\frac{1}{Y'_{as}}\right)H^+ + \left(\frac{1+3Y'_{as}}{Y'_{as}}\right)H_2O\end{aligned} \quad (5\text{-}10)$$

The stoichiometry in terms of the anabolic yield for the growth process of acetoclastic SRB is taken directly from Equation 5-10 and listed in Table 5-3.

Let Y_{as} = metabolic yield. Therefore:

$$Y_{as} = \frac{2Y'_{as}}{1+5Y'_{as}} \quad (5\text{-}11)$$

and

$$Y'_{as} = \frac{Y_{as}}{2-5Y_{as}} \quad (5\text{-}12)$$

Table 5-3: Stoichiometry for acetoclastic SRB in terms of the anabolic organism yield

Component	Unit	Stoichiometric coefficient
HAc	mol	$-\left(\frac{1+5Y'_{as}}{2Y'_{as}}\right)$
SO_4^{2-}	mol	$-\left(\frac{1}{2Y'_{as}}\right)$
NH_4^+	mol	-1
Z_{as}	mol	1
H_2S	mol	$\frac{1}{2Y'_{as}}$
H_2CO_3	mol	$\frac{1}{Y'_{as}}$
H^+	mol	$1-\frac{1}{Y'_{as}}$
H_2O	mol	$\frac{1+3Y'_{as}}{Y'_{as}}$

Substituting Equation 5-12 into the stoichiometry shown in Table 5-3 provides the stoichiometry for acetoclastic SRB in terms of the true (metabolic) yield, shown in Table 5-4.

Table 5-4: Stoichiometry for acetoclastic SRB in terms of the true organism yield

Component	Unit	Stoichiometric coefficient
HAc	mol	$-\left(\frac{1}{Y_{as}}\right)$
SO_4^{2-}	mol	$-\left(\frac{1}{Y_{as}}-\frac{5}{2}\right)$
NH_4^+	mol	-1
Z_{as}	mol	1
H_2S	mol	$\frac{1}{Y_{as}}-\frac{5}{2}$
H_2CO_3	mol	$\frac{2}{Y_{as}}-5$
H^+	mol	$6-\frac{2}{Y_{as}}$
H_2O	mol	$\frac{2}{Y_{as}}-2$

5.1.3 Hydrogenotrophic Sulphidogenesis

A similar approach was adopted for the growth of hydrogenotrophic sulphidogenesis as was for growth of acetogenic and acetoclastic sulphidogenesis. Kalyuzhnyi et al. (1998) proposed the sequence for use of hydrogen as a substrate:

$$4H_2 + SO_4^{2-} + 2H^+ \rightarrow H_2S + 4H_2O \qquad (5\text{-}13)$$

The growth of hydrogenotrophic methanogens is described in the UCTADM1 (Sötemann, et al., 2005b):

$$5CO_2 + 10H_2 + NH_4^+ \rightarrow C_5H_7O_2N + 8H_2O + H^+ \qquad (5\text{-}14)$$

Multiplying Equation 5-14 by the anabolic organism yield (Y'_{hs}) and adding Equation 5-13 to Equation 5-14:

$$\begin{aligned} &5Y'_{hs}\,CO_2 + \left(4+10Y'_{hs}\right)H_2 + SO_4^{2-} + Y'_{hs}\,NH_4^{+} + 2H^{+} \\ &\rightarrow Y'_{hs}\,C_5H_7O_2N + H_2S + Y'_{hs}\,H^{+} + \left(4+8Y'_{hs}\right)H_2O \end{aligned} \tag{5-15}$$

Dividing Equation 5-15 by $2Y'_{hs}$ and simplifying:

$$\begin{aligned} &5CO_2 + \left(\frac{4+10Y'_{hs}}{Y'_{hs}}\right)H_2 + \frac{1}{Y'_{hs}}SO_4^{2-} + NH_4^{+} \\ &\rightarrow C_5H_7O_2N + \frac{1}{Y'_{hs}}H_2S + \left(1-\frac{2}{Y'_{hs}}\right)H^{+} + \left(\frac{4+8Y'_{hs}}{Y'_{hs}}\right)H_2O \end{aligned} \tag{5-16}$$

The stoichiometry in terms of anabolic organism yield for the growth process of hydrogenotrophic SRB is taken directly from Equation 5-16 and listed in Table 5-5:

Table 5-5: Stoichiometry for hydrogenotrophic SRB in terms of anabolic yield

Component	Unit	Stoichiometric coefficient
H_2CO_3	mol	-5
H_2	mol	$-\left(\frac{4+10Y'_{hs}}{Y'_{hs}}\right)$
SO_4^{2-}	mol	$-\left(\frac{1}{Y'_{hs}}\right)$
NH_4^{+}	mol	-1
Z_{hs}	mol	1
H_2S	mol	$\frac{1}{Y'_{hs}}$
H^{+}	mol	$1-\frac{2}{Y'_{hs}}$
H_2O	mol	$\frac{4+8Y'_{hs}}{Y'_{hs}}$

Let Y_{hs} = metabolic yield. Therefore:

$$Y_{hs} = \frac{Y'_{hs}}{4 + 10Y'_{hs}} \tag{5-17}$$

and

$$Y'_{hs} = \frac{4Y_{hs}}{1 - 10Y_{hs}} \tag{5-18}$$

Substituting Equation 5-18 into the stoichiometry shown in Table 5-5 gives the stoichiometry for hydrogenotrophic SRB in terms of the true (metabolic) organism yield, shown in Table 5-6:

Table 5-6: Stoichiometry for hydrogenotrophic SRB in terms of the true organism yield

Component	Unit	Stoichiometric coefficient
H_2CO_3	mol	-5
H_2	mol	$-\left(\frac{1}{Y_{hs}}\right)$
SO_4^{2-}	mol	$-\left(\frac{1}{4Y_{hs}} - \frac{5}{2}\right)$
NH_4^+	mol	-1
Z_{hs}	mol	1
H_2S	mol	$\frac{1}{4Y_{hs}} - \frac{5}{2}$
H^+	mol	$6 - \frac{1}{2Y_{hs}}$
H_2O	mol	$\frac{1}{Y_{hs}} - 2$

5.2 Kinetic Process Rates

5.2.1 Growth

Bacterial growths of each sulphidogenic organism group were modelled using Monod kinetics with simultaneous inhibition by pH and undissociated sulphide. The undissociated sulphide inhibition was reported as first order for all bacterial groups. The principles of the kinetic description are taken from Kalyuzhnyi et al. (1998). Thus, a specific growth rate equation for SRB was expressed as:

$$\mu_j = \mu_{\max,j} \frac{[S_i] F(pH)}{K_{s,j} + [S_i]} \left[1 - \frac{H_2S_f}{Ki_j}\right] \left[\frac{\left[SO_4^{2-}\right]}{Kn + \left[SO_4^{2-}\right]}\right] \quad (5\text{-}19)$$

The method of approach used by Kalyuzhnyi et al. (1998) in defining the kinetic rates was the same as that used in the UCTADM1 (Sötemann, et al., 2005b). A decision was made to include total substrate concentrations with respect to propionate and acetate for the respective organism growth processes in the model. This decision was based on the fact that Sötemann et al. (2005b) obtained kinetic parameters from Sam-Soon et al. (1991) which were based on total substrate concentrations in mg COD/ℓ. The kinetic principles of the Kalyuzhnyi et al. (1998) model were adapted from the model of Kalyuzhnyi and Fedorovich (1998), which were also based on total substrate concentrations in g COD/ℓ, and therefore kinetic parameters were selected based on this. Total substrate concentrations for propionate and acetate, represented by the addition of the undissociated and dissociated forms, were included in the respective Monod growth process terms of acetogenesis, acetoclastic methanogenesis, acetogenic sulphidogenesis and acetoclastic sulphidogenesis in the UCTADM1.

A major mismatch between the two reaction schemes of Sötemann et al. (2005b) and Kalyuzhnyi et al. (1998) concerned the representation of pH and H_2S inhibition. The UCTADM1 did not consider H_2S inhibition, since H_2S is not present in the absence of sulphate reduction. The model proposed by Kalyuzhnyi et al. (1998) did not explicitly consider pH inhibition because it is difficult to distinguish between the effects of pH and H_2S inhibition experimentally. Sulphide is present in solution as H_2S and HS^-, and only the undissociated form appears to be toxic to the organisms. As the pH drops, HS^- is progressively converted to H_2S, and this occurs chiefly in the pH range where pH inhibition becomes significant. Hence the H_2S inhibition coefficients in the Kalyuzhnyi et al. (1998) model effectively contain the pH inhibition effect also. Hence it was decided to adopt a consistent set of inhibition terms

(Kalyuzhnyi, et al., 1998) applied to all the reactions including those in the UCTADM1, in the hope that they would reflect a proper balance between the two sets of biological reactions. The pH inhibition terms for the non-sulphidogenic reactions in the UCTADM1 were deactivated by setting the coefficients to very high values.

However, when this was implemented a problem was found with the form of the H_2S inhibition terms used by Kalyuzhnyi et al., (1998), represented by:

$$1-\frac{[H_2S]}{Ki} \tag{5-20}$$

When the H_2S concentration becomes higher than Ki (H_2S inhibition coefficient for a specific organism group), the inhibition term becomes negative, which causes the reaction to reverse. To overcome this problem, the form of the inhibition term was changed to:

$$\exp\left(-\left(\frac{[H_2S]}{0.6065Ki}\right)^2\right) \tag{5-21}$$

The factor 0.6065 was chosen to get the two forms to match at the 50 % inhibition point using the same value of Ki, as illustrated in Figure 5-1. The form of the sulphide inhibition term presented in Equation 5-21 was also added to the existing specific growth rate equations for acidogenic, acetogenic and methanogenic bacterial groups in the UCTADM1.

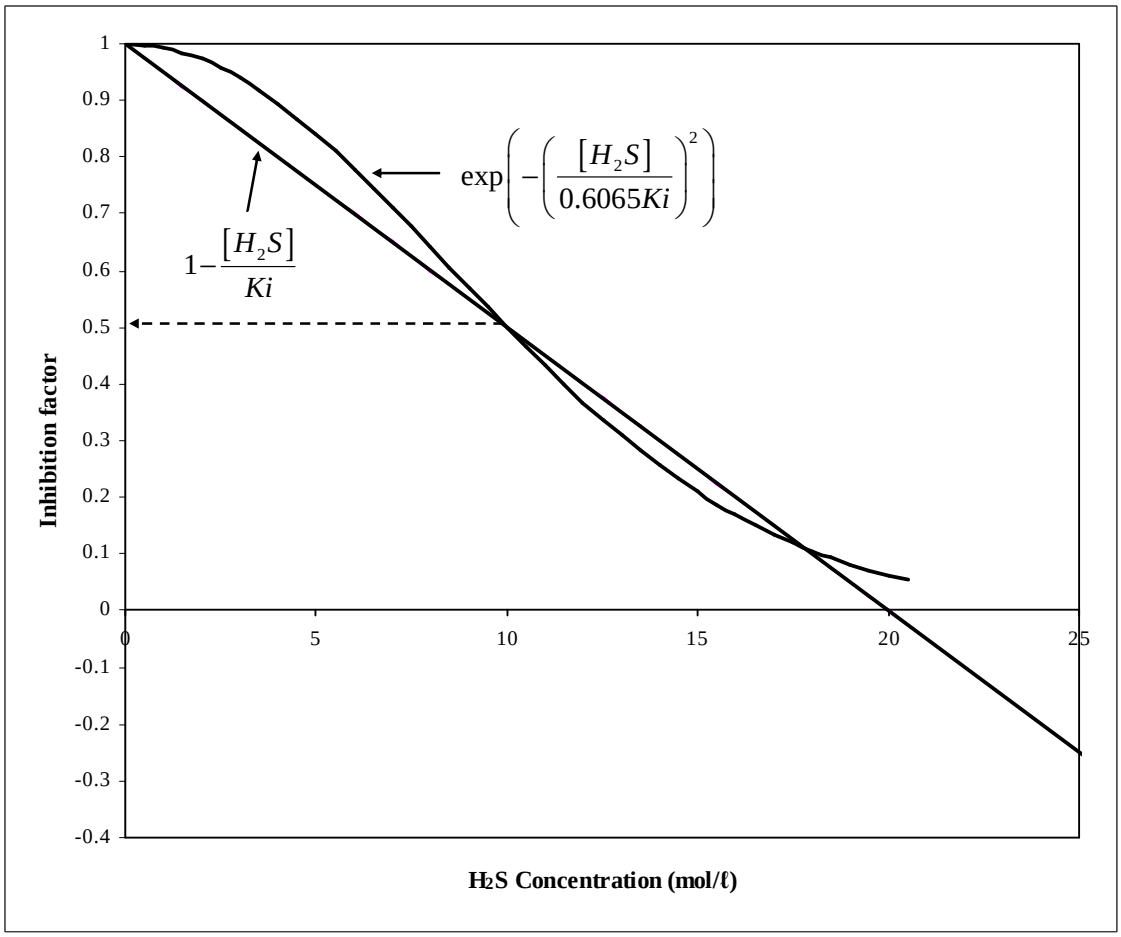

Figure 5-1: Comparison of inhibition factor forms

5.2.1.1 Acetogenic SRB

The specific growth rate of the acetogenic sulphidogenic organisms, including the revised form of the sulphide inhibition term in { } is given as follows:

$$r_{Z_{ps}} = \frac{\mu_{\max,ps}\left(\left[H\,\mathrm{Pr}\right]+\left[\mathrm{Pr}^-\right]\right)}{K_{S,ps}+\left(\left[H\,\mathrm{Pr}\right]+\left[\mathrm{Pr}^-\right]\right)}\left\{\exp\left(-\left(\frac{[H_2S]}{0.6065Ki_{ps}}\right)^2\right)\right\}\left(\frac{\left[SO_4^{2-}\right]}{Kn_{ps}+\left[SO_4^{2-}\right]}\right)\left[Z_{ps}\right] \quad (5\text{-}22)$$

where:

$\mu_{max,ps}$ = maximum specific growth rate constant for acetogenic sulphidogens (d^{-1})

$K_{S,ps}$ = half saturation concentration for acetogenic sulphidogen growth on propionic acid (mol/ℓ)

$Ki_{,ps}$ = inhibition constant i.e. the hydrogen sulphide concentration at which the growth of acetogenic sulphidogens is half the maximum rate (mol/ℓ)

$Kn_{,ps}$ = half saturation concentration for acetogenic sulphidogen growth on sulphate (mol /ℓ)

[HPr] = undissociated propionate concentration (mol/ℓ)

$[Pr^-]$ = dissociated propionate concentration (mol/ℓ)

$[SO_4^{2-}]$ = total sulphate concentration (mol/ℓ)

$[Z_{ps}]$ = acetogenic sulphidogen organism concentration (mol/ℓ)

5.2.1.2 Acetoclastic SRB

The equation for the specific growth rate of acetoclastic SRB includes a term for sulphide inhibition in { } and is given by:

$$r_{Z_{as}} = \frac{\mu_{\max,as}\left(\left[HAc\right]+\left[Ac^-\right]\right)}{K_{S,as}+\left(\left[HAc\right]+\left[Ac^-\right]\right)}\left\{\exp\left(-\left(\frac{\left[H_2S\right]}{0.6065Ki_{as}}\right)^2\right)\right\}\left(\frac{\left[SO_4^{2-}\right]}{Kn_{as}+\left[SO_4^{2-}\right]}\right)\left[Z_{as}\right] \quad (5\text{-}23)$$

where:

$\mu_{max,as}$ = maximum specific growth rate constant for acetoclastic sulphidogens (d^{-1})

$K_{S,as}$ = half saturation concentration for acetoclastic sulphidogen growth on acetic acid (mol /ℓ)

$Ki_{,as}$ = inhibition constant i.e. the hydrogen sulphide concentration at which the growth of acetoclastic sulphidogens is half the maximum rate (mol/ℓ)

$Kn_{,as}$ = half saturation concentration for acetoclastic sulphidogen growth on sulphate (mol /ℓ)

[HAc] = undissociated acetate concentration (mol/ℓ)

$[Ac^-]$ = dissociated acetate concentration (mol/ℓ)

$[Z_{as}]$ = acetoclastic sulphidogen organism concentration (mol/ℓ)

5.2.1.3 Hydrogenotrophic SRB

The specific growth rate for hydrogenotrophic sulphidogens is similar to that of acetogenic and acetoclastic SRB, as follows:

$$r_{Z_{hs}} = \frac{\mu_{\max,hs}\left[H_2\right]}{K_{S,hs}+\left[H_2\right]}\left\{\exp\left(-\left(\frac{\left[H_2S\right]}{0.6065Ki_{hs}}\right)^2\right)\right\}\left(\frac{\left[SO_4^{2-}\right]}{Kn_{hs}+\left[SO_4^{2-}\right]}\right)\left[Z_{hs}\right] \quad (5\text{-}24)$$

where:

$\mu_{max,hs}$ = maximum specific growth rate constant for hydrogenotrophic sulphidogens (d^{-1})

$K_{S,hs}$ = half saturation concentration for hydrogenotrophic sulphidogen growth on acetic acid (mol/ℓ)

$Ki_{,hs}$ = inhibition constant i.e. the hydrogen sulphide concentration at which the growth of hydrogenotrophic sulphidogens is half the maximum rate (mol/ℓ)

$Kn_{,hs}$ = half saturation concentration for hydrogenotrophic sulphidogen growth on sulphate (mol/ℓ)

$[H_2]$ = hydrogen concentration (mol/ℓ)

$[Z_{hs}]$ = hydrogenotrophic sulphidogen organism concentration (mol/ℓ)

5.2.2 Endogenous Decay

The endogenous decay or death of organisms is described in Kalyuzhnyi et al. (1998) by first order kinetics. Bacterial decay in the UCTADM1 is also described by first order kinetics, hence this approach is used here.

5.2.2.1 Acetogenic SRB

The specific rate equation for the decay of acetogenic SRB is expressed by first order kinetics according to:

$$r_{Z_{ps}} = b_{ps}\left[Z_{ps}\right] \tag{5-25}$$

where:

b_{ps} = specific decay constant for acetogenic sulphidogens (d^{-1})

$[Z_{ps}]$ = acetogenic sulphidogen organism concentration (mol/ℓ)

5.2.2.2 Acetoclastic SRB

The endogenous decay of acetoclastic sulphidogens is represented with the following specific rate equation:

$$r_{Z_{as}} = b_{as}\left[Z_{as}\right] \tag{5-26}$$

where:

b_{as} = specific decay constant for acetoclastic sulphidogens (d^{-1})

$[Z_{as}]$ = acetoclastic sulphidogen organism concentration (mol/ℓ)

5.2.2.3 Hydrogenotrophic SRB

The specific decay rate for hydrogenotrophic sulphidogens is similar to that of acetogenic and acetoclastic SRB, as follows:

$$r_{Z_{hs}} = b_{hs}\left[Z_{hs}\right] \tag{5-27}$$

where:

b_{hs} = specific decay constant for hydrogenotrophic sulphidogens (d^{-1})

$[Z_{hs}]$ = hydrogenotrophic sulphidogen organism concentration (mol/ℓ)

5.2.3 Chemical Equilibrium Processes

It was essential that chemical equilibrium processes for biological sulphate reduction be integrated with the biomass population biology and the UCTADM1. This involved the addition of a further two equilibrium dissociation processes with respect to sulphide. The specific rate constant for the forward dissociation reactions for each sulphidogenic equilibrium process was calculated from the reverse dissociation constant. Due to the values of the reverse dissociation constant not being available in the literature, they were determined for each process by using the calculator function in WEST®. These values may be found in Table A-8, Appendix A. All thermodynamic data was obtained from Stumm and Morgan (1996).

5.2.3.1 Dissociation of Hydrogen Sulphide

The ionic equilibrium reaction for the dissociation of hydrogen sulphide can be shown as follows:

$$H_2S \leftrightarrow H^+ + HS^- \tag{5-28}$$

The forward dissociation reaction is given by:

$$Forward\ dissociation\left(H_2S\right) = Kf_{HS}\left[H_2S\right] \tag{5-29}$$

and the reverse dissociation reaction is expressed as:

$$\text{Re}verse\ dissociation\left(H_2S\right) = Kr_{HS}\left[HS^-\right]\left[H^+\right] \tag{5-30}$$

with

$$Kf_{HS} = Kr_{HS}\frac{10^{-pK_{HS}}}{f_m{}^2} \tag{5-31}$$

where:

Kf_{HS} = forward dissociation constant for H_2S (mol/ℓ)

Kr_{HS} = reverse dissociation constant for H_2S (mol/ℓ)

$[H_2S]$ = undissociated hydrogen sulphide concentration (mol/ℓ)

$[HS^-]$ = dissociated hydrogen sulphide concentration (mol/ℓ)

$[H^+]$ = hydrogen ion concentration (mol/ℓ)

pK_{HS} = pK constant for the dissociation of H_2S

f_m = monovalent activity coefficient

The standard enthalpy equation for the effect of temperature on the equilibrium constant is given by Smith et al. (1996), as follows:

$$\frac{d\ln K}{dT} = \frac{\Delta H^o}{RT^2} \tag{5-32}$$

T = temperature in Kelvin (K)

K = equilibrium constant at 298.15 K

ΔH^o = heat of reaction at 298.15 K

R = universal gas constant (kJ/mol.K)

Thermodynamic data:

Heats of formation (at a temperature of 298.15 K):

H_2S = -39.75 kJ/mol

H^+ = 0

HS^- = -17.6 kJ/mol

Universal gas constant

R = 8.314 E-03 kJ/mol.K

Equilibrium constant (at a temperature of 298.15 K)

K = 9.77 E-08

Integrating Equation 5-32 and including the above thermodynamic data with a conversion factor from ln K to $\log_{10}$K:

$$\log_{10} K = \frac{-1.1568E+03}{T} - 3.1301 \tag{5-33}$$

From the definition of pK = - $\log_{10}$K, therefore:

$$pK_{HS} = \frac{1.1568E+03}{T} + 3.1301 \tag{5-34}$$

5.2.3.2 Dissociation of Bisulphide

The method of approach is similar to that used for the dissociation of H_2S. The ionic equilibrium reaction for the dissociation of bisulphide ion can be shown as follows:

$$HS^- \leftrightarrow H^+ + S^{2-} \tag{5-35}$$

The forward dissociation reaction is given by:

$$Forward\ dissociation\left(HS^-\right) = Kf_S\left[HS^-\right] \tag{5-36}$$

and the reverse dissociation reaction is expressed as:

$$\mathrm{Re}verse\ dissociation\left(HS^-\right) = Kr_S\left[S^{2-}\right]\left[H^+\right] \tag{5-37}$$

with

$$Kf_S = Kr_S \frac{10^{-pK_S}}{f_d} \tag{5-38}$$

where:

Kf_S = forward dissociation constant for HS^- (mol/ℓ)

Kr_S = reverse dissociation constant for HS^- (mol/ℓ)

$[HS^-]$ = dissociated hydrogen sulphide concentration (mol/ℓ)

$[S^{2-}]$ = elemental sulphur concentration (mol/ℓ)

$[H^+]$ = hydrogen ion concentration (mol/ℓ)

pK_S = pK constant for the dissociation of HS^-

f_d = divalent activity coefficient

Thermodynamic data:

Heats of formation (at a temperature of 298.15 K):

HS^- = -17.6 kJ/mol

H^+ = 0

S^{2-} = 33 kJ/mol

Universal gas constant

R = 8.314 E-03 kJ/mol.K

Equilibrium constant (at a temperature of 298.15 K)

K = 1 E-19

The standard enthalpy equation (Smith, et al., 1996) was again used, and by integrating Equation 5-32 and including the above thermodynamic data with a conversion factor from ln K to $\log_{10}$K:

$$\log_{10} K = \frac{-2.6427E+03}{T} - 10.1363 \tag{5-39}$$

From the definition of pK = - $\log_{10}$K, therefore:

$$pK_S = \frac{2.6427E+03}{T} + 10.1363 \tag{5-40}$$

5.2.4 Gas Exchange Processes

The physical processes for hydrogen sulphide gas exchange with the atmosphere were included. Similarly to CO_2 in the UCTADM1 by Sötemann et al. (2005b), H_2S was also modelled with both expulsion and dissolution. The equilibrium reaction of H_2S gas exchange between the solution and the atmosphere is given as follows:

$$H_2S_{(aq)} \leftrightarrow H_2S_{(g)} \tag{5-41}$$

The dissolution of H_2S is shown by the following equation:

$$Dissolution\left(H_2S\right) = Kr_{H_2S}.pH_2S.KH_{H_2S} \tag{5-42}$$

and the expulsion of H_2S is expressed as:

$$Expulsion\left(H_2S\right) = Kr_{H_2S}\left[H_2S_{(aq)}\right] \tag{5-43}$$

with

$$KH_{H_2S} = 10^{-pK_{H_2S}} \tag{5-44}$$

where:

Kr_{H2S} = reverse dissociation constant for H_2S expulsion

pH_2S = $H_2S_{(g)}$ partial pressure

KH_{H2S} = Henry's Law constant for H_2S

$[H_2S_{(aq)}]$ = aqueous hydrogen sulphide concentration (mol/ℓ)

$[H_2S_{(g)}]$ = gaseous hydrogen sulphide concentration (mol/ℓ)

pKH_{H2S} = pK constant for the dissolution of H_2S

Thermodynamic data:

Heats of formation (at a temperature of 298.15 K):

$H_2S_{(aq)}$ = -39.75 kJ/mol

$H_2S_{(g)}$ = -20.63 kJ/mol

Universal gas constant

R = 8.314 E-03 kJ/mol.K

Equilibrium constant (at a temperature of 298.15 K)

K = 1.05 E-01

Integrating Equation 5-32 and including the above thermodynamic data with a conversion factor from ln K to $\log_{10}$K:

$$\log_{10} K = \frac{-9.9858E+02}{T} + 2.3705 \tag{5-45}$$

From the definition of pK = - $\log_{10}$K, therefore:

$$pK_S = \frac{9.9858E+02}{T} - 2.3705 \tag{5-46}$$

5.3 Model Kinetic Parameters

Sötemann et al. (2005b) obtained kinetic constants (on a molar basis at 37 ^{o}C) from Sam-Soon et al. (1991) for the calibration and validation of the UCTADM1 excluding sulphate reduction. The hydrolysis kinetic parameters were obtained by calibration (refer Table 2-3, Chapter 2). Kalyuzhnyi et al. (1998) proposed a complete set of kinetic parameters (on a mass basis at 30 ^{o}C) for the anaerobic digestion of soluble organic wastewater containing sulphate (refer Table 2-4, Chapter 2). Both sets of kinetic parameters by Sam-Soon et al. (1991) and Kalyuzhnyi et al. (1998) were based on mathematical models developed for upflow anaerobic sludge blanket (UASB) type bioreactors. The above-mentioned kinetic parameter sets needed to be converted to a common set of units.

The kinetic constants by Sötemann et al. (2005b) and Kalyuzhnyi et al. (1998) are given for laboratory temperatures of 37 ^{o}C and 30 ^{o}C respectively, while the operating temperature of the six digesters used by Ristow et al. (2005) in the UCT experimental investigation of PSS hydrolysis and the pilot RSBR were 35 ^{o}C and 23 ^{o}C respectively. The half saturation constant is not strongly dependent on temperature whereas the yield coefficient is slightly dependent on temperature, but this effect can be regarded as negligible. The maximum specific growth rates and specific decay rates are dependent on temperature. To account for a temperature variation when comparing the laboratory operating temperatures of Sötemann et al. and (2005b) Kalyuzhnyi et al. (1998) to that of Ristow et al. (2005) and the pilot plant, a temperature correction factor was needed, which would preserve the relative relationship between all the rate coefficients. To estimate the factor, it was noted that the ADM1 task team (Batstone, et al., 2002) concluded that changes in the rate of hydrolysis could be described by a rate equation in the form of:

$$\frac{K_2}{K_1} = e^{\tau(T_2 - T_1)} \tag{5-47}$$

where:

K_2/K_1 = temperature correction factor

T_1 = target operating temperature (^{o}C)

T_2 = current operating temperature (^{o}C)

τ = 0.0667 calculated from data at 35 ^{o}C and 25 ^{o}C (Gujer and Zehnder, 1983)

The set of kinetic constants from Sötemann et al. (2005b) were presented on a molar basis. However, the surface mediated reaction kinetics that were accepted by Sötemann et al. (2005b) for incorporation into the UCTADM1 needed to be converted from mole units to mass COD units to be integrated with the current representation of biodegradable particulate COD (S_{bp}). The maximum specific growth rate and specific decay rate constants were multiplied by equation 5-47 to represent the interaction of the respective organism groups at a desired operating temperature. Table 5-7 shows the set of kinetic parameters by Sötemann et al. (2005b) that will be investigated further for calibration of the UCTADM1 with sulphate reduction.

Table 5-7: Kinetic and stoichiometric constants of Sötemann et al. (2005b) at 35 °C and 23 °C

Organism Group	μ_{max} 35 °C (d^{-1})	μ_{max} 23 °C (d^{-1})	K_s (mol/ℓ)	Y (mol org/mol substrate)	b 35 °C (d^{-1})	b 23 °C (d^{-1})
Z_{ai}	0.700	0.314	7.80E-04	0.107	0.036	0.016
Z_{ae}	1.006	0.452	8.90E-05	0.028	0.013	0.006
Z_{am}	3.842	1.726	1.30E-05	0.016	0.032	0.015
Z_{hm}	1.050	0.472	1.56E-04	0.004	0.009	0.004
Hydrogen inhibition coefficient for high pH_2 (mol H_2/ℓ):					6.25E-4	
Surface mediated reaction (Contois): $k_{max,HYD}$ (g COD S_{bp}/mol Z_{ai}.d)					769	
			$K_{SS,HYD}$ (g COD S_{bp}/mol Z_{ai})		1225	

The kinetic parameters used in the mathematical model developed by Kalyuzhnyi et al. (1998) were specified on a mass basis. The units of these constants need to be converted from mass units to mole units prior to the processes of sulphate reduction being integrated with the UCTADM1. Conversion factors (Table 5-8) together with molecular weights were used in obtaining kinetic constants on a molar basis.

Table 5-8: Conversion factors used in the model

Component	Conversion factor	Unit
Glucose ($C_6H_{12}O_6$)	192	g COD/mol
Propionate (CH_3CH_2COOH)	112	g COD/mol
Acetate (CH_3COOH)	64	g COD/mol
Hydrogen (H_2)	16	g COD/mol
Sulphur (S^{2-})	32	g S/mol
Sulphate (SO_4^{2-})	96	g/mol

As performed for the kinetic parameter set of Sötemann et al. (2005b), the maximum specific growth rate and specific decay rate constants were multiplied by the temperature correction factor of Equation 5-47.

Table 5-9 lists the kinetic parameters (on a molar basis) of Kalyuzhnyi et al. (1998), where the growth and decay rate constants have been corrected to operating temperatures of 35 ^{o}C and 23 ^{o}C for the reactors used in the UCT experimental investigation of PSS hydrolysis, and the pilot RSBR respectively. The other kinetic parameters apply to both operating temperatures.

It was decided to investigate both sets of kinetic parameters i.e. from Sötemann et al. (2005b) and Kalyuzhnyi et al. (1998) for the modelling of bioreactors used in the UCT experimental investigation as well as the pilot RSBR, and to ascertain the compatibility of these constants with respect to the above-mentioned systems. The complete set of kinetic parameters by Kalyuzhnyi et al. (1998) would first be applied to each of the systems, and if unsuccessful, a combination of both sets will thereafter be implemented.

Table 5-9: Kinetic parameters of Kalyuzhnyi et al. (1998) on a molar basis at 35 ^{o}C and 23 ^{o}C

Organism Group	**μ_{max} 35 ^{o}C (d^{-1})**	**μ_{max} 23 ^{o}C (d^{-1})**	**K_s (mol/ℓ)**	**K_n (mol/ℓ)**	**K_i (mol/ℓ)**	**Y (mol org/ mol substrate)**	**b 35 ^{o}C (d^{-1})**	**b 23 ^{o}C (d^{-1})**
Z_{ai}	5.583	2.508	1.46E-04	-	1.72E-02	0.058	0.126	0.056
Z_{ae}	0.223	0.100	2.21E-03	-	5.94E-03	0.016	0.020	0.009
Z_{ps}	0.814	0.366	2.63E-03	7.71E-05	5.78E-03	0.027	0.026	0.012
Z_{am}	0.369	0.166	1.88E-03	-	5.78E-03	0.012	0.028	0.013
Z_{as}	0.854	0.384	3.75E-04	2.00E-04	5.13E-03	0.019	0.038	0.017
Z_{hm}	1.396	0.627	7.50E-06	-	5.16E-03	0.002	0.056	0.025
Z_{hs}	3.908	1.755	4.38E-06	2.00E-04	1.72E-02	0.007	0.084	0.038

5.4 Conversion of Model Units

The UCTADM1 including sulphate reduction is represented by units on a molar basis. However the WEST® modelling and simulation platform is based on SI mass units which would result in confusion when interpreting units when working with the software program. It was therefore decided to standardise units for each component in the UCTADM1 by converting molar concentration units (in mol/ℓ) to mass concentration units (in g/m^3). This was achieved by multiplying the stoichiometric coefficients of each compound in the Petersen matrix by their respective molecular weights as well as the volume conversion from litre to cubic metre. Process rate equations were also adjusted accordingly to incorporate this conversion.

The Petersen matrix representation of the UCTADM1 including sulphate reduction, which has been implemented in WEST®, can be viewed in Tables A-3 to A-6, Appendix A. Tables A-7, A-8 and A-9 include the kinetic process rate equations, parameters and variables used in the model respectively.

CHAPTER 6

METHODOLOGY ADOPTED IN WEST® IMPLEMENTATION OF THE MODEL

The mathematical model and calculation algorithms, formulated and developed in Chapter 5 for biological sulphate reduction, were integrated with the UCTADM1 of Sötemann et al. (2005b) resulting in a model that is able to represent the biology of acidogenic, methanogenic and sulphate reducing bacteria as well as their respective biological processes. This chapter outlines the method of approach adopted in characterising available influent data as well as the implementation of experimental and pilot plant systems thereby rendering it suitable for modelling within the WEST® simulation environment.

6.1 Development of an Influent Characterisation Method

The accurate characterisation of the influent or feed to any biological system, be it in reality through experiments or via modelling and simulation, is vital in attaining a better understanding of biological processes, interaction between organisms, and the subsequent end-result of a given system under investigation.

In the case of the UCTADM1, the characterisation of PSS into its constituent fractions forms the basis of specifying the various sewage sludge organic compounds in addition to inorganic compounds as input to the model. Thus quantifying and specifying the influent sludge organic fractions together with inorganic compounds are essential both in model calibration and simulation. In UCTADM1, the weak acid/base chemistry is integrated with the biological and physical processes, and the individual weak acid/base species specified as compounds in the model. This requires that the influent weak acid/bases are speciated according to the influent pH and total species concentrations. This section explains the basis of the characterisation structure that was developed to use available influent data from both the UCT experimental investigation and the pilot RSBR to specify the input (in flux units of g/d) to WEST®, hence enabling the effective simulation of these systems. The characterisation procedure was performed externally to the WEST® simulation platform. It must be noted that the phosphate system was not considered in the model due to the unavailability of important influent information regarding the characterisation into its constituent components, such as the compositions of the biodegradable particulate and unbiodegradable particulate fractions of the feed COD and the unknown

phosphorous content of PSS.

6.1.1 COD

The PSS total influent COD (S_{ti}) consists of a biodegradable particulate fraction (S_{bpi}), unbiodegradable particulate fraction (S_{upi}), biodegradable soluble fraction in the form of glucose (S_{bsi}), unbiodegradable soluble fraction (S_{usi}), and volatile fatty acids (S_{VFAi}). The total COD balance for the feed is given in units of mg COD/ℓ by:

$$S_{ti} = S_{bpi} + S_{upi} + S_{bsi} + S_{usi} + S_{VFAi} \tag{6-1}$$

and the total soluble influent COD (S_{si}) in mg COD/ℓ is given by:

$$S_{si} = S_{bsi} + S_{usi} + S_{VFAi} \tag{6-2}$$

Ristow et al. (2005) made the assumption that the unbiodegradable particulate COD fraction forms 33.45 % of the total COD. Furthermore, an assumption was made that the biodegradable soluble COD fraction is equivalent to that of volatile fatty acids. The unbiodegradable COD fractions remain the same through the system i.e. effluent concentration is same as the influent concentration. Using Equation 6-1 and Equation 6-2 as well as taking into consideration the above-mentioned assumptions, the various COD fractions can be determined by the following equations:

$$S_{upi} = 0.3345 \times S_{ti} \tag{6-3}$$

$$S_{usi} = S_{us}\left(Effluent\right) \tag{6-4}$$

$$S_{bsi} = S_{VFAi} = \frac{\left(S_{si} - S_{usi}\right)}{2} \tag{6-5}$$

$$S_{bpi} = S_{ti} - S_{bsi} - S_{VFAi} - S_{usi} - S_{upi} \tag{6-6}$$

Multiplying by the flowrate in the reactor, all COD fractions were converted from concentration units of mg COD/ℓ to flux units of g COD/d, with the exception of S_{bsi}, which was converted to

flux units of g/d, by additionally dividing by the assumed COD/Glucose ratio.

6.1.2 pH

The calculation of the hydrogen and hydroxyl ion feed flux was based on the influent pH to the reactor. From the definition of pH:

$$pH = -\log_{10}\left[H^+\right] \tag{6-7}$$

therefore the molar concentration of H^+ and OH^- can be calculated respectively as follows:

$$\left[H^+\right] = 10^{-(pH)} \tag{6-8}$$

$$\left[OH^-\right] = 10^{-(14-pH)} \tag{6-9}$$

The molar concentrations (mol/ℓ) were converted to flux units (g/d) by multiplying with the reactor flowrate (ℓ /d) and their respective molecular weights (g/mol).

6.1.3 Volatile Fatty Acids

The compounds that form the VFA component of PSS are the undissociated and dissociated forms of propionate and acetate. These compounds can be fractioned from the above-mentioned VFA component of influent COD (S_{VFAi}) as illustrated in Figure 6-1, where:

S_{VFAi}	=	volatile fatty acid component of influent COD (mg COD/ℓ) (from above)
in_f_HAc	=	fraction total VFA that is acetate
Ac_{tot}	=	acetate system (HAc + Ac^-) total concentration (mol/ℓ)
Pr_{tot}	=	propionate system (HPr + Pr^-) total concentration (mol/ℓ)
ThOD HAc	=	theoretical oxygen demand for acetic acid (g COD/mol)
ThOD HPr	=	theoretical oxygen demand for propionic acid (g COD/mol)
K_a	=	equilibrium constant for dissociation acetic acid at 25 ^oC
K_p	=	equilibrium constant for dissociation of propionic acid at 25 ^oC
$[H^+]$	=	Influent hydrogen ion molar concentration (mol/ℓ) (from above)

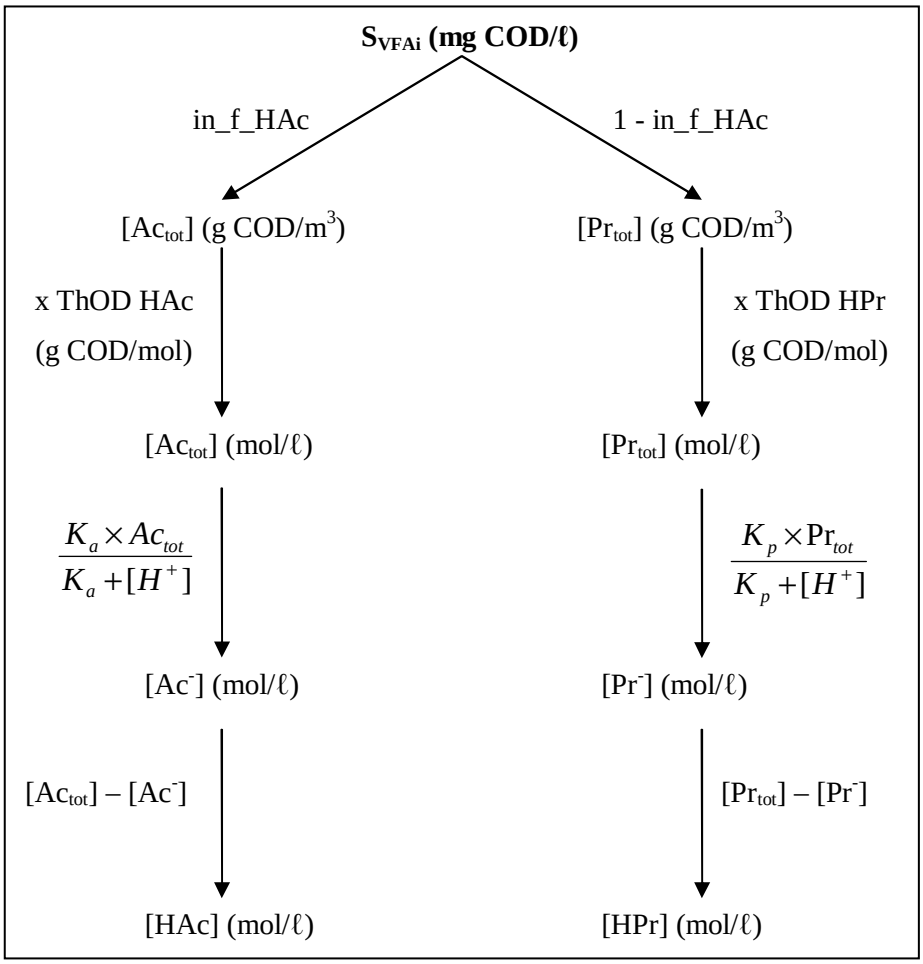

Figure 6-1: Method of approach in fractioning the VFA component of the influent COD into the undissociated and dissociated forms of acetate and propionate

The molar concentrations of the undissociated and dissociated forms of acetate and propionate were converted to flux units by multiplying with the reactor flowrate and their respective molecular weights.

6.1.4 Free and Saline Ammonia

The calculation of ammonia and the ammonium ion influx was based on the influent FSA concentration (mg N/ℓ) together with the ammonium ion equilibrium constant. The calculation of the influent ammonia and ammonium ion concentrations on a molar basis are given by the following equations respectively:

$$[NH_3] = \frac{K_n \times \left(\frac{FSA}{AW_N \times 1000} \right)}{K_n \times [H^+]} \quad (6\text{-}10)$$

$$[NH_4^+] = \frac{[NH_3] \times [H^+]}{K_n} \quad (6\text{-}11)$$

where:

K_n = equilibrium constant for dissociation ammonium ion at 25 ^oC

FSA = influent FSA concentration expressed as nitrogen (mg N/ ℓ)

AW_N = atomic weight of nitrogen (g/mol)

$[H^+]$ = influent hydrogen ion molar concentration (mol/ℓ) (from above)

The reactor flowrate together with the molecular weights of NH_3 and NH_4^+ were used to convert molar concentrations to fluxes.

6.1.5 Alkalinity

The influx of components belonging to the carbonate system was determined from the influent alkalinity (mg/ℓ as $CaCO_3$) and the equilibrium constants of this system. The molar concentrations of CO_3^{2-}, HCO_3^- and H_2CO_3 are calculated from the influent alkalinity and carbonate equilibrium constants by following equations respectively:

$$[CO_3^{2-}] = \frac{\left(\frac{Alkalinity}{MW_{CaCO_3} \times 1000} \times 2 \right) + [H^+] - [OH^-]}{2 + \left(\frac{[H^+]}{K_{c2}} \right)} \quad (6\text{-}12)$$

$$[HCO_3^-] = \frac{[CO_3^{2-}] \times [H^+]}{K_{c2}} \quad (6\text{-}13)$$

$$[H_2CO_3] = \frac{[HCO_3^-] \times [H^+]}{K_{c1}} \quad (6\text{-}14)$$

where:

Alkalinity = influent alkalinity expressed in mg/ℓ as $CaCO_3$

MW_{CaCO3} = molecular weight of calcium carbonate (g/mol)

$[H^+]$ = influent hydrogen ion molar concentration (mol/ℓ) (from above)

$[OH^-]$ = influent hydroxyl ion molar concentration (mol/ℓ) (from above)

K_{c1} = equilibrium constant for dissociation of carbonic acid at 25 ^oC

K_{c2} = equilibrium constant for dissociation of bicarbonate at 25 ^oC

The molar concentrations of CO_3^{2-}, HCO_3^- and H_2CO_3 were converted to flux units by multiplying with the reactor flowrate and their respective molecular weights.

6.1.6 Sulphate

The available influent sulphate concentration in mass units of mg/ℓ did not require much manipulation in determining its influx value. This concentration was simply multiplied with the reactor flowrate in ℓ/d to obtain the influent flux in g/d.

6.1.7 Influent Data

The characterisation structure developed here was used in the manipulation of available influent data from Ristow et al. (2005) and Ristow (2005) to specify input fluxes for subsequent simulation of UCT laboratory experiments and the pilot plant RSBR respectively in WEST®. The equilibrium constants used the characterisation methodology were obtained from Stumm and Morgan (1996) and are listed in Table 6-1.

Table 6-1: Equilibrium constants at 25 ^oC at infinite dilution used to characterise the influent of various systems

(Stumm and Morgan, 1996)

Symbol	Value	Description
K_a	1.75E-05	equilibrium constant for dissociation acetic acid
K_p	1.32E-05	equilibrium constant for dissociation of propionic acid
K_n	5.60E-10	equilibrium constant for dissociation ammonium ion
K_{c1}	4.35E-07	equilibrium constant for dissociation of carbonic acid
K_{c2}	4.69E-11	equilibrium constant for dissociation of bicarbonate

6.2 WEST® Implementation of UCT Laboratory Experiments

The experimental data used in the model were obtained from Ristow et al. (2005), who investigated the hydrolysis of PSS under methanogenic, acidogenic and sulphidogenic conditions, carried out in completely mixed reactors at 35 ^{o}C. Acidogenic or acid forming systems were not considered in model calibration as this would merely simulate the build up of excess VFAs, a drastic decrease in pH, and result in subsequent digester failure.

Ristow et al. (2005) collected, prepared and analysed a series of feed batches that were used during the steady state operating periods of methanogenic, acidogenic and sulphate reducing systems. The pH and alkalinity of these feed batches that were used in the feed characterisation procedure are reported in Table B-1, Appendix B. The measured and calculated values of the various fractions of the feed COD, pH, alkalinity, FSA, sulphate (where applicable) and the digester operating conditions for each steady state laboratory experiment were obtained from Ristow et al. (2005) for the characterisation of the influent and subsequent simulation in WEST®. The influent characterisation procedure was performed externally to the simulation software according to the procedure outlined in Section 6.1.

PSS seldom remain in their original state and undergo hydrolysis and acidogenesis within the primary settling tank, and in transport and storage for laboratory investigations (Sötemann, et al., 2005b). Further, this results in the production of VFAs which has a significant influence on the prediction of pH when simulating anaerobic digesters, since the uptake of dissociated VFA generates significant alkalinity. This production of VFA is reflected in the S_{VFAi} fraction of the feed. Ristow et al. (2005) made that assumption above that the S_{VFAi} fraction is equivalent to the S_{bsi} fraction of influent COD. However this is not certain and since equality of S_{bsfi} and S_{VFAi} was not directly measured for all the feed batches, this assumption was evaluated. The steady state model of Sötemann et al. (2005a) was used to regress data from each steady state experiment of Ristow et al. (2005), thereby predicting the influent COD that is VFA. This was achieved by specifying a feed input of S_{ti}, S_{VFAi}, pH, alkalinity, FSA, S_{upi} fraction, relative proportions of carbon, hydrogen, oxygen and nitrogen in PSS; and together with flow variables and effluent data of S_t, FSA, alkalinity and pH; the model was used to minimise the sum of squared errors of effluent alkalinity, FSA and CO_2 partial pressure to predict a value of S_{VFAi}. The values of S_{VFAi} obtained were significantly higher than that predicted by Ristow et al. (2005), particularly for steady state experiments supplied with influent from feed batch number F12. However, with the exception of a few steady state experiments (steady state numbers 7, 8, 10 and 11) fed with influent from feed batch number F13, the remaining steady state S_{VFAi} experimental values remained unchanged. All S_{VFAi} was assumed to be acetate. A summary

of the characterised influent used as input for simulation in WEST® for each steady state experiment is shown in Table B-2 to Table B-4, Appendix B.

The experimental setup was modelled in WEST® using the UCTADM1 which is symbolically represented by an anaerobic digester icon together with an input and output node representing the interface of the model and contain the characteristics of the feed and of the treated water respectively (refer to Figure 6-1).

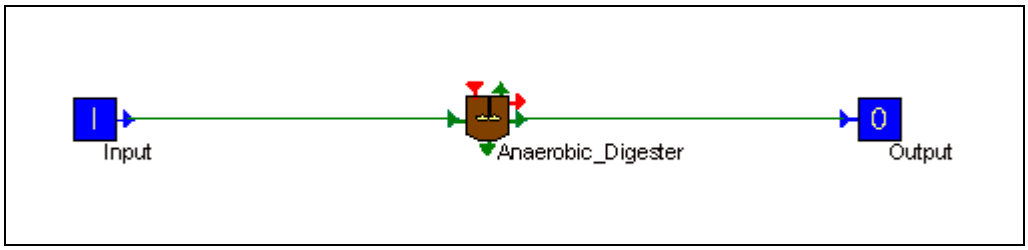

Figure 6-1: Configuration of the UCT experimental system in WEST®

The kinetic parameters used in the model were not derived from the UCT laboratory experiments, but were independent and obtained from Sötemann et al. (2005b) and Kalyuzhnyi et al. (1998), refer to Section 2.2.9, Chapter 2. It is therefore imperative to select a set of kinetic constants accurately predict the behaviour of these experimental systems. The single, complete set of kinetic parameters from Kalyuzhnyi et al. (1998) was initially selected for the simulation of experimental data sets. Hydrolysis kinetic parameters were obtained from Sötemann et al. (2005b). However, upon preliminary simulations, it was observed that simulation of experimental systems showed a negative response to these kinetic parameters i.e. death of organisms and no degradation of influent COD even if hydrolysis kinetic constants were manipulated. It was subsequently decided to use a combination of kinetic parameters from Sötemann et al. (2005b) and Kalyuzhnyi et al. (1998). In addition to hydrolysis kinetic parameters, kinetic and stoichiometric constants for the four anaerobic digestion organism groups of acidogens, acetogens, acetoclastic methanogens and hydrogenotrophic methanogens were obtained from Sötemann et al. (2005b) as per Table 5-7, Chapter 5. The remaining kinetic parameters for acetogenic, acetoclastic and hydrogenotrophic SRB were acquired from Kalyuzhnyi et al. (1998) according to Table 5-9, Chapter 5. Merging these two sets of kinetic parameters proved positive and considering that no kinetic parameters, other than that of hydrolysis (refer to Section 7.3, Chapter 7) were calibrated, the simulation results (discussed in Sections 7.1 and 7.2, Chapter 7) of methanogenic and sulphidogenic systems, with exception of desired sulphate removal efficiencies, fitted well to the experimental data. The complete set of kinetic parameters, except for those of hydrolysis, used in application of the model to

methanogenic and sulphidogenic experimental data sets at 35 ^{o}C is shown in Table 6-2.

Table 6-2: Kinetic parameters used in modelling experimental data sets at 35 ^{o}C

Organism Group	μ_{max} (d^{-1})	K_s (mol/ℓ)	K_n (mol/ℓ)	K_i (mol/ℓ)	Y (mol org/mol substrate)	b (d^{-1})
Z_{ai}	0.700	7.80E-04	-	1.72E-02	0.107	0.036
Z_{ae}	1.001	8.90E-05	-	5.94E-03	0.028	0.013
Z_{ps}	0.814	2.63E-03	7.71E-05	5.78E-03	0.027	0.026
Z_{am}	3.842	1.30E-05	-	5.78E-03	0.016	0.032
Z_{as}	0.854	3.75E-04	2.00E-04	5.13E-03	0.019	0.038
Z_{hm}	1.050	1.56E-04	-	5.16E-03	0.004	0.009
Z_{hs}	3.908	4.38E-06	2.00E-04	1.72E-02	0.007	0.084

Simulation of steady state sulphidogenic systems were conducted in anaerobic digesters under sulphate reducing conditions, where they were operated with excess sulphate. Comparison of sulphate reducing systems to other sulphate reducing systems and to the corresponding methanogenic system was made possible with the change of a single parameter between respective systems within the model. It was not possible to induce unstable methanogenic operation and washing out of methanogens by progressively reducing retention times in the digester during simulation, thereby demonstrating the absence of methanogenic organisms for all systems other than steady state number 6 (where all organism groups were present) as undertaken by Ristow et al. (2005). The initial masses for respective organism groups for the simulation of all sulphidogenic systems were assumed to be equivalent i.e. $Z_{ae} = Z_{ps}$, $Z_{am} = Z_{as}$ and $Z_{hm} = Z_{hs}$.

Variables were included in the model to allow a direct comparison of the WEST® output data with the effluent experimental data for the purpose of validation. These additional terms may be found in Table A-9, Appendix A.

6.3 WEST® Implementation of the Pilot Plant RSBR

Available pilot plant data that was obtained from Ristow (2005), and presented in Figure 3-1, Chapter 3, was used to simulate the configuration of the RSBR in WEST®. Other than temperatures and flowrates, only the total COD for the PSS stream; and the pH, alkalinity and sulphate concentration of the mine water stream are known. The total COD of 30 g/ℓ was fractionated into its various components by using steady state experimental data as a guideline in terms of the average fraction that each component forms of the total COD. The remainder of the feed characteristics had to be constructed from judicious assumptions.

Insufficient feed data was available to predict the fraction of VFA in the feed COD using the steady state model of Sötemann et al. (2005a). It was therefore decided to revert to the assumption made by Ristow et al. (2005) that the S_{VFAi} fraction is equivalent to the S_{bsi} fraction of influent COD. All S_{VFAi} was again assumed as being acetate only. PSS was obtained directly from ERWAT without being stored prior to feeding, and therefore a pH value of 7 was estimated for PSS in its pristine state. An FSA value of 39 mg N/ℓ was taken from the measured data of steady state number 1 above, which has a feed COD of PSS closest to that of the pilot plant. Influent alkalinity of this stream was assumed to be 300 mg/ℓ as $CaCO_3$ to correspond to some extent to an influent pH of 7 for PSS. The mine water feed stream to the pilot plant would only represent the concentration of sulphate, together with pH and alkalinity. Influent sulphate concentration of 1300 mg/ℓ, a pH value of 7 and an alkalinity of 350 mg/ℓ as $CaCO_3$ were obtained from available influent data in Figure 3-1, Chapter 3. The characterisation method was again performed externally to the simulation software according to the method outlined in Section 6.1. Refer to Table B-5, Appendix B, for the summarised influent characterisation of the PSS and mine water feed streams to the RSBR that was used as input for simulation in WEST®.

The pilot plant configuration of the RSBR was modelled and represented by using various symbolic icons (refer to Figure 6-2). The core of the model configuration is an anaerobic digester which includes the UCTADM1. Two input nodes contain the characteristics of the PSS and mine water feed, and three outlets of gas, overflow and recycle streams represent the reactor effluent. Two additional parameters were created to represent the fraction of the feed flow that is recycled and the ratio of particulate concentration in the overflow to particulate concentration in the reactor. The recycle ratio was set to 50 % and the latter concentration ratio was set to a very low value of 0.0001 to allow the overflow effluent stream to be practically free of solids. The RSBR was modelled such that only the gaseous components of methane, carbon dioxide and hydrogen sulphide exit only through the gas stream. The recycle stream is mediated by

a splitter which removes or wastes 1 m^3/d of sludge via the "sludge off" node. A loop breaker is used to prevent the formation of an algebraic loop during simulation. The recycle stream is mixed with the influent PSS and mine water which is then fed to the anaerobic digester. The pilot plant was simulated for a period of 365 days which allowed steady state operation to be observed.

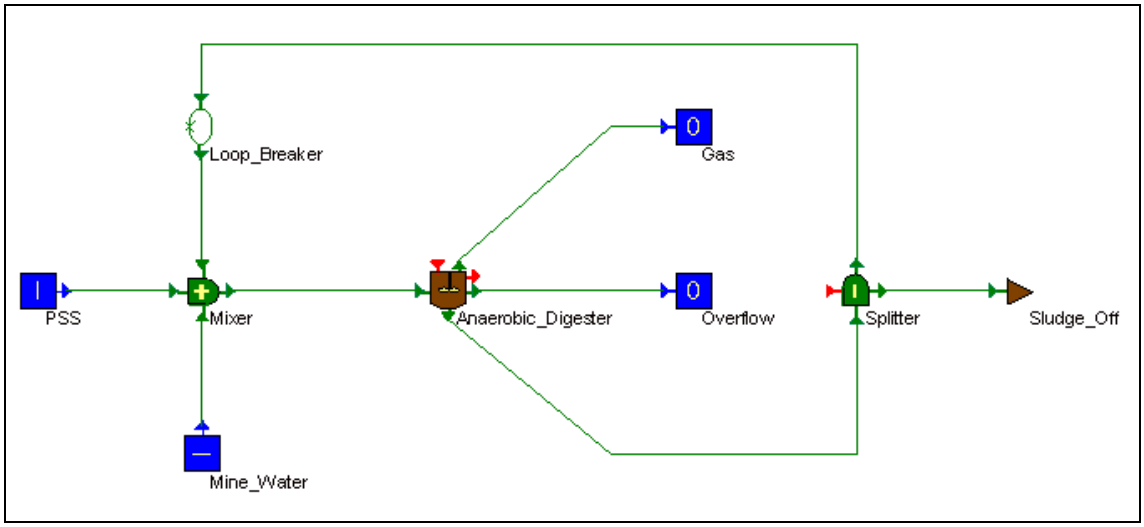

Figure 6-2: Configuration of the pilot plant RSBR model in WEST®

The RSBR operating conditions of the pilot plant were very different from those prevailing for all the UCT experiments. The pilot plant was operated at an ambient temperature of 23 ^oC as compared to that of 35 ^oC for the laboratory experiments. As in the case of laboratory experiments above, the complete set of kinetic parameters from Kalyuzhnyi et al. (1998) was initially selected for the simulation of experimental data sets with hydrolysis kinetic parameters from Sötemann et al. (2005b). However, upon preliminary simulations, it was observed that the experimental systems showed a negative response to these kinetic parameters i.e. death of organisms and no degradation of influent COD. A combination of kinetic parameters from Sötemann et al. (2005b) and Kalyuzhnyi et al. (1998) corrected to 23 ^oC was subsequently used as per Tables 5-7 and 5-9 in Chapter 5. Merging these two sets of kinetic parameters with no manipulation of kinetic parameters proved positive. Model outputs (to be discussed in Section 8.1, Chapter 8) with exception of desired sulphate removal efficiencies fitted fairly well to available pilot plant data. The complete set of kinetic parameters used in the model with available pilot plant data of the RSBR at 23 ^oC is listed in Table 6-3.

Table 6-3: Kinetic parameters used in modelling the pilot plant RSBR at 23 ^{o}C

Organism Group	μ_{max} (d^{-1})	K_s (mol/ℓ)	K_n (mol/ℓ)	K_i (mol/ℓ)	Y (mol org/mol substrate)	b (d^{-1})
Z_{ai}	0.314	7.80E-04	-	1.72E-02	0.107	0.016
Z_{ae}	0.452	8.90E-05	-	5.94E-03	0.028	0.006
Z_{ps}	0.366	2.63E-03	7.71E-05	5.78E-03	0.027	0.012
Z_{am}	1.726	1.30E-05	-	5.78E-03	0.016	0.015
Z_{as}	0.384	3.75E-04	2.00E-04	5.13E-03	0.019	0.017
Z_{hm}	0.472	1.56E-04	-	5.16E-03	0.004	0.004
Z_{hs}	1.755	4.38E-06	2.00E-04	1.72E-02	0.0071	0.038

6.4 Model Verification

An important asset in modelling is model verification which proves that the model conforms to 100% COD, C, H, O, N and S mass balances. Performing a continuity check through calculation of a series of continuity equations is a valuable tool for model verification. These equations are the mathematical equivalent of the principle that in chemical reactions, elements, theoretical oxygen demand and net electrical charges may neither be formed nor destroyed. The continuity check determines whether the result of the equation is equal to zero or not. If the result is different from zero the element is either formed or destroyed in the biological system.

A continuity check was performed on model influent and effluent flux data. A single methanogenic system (Steady State Number 1) and a sulphidogenic system (Steady State Number 6) were used to perform a continuity check on and hence verify the model. With the exception of COD, the Ristow et al., (2005) influent and effluent experimental data proved insufficient in performing a continuity check as per to the method adopted in the model. The results of the continuity check in flux (g/d) and percentage error between influent and effluent data for both model systems are tabulated in Table 6-4.

Table 6-4: Model continuity check results for Steady States 1 and 6

	Steady State Number 1		Steady State Number 6	
	(g/d)	**% Error**	**(g/d)**	**% Error**
COD	10.46	15.44	9.91	14.63
C	3.26	14.37	3.26	14.36
H	0.21	0.12	0.22	0.12
O	-0.54	-0.04	-0.50	-0.03
N	0.27	20.60	0.27	20.59
S	0	0	0	0

As is evident from Table 6-4, only the sulphur balance reflects full closure with the largest margin of error observed for COD, C and N. The margin of error in methanogenic and sulphidogenic models is very similar to one another. This trend was also observed when the continuity check was performed upon the initial translation of the UCTADM1 (without sulphate reduction) from AQUASIM to WEST® with margins of error very similar in both software platforms to that observed in Steady States 1 and 6. A COD conversion of 110.30 % was calculated from available Ristow, et al. (2005) data (feed COD, effluent COD and methane gas production) for Steady State Number 1 as compared to the 84.56 % conversion calculated in the model continuity check (Table 6-4). No mass balances were performed for sulphate-reducing systems by Ristow, et al (2005), however a COD conversion of 98.10 % was calculated for Steady State Number 6 based on the best available data (feed COD, effluent COD, methane gas production and effluent sulphide) as compared to 85.37 % calculated in the model continuity check (Table 6-4). Ristow, et al. (2005) indicates that 90 – 110 % COD recovery falls within the acceptable range for particulate fed systems and confirms that the methods used to analyse the various parameters are accurate and consistent.

Lower conversions of COD, C and N within the model may indicate that there is an error in the derivation of the model and hence in the reaction stoichiometry of the Petersen matrix with the probability of inheriting the mass balance error from the AQUASIM model stoichiometry during coding into WEST®. Upon investigating the detail of the continuity check, it became obvious that the discrepancy in COD could be attributed to the biodegradable particulate COD

producing inadequate amounts of methane, carbon dioxide and biomass. Further, the N:C balance discrepancy is approximately the same as N:C balance in biodegradable particulate COD. This again could be attributed to inaccurate reaction stoichiometry in the production of methane, carbon dioxide and biomass.

Upon further manipulation of the model to allow stoichiometric coefficients to be visible which were previously hidden by default in the simulation output, it was discovered that WEST® incorrectly computed a single stoichiometric coefficient viz. 'EndogenousProt'. This term was programmed as a variable within the software to simplify the stoichiometry of certain reactions. The 'EndogenousProt' coefficient was calculated from 'HydrolysisProt' which was also programmed into the model as a variable. The software accepts the computation of 'HydrolysisProt', but incorrectly calculates that of 'EndogenousProt' and carries the error through the simulation. Both coefficients were subsequently re-programmed as parameters within Petersen Matrix, MSL code re-generated, model re-configured and a new model experimentation environment created. Considering that the model baseline data was the same as the previous one, the continuity check with respective input and output fluxes resulted in a margin of error that was 5 % when compared to the previous WEST® and AQUASIM models for which mass balances did not close.

In summary, it can be concluded that the major portion of mass balance errors can be attributed to incorrect reaction stoichiometry that was inherited via the translation of the AQUASIM model into WEST® with a minor portion due to inconsistencies in computation of reaction stoichiometry within the WEST® software.

CHAPTER 7

RESULTS AND DISCUSSION OF MODELLING EXPERIMENTAL SYSTEMS

This chapter summarises simulation results from application of the extended UCTADM1 in WEST® to experimental data sets from the UCT laboratory investigation of PSS hydrolysis. Model predictions are discussed by comparison to that of respective steady state methanogenic and sulphidogenic steady experimental data. Model kinetic parameters that are most sensitive are selected for optimisation and calibration. It must be noted that the experimental data was not collected specifically for the purpose of this modelling exercise, but is sufficiently well defined for model application and hence validation.

Detailed data regarding the simulation of respective steady state experimental systems are listed in Appendix C, where model outputs are compared to measured data with relative errors calculated between each other. Simulated profiles of certain effluent variables from WEST® are also shown for each steady state system.

7.1 Methanogenic Systems

The steady states measured for varying hydraulic retention times and feed COD concentrations under stable methanogenic operation listed in Table 3-1, Chapter 3, were simulated in WEST®. The results include total and soluble COD concentrations, pH, VFA, alkalinity, FSA, TKN methane production and methane composition. The summary of results for the steady state simulation of methanogenic systems including the model variables are presented in Table 7-1. Influent total and soluble COD concentrations for steady states 1 - 8, 10 and 11 have been adjusted to include the additional influent fraction of S_{VFAi} (as discussed in Section 6.2, Chapter 6).

Table 7-1: Summary of results from the simulation of each steady state methanogenic system

		INFLUENT			EFFLUENT								
Steady State Number	**Reactor Volume (ℓ)**	**Retention Time (d)**	**Total COD (S_{ti}) (mg COD/ℓ)**	**Soluble COD (S_{si}) (mg COD/ℓ)**	**Total COD (S_t) (mg COD/ℓ)**	**Soluble COD (S_s) (mg COD/ℓ)**	**pH**	**VFA (mg HAc/ℓ)**	**Alkalinity (mg/ℓ as $CaCO_3$)**	**Methane Production (ℓ/d)**	**Methane Composition (% vol)**	**FSA (mg N/ℓ)**	**TKN (mg N/ℓ)**
1	16	10	28876	5254	11079.48	215.73	6.83	1.01	2475.25	12.23	59.86	205.02	488.13
2	16	8	26439	3161	11223.93	215.60	6.57	1.62	1407.98	13.19	58.62	196.21	480.68
3	20	20	26654	3027	10402.06	200.76	6.62	0.60	1576.84	7.05	58.70	240.00	516.39
4	20	15	26608	3302	10370.99	189.51	6.61	0.99	1561.55	9.38	58.71	218.18	494.35
5	20	15	14011	1825	5711.95	129.93	6.34	1.38	854.83	4.83	57.01	111.53	259.35
7	16	6.67	25228	2374	12549.55	257.55	6.63	1.90	1518.46	13.19	61.52	239.92	529.95
8	16	5.71	25061	2604	12713.84	273.94	6.62	2.38	1470.85	15.01	61.37	246.47	538.51
9	16	5	24880	2693	12847.97	382.47	6.60	2.96	1412.22	16.71	61.34	247.66	539.42
10	20	15	39984	3715	17033.63	276.86	6.83	0.67	2442.00	13.30	61.11	459.10	893.84
11	20	15	39965	4165	17214.72	325.84	6.85	0.66	2535.34	13.17	61.14	466.54	902.59
12	20	10	39810	4436	18629.35	293.88	6.83	1.01	2425.72	18.38	61.17	437.82	888.51
13	20	10	13270	1174	6147.25	147.03	6.35	1.63	820.53	6.19	60.56	141.18	290.30
14	20	8	13269	1524	6384.39	152.34	6.40	2.01	903.30	7.47	60.76	143.00	295.88
17	20	60	9810	1204	3657.88	100.84	6.18	0.44	619.27	0.90	55.38	104.38	205.97
18	16	8	1949	283	864.43	97.48	7.50	1.00	1536.15	0.94	94.72	18.67	39.44
19	16	8	1949	283	864.69	97.76	7.02	1.15	1328.49	0.94	86.40	19.69	40.46
21	20	8	34819	3829	15490.07	252.20	6.73	1.39	1952.11	20.97	60.45	245.52	631.80
23	20	6.67	34819	4399	15405.23	264.17	6.76	1.69	2081.30	25.24	60.56	257.31	642.65
24	20	6.67	13580	1846	6094.14	154.92	6.38	2.65	893.28	9.73	59.48	107.58	258.20
25	20	10	1950	254	935.25	85.15	5.65	9.36	193.85	0.88	52.20	16.36	37.95
26	20	8	1949	283	921.82	117.40	5.65	11.89	194.80	1.11	52.32	18.24	39.38
27	16	8	2017	224	920.30	63.58	6.58	1.60	949.28	0.95	72.85	20.31	42.43
28	20	5.71	41442	2583	20388.97	363.72	6.66	2.27	1671.18	32.13	60.63	280.51	759.16
31	20	5.71	13186	956	7007.94	193.50	6.20	4.88	595.68	9.42	59.16	86.68	243.37

7.1.1 Total and Soluble COD

The model was able to accurately predict the effluent total COD concentration when compared to the experimental data for each steady state system. This is clearly evident in Figure 7-1. This is to be expected since the model predicted total COD concentration is the result of fitted hydrolysis kinetic parameters (refer to Section 7.3).

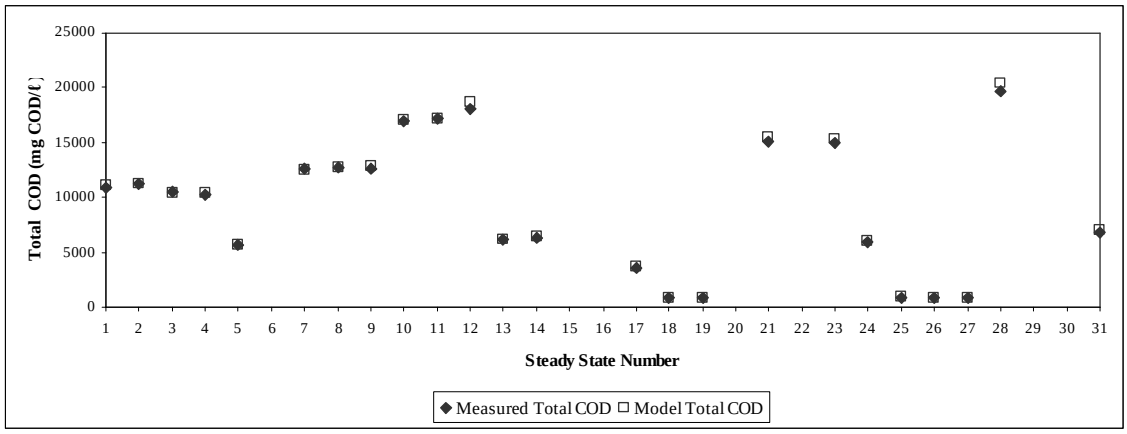

Figure 7-1: Measured and predicted effluent total COD concentrations for respective steady state methanogenic systems

As is shown in Figure 7-2, a somewhat greater effluent soluble COD concentration was predicted by the model than was observed experimentally for all steady state methanogenic systems. This variation across all steady states is due to the insufficient utilisation of the biodegradable soluble COD fraction in the form of the intermediate glucose (refer Section 2.2.2, Chapter 2). This is possibly due to the equilibrium established in the completely mixed reactor between the hydrolysis process producing this component and the acidogenic process consuming it. The difference in relation to the COD utilised is very small and therefore one could increase the acidogenesis rate because ultimately it is limited by the hydrolysis rate. This requires further investigation.

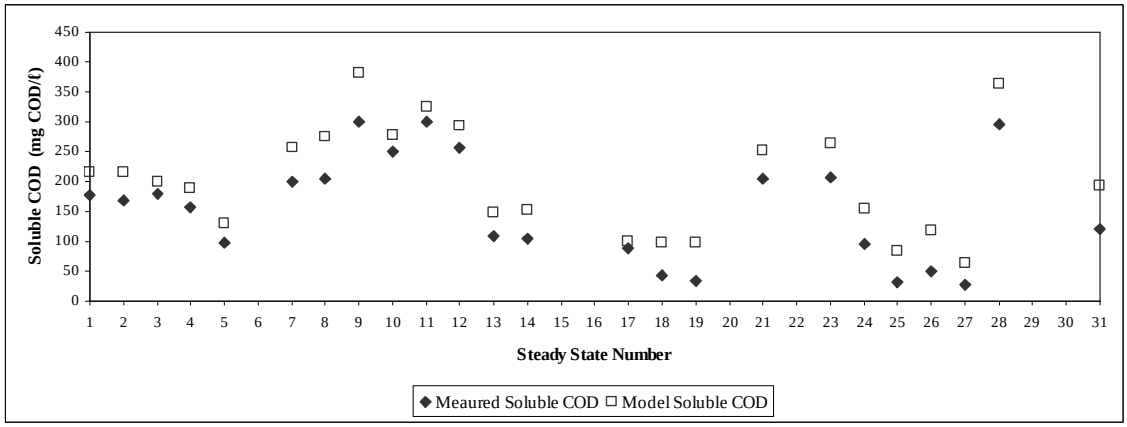

Figure 7-2: Measured and predicted effluent soluble COD concentrations for respective steady state methanogenic systems

7.1.2 pH and Alkalinity

The predicted steady state model operating pH and effluent alkalinity values for each methanogenic system are compared to the measured values in Figure 7-3. The pH for steady states 18, 19 and 27 were controlled to 7.5, 7, and 6.5 respectively. This was done in the model by adding either hydrogen or hydroxyl ion to the influent to maintain a given pH.

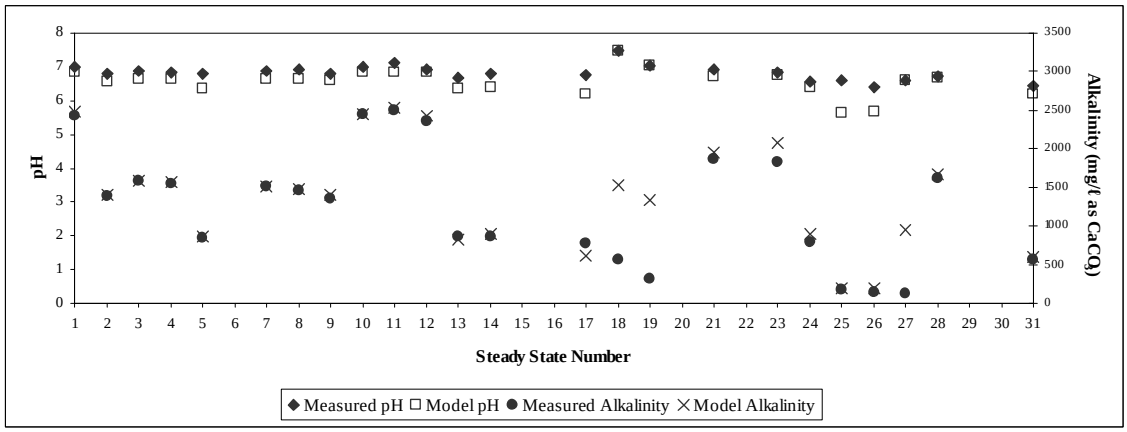

Figure 7-3: Measured and predicted operating pH and effluent alkalinity concentrations for respective steady state methanogenic systems

However this method as well as alternate pH correction techniques in model application must be investigated further. The model pH and alkalinity compare remarkably well to the experimental data for most steady states indicating that bioprocesses and mixed weak acid base chemistry has been correctly integrated and accurately modelled.

7.1.3 VFA

Figure 7-4 shows the comparison of the predicted model effluent VFA concentrations with the measured values for each of the steady state systems. The requirement for a stable methanogenic system, according to Ristow et al. (2005), is a VFA concentration of 50 mg HAc/ℓ or less. The model predicts almost complete utilisation of substrate VFA by organisms for most steady states as shown in Figure 7-4.

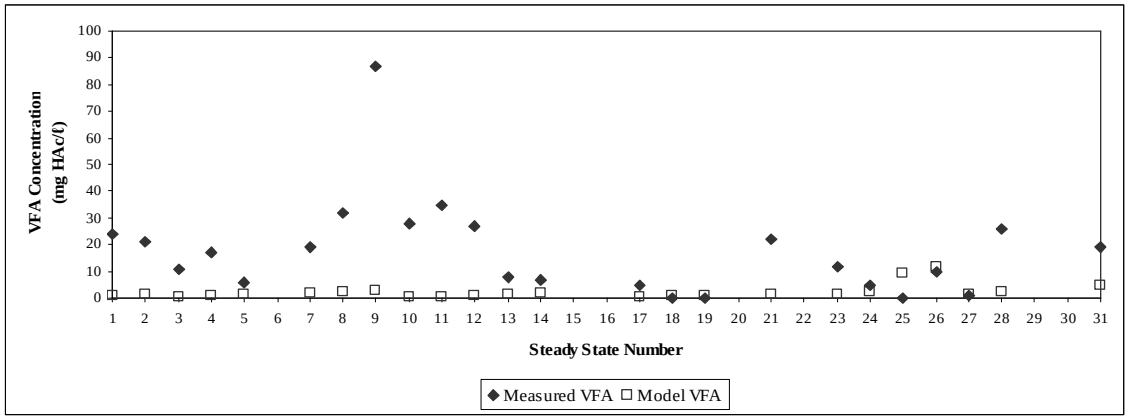

Figure 7-4: Measured and predicted effluent VFA concentrations for respective steady state methanogenic systems

Although in most cases the predicted values are much lower than measured values, the differences are small in terms of the total COD input (refer to Table 7-1) and hence the requirement for stable methanogenic operation is met.

7.1.4 Methane Production and Gas Composition

The end product of the methanogenic anaerobic digestion process is methane and its production is a good indication of the stability of the system. The comparisons of the model and experimental methane production as well as the methane gas composition are shown in Figure 7-5. It is evident that the model compares relatively well to the measured values for both methane production and methane composition, although it predicts a slightly higher methane production for most steady states. The gas produced consists of methane and carbon dioxide only, and therefore by difference, the carbon dioxide composition is determined. The main difference between the predicted methane and gas composition is due to the model data not conforming exactly to 100% COD and C mass balances.

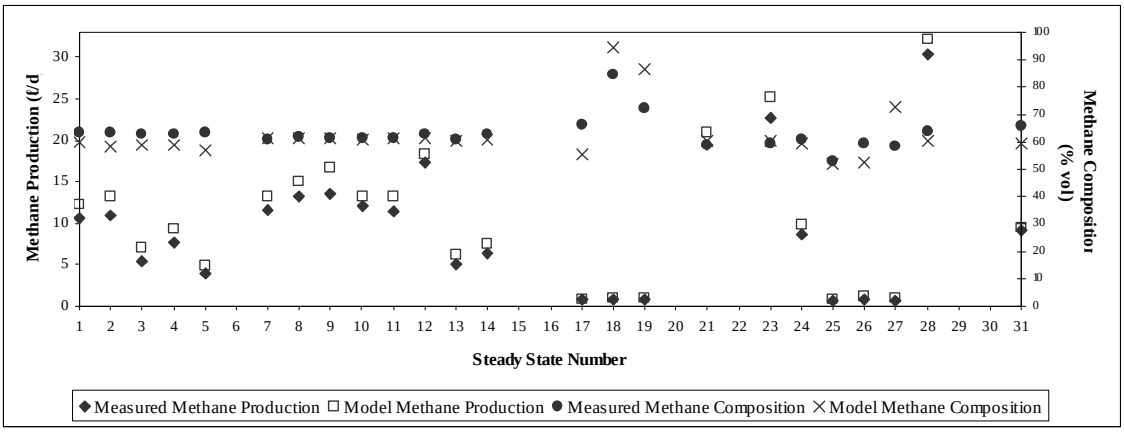

Figure 7-5: Measured and predicted methane production and methane composition for respective steady state methanogenic systems

7.1.5 FSA and TKN

Figures 7-6 and 7-7 illustrate the comparison of predicted effluent TKN and FSA concentrations to measured data for each steady state system respectively. Model predictions of FSA compare fairly well with the exception of a steady states 7 – 12 and 28 which predict a greater effluent value than that measured.

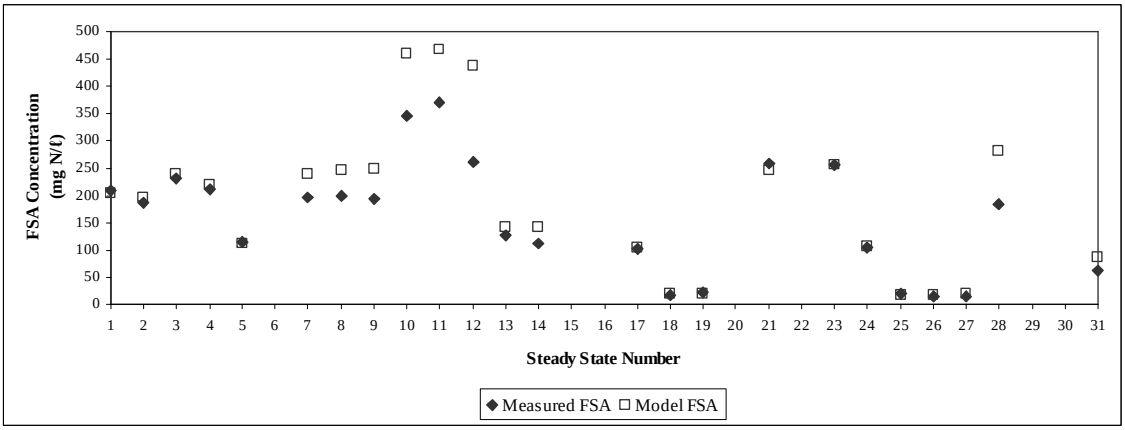

Figure 7-6: Measured and predicted effluent FSA concentrations for respective steady state methanogenic systems

As in the case of FSA concentrations, the predicted TKN values in Figure 7-7 compare reasonably well to measured effluent data, with the exception of same steady state systems as shown in Figure 7-6 in which higher values are predicted. Again the difference is due to the data not conforming to the 100% N mass balance.

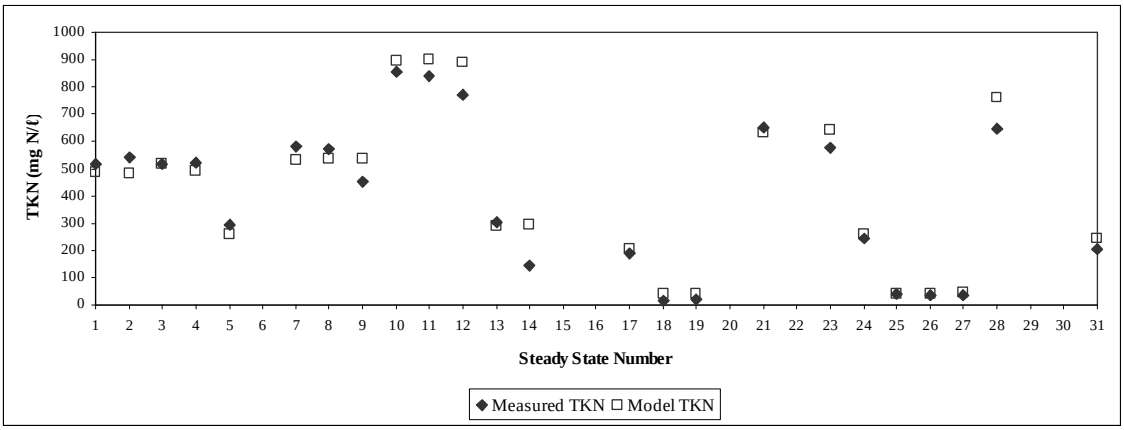

Figure 7-7: Measured and predicted effluent TKN for respective steady state methanogenic systems

7.2 Sulphidogenic Systems

All sulphidogenic steady state experiments with the exception of steady state number 16 listed in Table 3-3, Chapter 3, were modelled and simulated in WEST®. According to Ristow et al. (2005), no steady state operation was observed for this particular experiment. The summary of results for the steady state simulation of sulphidogenic systems including the model variables are presented in Table 7-2. Variables include total and soluble COD concentrations, pH, VFA, alkalinity, FSA, TKN and sulphate concentrations.

Table 7-2: Summary of results from the simulation of each steady state sulphidogenic system

			INFLUENT			EFFLUENT							
Steady State Number	**Reactor Volume (ℓ)**	**Retention Time (d)**	**Total COD (S_{ti}) (mg COD/ℓ)**	**Soluble COD (S_{si}) (mg COD/ℓ)**	**Sulphate (mg SO_4/ℓ)**	**Total COD (S_t) (mg COD/ℓ)**	**Soluble COD (S_s) (mg COD/ℓ)**	**Sulphate (mg SO_4/ℓ)**	**pH**	**VFA (mg HAc/ℓ)**	**Alkalinity (mg/ℓ as $CaCO_3$)**	**FSA (mg N/ℓ)**	**TKN (mg N/ℓ)**
6	16	10	28876	5254	1000	11109.43	221.95	1.19	6.99	0.92	3492.40	203.05	486.41
15	16	8	13269	1524	9600	5969.54	192.45	5952.53	6.87	0.98	2483.95	141.72	288.68
20	16	8	1949	283	2000	1117.75	247.63	1522.68	7.52	0.16	1812.58	17.41	39.21
22	16	8	1949	283	2000	994.07	123.95	1522.68	6.41	0.17	873.92	19.43	41.23
36	16	8	1949	283	2000	996.00	125.87	1522.68	6.46	0.17	937.84	22.42	44.22
41	20	16	2012	212	2000	898.94	66.44	1424.99	6.32	0.13	789.57	19.55	41.46
42	20	13.3	2017	224	2000	918.44	69.90	1438.52	6.31	0.14	776.91	22.54	44.59
46	20	10	989	102	1000	477.42	71.89	734.09	5.98	0.14	414.56	13.06	23.76
47	16	8	1900	203	2000	1206.19	392.69	1487.19	8.27	0.17	2104.80	14.76	35.67

7.2.1 Total and Soluble COD

As illustrated in Figure 7-8, with the exception of steady state number 15, the model was able to accurately predict the effluent total COD concentration when compared to the experimental data for each steady state sulphidogenic system. This is due to the experimental feed of steady state 15 having being supplemented with Fe to precipitate FeS hence eliminating sulphide toxicity (refer to Section 3.1.7, Chapter 3). The model does not include the Fe component, and therefore total COD was regarded usually as in the simulation of other steady state systems. The absence of the Fe component in the predicted COD results the difference between modelled and measured values. According to Ristow et al. (2005), the ferrous sulphide contribution to total effluent COD is 6639 mg COD/ ℓ which compares fairly well to the difference of 7031 mg COD/ℓ between the modelled value and actual measurement. The predicted effluent total COD concentrations are a result of the optimised hydrolysis kinetic parameters (refer to Section 7.3). Influent total and soluble COD concentrations have been adjusted to include the additional predicted fraction of S_{VFAi} for steady state number 6 only.

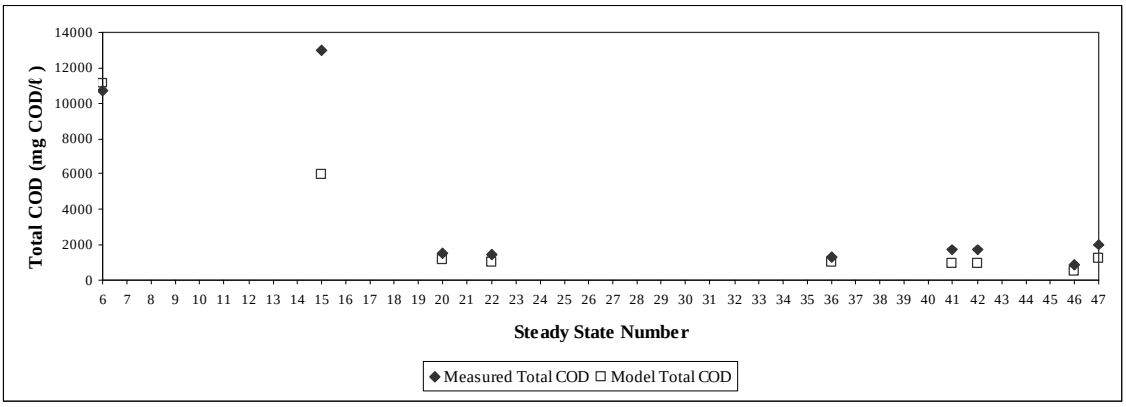

Figure 7-8: Measured and predicted effluent total COD concentrations for respective steady state sulphidogenic systems

When comparing effluent soluble COD of the model to the measured data for each steady state system in Figure 7-9, it can be seen that reasonable correspondences are only achieved for steady states 6 and 15. A factor that potentially influences the soluble COD concentration most is the contribution of COD due to total dissolved sulphides. As a result of the aqueous sulphide concentration not reported for experimental systems, it is not possible to validate this deduction. This probability and other potential reasons for this deviation need to be investigated further.

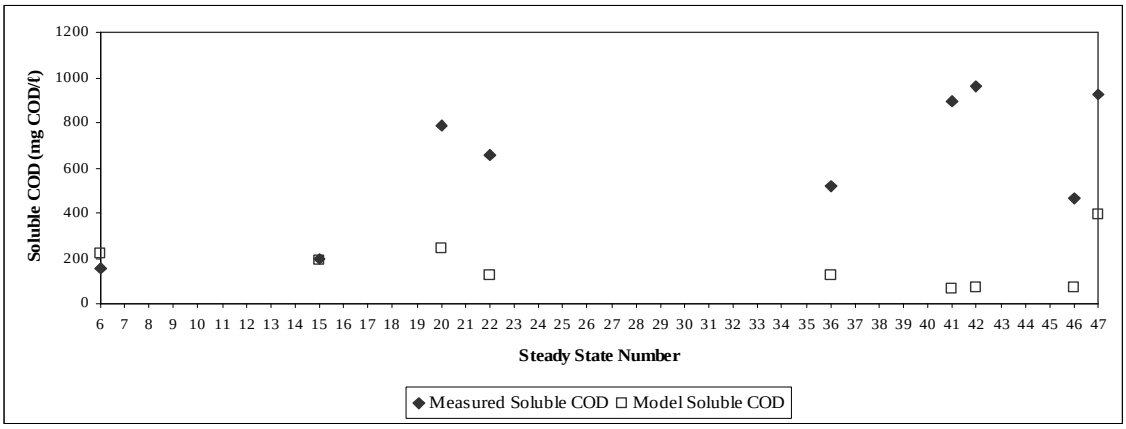

Figure 7-9: Measured and predicted effluent soluble COD concentrations for respective steady state sulphidogenic systems

7.2.2 pH and Alkalinity

The predicted model operating pH and effluent alkalinity values for each sulphidogenic system are compared to the measured values in Figure 7-10. The pH for all steady state systems, excluding steady state numbers 41, 42 and 46, were controlled by manually adding either hydrogen or hydroxyl ion to the influent to maintain a given pH. As pointed out for methanogenic systems, this method as well as alternate pH correction techniques in model application must be investigated further. The model predicts a lower pH for systems where pH was observed from steady state operation.

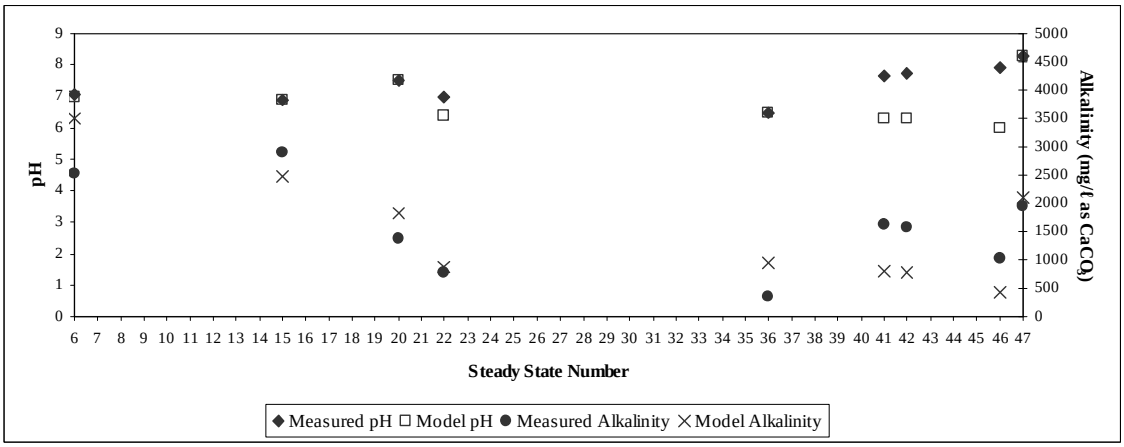

Figure 7-10: Measured and predicted operating pH and effluent alkalinity concentrations for respective steady state sulphidogenic systems

For steady state experiments where pH was not controlled, and steady state operation allowed to prevail, the model yielded alkalinity values lower than that measured. However in the case

where pH was controlled, the model demonstrated effluent alkalinity that was of an erratic nature and hence no clear trend could be deduced. This requires further investigation.

Digester performance is influenced directly by organic acids, pH and alkalinity which related to one another. If in certain systems where methanogenic activity cannot remove hydrogen and organic acids as quickly as they are produced, the result is an increase in acid concentration and if pH is not controlled, the pH will drop to a level where fermentation can be terminated. Ammonia and bicarbonate are major components that directly contribute to alkalinity. Deviation in pH and alkalinity regarding steady state sulphidogenic systems must be further optimised through a correct balance of the contributing factors mentioned above.

7.2.3 VFA

Figure 7-11 shows the comparison of predicted model values of effluent VFA concentration to measured experimental values. The model representative of steady state numbers 15, 20, 36, 41 and 46 is able to reasonably predict the effluent VFA concentration when compared to measured data. Greater deviations of the model from measured data are observed for steady state numbers 6, 22, 42 and 47.

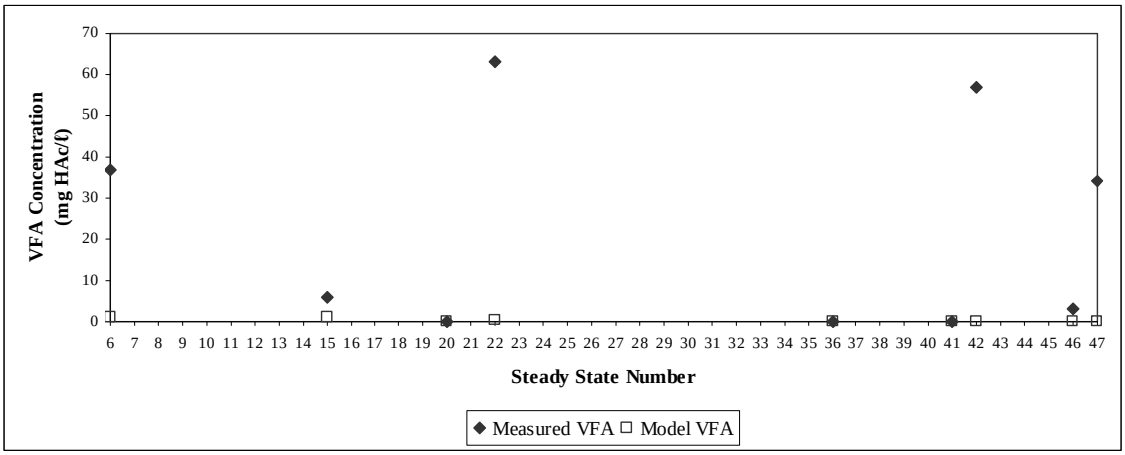

Figure 7-11: Measured and predicted effluent VFA concentrations for respective steady state sulphidogenic systems

As in the case of methanogenic systems, stable sulphate reducing conditions were accepted to require a negligible VFA concentration i.e. less than 50 mg HAc/ℓ. Predicted VFA concentrations range from 0.13 mg HAc/ℓ to 0.98 mg HAc/ℓ for all steady state simulations, hence maintaining stable sulphate reducing conditions.

7.2.4 Sulphate

The predicted model values of effluent sulphate concentration are compared to the experimental values as illustrated in Figure 7-12. It can be seen that the model predicts reasonable sulphate reduction for steady states 6 only when compared to the measured values. The model is able to reduce sulphate by 99.88 % for steady state 6 and according to Ristow et al. (2005) complete sulphate reduction was probable for this steady state. This is due to using a very high influent COD:SO_4 ratio of 28.88, which can result in the complete reduction of sulphate. For the remaining steady state systems predicted effluent sulphate concentrations are significantly higher than the respective measured values with an average sulphate removal efficiency of 27.33 %. It is clearly evident that high model sulphate removal efficiencies are obtained at high COD:SO_4 ratios as in the case of steady state 6. COD:SO_4 ratios for the remaining steady states range from 0.95 to 1.38 for steady states 47 (25.64 % sulphate removal) and 15 (37.99 % sulphate removal) respectively, hence substantiating the deduction made above. With the exception of steady state 6, the model does not properly represent competition between methanogenic and sulphidogenic organisms as discussed in literature (refer to Chapter 2) and as occurs in reality. Other than steady state 6, sulphidogens are clearly out-competed for substrate by methanogens, resulting in methane production within the model; whereas negligible methane data was recorded for the remaining steady state experiments (refer to Appendix C for detailed steady state data). However it must be noted that the laboratory experiments were not designed to investigate competition between methanogenic and sulphidogenic organisms but rather to determine the rate of hydrolysis of PSS under methanogenic, acidogenic and sulphate-reducing conditions and the influences thereof, to which independent sets of kinetic parameters were applied.

Undissociated aqueous sulphide concentrations range from 0.96 mg/ℓ to 8.86 mg/ℓ for steady states 6 and 20 respectively, therefore maintaining sulphide inhibition to a minimum. No experimental measurement for effluent sulphate was made for steady state number 41. Considering that the sulphur mass balance in the model conforms to 100% closure, one can be sure that the derivation of the model stoichiometry is correct.

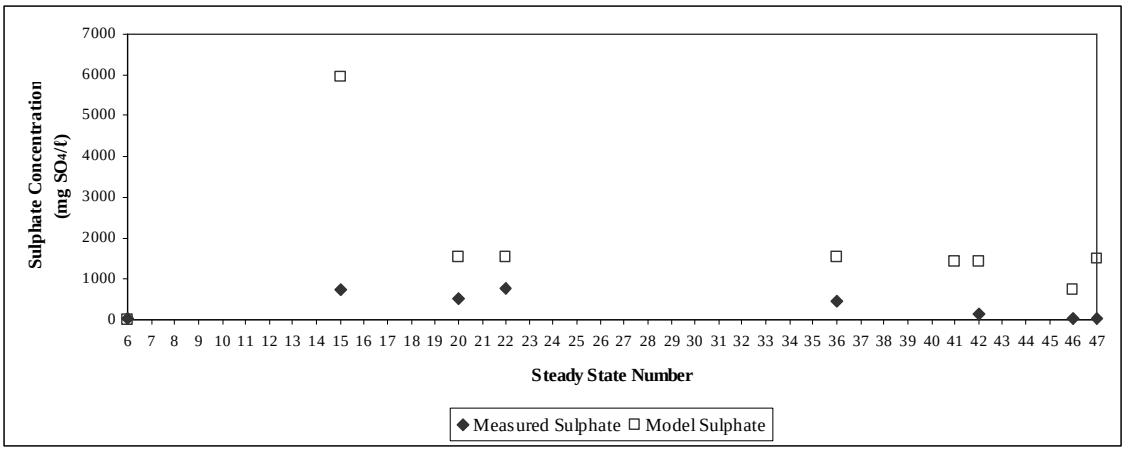

Figure 7-12: Measured and predicted effluent sulphate concentrations for respective steady states

7.2.5 FSA and TKN

Other than steady state number 15 in Figure 7-13, predicted FSA compare reasonably well to measured data for sulphidogenic systems. It must be noted that FSA measurements were not recorded for steady state numbers 46 and 47.

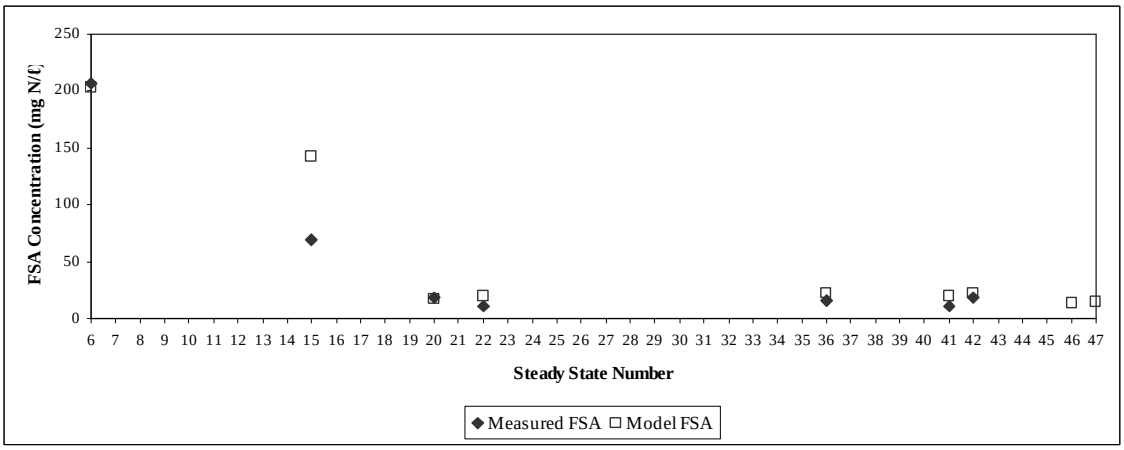

Figure 7-13: Measured and predicted effluent FSA concentrations for respective steady state sulphidogenic systems

As illustrated in Figure 7-14, except for steady states 6 and 42, the model is able predict TKN fairly well when compared to actual measurements. Effluent nitrogen content of organisms and biodegradable particulate COD for TKN is under-predicted for steady states 6 and 42, and therefore implies that effluent organism concentration and biodegradable particulate COD is low. Once again, no measurements were recorded for steady states 46 and 47. Discrepancies

could be due to the data not conforming to the 100% N mass balance.

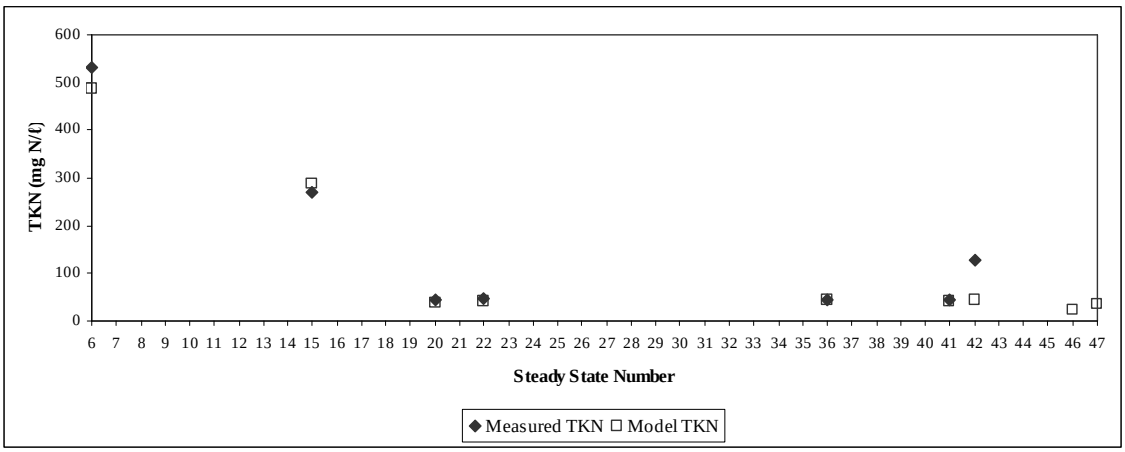

Figure 7-14: Measured and predicted effluent TKN for respective steady state sulphidogenic systems

7.3 Parameter Calibration

7.3.1 Sensitivity Analysis

Sensitivity of a given variable due to a perturbation of a given parameter will indicate which parameters need to be calibrated, in order to get accurate simulation outputs. Sensitivity analysis was performed on the model for each steady state simulation in WEST® to identify and determine the model parameters that influence simulated outputs. The absolute and relative sensitivity of a given variable due to a change in the given parameter was calculated by using the sensitivity function in WEST®. In application of the model and analysing all the steady state sensitivity output data from sensitivity analyses, it was clearly evident and therefore determined that the hydrolysis maximum specific rate constant ($k_{max,HYD}$) and half saturation constant ($K_{SS,HYD}$) were most sensitive and influenced simulation results significantly. This result was not unexpected and is in agreement with the literature in Chapter 2, showing that hydrolysis is the rate-limiting step in the anaerobic digestion process treating PSS. Accordingly, for each system simulated, these two constants were calibrated using the optimiser function in WEST®.

7.3.2 Parameter Regression

The values of the hydrolysis kinetic constants were expected to vary from one simulation to another depending on the operating conditions and the amount of particulate organic matter fed into a given system. Initial values of 769 g COD S_{bp}/mol Z_{ai}.d and 1225 g COD S_{bp}/mol Z_{ai}

for $k_{max,HYD}$ and $K_{SS,HYD}$ respectively were obtained from Sötemann et al. (2005b) who used the data set of Izzett et al. (1992) to calibrate constants for these hydrolysis kinetics. The next step involved determining the values of these kinetics parameters that would best describe a given system effectively. This was achieved by using the optimiser function in WEST®, whereby model parameters are adjusted to fit the model output on the experimental data set. An "end-value optimisation" function was applicable to steady state simulations and was performed on each steady state system discussed above. In an end-value optimisation simulation, a set of model parameters is tuned in order to minimise a defined variable, referred to as the cost variable. During optimisation the algorithm tries to find the optimum for the different parameters so that the result of the simulation fits the measured data. The "cost variable" selected for optimisation of hydrolysis kinetic parameters was effluent total COD. This cost variable was minimised by comparing the relationship and minimising the sum of squared errors between the model output and measured value of effluent total COD while hydrolysis kinetic parameters were simultaneously optimised to obtain the optimal fit. Table 7-3 contain the results of optimisation performed on hydrolysis kinetic parameters from simulation of each steady state experiment.

It must be noted that the parameter regression methodology as applied above for hydrolysis kinetics was applied to the remaining kinetic parameters. However, this proved unsuccessful in influencing the end result of simulating competition between methanogenic and sulphidogenic organisms, especially with regard to sulphate removal efficiencies, to obtain the desired interaction as per literature and experimental data indicate.

The hydrolysis maximum specific rate constants and half saturation kinetic rates determined via regression were averaged for methanogenic and sulphidogenic systems to check if the values differed from each other as well as to that of experimental data. The results in Table 7-4 do not differ significantly for respective systems with a 3 % deviation in hydrolysis maximum specific rate constant and 5 % for the half saturation kinetic rate. Ristow et al., (2005) concluded that PSS hydrolysis rate is closely similar under methanogenic and sulphate-reducing conditions (where sulphide is not inhibitory) and hence sulphate reduction does appear to influence the PSS hydrolysis rate. This conclusion validates the result obtained above through parameter regression. Calibrated kinetic constants calculated from methanogenic experimental data by Ristow et al., (2005) for $k_{max,HYD}$ and $K_{SS,HYD}$ were 11.2 mg COD S_{bp}/mg Z_{ai}.d (1267 g COD S_{bp}/mol Z_{ai}.d) and 13 mg COD S_{bp}/mg Z_{ai} (1471 g COD S_{bp}/mol Z_{ai}) respectively. This data differs significantly from averaged regressed methanogenic data with errors of 51 % and 288 % for $k_{max,HYD}$ and $K_{SS,HYD}$ respectively. The deviation between the experimental data and the

predicted results with respect the average hydrolysis constants need to be assessed when applied to new methanogenic and sulphate-reducing systems.

Table 7-3: Results of optimisation performed on hydrolysis kinetic parameters from the model for each steady state system

Steady state number	$k_{max,HYD}$ (g COD S_{bp}/mol Z_{ai}.d)	$K_{SS,HYD}$ (g COD S_{bp}/mol Z_{ai})
1	900	300
2	900	300
3	900	300
4	1100	50
5	900	300
6	900	300
7	700	570
8	745	550
9	795	520
10	725	560
11	690	600
12	610	600
13	700	595
14	690	600
15	830	330
17	1100	50
18	1100	50
19	1100	50
20	730	430
21	800	395
22	730	430
23	860	320
24	850	350
25	700	500
26	930	270
27	880	330
28	775	425
31	680	515
36	730	430
41	760	430
42	750	430
46	1000	150
47	900	300

Table 7-4: Regressed average hydrolysis kinetic parameters for methanogenic and sulphidogenic systems

System Type	Average $k_{max,HYD}$ (g COD S_{bp}/mol Z_{ai}.d)	Average $k_{SS,HYD}$ (g COD S_{bp}/mol Z_{ai}.d)
Methanogenic	839	379
Sulphidogenic	814	359

CHAPTER 8

APPLICATION OF THE MODEL TO THE PILOT PLANT

This chapter discusses simulation results from application of the extended UCTADM1 in WEST® to available pilot plant RSBR operating data in Section 3.2, Chapter 3. In addition the model was further used to investigate various operating scenarios as at the time of this study the pilot plant was still at the stage of ironing out equipment teething problems and not much was known about process related issues.

The available data includes estimated values and qualitative statements and it is therefore not known how representative or reliable these values are. The model presented here and the results thereof must be considered as very much a preliminary one, and any specific conclusions can only be tentative and should therefore only be taken as indicating qualitative trends.

8.1 RSBR Simulation

The summary of results for the steady state simulation of the pilot RSBR including are presented in Table 8-1. Available operating data for comparison to model output data include pH, VFA, alkalinity, and sulphate concentration. Table 8-2 summarises the comparison between model outputs and available measured data.

The model exhibited a sulphate conversion lower than that measured when applied to the pilot plant. Although the effluent sulphate concentration is not given specifically (< 200 mg/ℓ), a sulphate concentration of 702.07 mg SO_4/ℓ predicted by the model is much higher than this estimation. As discussed above for steady state sulphidogenic systems, the under prediction of sulphate removal efficiency is attributed to the use of a low COD:SO_4 ratio. In the case of the pilot plant the COD:SO_4 ratio was calculated to be 1.32, hence resulting in only 45.99 % sulphate conversion based estimated pilot plant effluent sulphate concentration of lower 200 mg/ℓ. In addition, a low undissociated aqueous sulphide concentration of 2.27 mg/ℓ was predicted, thereby maintaining sulphide inhibition to a minimum.

Table 8-1: Summary of results from the simulation of the pilot plant RSBR

Variable	Value
Reactor Volume (ℓ)	250 000
Retention Time (d)	1
Feed Total COD (mg COD/ℓ)	30 000
Feed Soluble COD (mg COD/ℓ)	2694
Feed Sulphate (mg SO_4/ℓ)	1300
Effluent Total COD (mg COD/ℓ)	8681.34
Effluent Soluble COD (mg COD/ℓ)	37.92
Effluent Sulphate (mg SO_4/ℓ)	702.07
Reactor pH	7.18
Effluent VFA (mg HAc/ℓ)	0.07
Effluent Alkalinity (mg/ℓ as $CaCO_3$)	1001.45
Methane Production (ℓ/d)	72.77
Gas composition (% CH_4)	15.58
Total Gas production (ℓ/d)	130.43
Effluent FSA (mg N/ℓ)	19.02
Effluent TKN (mg N/ℓ)	119.90

Table 8-2: Comparison between pilot plant measurements and model predictions

	Measured	Model
Effluent Sulphate (mg SO_4/ℓ)	< 200	702.07
Effluent pH	~ 7.7 (not confirmed)	7.18
Effluent Alkalinity (mg/ℓ as $CaCO_3$)	1500	1001.45
Effluent VFA (mg HAc/ℓ)	< 50	0.07

As in most steady state systems, sulphidogens are clearly out competed for substrate by methanogens within the pilot plant model resulting in methane production (72.77 ℓ/d) and elevated methane gas compositions (15.58 %) although no physical measurements were recorded for comparison purposes. It must be noted that the model used to simulate the pilot plant is the same as that derived to model laboratory experiments, however with kinetic parameters corrected to 23 ^{o}C instead of 35 ^{o}C. Model trends exhibited for the pilot plant were similar to those displayed in the simulation of steady state experimental systems.

A pH value of 7.18 was predicted compared to an unconfirmed pH measurement of less than 7.7. As in the case of steady state sulphidogenic systems, the model predicts a lower pH for the pilot plant where pH was observed from steady state operation. A simulated alkalinity at 1001.45 mg/ℓ was observed in model as compared to 1500 mg/ℓ measured for the pilot plant. This trend is similar to that observed for sulphidogenic steady state experiments where the model yielded alkalinity values lower than that measured for steady state operation. According to Greben et al. (2005), improved sulphate removal results in an increased alkalinity production and in an increased reactor pH, which in turn is favourable for decrease in the redox potential, when a dominant redox couple such as sulphate:sulphide is present in a solution. As per the comparison in Table 8-2, this could be the probable reason for high sulphate removal measured for a system with a high alkalinity and low sulphate removal predicted from the model with low alkalinity. Similarly to steady state sulphidogenic systems, the digester performance is influenced directly by organic acids, pH and alkalinity which related to one another. If in certain systems where methanogenic activity cannot remove hydrogen and organic acids as quickly as they are produced, the result is an increase in acid concentration and if pH is not controlled, the pH will drop to a level where fermentation can be terminated. Ammonia and bicarbonate are major components that directly contribute to alkalinity. Deviation in pH and alkalinity regarding steady state sulphidogenic systems must be further optimised through a correct balance of the contributing factors mentioned above.

A simulated effluent VFA concentration of 0.07 mg/ℓ is adequate to maintain stable sulphidogenic conditions as discussed in the case of experimental systems. Operating and model data for the pilot plant together with simulated profiles of certain effluent variables from WEST® may be found in Appendix D.

8.2 Investigation of operating scenarios using the model

As a result of the pilot plant still being in the stage of ironing out equipment teething problems at the time of this study, not much was known about process related issues. The model

provides an extremely useful tool to explore various scenarios, to select the more promising for experimental evaluation. Accordingly, the model was used to explore the effects of changing the ratio between PSS and AMD fed to the reactor. This work follows that of Ristow et al. (2006), however updated in the form of sludge and mine water flowrate ranges applied to the current model.

As mentioned above, the preliminary nature of the model application using available pilot plant operating data, indicates that the reliability of results of this section of the investigation is unknown, and should therefore only be taken as indicating qualitative trends. Nevertheless, Ristow (2005) confirmed that the pilot plant reflects certain important features of the model that have emerged while simulating various scenarios:

- The process seems to be quite resilient in the face of upsets. In particular, it does not seem to suffer from the pH related instabilities typical of methanogenic anaerobic digestion.
- Production of methane is negligible under the current operating conditions.
- H_2S inhibition is not an important factor under the current operating conditions.

8.2.1 Qualitative Characteristics of the Model

A simplified conceptual view of the model is useful for qualitative understanding of its behaviour. The rate limiting process is the first step of hydrolysing the particulate COD, and thus the dominant factor determining the model's characteristics. Once the substrate has been solubilised, the methanogenic and sulphate reducing populations of organisms compete for it, and the outcome of this competition determines the second level of characteristics, i.e. how much COD goes into sulphate reduction, and how much into methane production. Issues such as sulphide inhibition fall into a third level, and do not seem to be significant under the conditions experienced by the pilot plant.

8.2.2 Investigation of the COD:SO_4 feed ratio

It is assumed here that the sulphate rich mine water is in excess, so that obtaining the maximum sulphate reduction for the COD used is desirable. Under this assumption there is still a compromise to be made between the effluent quality of the treated water and the load of sulphate removed. If the treated water is to be discharged to a receiving body, the load is the important criterion, whereas if it is to be reused, the quality is relevant. In considering the latter option, there is a follow-up unit operation to remove the sulphide generated, so that the water

quality can be expressed in terms of the residual sulphate concentration. The model was run with a mine water flowrate of 230 m^3/d (the same as the nominal feed rate to the pilot plant), and a range of sludge flow rates from 1.32 to 39.6 m^3/d (the current nominal feed rate to the pilot plant is 13.2 m^3/d). The results are summarised in Figure 8-1, which plots ratios representing the effluent quality and the COD utilisation against the ratio of COD to sulphate fed.

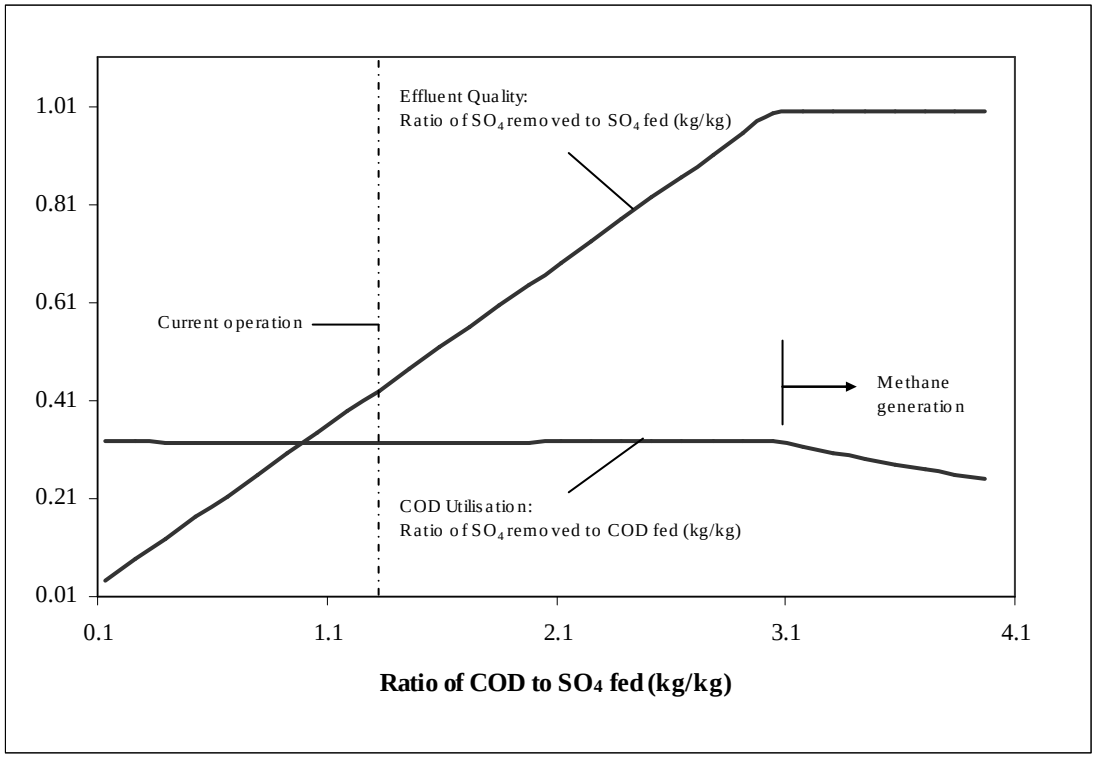

Figure 8-1: Simulated SO_4 removal and COD utilisation ratios for a varying sludge feed rate

The lower the ratio of COD to sulphate fed, the more sulphate is reduced by a given amount of COD. COD utilisation remains effectively constant until the sulphate nears complete removal. The model predicts that this trend continues with stable operation down to much lower COD:SO_4 ratios than current operation; this may or may not be realistic. The sulphate removal ratio increases almost linearly up to almost complete removal. This is a consequence of the reactions being limited by the hydrolysis rate.

The series of simulations reflected in Figure 8-1 held the mine water feed rate constant while varying the sludge feed rate in order to vary the COD: SO_4 ratio. The ratio could also be altered by holding the sludge feed rate constant and varying the mine water feed rate. The model was run with a sludge flowrate of 13.2 m^3/d (the same as the nominal feed rate to the pilot plant),

and a range of mine water flow rates from 23 to 690 m^3/d (the current nominal feed rate to the pilot plant is 230 m^3/d). This gives a similar system response, as shown in Figure 8-2.

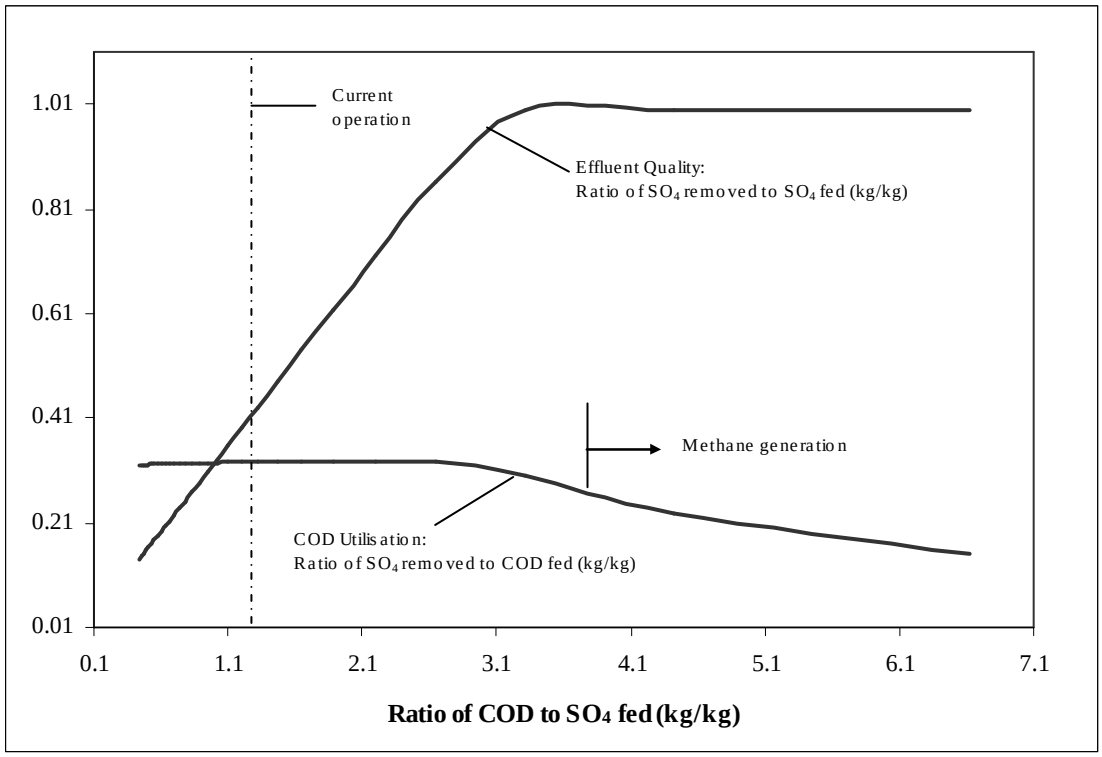

Figure 8-2: Simulated SO_4 removal and COD utilisation ratios for a varying mine water feed rate

In this case the effluent quality responds very much as before. The COD utilisation remains effectively constant until complete sulphate removal is approached. This is again a consequence of the limiting hydrolysis rate, since the sludge residence time is held constant, the reaction rate remains constant.

Figures 8-1 and 8-2 tend to obscure the effect of the limitation of reactor volume, although it is implied in the results. When designing a system, the reactor size would be a variable, which adds a degree of freedom to the system response. The above diagrams should be seen as examples of how the model could be used, rather than as definitive characteristics of the process, particularly in view of the uncertainties in the kinetic parameter values.

CHAPTER 9

CONCLUSIONS AND RECOMMENDATIONS

It can be summarised and concluded from the outcome of this study that:

1. The modelling and simulation package WEST® (**W**astewater Treatment Plant **E**ngine for **S**imulation and **T**raining) was used as the platform for the successful translation and coding of biological processes of the basic University of Cape Town Anaerobic Digestion Model No.1 (UCTADM1) from AQUASIM via the methodology outlined in Chapter 4.

2. The basic UCTADM1 for the production of methane was extended with the development of a mathematical model (as per the method of approach discussed in Chapter 5) incorporating the processes of biosulphidogenic reduction and the biology of sulphate reducing bacteria (SRB). Kinetic parameters used in the model were obtained from Sötemann et al. (2005b) and Kalyuzhnyi et al. (1998). This sulphidogenic mathematical model was subsequently integrated with the methanogenic model in WEST® which would facilitate competition between these 2 organism groups to be demonstrated.

3. A continuity check was performed on model influent and effluent flux data for a single methanogenic and sulphidogenic system. The Ristow et al., (2005) influent and effluent experimental data proved insufficient in performing a continuity check as that undertaken in the model. Only the sulphur balance reflected full closure with the largest margin of error observed for COD, C and N. The margin of error in methanogenic and sulphidogenic models was very similar to one another, however lower than that of Ristow, et al. (2005) for COD conversion. This trend was also observed when the continuity check was performed upon the initial translation of the UCTADM1 (without sulphate reduction) from AQUASIM to WEST® with margins of error very similar in both software platforms to that observed in both steady state models. This indicated that there may possibly be an error in the derivation of the model and hence in the reaction stoichiometry of the Petersen matrix with the probability of inheriting the mass balance error from the AQUASIM model stoichiometry during coding into WEST®. Upon further manipulation of the model to allow stoichiometric coefficients to be visible which were previously hidden by default, it was discovered that WEST® incorrectly computed a single stoichiometric coefficient viz. 'EndogenousProt' which was programmed into the model as a variable to simplify the stoichiometry of certain reactions. Once rectified, a subsequent continuity check

resulted in a margin of error that was 5 % when compared to the previous WEST® and AQUASIM models for which mass balances did not close. It can therefore be concluded that the major portion of mass balance errors can be attributed to incorrect reaction stoichiometry that was inherited via the translation of the AQUASIM model into WEST® with the remainder due to inconsistencies in computation of reaction stoichiometry within the WEST® software.

4. WEST® was subsequently used in application of the extended UCTADM1 to data sets from the UCT laboratory experiments carried out in completely mixed reactors. Application of the WEST® implementation of the model to the experimental methanogenic anaerobic digestion systems (described in Section 3.1.5, Chapter 3) gave reasonably close correlations (refer to Section 7.1, Chapter 7) between predicted and measured data for a single set of stoichiometric and kinetic constants, with the exception of the hydrolysis rate constants, which were regressed (refer to Section 7.3, Chapter 7) using the optimiser function in WEST®. The regressed hydrolysis maximum specific rate constants and half saturation kinetic rates were then averaged for methanogenic and sulphidogenic systems to check if the values differed from each other as well as to that of experimental data. The results did not differ significantly for respective systems with a 3 % deviation in hydrolysis maximum specific rate constant and 5 % for the half saturation kinetic rate which is in accordance with conclusions of Ristow et al., (2005). Calibrated kinetic constants calculated from methanogenic experimental data by Ristow et al., (2005) when compared to averaged regressed methanogenic data resulted in errors of 51 % and 288 % for $k_{max,HYD}$ and $K_{SS,HYD}$ respectively.

5. Application of the extended UCTADM1 to experimental sulphidogenic anaerobic systems demonstrated simulation results (refer to Section 7.2, Chapter 7) fairly close to measured data with the exception of effluent soluble COD and sulphate concentrations. The probability of soluble COD concentration being influenced by the contribution of COD due to total dissolved sulphides in addition to other potential factors must be investigated further. Model sulphate removal efficiencies for steady state sulphidogenic systems range from 25.64 % to 99.88 %. This characteristic of the model is due to varying influent COD:SO_4 ratios ranging from 0.95 to 28.88 with maximum model sulphate removal efficiencies being achieved at the highest ratio. As a result sulphidogens, with the exception of a single simulated system (steady state 6 with the highest COD:SO_4 ratio), are out competed for substrate by methanogens within the model, hence the model does not

properly represent competition between methanogenic and sulphidogenic.

6. The extended model as applied to UCT laboratory experiments was subsequently applied (refer to Section 8.1, Chapter 8) to available operating data from the Rhodes BioSURE pilot plant's recycling sludge bed reactor (RSBR) responsible for the anaerobic co-disposal of primary sewage sludge (PSS) and high sulphate acid mine drainage (AMD). The model predicted a sulphate conversion of 45.99 % based on estimated pilot plant effluent sulphate concentration of lower than 200 mg/ℓ. This is due to a low COD:SO_4 ratio of 1.32 as discussed above, resulting in methanogens out-competing sulphidogens. A pH of 7.18 was predicted as compared to an unconfirmed measurement of less than 7.7 and alkalinity of 1001.45 mg/ℓ predicted as compared to 1500 mg/ℓ measured. A low simulated VFA concentration of less than 50 mg/ℓ ensured stable sulphidogenic conditions. The model trends observed for the pilot plant simulation are similar to those observed for sulphidogenic steady state experiments. Clearly, this application is extremely rough and rests on numerous assumptions; however it is the best that could be achieved with the available information. Nevertheless, it established the model at a similar stage of development to that of the pilot plant itself, which provided an opportunity for the modelling and experimental programmes to evolve together and mutually reinforce each other.

7. The model was further used as a tool to explore various operating scenarios (refer to Section 8.2, Chapter 8) as at the time of this study the pilot plant was still at the stage of ironing out equipment teething problems and not much was known about process related issues. The model was run with a mine water flowrate the same as the nominal feed rate to the pilot plant and with a varying range of sludge flow rates and vice versa. The result for both scenarios demonstrated that the lower the ratio of COD to sulphate fed, the more sulphate is reduced by a given amount of COD where COD utilisation remains effective constant until the sulphate nears complete removal. The sulphate removal ratio increased almost linearly up to almost complete removal as a consequence of the reactions being limited by the hydrolysis rate.

Based on the work conducted in this study and in conjunction with Ristow et al. (2006), the following are recommended as areas for future research:

1. A detailed investigation into the derivation of the model stoichiometry is required to identify which stoichiometric coefficients result in an incomplete closure of the model mass balances particularly with regard to COD, C and N. A probable commencement area would

be in the conversion of biodegradable particulate COD into methane, carbon dioxide and biomass. The inconsistency in computation regarding variations of reaction stoichiometry as programmed within WEST® need to be presented to the developers (HEMMIS) of the software to allow for rectification in subsequent versions.

2. The most obvious needs for further research are to reduce the uncertainties in the kinetic parameters values that are appropriate for the operating conditions of laboratory experiments and the pilot plant. The most important aspect of the operating conditions seem to be:

   - *Operating temperatures at 35 °C and 23 °C for laboratory experiments and pilot plant respectively.*

     Temperature dependences are unavailable for methanogenic and sulphidogenic anaerobic digestion reaction rates, nor the pilot plant. Kinetic parameters obtained from literature had to be temperature corrected to operating temperatures of experimental and pilot systems for model application. However, the approximate and interactive nature of the model makes it probable that the entire set of reaction parameters needs to be determined together, rather than attributing an independent reality to any subset.

   - *Experiment design*

     The conventional way of addressing the need for a single set of kinetic parameters would be to embark on a comprehensive programme of experiments similar to the ones carried out in the UCT laboratory. This exercise should focus on demonstrating the competition between methanogenic and sulphidogenic organisms with the ultimate objective of deriving a single set of kinetic parameters that is representative of the systems under investigation. Although the efficacy of this approach is proven, the requirements in terms of time, expense and experimental effort are known to be high.

2. A cooperative project should be established between the modelling and pilot plant teams to take advantage of the opportunity to maximise the benefits of the combined modelling and experimental effort. Thus the model could be used to explore gaps in the understanding of the process and suggest experiments to be tried on the pilot plant. The data from the pilot plant can then be fed back to improve the model. This is the basic strategy of 'optimal experimental design' as outlined by Dochain and Vanrolleghem (2001). What is novel here is the opportunity to apply the technique to such a large scale reactor, and it may represent a significant advance in the practice of piloting biological treatment processes, which frequently only confirm the operability of a process and add little to the scientific

knowledge of the process. Therefore it is strongly recommended that the pilot plant investigation be supported by a simultaneous modelling investigation. To be fully effective, this should have a strong interaction with the experimental work. Theoretically this would be best achieved if the modelling and experimentation were carried out by the same team, but it could also be carried out by separate teams as long there is sufficient communication between them.

3. The hydrolysis of biodegradable particulate organic COD governs the overall rate of methanogenesis and sulphidogenesis as this step is the slowest process of the bioprocess sequence. The deviation between the experimental data and the predicted results with respect the average regressed hydrolysis constants as concluded above need to be assessed when applied to new methanogenic and sulphate-reducing systems.

4. The exercise of applying the model to the pilot plant operation demonstrated that it is not necessary to know all the parameters to the same degree of accuracy, and that it may well be that only a small number of them are critically important. Clearly the experience of the actual pilot plant operation is the best source of information for determining which parameters are critical. With the variability and contingencies of pilot plant operating conditions, it may not always be possible to determine parameters accurately, and laboratory tests might be needed to complement the pilot plant data. Here the 'serum bottle tests' which have been extensively developed could be useful. They are relatively rapid and inexpensive, and, while not able to provide comprehensive data about a process, can be tailored to investigate specific questions by spiking the test mixture with specific components.

5. The pilot plant reactor uses settling of the sludge to retain sludge in the reactor and produce a clarified effluent. Lacking any information on the settling characteristics of the sludge, this is represented in the current model as a single parameter which sets the ratio between the sludge concentration in the reactor and the effluent, which was set to an arbitrarily low value (0.0001) based entirely on qualitative observation of the clarity of the effluent under current operating conditions. In reality the retention ratio must be a function of the settling characteristics of the sludge and the flow regime in the reactor, and it sets important operating conditions and physical constraints for the reactor operation which are not currently represented in the model. These relate to the biomass concentration in the reactor and the sludge retention time. In operating the pilot plant, sludge withdrawal rate is set so as to maintain the sludge level in the reactor and prevent it overflowing into the effluent. In

the model simulations presented in this study, the sludge withdrawal flow rate was set at 1 m^3/d, the value estimated by the operators for current operation. It is quite likely that this rate would need to be adjusted to maintain the sludge separation when varying the feed rates to the reactor.

REFERENCES

BATSTONE DJ, KELLER J, ANGELIDAKI I, KALYUZHNYI SV, PAVLOSTATHIS SG, ROZZI A, SANDERS WTM, SIEGRIEST H and VAVILIN VA (2002) *Anaerobic Digestion Model No. 1,* Scientific and Technical Report No. 13, IWA Task Group for Mathematical Modelling of Anaerobic Digestion Processes, International Water Association, London.

BURGESS JE and STUETZ RM (2002) Activated sludge for the treatment of sulphur-rich wastewaters. *Minerals Engineering* **15** 839-846.

BURGESS SG and WOOD LB (1961) Pilot plant studies in production of sulphur from sulphate-enriched sewage sludge. *J. Sci. Food Agric.* **12** 326-341.

CHRISTENSEN B, LAAKE M and LIEN T (1996) Treatment of acid mine water by sulfate-reducing bacteria; Results from a bench scale experiment. *Water Research* **30** (7) 1617-1624.

DOCHAIN D and VANROLLEGHEM PA (2001) *Dynamic Modelling and Estimation in Wastewater Treatment Processes.* IWA Publishing, London.

DU PREEZ LA, ODENDAAL JP, MAREE JP and PONSONBY M (1992) Biological removal of sulphate from industrial effluents using using producer gas as an energy source. *Environmental Technology* **13** 875-882.

EASTMAN JA and FERGUSON JF (1981) Solubilization of particulate organic carbon during the acid phase of anaerobic digestion. *J. WPCF* **53** (3) 352-366.

GAZEA B, ADAM K and KONTOPOULOS A (1996) A review of passive systems for the treatment of acid mine drainage. *Minerals Engineering* **9** (1) 23-42.

GIBERT O, DE PABLO J, CORTINA JL and AYORA C (2004) Chemical characterisation of natural organic substrates for biological mitigation of acid mine drainagce. *Water Research* **38** 4186-4196.

GREBEN HA, MAREE JP, ELOFF E and MURRAY K (2005) Improved sulphate removal rates at increased sulphide concentration in the sulphidogenic bioreactor. *Water SA* **31** (3) 351-358.

GUJER W and ZEHNDER AJB (1983) Conversion processes in anaerobic digestion. *Water Science and Technology* **15** 127-167.

HANSFORD GS (2004) The mechanisms and kinetics of biological treatment of metal-containing effluent. WRC Report No. 1080/1/04, Water Research Commission, PO Box 824, Pretoria 0001, South Africa.

HENZE M, GRADY CPL, GUJER W, MARAIS G and MATSUO T (1987) *Activated Sludge Model No. 1*. IAWPRC Scientific and Technical Reports No. 1, International Association on Water Pollution Research and Control, IAWPRC, London.

HENZE M and HARREMÖES P (1983) Anaerobic treatment of wastewater in fixed film reactors-A literature review. *Water Science and Technology* **15** 1-101.

KALYUZHNYI SV, FEDOROVICH VV, LENS P, POL LH and LETTINGA G (1998) Mathematical modelling as a tool to study population dynamics between sulfate reducing and methanogenic bacteria. *Biodegradation* **9** 187-199.

KNOBEL AN and LEWIS AE (2002) A mathematical model of a high sulphate wastewater anaerobic treatment system. *Water Research* **36** 257-265.

LEDIN M and PEDERSEN K (1996) The environmental impact of mine wastes-Roles of microorganisms and their significance in treatment of mine wastes. *Earth-Science Reviews* **41** 67-108.

MAREE JP and HILL E (1989) Biological removal of sulphate from industrial effluents and concomitant production of sulphur. *Water Science and Technology* **21** 265-276.

MCCARTY PL (1974) Anaerobic processes. *Proc. Birmingham Short Course on Design Aspects of Biological Treatment, International Association of Water Pollution Research, September 18*, Birmingham, England.

MOLWANTWA JB, WHITTINGTON-JONES KJ and ROSE PD (2004) An investigation into the mechanism underlying enhanced hydrolysis of complex carbon in a biosulphidogenic recycling sludge bed reactor (RSBR). *Water SA* **30** (5) 150-154.

MOSEY FE (1983) Mathematical modelling of the anaerobic digestion process: Regulatory mechanisms for the formation of short-chain volatile fatty acids from glucose. *Water Science and Technology* **15** 209-232.

MURPHY N, TAYLOR J and LEAKE M (1999) *Coming to Terms with Acid Drainage*. Technical paper on acid mine drainage. Earth Systems Pty Ltd, Victoria, Australia. http://www.earthsystems.com.au/downloads/BestPrac.doc.

OLESZKIEWICZ JA and HILTON BL (1986) Anaerobic treatment of high sulphate wastes. *Can. J. Civ. Eng.* **13** 423-428.

OUDE ELFERINK SJWH, VISSER A, HULSHOFF POL LW and STAMS AJM (1994) Sulfate reduction in methanogenic bioreactors. *FEMS Microbiology Reviews* **15** 119-136.

PAVLOSTATHIS SG and GIRALDO-GOMEZ E (1991) Kinetics of anaerobic treatment. *Water Science and Technology* **24** (8) 35-59.

PETRIK L, WHITE R, KLINK M, SOMERSET V, KEY D, IWUOHA E, BURGERS C and FEY MV (2005) Utilization of fly ash for acid mine drainage remediation. WRC Report No. 1242/1/05, Water Research Commission, PO Box 824, Pretoria 0001, South Africa.

PULLES W (2003) The status of mine water pollution in South Africa. *Proc. 6th ICARD, July 12-18*, Cairns, Australia.

RISTOW NE (1999) The modelling of a falling sludge bed reactor using AQUASIM. MSc Thesis. Department of Chemical Eng., University of Cape Town, Cape Town, South Africa.

RISTOW NE (2005) Personal communication.

RISTOW NE, SÖTEMANN SW, LOEWENTHAL RE, WENTZEL MC and EKAMA GA (2005) Hydrolysis of primary sewage sludge under methanogenic, acidogenic, and sulfate-reducing conditions. WRC Report No. 1216/1/05, Water Research Commission, PO Box 824, Pretoria 0001, South Africa.

RISTOW NE, SÖTEMANN SW, RAJKUMAR S, WENTZEL MC, BROUCKAERT CJ, BUCKLEY CA, EKAMA GA and ROSE PD (2006) Integrated physical, chemical, and biological processes kinetic models for anaerobic digestion of primary sewage sludge. WRC Report - submitted for publication, Water Research Commission, PO Box 824, Pretoria 0001, South Africa.

RISTOW NE, SÖTEMANN SW, WENTZEL MC, EKAMA GA and LOEWENTHAL RE (2004) Considerations for the use of primary sewage sludge and sulfate-reducing bacteria for the treatment of sulfate-rich wastes. *Proc. WISA Biennial Conference, May 2-6*, Cape Town, South Africa.

RISTOW NE, WHITTINGTON-JONES KJ, CORBETT CJ, ROSE PD and HANSFORD GS (2002) Modelling of a recycling sludge bed reactor using AQUASIM. *Water SA* **28** (1) 111-120.

ROBERTS R, DAVIES WJ and FORSTER CF (1999) Two-stage, thermophilic-mesophilic anaerobic digestion of sewage sludge. *Trans IChemE* **77** (B) 93-97.

ROSE PD (2002) Salinity, sanitation, and sustainability - A study in environmental biotechnology and integrated wastewater beneficiation in South Africa. WRC Report No. TT 187/02, Water Research Commission, PO Box 824, Pretoria 0001, South Africa.

ROSE PD, CORBETT CJ, WHITTINGTON-JONES KJ and HART OO (2002) The Rhodes BioSURE Process ® - Part 1: Biodesalination of mine drainage wastewaters. WRC Report No. TT 195/02, Water Research Commission, PO Box 824, Pretoria 0001, South Africa.

SACKS J and BUCKLEY CA (2004) Anaerobic digestion of high-strength or toxic organic effluents in available digester capacity. WRC Report No. 762/1/04, Water Research Commission, PO Box 824, Pretoria 0001, South Africa.

SAM-SOON PALNS, WENTZEL MC, DOLD PL, LOEWENTHAL RE and MARAIS G_VR (1991) Mathematical modelling of upflow anaerobic sludge bed (UASB) systems treating carbohydrate waste waters. *Water SA* **17** (2) 91-106.

SMITH JM, VAN HESS HC and ABBOTT MM (1996) *Introduction to Chemical Engineering Thermodynamics* (5th ed.). McGraw-Hill International Editions.

SÖTEMANN SW, RISTOW NE, WENTZEL MC and EKAMA GA (2005a) A steady state model for anaerobic digestion of sewage sludges. *Water SA* **31** (4) 511-527.

SÖTEMANN SW, VAN RENSBURG P, RISTOW NE, WENTZEL MC, LOEWENTHAL RE and EKAMA GA (2005b) Integrated chemical/physical and biological processes modelling Part 2-Anaerobic digestion of sewage sludges. *Water SA* **31** (4) 545-568.

STUMM W and MORGAN JJ (1996) *Aquatic Chemistry-Chemical Equilibria and Rates in Natural Waters* (3^{rd} ed.). John Wiley & Sons, Inc.

UEKI K, KOTAKA K, ITOH K and UEKI A (1988) Potential availability of anaerobic treatment with digester slurry of animal waste for the reclamation of acid mine water containing sulphate and heavy metals. *J. Ferment. Technol.* **66** 43-50.

VAN RENSBURG P, WENTZEL MC and EKAMA GA (2001) Integrated modelling of the chemical, biological and physical processes in anaerobic digestion of primary sludge. Research Report No. W113, University of Cape Town, Dept. of Civil Eng., Cape Town, South Africa.

VANHOOREN H, MEIRLAEN J, AMERLINCK Y, CLAEYS F, VANGHELUWE H and VANROLLEGHEM PA (2003) WEST: Modelling biological wastewater treatment. *J. Hydroinformatics* **5** (1) 27-50.

WHITTINGTON-JONES KJ, CORBETT CJ and ROSE PD (2002) The Rhodes BioSURE Process ® - Part 2: Enhanched hydrolysis of organic carbon substrates - Development of the recycling sludge bed reactor. WRC Report No. TT 196/02, Water Research Commission, PO Box 824, Pretoria 0001, South Africa.

WISA (2005) At the forefront of wastewater technology. *Water Sewage & Effluent* **25** (4) 36-37.

WRC (2005) Mine Water Pollution: Research seeks answers for century-old problem. *The Water Wheel* **4** (2) 16-21.

APPENDIX A

UCT ANAEROBIC DIGESTION MODEL NO. 1 (UCTADM1)

Table A-1: Petersen matrix representation of biochemical rate coefficients ($\upsilon_{i,j}$) and kinetic process rate equations (ρ_j) for components (i = 1-27, j = 1-30) in the UCTADM1 (excluding sulphate reduction)

Component →	i	1	2	3	4	5	6	7	8	9	10	11	12	13	14	15	16	17	18	19	20	21	22	23	24	25	26	27	Process Rate (ρ)
j	Process ↓	H_2O	HPr	Pr^-	HAc	Ac^-	NH_4^+	NH_3	H_2	H^+	OH^-	$H_2PO_4^-$	$H_2PO_4^-$	HPO_4^{2-}	PO_4^{3-}	H_2CO_3	HCO_3^-	CO_3^{2-}	S_{bs}	S_{ch}	S_{bp}	S_{up}	Z_{ac}	Z_{ae}	Z_{am}	Z_{hm}	$CH_4(g)$	$CO_2(g)$	
1	Hydrolysis							$\frac{PsN\times MW_{NH_3}}{\frac{Hydrolysis\ Prot}{2}\times AW_O}$								$\frac{\left(\frac{6\times Hydrolysis\ Prot}{24}-PsC\right)\times MW_{CO_2}}{\frac{Hydrolysis\ Prot}{2}\times AW_O}$			$\frac{\frac{Hydrolysis\ Prot}{24}\times MW_{C_6H_{12}O_6}}{\frac{Hydrolysis\ Prot}{2}\times AW_O}$		−1									ρ_1
2	Acidogenesis (low and high pH_2)				$\frac{2}{Y_{ai}}$		−1		$\frac{4}{Y_{ai}}$	1						$\frac{2}{Y_{ai}}$			$-\frac{1+\frac{5}{6}Y_{ai}}{Y_{ai}}$				1					ρ_2
3	Acidogenesis (high pH_2 only)		$\frac{1}{Y_{ai}}$		$\frac{1}{Y_{ai}}$		−1		$\frac{1}{Y_{ai}}$	1									$-\frac{1+\frac{5}{6}Y_{ai}}{Y_{ai}}$				1					ρ_3
4	Acidogen Endogenous Decay							$(1-Endogenous\ Prot\times PsN)$								$(5-Endogenous\ Prot\times PsC)$					160		−1						ρ_4
5	Acetogenesis		$-\frac{1+\frac{3}{2}Y_{ae}}{Y_{ae}}$		$\frac{1}{Y_{ae}}$		−1		$\frac{1}{2}+\frac{3}{Y_{ae}}$	1						$\left(\frac{1}{Y_{ae}}-\frac{1}{2}\right)$								1					ρ_5
6	Acetogen Endogenous Decay							$(1-Endogenous\ Prot\times PsN)$								$(5-Endogenous\ Prot\times PsC)$					160			−1					ρ_6
7	Acetoclastic Methanogenesis				$-\frac{1+\frac{5}{2}Y_{am}}{Y_{am}}$		−1			1						$\frac{1}{Y_{am}}$									1		$\frac{1}{Y_{am}}$		ρ_7
8	Acetoclastic Methanogen Endogenous Decay							$(1-Endogenous\ Prot\times PsN)$								$(5-Endogenous\ Prot\times PsC)$					160				−1				ρ_8
9	Hydrogenotrophic Methanogenesis						−1		$-\frac{4+10Y_{hm}}{Y_{hm}}$	1						$-\frac{1+5Y_{hm}}{Y_{hm}}$										1	$\frac{1}{Y_{hm}}$		ρ_9
10	Hydrogenotrophic Methanogen Endogenous Decay							$(1-Endogenous\ Prot\times PsN)$								$(5-Endogenous\ Prot\times PsC)$					160					−1			ρ_{10}
11	Forward Dissociation of H_3PO_4									1		−1	1																ρ_{11}
12	Reverse Dissociation of H_2PO_4									−1		1	−1																ρ_{12}
13	Forward Dissociation of $H_2PO_4^-$									1			−1	1															ρ_{13}
14	Reverse Dissociation of $H_2PO_4^-$									−1			1	−1															ρ_{14}
15	Forward Dissociation of HPO_4^{2-}									1				−1	1														ρ_{15}
16	Reverse Dissociation of HPO_4^{2-}									−1				1	−1														ρ_{16}
17	Forward Dissociation of H_2CO_3									1						−1	1												ρ_{17}
18	Reverse Dissociation of H_2CO_3									−1						1	−1												ρ_{18}
19	Forward Dissociation of HCO_3^-									1							−1	1											ρ_{19}
20	Reverse Dissociation of HCO_3^-									−1							1	−1											ρ_{20}
21	Forward Dissociation of NH_4^+						−1	1		1																			ρ_{21}
22	Reverse Dissociation of NH_4^+						1	−1		−1																			ρ_{22}
23	Forward Dissociation of HPr		−1	1						1																			ρ_{23}
24	Reverse Dissociation of HPr		1	−1						−1																			ρ_{24}
25	Forward Dissociation of HAc				−1	1				1																			ρ_{25}
26	Reverse Dissociation of HAc				1	−1				−1																			ρ_{26}
27	Forward Dissociation of H_2O									1	1																		ρ_{27}
28	Reverse Dissociation of H_2O									−1	−1																		ρ_{28}
29	Dissolution of $CO_2(g)$															1												−1	ρ_{29}
30	Expulsion of $CO_2(g)$															−1												1	ρ_{30}
	Unit		mol/ℓ	mol/ℓ	mol/ℓ	mol/ℓ	mol/ℓ	mol/ℓ	mol/ℓ	mol/ℓ	mol/ℓ	mol/ℓ	mol/ℓ	mol/ℓ	mol/ℓ	mol/ℓ	mol/ℓ	mol/ℓ	mol/ℓ	mol/ℓ	$gCOD/\ell$	$gCOD/\ell$	$gCOD/\ell$	mol/ℓ	mol/ℓ	mol/ℓ	mol/ℓ	mol/ℓ	mol/ℓ	

Table A-2: Key of process rates (ρ = 1-30) in Petersen matrix representation of the UCTADM1 (excluding sulphate reduction)

Process Rate (ρ)
ρ_1 : $\left(\frac{HydK\max \times \frac{[S_{bp}]}{[Z_{ai}]}}{Ks_{Hyd} + \frac{[S_{bp}]}{[Z_{ai}]}} \right) \times [Z_{ai}]$
ρ_2 : $\left(\frac{\mu \max_a \times [S_{bs}]}{Ks_a + [S_{bs}]} \right) \times \left(1 - \frac{[H_2]}{K_{H_2} + [H_2]} \right) \times [Z_{ai}]$
ρ_3 : $\left(\frac{\mu \max_a \times [S_{bs}]}{Ks_a + [S_{bs}]} \right) \times \left(\frac{[H_2]}{K_{H_2} + [H_2]} \right) \times [Z_{ai}]$
ρ_4 : $b_a \times [Z_{ai}]$
ρ_5 : $\left(\frac{\mu \max_{ae} \times [H\,\mathrm{Pr}]}{Ks_{ae} + [H\,\mathrm{Pr}]} \right) \times \left(1 - \frac{[H_2]}{K_{H_2} + [H_2]} \right) \times [Z_{ae}]$
ρ_6 : $b_{ae} \times [Z_{ae}]$
ρ_7 : $\left(\frac{\mu \max_{am} \times [HAc]}{(Ks_{am} + [HAc]) \times \left(1 + \frac{[H]}{Ki_{am}} \right)} \right) \times [Z_{am}]$
ρ_8 : $b_{am} \times [Z_{am}]$
ρ_9 : $\left(\frac{\mu \max_{hm} \times [H_2]}{(Ks_{hm} + [H_2]) \times \left(1 + \frac{[H]}{Ki_{hm}} \right)} \right) \times [Z_{hm}]$
ρ_{10} : $b_{hm} \times [Z_{hm}]$
ρ_{11} : $Kf_{p1} \times [H_3PO_4]$

ρ_{12} : $Kr_{p1} \times [H_2PO_4] \times [H]$

ρ_{13} : $Kf_{p2} \times [H_2PO_4]$

ρ_{14} : $Kr_{p2} \times [HPO_4] \times [H]$

ρ_{15} : $Kf_{p3} \times [HPO_4]$

ρ_{16} : $Kr_{p3} \times [PO_4] \times [H]$

ρ_{17} : $Kf_{c1} \times [H_2CO_3]$

ρ_{18} : $Kr_{c1} \times [HCO_3] \times [H]$

ρ_{19} : $Kf_{c2} \times [HCO_3]$

ρ_{20} : $Kr_{c2} \times [CO_3] \times [H]$

ρ_{21} : $Kf_n \times [NH_4]$

ρ_{22} : $Kr_n \times [NH_3] \times [H]$

ρ_{23} : $Kf_{\mathrm{Pr}} \times [H\,\mathrm{Pr}]$

ρ_{24} : $Kr_{\mathrm{Pr}} \times [\mathrm{Pr}] \times [H]$

ρ_{25} : $Kf_a \times [HAc]$

P_{26} : $Kr_a \times [Ac] \times [H]$

ρ_{27} : Kf_W

ρ_{28} : $Kr_W \times [OH] \times [H]$

ρ_{29} : $Kr_{CO_2} \times p_{CO_2} \times KH_{CO_2}$

ρ_{30} : $Kr_{CO_2} \times [H_2CO_3]$

Table A-3: Petersen matrix representation of biochemical rate coefficients ($\upsilon_{i,j}$) and kinetic process rate equations (ρ_j) for water (i = 1; j = 1-42)

and soluble components (i = 2-13; j = 1-42) in the UCTADM1 (including sulphate reduction)

Component →	i	1	2	3	4	5	6	7	8	9	10	11	12	13	Process Rate (ρ_j)
j	**Process ↓**	H_2O	HPr	Pr^-	HAc	Ac^-	NH_4^+	NH_3	H_2	H^+	OH^-	H_3PO_4	$H_2PO_4^-$	HPO_4^{2-}	
1	Hydrolysis							$\left(\frac{\frac{PsN\times MW_{NH_3}}{Hydrolysis\ Prot\times AW_O}}{\frac{2}{MW_{NH_3}}}\right)\times MW_{NH_3}\times 1000$							ρ_1
2	Acidogenesis (low and high pH_2)				$\frac{2}{Y_{ai}}\times MW_{HAc}\times 1000$		$-1\times MW_{NH_4}\times 1000$		$\frac{4}{Y_{ai}}\times MW_{H_2}\times 1000$	$1\times MW_H\times 1000$					ρ_2
3	Acidogenesis (high pH_2 only)		$\frac{1}{Y_{ai}}\times MW_{HPr}\times 1000$		$\frac{1}{Y_{ai}}\times MW_{HAc}\times 1000$		$-1\times MW_{NH_4}\times 1000$		$\frac{1}{Y_{ai}}\times MW_{H_2}\times 1000$	$1\times MW_H\times 1000$					ρ_3
4	Acidogen Endogenous Decay							$(1-Endogenous\ Prot\times PsN)\times MW_{NH_3}\times 1000$							ρ_4
5	Acetogenesis		$\left(-\frac{1+\frac{3}{2}Y_{ae}}{Y_{ae}}\right)\times MW_{HPr}\times 1000$		$\frac{1}{Y_{ae}}\times MW_{HAc}\times 1000$		$-1\times MW_{NH_4}\times 1000$		$\left(\frac{1}{2}+\frac{3}{Y_{ae}}\right)\times MW_{H_2}\times 1000$	$1\times MW_H\times 1000$					ρ_5
6	Acetogen Endogenous Decay							$(1-Endogenous\ Prot\times PsN)\times MW_{NH_3}\times 1000$							ρ_6
7	Acetoclastic Methanogenesis				$\left(-\frac{1+\frac{5}{2}Y_{am}}{Y_{am}}\right)\times MW_{HAc}\times 1000$		$-1\times MW_{NH_4}\times 1000$			$1\times MW_H\times 1000$					ρ_7
8	Acetoclastic Methanogen Endogenous Decay							$(1-Endogenous\ Prot\times PsN)\times MW_{NH_3}\times 1000$							ρ_8
9	Hydrogenotrophic Methanogenesis						$-1\times MW_{NH_4}\times 1000$		$\left(-\frac{4+10Y_{hm}}{Y_{hm}}\right)\times MW_{H_2}\times 1000$	$1\times MW_H\times 1000$					ρ_9
10	Hydrogenotrophic Methanogen Endogenous Decay							$(1-Endogenous\ Prot\times PsN)\times MW_{NH_3}\times 1000$							ρ_{10}
11	Acetogenic Sulphidogenesis		$-\frac{1}{Y_{ps}}\times MW_{HPr}\times 1000$		$\left(\frac{1}{Y_{ps}}-\frac{3}{2}\right)\times MW_{HAc}\times 1000$		$-1\times MW_{NH_4}\times 1000$		$\frac{1}{2}\times MW_{H_2}\times 1000$	$\left(\frac{13}{4}-\frac{3}{2Y_{ps}}\right)\times MW_H\times 1000$					ρ_{11}
12	Acetogenic Sulphidogen Endogenous Decay							$0.761\times MW_{NH_3}\times 1000$							ρ_{12}
13	Acetoclastic Sulphidogenesis				$-\frac{1}{Y_{as}}\times MW_{HAc}\times 1000$		$-1\times MW_{NH_4}\times 1000$			$\left(6-\frac{2}{Y_{as}}\right)\times MW_H\times 1000$					ρ_{13}
14	Acetoclastic Sulphidogen Endogenous Decay							$0.761\times MW_{NH_3}\times 1000$							ρ_{14}
15	Hydrogenotrophic Sulphidogenesis						$-1\times MW_{NH_4}\times 1000$		$-\frac{1}{Y_{hs}}\times MW_{H_2}\times 1000$	$\left(6-\frac{1}{2Y_{hs}}\right)\times MW_H\times 1000$					ρ_{15}
16	Hydrogenotrophic Sulphidogen Endogenous Decay							$0.761\times MW_{NH_3}\times 1000$							ρ_{16}
17	Forward Dissociation of H_2S(aq)									$1\times MW_H\times 1000$					ρ_{17}
18	Reverse Dissociation of H_2S(aq)									$-1\times MW_H\times 1000$					ρ_{18}
19	Forward Dissociation of HS^-									$1\times MW_H\times 1000$					ρ_{19}
20	Reverse Dissociation of HS^-									$-1\times MW_H\times 1000$					ρ_{20}
21	Forward Dissociation of H_3PO_4									$1\times MW_H\times 1000$		$-1\times MW_{H_3PO_4}\times 1000$	$1\times MW_{H_2PO_4}\times 1000$		ρ_{21}
22	Reverse Dissociation of H_3PO_4									$-1\times MW_H\times 1000$		$1\times MW_{H_3PO_4}\times 1000$	$-1\times MW_{H_2PO_4}\times 1000$		ρ_{22}
23	Forward Dissociation of $H_2PO_4^-$									$1\times MW_H\times 1000$			$-1\times MW_{H_2PO_4}\times 1000$	$1\times MW_{HPO_4}\times 1000$	ρ_{23}
24	Reverse Dissociation of $H_2PO_4^-$									$-1\times MW_H\times 1000$			$1\times MW_{H_2PO_4}\times 1000$	$-1\times MW_{HPO_4}\times 1000$	ρ_{24}
25	Forward Dissociation of HPO_4^{2-}									$1\times MW_H\times 1000$				$-1\times MW_{HPO_4}\times 1000$	ρ_{25}
26	Reverse Dissociation of HPO_4^{2-}									$-1\times MW_H\times 1000$				$1\times MW_{HPO_4}\times 1000$	ρ_{26}
27	Forward Dissociation of H_2CO_3									$1\times MW_H\times 1000$					ρ_{27}
28	Reverse Dissociation of H_2CO_3									$-1\times MW_H\times 1000$					ρ_{28}
29	Forward Dissociation of HCO_3^-									$1\times MW_H\times 1000$					ρ_{29}
30	Reverse Dissociation of HCO_3^-									$-1\times MW_H\times 1000$					ρ_{30}
31	Forward Dissociation of NH_4^+						$-1\times MW_{NH_4}\times 1000$	$1\times MW_{NH_3}\times 1000$		$1\times MW_H\times 1000$					ρ_{31}
32	Reverse Dissociation of NH_4^+						$1\times MW_{NH_4}\times 1000$	$-1\times MW_{NH_3}\times 1000$		$-1\times MW_H\times 1000$					ρ_{32}
33	Forward Dissociation of HPr		$-1\times MW_{HPr}\times 1000$	$1\times MW_{Pr}\times 1000$						$1\times MW_H\times 1000$					ρ_{33}
34	Reverse Dissociation of HPr		$1\times MW_{HPr}\times 1000$	$-1\times MW_{Pr}\times 1000$						$-1\times MW_H\times 1000$					ρ_{34}
35	Forward Dissociation of HAc				$-1\times MW_{HAc}\times 1000$	$1\times MW_{Ac}\times 1000$				$1\times MW_H\times 1000$					ρ_{35}
36	Reverse Dissociation of HAc				$1\times MW_{HAc}\times 1000$	$-1\times MW_{Ac}\times 1000$				$-1\times MW_H\times 1000$					ρ_{36}
37	Forward Dissociation of H_2O									$1\times MW_H\times 1000$	$1\times MW_{OH}\times 1000$				ρ_{37}
38	Reverse Dissociation of H_2O									$-1\times MW_H\times 1000$	$-1\times MW_{OH}\times 1000$				ρ_{38}
39	Dissolution of CO_2(g)														ρ_{39}
40	Expulsion of CO_2(g)														ρ_{40}
41	Dissolution of H_2S(g)														ρ_{41}
42	Expulsion of H_2S(g)														ρ_{42}
	Unit		g/m^3	g/m^3	g/m^3	g/m^3	g/m^3	g/m^3	g/m^3	g/m^3	g/m^3	g/m^3	g/m^3	g/m^3	

Table A-4: Petersen matrix representation of biochemical rate coefficients ($\upsilon_{i,j}$) and kinetic process rate equations (ρ_j) for soluble components (i = 14-22; j = 1-42)

in the UCTADM1 (including sulphate reduction)

Component →	i	14	15	16	17	18	19	20	21	22	Process Rate (ρ)
j	**Process ↓**	PO_4^{3-}	H_2CO_3	HCO_3^-	CO_3^{2-}	SO_4^{2-}	H_2S(aq)	HS^-	S^{2-}	S_{ln}	
1	Hydrolysis		$-\left(\frac{\left(\frac{6\times Hydrolysis\ Prot}{24}-PsC\right)\times MW_{CO_2}}{\frac{Hydrolysis\ Prot}{2}\times AW_O}\right)\times MW_{H_2CO_3}\times 1000$							$\left(\frac{\frac{Hydrolysis\ Prot}{24}\times MW_{C_6H_{10}O_5}}{\frac{Hydrolysis\ Prot}{2}\times AW_O}\right)\times MW_{C_6H_{10}O_5}\times 1000$	ρ_1
2	Acidogenesis (low and high pH_2)		$\frac{2}{Y_{ai}}\times MW_{H_2CO_3}\times 1000$							$-\frac{1+\frac{5}{6}Y_{ai}}{Y_{ai}}\times MW_{C_6H_{10}O_5}\times 1000$	ρ_2
3	Acidogenesis (high pH_2 only)									$-\frac{1+\frac{5}{6}Y_{ai}}{Y_{ai}}\times MW_{C_6H_{10}O_5}\times 1000$	ρ_3
4	Acidogen Endogenous Decay		$(5-Endogenous\ Prot\times PsC)\times MW_{H_2CO_3}\times 1000$								ρ_4
5	Acetogenesis		$\left(\frac{1}{Y_{ac}}-\frac{1}{2}\right)\times MW_{H_2CO_3}\times 1000$								ρ_5
6	Acetogen Endogenous Decay		$(5-Endogenous\ Prot\times PsC)\times MW_{H_2CO_3}\times 1000$								ρ_6
7	Acetoclastic Methanogenesis		$\frac{1}{Y_{am}}\times MW_{H_2CO_3}\times 1000$								ρ_7
8	Acetoclastic Methanogen Endogenous Decay		$(5-Endogenous\ Prot\times PsC)\times MW_{H_2CO_3}\times 1000$								ρ_8
9	Hydrogenotrophic Methanogenesis		$\left(-\frac{1+5Y_{hm}}{Y_{hm}}\right)\times MW_{H_2CO_3}\times 1000$								ρ_9
10	Hydrogenotrophic Methanogen Endogenous Decay		$(5-Endogenous\ Prot\times PsC)\times MW_{H_2CO_3}\times 1000$								ρ_{10}
11	Acetogenic Sulphidogenesis		$\left(\frac{1}{Y_{as}}-2\right)\times MW_{H_2CO_3}\times 1000$			$-\left(\frac{3}{4Y_{as}}-\frac{9}{8}\right)\times MW_{SO_4}\times 1000$	$\left(\frac{3}{4Y_{as}}-\frac{9}{8}\right)\times MW_{H_2S}\times 1000$				ρ_{11}
12	Acetogenic Sulphidogen Endogenous Decay		$0.7335\times MW_{H_2CO_3}\times 1000$								ρ_{12}
13	Acetoclastic Sulphidogenesis		$\left(\frac{2}{Y_{as}}-5\right)\times MW_{H_2CO_3}\times 1000$			$-\left(\frac{1}{Y_{as}}-\frac{5}{2}\right)\times MW_{SO_4}\times 1000$	$\left(\frac{1}{Y_{as}}-\frac{5}{2}\right)\times MW_{H_2S}\times 1000$				ρ_{13}
14	Acetoclastic Sulphidogen Endogenous Decay		$0.7335\times MW_{H_2CO_3}\times 1000$								ρ_{14}
15	Hydrogenotrophic Sulphidogenesis		$-5\times MW_{H_2CO_3}\times 1000$			$-\left(\frac{1}{4Y_{hs}}-\frac{5}{2}\right)\times MW_{SO_4}\times 1000$	$\left(\frac{1}{4Y_{hs}}-\frac{5}{2}\right)\times MW_{H_2S}\times 1000$				ρ_{15}
16	Hydrogenotrophic Sulphidogen Endogenous Decay		$0.7335\times MW_{H_2CO_3}\times 1000$								ρ_{16}
17	Forward Dissociation of H_2S(aq)						$-1\times MW_{H_2S}\times 1000$	$1\times MW_{HS}\times 1000$			ρ_{17}
18	Reverse Dissociation of H_2S(aq)						$1\times MW_{H_2S}\times 1000$	$-1\times MW_{HS}\times 1000$			ρ_{18}
19	Forward Dissociation of HS^-							$-1\times MW_{HS}\times 1000$	$1\times MW_S\times 1000$		ρ_{19}
20	Reverse Dissociation of HS^-							$1\times MW_{HS}\times 1000$	$-1\times MW_S\times 1000$		ρ_{20}
21	Forward Dissociation of H_3PO_4										ρ_{21}
22	Reverse Dissociation of H_3PO_4										ρ_{22}
23	Forward Dissociation of $H_2PO_4^-$										ρ_{23}
24	Reverse Dissociation of $H_2PO_4^-$										ρ_{24}
25	Forward Dissociation of HPO_4^{2-}	$1\times MW_{PO_4}\times 1000$									ρ_{25}
26	Reverse Dissociation of HPO_4^{2-}	$-1\times MW_{PO_4}\times 1000$									ρ_{26}
27	Forward Dissociation of H_2CO_3		$-1\times MW_{H_2CO_3}\times 1000$	$1\times MW_{HCO_3}\times 1000$							ρ_{27}
28	Reverse Dissociation of H_2CO_3		$1\times MW_{H_2CO_3}\times 1000$	$-1\times MW_{HCO_3}\times 1000$							ρ_{28}
29	Forward Dissociation of HCO_3^-			$-1\times MW_{HCO_3}\times 1000$	$1\times MW_{CO_3}\times 1000$						ρ_{29}
30	Reverse Dissociation of HCO_3^-			$1\times MW_{HCO_3}\times 1000$	$-1\times MW_{CO_3}\times 1000$						ρ_{30}
31	Forward Dissociation of NH_4^+										ρ_{31}
32	Reverse Dissociation of NH_4^+										ρ_{32}
33	Forward Dissociation of HPr										ρ_{33}
34	Reverse Dissociation of HPr										ρ_{34}
35	Forward Dissociation of HAc										ρ_{35}
36	Reverse Dissociation of HAc										ρ_{36}
37	Forward Dissociation of H_2O										ρ_{37}
38	Reverse Dissociation of H_2O										ρ_{38}
39	Dissolution of CO_2(g)		$1\times MW_{H_2CO_3}\times 1000$								ρ_{39}
40	Expulsion of CO_2(g)		$-1\times MW_{H_2CO_3}\times 1000$								ρ_{40}
41	Dissolution of H_2S(g)						$1\times MW_{H_2S}\times 1000$				ρ_{41}
42	Expulsion of H_2S(g)						$-1\times MW_{H_2S}\times 1000$				ρ_{42}
	Unit	g/m^3	g/m^3	g/m^3	g/m^3	g/m^3	g/m^3	g/m^3	g/m^3	g/m^3	

Table A-5: Petersen matrix representation of biochemical rate coefficients ($\upsilon_{i,j}$) and kinetic process rate equations (ρ_j) for particulate components (i = 23-32; j = 1-42) in the UCTADM1 (including sulphate reduction)

Component →	i	23	24	25	26	27	28	29	30	31	32	Process Rate (ρ)
j	Process ↓	S_{us}	S_{bp}	S_{up}	Z_{ai}	Z_{ae}	Z_{am}	Z_{hm}	Z_{ps}	Z_{as}	Z_{hs}	
1	Hydrolysis		-1×1000									ρ_1
2	Acidogenesis (low and high pH_2)				$1\times MW_{C_5H_7O_2N}\times1000$							ρ_2
3	Acidogenesis (high pH_2 only)				$1\times MW_{C_5H_7O_2N}\times1000$							ρ_3
4	Acidogen Endogenous Decay		160×1000		$-1\times MW_{C_5H_7O_2N}\times1000$							ρ_4
5	Acetogenesis					$1\times MW_{C_5H_7O_2N}\times1000$						ρ_5
6	Acetogen Endogenous Decay		160×1000			$-1\times MW_{C_5H_7O_2N}\times1000$						ρ_6
7	Acetoclastic Methanogenesis						$1\times MW_{C_5H_7O_2N}\times1000$					ρ_7
8	Acetoclastic Methanogen Endogenous Decay		160×1000				$-1\times MW_{C_5H_7O_2N}\times1000$					ρ_8
9	Hydrogenotrophic Methanogenesis							$1\times MW_{C_5H_7O_2N}\times1000$				ρ_9
10	Hydrogenotrophic Methanogen Endogenous Decay		160×1000					$-1\times MW_{C_5H_7O_2N}\times1000$				ρ_{10}
11	Acetogenic Sulphidogenesis								$1\times MW_{C_5H_7O_2N}\times1000$			ρ_{11}
12	Acetogenic Sulphidogen Endogenous Decay		160×1000						$-1\times MW_{C_5H_7O_2N}\times1000$			ρ_{12}
13	Acetoclastic Sulphidogenesis									$1\times MW_{C_5H_7O_2N}\times1000$		ρ_{13}
14	Acetoclastic Sulphidogen Endogenous Decay		160×1000							$-1\times MW_{C_5H_7O_2N}\times1000$		ρ_{14}
15	Hydrogenotrophic Sulphidogenesis										$1\times MW_{C_5H_7O_2N}\times1000$	ρ_{15}
16	Hydrogenotrophic Sulphidogen Endogenous Decay		160×1000								$-1\times MW_{C_5H_7O_2N}\times1000$	ρ_{16}
17	Forward Dissociation of H_2S(aq)											ρ_{17}
18	Reverse Dissociation of H_2S(aq)											ρ_{18}
19	Forward Dissociation of HS^-											ρ_{19}
20	Reverse Dissociation of HS^-											ρ_{20}
21	Forward Dissociation of H_3PO_4											ρ_{21}
22	Reverse Dissociation of H_3PO_4											ρ_{22}
23	Forward Dissociation of $H_2PO_4^-$											ρ_{23}
24	Reverse Dissociation of $H_2PO_4^-$											ρ_{24}
25	Forward Dissociation of HPO_4^{2-}											ρ_{25}
26	Reverse Dissociation of HPO_4^{2-}											ρ_{26}
27	Forward Dissociation of H_2CO_3											ρ_{27}
28	Reverse Dissociation of H_2CO_3											ρ_{28}
29	Forward Dissociation of HCO_3^-											ρ_{29}
30	Reverse Dissociation of HCO_3^-											ρ_{30}
31	Forward Dissociation of NH_4^+											ρ_{31}
32	Reverse Dissociation of NH_4^+											ρ_{32}
33	Forward Dissociation of HPr											ρ_{33}
34	Reverse Dissociation of HPr											ρ_{34}
35	Forward Dissociation of HAc											ρ_{35}
36	Reverse Dissociation of HAc											ρ_{36}
37	Forward Dissociation of H_2O											ρ_{37}
38	Reverse Dissociation of H_2O											ρ_{38}
39	Dissolution of CO_2(g)											ρ_{39}
40	Expulsion of CO_2(g)											ρ_{40}
41	Dissolution of H_2S(g)											ρ_{41}
42	Expulsion of H_2S(g)											ρ_{42}
	Unit	$gCOD/m^3$	$gCOD/m^3$	$gCOD/m^3$	g/m^3	g/m^3	g/m^3	g/m^3	g/m^3	g/m^3	g/m^3	

Table A-6: Petersen matrix representation of biochemical rate coefficients ($\upsilon_{i,j}$) and kinetic process rate equations (ρ_j) for gaseous components (i = 33-35; j = 1-42) in the UCTADM1 (including sulphate reduction)

Component →	i	33	34	35	Process Rate (ρ)
j	Process ↓	CH_4(g)	CO_2(g)	H_2S(g)	
1	Hydrolysis				ρ_1
2	Acidogenesis (low and high pH_2)				ρ_2
3	Acidogenesis (high pH_2 only)				ρ_3
4	Acidogen Endogenous Decay				ρ_4
5	Acetogenesis				ρ_5
6	Acetogen Endogenous Decay				ρ_6
7	Acetoclastic Methanogenesis	$\frac{1}{Y_{am}} \times MW_{CH_4} \times 1000$			ρ_7
8	Acetoclastic Methanogen Endogenous Decay				ρ_8
9	Hydrogenotrophic Methanogenesis	$\frac{1}{Y_{hm}} \times MW_{CH_4} \times 1000$			ρ_9
10	Hydrogenotrophic Methanogen Endogenous Decay				ρ_{10}
11	Acetogenic Sulphidogenesis				ρ_{11}
12	Acetogenic Sulphidogen Endogenous Decay				ρ_{12}
13	Acetoclastic Sulphidogenesis				ρ_{13}
14	Acetoclastic Sulphidogen Endogenous Decay				ρ_{14}
15	Hydrogenotrophic Sulphidogenesis				ρ_{15}
16	Hydrogenotrophic Sulphidogen Endogenous Decay				ρ_{16}
17	Forward Dissociation of $H_2S_{(aq)}$				ρ_{17}
18	Reverse Dissociation of $H_2S_{(aq)}$				ρ_{18}
19	Forward Dissociation of HS^-				ρ_{19}
20	Reverse Dissociation of HS^-				ρ_{20}
21	Forward Dissociation of H_3PO_4				ρ_{21}
22	Reverse Dissociation of H_3PO_4				ρ_{22}
23	Forward Dissociation of $H_2PO_4^-$				ρ_{23}
24	Reverse Dissociation of $H_2PO_4^-$				ρ_{24}
25	Forward Dissociation of HPO_4^{2-}				ρ_{25}
26	Reverse Dissociation of HPO_4^{2-}				ρ_{26}
27	Forward Dissociation of H_2CO_3				ρ_{27}
28	Reverse Dissociation of H_2CO_3				ρ_{28}
29	Forward Dissociation of HCO_3^-				ρ_{29}
30	Reverse Dissociation of HCO_3^-				ρ_{30}
31	Forward Dissociation of NH_4^+				ρ_{31}
32	Reverse Dissociation of NH_4^+				ρ_{32}
33	Forward Dissociation of HPr				ρ_{33}
34	Reverse Dissociation of HPr				ρ_{34}
35	Forward Dissociation of HAc				ρ_{35}
36	Reverse Dissociation of HAc				ρ_{36}
37	Forward Dissociation of H_2O				ρ_{37}
38	Reverse Dissociation of H_2O				ρ_{38}
39	Dissolution of CO_2(g)		$-1 \times MW_{CO_2} \times 1000$		ρ_{39}
40	Expulsion of CO_2(g)		$1 \times MW_{CO_2} \times 1000$		ρ_{40}
41	Dissolution of H_2S(g)			$-1 \times MW_{H_2S} \times 1000$	ρ_{41}
42	Expulsion of H_2S(g)			$1 \times MW_{H_2S} \times 1000$	ρ_{42}
	Unit	g/m^3	g/m^3	g/m^3	

Table A-7: Key of process rates (ρ = 1-42) in Petersen matrix representation of the UCTADM1 (including sulphate reduction)

	Process Rate (ρ)
ρ_1 :	$\left(\frac{HydK\max\times\frac{[S_{bp}]}{[Z_{ai}]}}{\frac{Ks_{Hyd}}{MW_{C_5H_7O_2N}}+\frac{[S_{bp}]}{[Z_{ai}]}}\right)\times\left(\frac{[Z_{ai}]}{[MW_{C_5H_7O_2N}\times1000]}\right)$
ρ_2 :	$\left(\frac{\mu\max_a\times[S_{bs}]}{(Ks_a\times MW_{C_6H_{12}O_6}\times1000)+[S_{bs}]}\right)\times\left(1-\frac{[H_2]}{(K_{H_2}\times MW_{H_2}\times1000)+[H_2]}\right)\times\left(\frac{[Z_{ai}]}{MW_{C_5H_7O_2N}\times1000}\right)$ $\times\exp\left(-\left(\frac{[H_2Saq]}{0.6065\times Ki_{ais}\times MW_{H_2S}\times1000}\right)^2\right)$
ρ_3 :	$\left(\frac{\mu\max_a\times[S_{bs}]}{(Ks_a\times MW_{C_6H_{12}O_6}\times1000)+[S_{bs}]}\right)\times\left(\frac{[H_2]}{(K_{H_2}\times MW_{H_2}\times1000)+[H_2]}\right)\times\left(\frac{[Z_{ai}]}{MW_{C_5H_7O_2N}\times1000}\right)\times\exp\left(-\left(\frac{[H_2Saq]}{0.6065\times Ki_{ais}\times MW_{H_2S}\times1000}\right)^2\right)$
ρ_4 :	$\left(\frac{b_a}{MW_{C_5H_7O_2N}\times1000}\right)\times[Z_{ai}]$

ρ_5 :

$$\left(\frac{\mu\max_{ae}\times\left(\left[H\,\mathrm{Pr}\right]+\left[\mathrm{Pr}\right]\right)}{((Ks_{ae}\times MW_{\mathrm{Pr}}\times 1000)+\left[H\,\mathrm{Pr}\right]+\left[\mathrm{Pr}\right])}\right)\times\left(1-\frac{\left[H_2\right]}{(K_{H_2}\times MW_{H_2}\times 1000)+\left[H_2\right]}\right)\times\left(\frac{\left[Z_{ae}\right]}{(MW_{C_5H_7O_2N}\times 1000)}\right)$$

$$\times\exp\left(-\left(\frac{\left[H_2Saq\right]}{0.6065\times Ki_{aes}\times MW_{H_2S}\times 1000}\right)^2\right)$$

ρ_6 :

$$\left(\frac{b_{ae}}{\left(MW_{C_5H_7O_2N}\times 1000\right)}\right)\times\left[Z_{ae}\right]$$

ρ_7 :

$$\left(\frac{\mu\max_{am}\times\left(\left[HAc\right]+\left[Ac\right]\right)}{((Ks_{am}\times MW_{HAc}\times 1000)+\left[HAc\right]+\left[Ac\right])\times\left(1+\frac{\left[H\right]}{Ki_{am}\times MW_{H}\times 1000}\right)}\right)\times\left(\frac{\left[Z_{am}\right]}{(MW_{C_5H_7O_2N}\times 1000)}\right)$$

$$\times\exp\left(-\left(\frac{\left[H_2Saq\right]}{0.6065\times Ki_{ams}\times MW_{H_2S}\times 1000}\right)^2\right)$$

ρ_8 :

$$\left(\frac{b_{am}}{(MW_{C_5H_7O_2N}\times 1000)}\right)\times\left[Z_{am}\right]$$

ρ_9 :

$$\left(\frac{\mu\max_{hm}\times[H_2]}{((Ks_{hm}\times MW_{H_2}\times 1000)+[H_2])\times\left(1+\frac{[H]}{(Ki_{hm}\times MW_H\times 1000}\right)}\right)\times\left(\frac{[Z_{hm}]}{(MW_{C_5H_7O_2N}\times 1000)}\right)\times\exp\left(-\left(\frac{[H_2Saq]}{0.6065\times Ki_{hms}\times MW_{H_2S}\times 1000}\right)^2\right)$$

ρ_{10} :

$$\left(\frac{b_{hm}}{MW_{C_5H_7O_2N}\times 1000}\right)\times[Z_{hm}]$$

ρ_{11} :

$$\left(\frac{\mu\max_{ps}\times([H\,\mathrm{Pr}]+[\mathrm{Pr}])}{(Ks_{ps}\times MW_{H\,\mathrm{Pr}}\times 1000)+[H\,\mathrm{Pr}]+[\mathrm{Pr}]}\right)\times\left(1-\frac{[H_2Saq]}{(Ki_{ps}\times MW_{H_2S}\times 1000)}\right)\times\left(\frac{[SO_4]}{(Kn_{ps}\times MW_{SO_4}\times 1000)+[SO_4]}\right)\times\left(\frac{[Z_{ps}]}{(MW_{C_5H_7O_2N}\times 1000)}\right)$$
$$\times\exp\left(-\left(\frac{[H_2Saq]}{0.6065\times Ki_{ps}\times MW_{H_2S}\times 1000}\right)^2\right)$$

ρ_{12} :

$$\left(\frac{b_{ps}}{(MW_{C_5H_7O_2N}\times 1000)}\right)\times[Z_{ps}]$$

ρ_{13} :

$$\left(\frac{\mu\max_{as}\times([HAc]+[Ac])}{(Ks_{as}\times MW_{HAc}\times 1000)+[HAc]+[Ac]}\right)\times\left(1-\frac{[H_2Saq]}{(Ki_{as}\times MW_{H_2S}\times 1000)}\right)\times\left(\frac{[SO_4]}{(Kn_{as}\times MW_{SO_4}\times 1000)+[SO_4]}\right)\times\left(\frac{[Z_{as}]}{(MW_{C_5H_7O_2N}\times 1000)}\right)$$
$$\times\exp\left(-\left(\frac{[H_2Saq]}{0.6065\times Ki_{as}\times MW_{H_2S}\times 1000}\right)^2\right)$$

ρ_{14} :

$$\left(\frac{b_{as}}{\left(MW_{C_5H_7O_2N}\times 1000\right)}\right)\times\left[Z_{as}\right]$$

ρ_{15} :

$$\left(\frac{\mu\max_{hs}\times\left[H_2\right]}{(Ks_{hs}\times MW_{H_2}\times 1000)+\left[H_2\right]}\right)\times\left(1-\frac{\left[H_2Saq\right]}{(Ki_{hs}\times MW_{H_2S}\times 1000)}\right)\times\left(\frac{\left[SO_4\right]}{(Kn_{hs}\times MW_{SO_4}\times 1000)+\left[SO_4\right]}\right)\times\left(\frac{Z_{hs}}{\left(MW_{C_5H_7O_2N}\times 1000\right)}\right)$$
$$\times\exp\left(-\left(\frac{\left[H_2Saq\right]}{0.6065\times Ki_{hs}\times MW_{H_2S}\times 1000}\right)^2\right)$$

ρ_{16} :

$$\left(\frac{b_{hs}}{\left(MW_{C_5H_7O_2N}\times 1000\right)}\right)\times\left[Z_{hs}\right]$$

ρ_{17} :

$$\left(\frac{Kf_{HS}}{\left(MW_{H_2S}\times 1000\right)}\right)\times\left[H_2Saq\right]$$

ρ_{18} :

$$\left(\frac{Kr_{HS}}{\left(MW_{HS}\times MW_{H}\times 1000000\right)}\right)\times\left[HS\right]\times\left[H\right]$$

ρ_{19} :

$$\left(\frac{Kf_{S}}{\left(MW_{HS}\times 1000\right)}\right)\times\left[HS\right]$$

ρ_{20} : $\left(\frac{Kr_S}{(MW_S \times MW_H \times 1000000}\right) \times [S] \times [H]$

ρ_{21} : $\left(\frac{Kf_{p1}}{MW_{H_3PO_4} \times 1000}\right) \times [H_3PO_4]$

ρ_{22} : $\left(\frac{Kr_{p1}}{MW_{H_2PO_4} \times MW_H \times 1000000}\right) \times [H_2PO_4] \times [H]$

ρ_{23} : $\left(\frac{Kf_{p2}}{MW_{H_2PO_4} \times 1000}\right) \times [H_2PO_4]$

ρ_{24} : $\left(\frac{Kr_{p2}}{MW_{HPO_4} \times MW_H \times 1000000}\right) \times [HPO_4] \times [H]$

ρ_{25} : $\left(\frac{Kf_{p3}}{MW_{HPO_4} \times 1000}\right) \times [HPO_4]$

ρ_{26} : $\left(\frac{Kr_{p3}}{MW_{PO_4} \times MW_H \times 1000000}\right) \times [PO_4] \times [H]$

ρ_{27} : $\left(\frac{Kf_{c1}}{MW_{H_2CO_3}\times 1000}\right)\times[H_2CO_3]$

ρ_{28} : $\left(\frac{Kr_{c1}}{MW_{HCO_3}\times MW_H\times 1000000}\right)\times[HCO_3]\times[H]$

ρ_{29} : $\left(\frac{Kf_{c2}}{MW_{HCO_3}\times 1000}\right)\times[HCO_3]$

ρ_{30} : $\left(\frac{Kr_{c2}}{MW_{CO_3}\times MW_H\times 1000000}\right)\times[CO_3]\times[H]$

ρ_{31} : $\left(\frac{Kf_n}{MW_{NH_4}\times 1000}\right)\times[NH_4]$

ρ_{32} : $\left(\frac{Kr_n}{MW_{NH_3}\times MW_H\times 1000000}\right)\times[NH_3]\times[H]$

ρ_{33} : $\left(\frac{Kf_{\mathrm{Pr}}}{MW_{H\,\mathrm{Pr}}\times 1000}\right)\times[H\,\mathrm{Pr}]$

ρ_{34} : $\left(\frac{Kr_{\mathrm{Pr}}}{MW_{\mathrm{Pr}}\times MW_H\times 1000000}\right)\times[\mathrm{Pr}]\times[H]$

ρ_{35} : $\left(\frac{Kf_a}{MW_{HAc}\times 1000}\right)\times[HAc]$

P_{36} : $\left(\frac{Kr_a}{MW_{Ac}\times MW_H\times 1000000}\right)\times[Ac]\times[H]$

ρ_{37} : Kf_W

ρ_{38} : $\left(\frac{Kr_W}{MW_{OH}\times MW_H\times 1000000}\right)\times[OH]\times[H]$

ρ_{39} : $Kr_{CO_2}\times p_{CO_2}\times KH_{CO_2}$

ρ_{40} : $\left(\frac{Kr_{CO_2}}{MW_{H_2CO_3}\times 1000}\right)\times[H_2CO_3]$

ρ_{41} : $Kr_{H_2S}\times p_{H_2S}\times KH_{H_2S}$

ρ_{42} : $\left(\frac{Kr_{H_2S}}{(MW_{H_sS}\times 1000)}\right)\times[H_2Saq]$

Table A-8: Parameters used in UCTADM1

(NB. Kinetic constants apply to modelling and simulation of steady state experiments only)

Parameter	Value	Unit	Description
PsC	3.5	-	Relative proportion of carbon in feed material
PsH	7	-	Relative proportion of hydrogen in feed material
PsN	0.196	-	Relative proportion of nitrogen in feed material
PsO	2	-	Relative proportion of oxygen in feed material
AW_C	12.011	g/mol	Atomic weight of carbon
AW_H	1.0079	g/mol	Atomic weight of hydrogen
AW_N	14.007	g/mol	Atomic weight of nitrogen
AW_O	15.999	g/mol	Atomic weight of oxygen
AW_P	30.974	g/mol	Atomic weight of phosphorous
AW_S	32.064	g/mol	Atomic weight of sulphur
HydKmax	769	g S_{bp}/mol Z_{ai}. d	Hydrolysis maximum specific rate constant
μmax_a	0.8	d^{-1}	Acidogenic biomass maximum specific growth rate constant
μmax_{ae}	1.15	d^{-1}	Acetogenic biomass maximum specific growth rate constant
μmax_{am}	4.39	d^{-1}	Acetoclastic methanogen biomass maximum specific growth rate constant
μmax_{hm}	1.2	d^{-1}	Hydrogenotrophic methanogen biomass maximum specific growth rate constant

μmax_{as}	0.854	d^{-1}	Acetoclastic sulphidogen biomass maximum specific growth rate constant
μmax_{ps}	0.814	d^{-1}	Acetogenic sulphidogen biomass maximum specific growth rate constant
μmax_{hs}	3.908	d^{-1}	Hydrogenotrophic sulphidogen biomass maximum specific growth rate constant
b_a	0.041	d^{-1}	Acidogenic biomass decay constant
b_{ae}	0.015	d^{-1}	Acetogenic biomass decay constant
b_{am}	0.037	d^{-1}	Acetoclastic methanogen biomass decay constant
b_{hm}	0.01	d^{-1}	Hydrogenotrophic methanogen biomass decay constant
b_{as}	0.038	d^{-1}	Acetoclastic sulphidogen biomass decay constant
b_{ps}	0.026	d^{-1}	Acetogenic sulphidogen biomass decay constant
b_{hs}	0.084	d^{-1}	Hydrogenotrophic sulphidogen biomass decay constant
Y_{ai}	0.1074	mol VSS/mol COD	Acidogenic biomass yield coefficient
Y_{ae}	0.0278	mol VSS/mol COD	Acetogenic biomass yield coefficient
Y_{am}	0.0157	mol VSS/mol COD	Acetoclastic methanogen biomass yield coefficient
Y_{hm}	0.004	mol VSS/mol COD	Hydrogenotrophic methanogen biomass yield coefficient
Y_{as}	0.0187	mol VSS/mol COD	Acetoclastic sulphidogen biomass yield coefficient

Y_{ps}	0.0268	mol VSS/mol COD	Acetogenic sulphidogen biomass yield coefficient
Y_{hs}	0.0071	mol VSS/mol COD	Hydrogenotrophic sulphidogen biomass yield coefficient
Ks_{Hyd}	1225	g S_{bp}/mol Z_{ai}	Hydrolysis half saturation constant
Ks_a	7.80E-04	mol/ℓ	Acidogenic biomass half saturation constant
Ks_{ae}	8.90E-05	mol/ℓ	Acetogenic biomass half saturation constant
Ks_{am}	1.30E-05	mol/ℓ	Acetoclastic methanogen biomass half saturation constant
Ks_{hm}	1.56E-04	mol/ℓ	Hydrogenotrophic methanogen biomass half saturation constant
Ks_{as}	3.75E-04	mol/ℓ	Acetoclastic sulphidogen biomass half saturation constant
Ks_{ps}	2.63E-03	mol/ℓ	Acetogenic sulphidogen biomass half saturation constant
Ks_{hs}	4.38E-06	mol/ℓ	Hydrogenotrophic sulphidogen biomass half saturation constant
Kn_{as}	2.00E-04	mol/ℓ	Acetoclastic sulphidogen biomass half saturation constant for sulphate
Kn_{ps}	7.71E-05	mol/ℓ	Acetogenic sulphidogen biomass half saturation constant for sulphate
Kn_{hs}	2.00E-04	mol/ℓ	Hydrogenotrophic sulphidogen biomass half saturation constant for sulphate
K_{H2}	6.25E-04	mol H_2/ℓ	Hydrogen inhibition coefficient for high pH_2
Ki_{am}	1.15E-06	mol/ℓ	Acetoclastic methanogen biomass hydrogen ion inhibition constant

Ki_{hm}	5.30E-04	mol/ℓ	Hydrogenotrophic methanogen biomass hydrogen ion inhibition constant
Ki_{ais}	1.72E-02	mol/ℓ	Acidogenic biomass hydrogen sulphide inhibition constant
Ki_{aes}	5.94E-03	mol/ℓ	Acetogenic biomass hydrogen sulphide inhibition constant
Ki_{ams}	5.78E-03	mol/ℓ	Acetoclastic methanogen biomass hydrogen sulphide inhibition constant
Ki_{hms}	5.16E-03	mol/ℓ	Hydrogenotrophic methanogen biomass hydrogen sulphide inhibition constant
Ki_{as}	5.13E-03	mol/ℓ	Acetoclastic sulphidogen biomass hydrogen sulphide inhibition constant
Ki_{ps}	5.78E-03	mol/ℓ	Acetogenic sulphidogen biomass hydrogen sulphide inhibition constant
Ki_{hs}	1.72E-02	mol/ℓ	Hydrogenotrophic sulphidogen biomass hydrogen sulphide inhibition constant
Kr_{CO2}	1E+05	-	Reverse dissociation constant for CO2 expulsion
Kr_{H2S}	1E+07	-	Reverse dissociation constant for H2S expulsion
Kr_{HS}	1E+10	-	Reverse dissociation constant for $H_2S \leftrightarrow HS^- + H^+$
Kr_{Pr}	1E+12	-	Reverse dissociation constant for $HPr \leftrightarrow Pr^- + H^+$
Kr_S	1E+10	-	Reverse dissociation constant for $HS^- \leftrightarrow S^{2-} + H^+$

Kr_W	1E+11	-	Reverse dissociation constant for $H_2O \leftrightarrow OH^- + H^+$
Kr_a	1E+14	-	Reverse dissociation constant for $HAc \leftrightarrow Ac^- + H^+$
Kr_{c1}	1E+10	-	Reverse dissociation constant for $H_2CO_3 \leftrightarrow HCO_3^- + H^+$
Kr_{c2}	1E+10	-	Reverse dissociation constant for $HCO_3^- \leftrightarrow CO_3^{2-} + H^+$
Kr_n	1E+12	-	Reverse dissociation constant for $NH_4^+ \leftrightarrow NH_3 + H^+$
Kr_{p1}	1E+08	-	Reverse dissociation constant for $H_3PO_4 \leftrightarrow H_2PO_4^- + H^+$
Kr_{p2}	1E+12	-	Reverse dissociation constant for $H_2PO_4\text{-} \leftrightarrow HPO_4^{2-} + H^+$
Kr_{p3}	1E+15	-	Reverse dissociation constant for $HPO_4^{2-} \leftrightarrow PO_4^{3-} + H^+$
MW_{Ac}	60.0516	g/mol	Molecular weight of Ac^-
$MW_{C5H7O2N}$	113.1153	g/mol	Molecular weight of biomass
$MW_{C6H12O6}$	180.1548	g/mol	Molecular weight of $C_6H_{12}O_6$
MW_{CH4}	16.0426	g/mol	Molecular weight of CH_4
MW_{CO2}	44.009	g/mol	Molecular weight of CO_2
MW_{CO3}	60.008	g/mol	Molecular weight of CO_3
MW_{CaCO3}	100.086	g/mol	Molecular weight of $CaCO_3$
MW_H	1.0079	g/mol	Molecular weight of H^+
MW_{H2}	2.0158	g/mol	Molecular weight of H_2
MW_{H2CO3}	62.0238	g/mol	Molecular weight of H_2CO_3

MW_{H2O}	18.0148	g/mol	Molecular weight of H_2O
MW_{H2PO4}	96.9856	g/mol	Molecular weight of H_2PO_4
MW_{H2S}	34.0798	g/mol	Molecular weight of H_2S
MW_{H3PO4}	97.9935	g/mol	Molecular weight of H_3PO_4
MW_{HAc}	61.0595	g/mol	Molecular weight of HAc
MW_{HCO3}	61.0159	g/mol	Molecular weight of HCO_3^-
MW_{HPO4}	95.9777	g/mol	Molecular weight of HPO_4^{2-}
MW_{HPr}	74.0784	g/mol	Molecular weight of HPr
MW_{HS}	33.0719	g/mol	Molecular weight of HS^-
MW_{NH3}	17.0307	g/mol	Molecular weight of NH_3
MW_{NH4}	18.0386	g/mol	Molecular weight of NH_4
MW_{OH}	17.0069	g/mol	Molecular weight of OH^-
MW_{PO4}	94.9698	g/mol	Molecular weight of PO_4^{3-}
MW_{Pr}	73.0705	g/mol	Molecular weight of Pr^-
MW_S	32.064	g/mol	Molecular weight of S^{2-}
MW_{SO4}	96.06	g/mol	Molecular weight of SO_4^{2-}
Patm	1	atm	Atmospheric pressure
R	0.0820575	ℓ.atm/mol.K	Universal gas constant
R_s	-	d	Reactor retention time
T_c	-	^oC	Temperature in degrees Celsius
in_f_GlucCOD	1.0656835	-	Influent COD/Glucose Ratio
in_f_HAcCOD	1.06568	-	Influent COD/HAc Ratio
in_f_HPrCOD	1.5118172	-	Influent COD/HPr Ratio
in_f_N_Xi	0.12	-	Fraction of influent Nitrogen content in Biomass

in_f_N_bp	0.01	g N/g COD	Fraction of influent Nitrogen content in biodegradable particulate COD
in_f_N_up	0.03	g N/g COD	Fraction of influent Nitrogen content in unbiodegradable particulate COD
in_f_P_bp	0.0046	g P/g COD	Fraction of influent Phosphorous content in biodegradable particulate COD
in_f_P_up	0.0046	g P/g COD	Fraction of influent Phosphorous content in unbiodegradable particulate COD
f_$C_5H_7O_2N$COD	1.4145559	-	COD/biomass ratio
inSC	284	mS/m	Conductivity of the influent
k_{CO2}	11.365	-	Henry's law coefficient for CO_2
k_{H2S}	2.3705	-	Henry's law coefficient for H_2S
V_r	-	ℓ	Reactor volume

Table A-9: Variables and their respective equations used in UCTADM1

Variable and equation	Unit	Description
$C_T = [H_2CO_3] + [HCO_3] + [CO_3]$	-	Total concentration of dissolved carbon species in digester
$Endogenous\,\mathrm{Pr}ot = \frac{320}{Hydrolysis\,\mathrm{Pr}ot \times AW_O}$	-	Intermediate step to simplify calculation for endogenous respiration
$Hydrolysis\,\mathrm{Pr}ot = PsH + 4PsC - 2PsO - 3PsN$	-	Intermediate step to simplify calculation for hydrolysis
$KH_{CO_2} = 10^{-pKH_{CO_2}}$	-	Henry's Law constant for CO_2
$KH_{H_2S} = 10^{-pKH_{H_2S}}$	-	Henry's Law constant for H_2S
$K_a = 10^{-pK_a}$	-	Equilibrium constant for HAc/Ac system
$K_{c1} = \frac{10^{-pK_{c1}}}{f_m \times f_m}$	-	Equilibrium constant for H_2CO_3/HCO_3 system
$K_{c2} = \frac{10^{-pK_{c2}}}{f_d}$	-	Equilibrium constant for HCO_3/CO_3 system

$Kf_{HS} = Kr_{HS} \times \frac{10^{-pK_{HS}}}{f_m \times f_m}$	-	Forward dissociation constant for $H_2S \leftrightarrow HS^- + H^+$
$Kf_{\mathrm{Pr}} = Kr_{\mathrm{Pr}} \times \frac{10^{-pK_{\mathrm{Pr}}}}{f_m \times f_m}$	-	Forward dissociation constant for $HPr \leftrightarrow Pr^- + H^+$
$Kf_S = Kr_S \times \frac{10^{-pK_S}}{f_d}$	-	Forward dissociation constant for $HS^- \leftrightarrow S^{2-} + H^+$
$Kf_W = Kr_W \times \frac{10^{-pK_W}}{f_m \times f_m}$	-	Forward dissociation constant for $H_2O \leftrightarrow OH^- + H^+$
$Kf_a = Kr_a \times \frac{10^{-pK_a}}{f_m \times f_m}$	-	Forward dissociation constant for $HAc \leftrightarrow Ac^- + H^+$
$Kf_{c1} = Kr_{c1} \times \frac{10^{-pK_{c1}}}{f_m \times f_m}$	-	Forward dissociation constant for $H_2CO_3 \leftrightarrow HCO_3^- + H^+$
$Kf_{c2} = Kr_{c2} \times \frac{10^{-pK_{c2}}}{f_d}$	-	Forward dissociation constant for $HCO_3^- \leftrightarrow CO_3^{2-} + H^+$

$Kf_n = Kr_n \times 10^{-pK_n}$	-	Forward dissociation constant for $NH_4^+ \leftrightarrow NH_3 + H^+$
$Kf_{p1} = Kr_{p1} \times \frac{10^{-pK_{p1}}}{f_m \times f_m}$	-	Forward dissociation constant for $H_3PO_4 \leftrightarrow H_2PO_4^- + H^+$
$Kf_{p2} = Kr_{p2} \times \frac{10^{-pK_{p2}}}{f_d}$	-	Forward dissociation constant for $H_2PO_4^- \leftrightarrow HPO_4^{2-} + H^+$
$Kf_{p3} = Kr_{p3} \times 10^{-pK_{p3}} \times \frac{f_d}{f_t \times f_m}$	-	Forward dissociation constant for $HPO_4^{2-} \leftrightarrow PO_4^{3-} + H^+$
$K_n = 10^{-pK_n}$	-	Equilibrium constant for NH_3/NH_4 system
$K_p = 10^{-pK_{Pr}}$	-	Equilibrium constant for HPr/Pr system
$K_W = \frac{10^{-pK_W}}{f_m \times f_m}$	-	Equilibrium constant for water system
$Q_i = \frac{V_r}{R_s}$	ℓ/d	Influent flowrate
$SC = inSC$	mS/m	Specific conductivity

$T_k = T_c + 273.15$	K	Temperature in degrees Kelvin
$f_d = 10^{-\left(1825000-(78.3\times T_k)^{-1.5}\right)\times 4\times\left(\left(\frac{(0.000168\times SC)^{0.5}}{1+(0.000168\times SC)^{0.5}}\right)-0.3\times 0.000168\times SC\right)}$	-	Divalent activity coefficient
$f_m = 10^{-\left(1825000-(78.3\times T_k)^{-1.5}\right)\times\left(\left(\frac{(0.000168\times SC)^{0.5}}{1+(0.000168\times SC)^{0.5}}\right)-0.3\times 0.000168\times SC\right)}$	-	Trivalent activity coefficient
$f_t = 10^{-\left(1825000-(78.3\times T_k)^{-1.5}\right)\times 9\times\left(\left(\frac{(0.000168\times SC)^{0.5}}{1+(0.000168\times SC)^{0.5}}\right)-0.3\times 0.000168\times SC\right)}$	-	Trivalent activity coefficient
$outALK = \left(\begin{array}{l} 2\times\frac{[CO_3]}{MW_{CO_3}}+\frac{[HCO_3]}{MW_{HCO_3}}+\frac{[OH]}{MW_{OH}}+\frac{[HS]}{MW_{HS}} \\ +2\times\frac{[S]}{MW_S}+\frac{[NH_3]}{MW_{NH_3}}-\frac{[H]}{MW_H} \end{array}\right)\times\frac{MW_{CaCO_3}}{2}$	mg/ℓ as $CaCO_3$	Effluent alkalinity
$outCH_4 gas = \frac{R\times T_k}{P_{atm}\times MW_{CH_4}}\times\frac{[CH_4]}{1000}\times Q_i$	ℓ/d	CH_4 gas production
$outCO_2 gas = \frac{R\times T_k}{P_{atm}\times MW_{CO_2}}\times\frac{[CO_2]}{1000}\times Q_i$	ℓ/d	CO_2 gas production

$outH_2Sgas = \frac{R \times T_k}{P_{atm} \times MW_{H_2S}} \times \frac{[H_2Sgas]}{1000} \times Q_i$	ℓ/d	H_2S gas production
$outS_{bp} = [S_{bp}]$	mgCOD/ℓ	Effluent COD that is biodegradable particulate
$outS_{bs} = [S_{bs}] \times in\_f\_GlucCOD$	mgCOD/ℓ	Effluent COD that is biodegradable soluble
$outS_{up} = [S_{up}]$	mgCOD/ℓ	Effluent COD that is unbiodegradable particulate
$outS_{us} = [S_{us}]$	mgCOD/ℓ	Effluent COD that is unbiodegradable soluble
$outS_{sulph} = \left(\frac{[S]}{MW_S} + \frac{[HS]}{MW_{HS}} + \frac{[H_2Saq]}{MW_{H_2S}} \right) \times 80$	mgCOD/ℓ	Effluent COD due to dissolved sulphides
$outS_{tot} = outS_{totpart} + outS_{totsol}$	mgCOD/ℓ	Total COD in Effluent
$outS_{totpart} = outS_{bp} + outS_{up} + outZ_{ae} + outZ_{ai} + outZ_{am} + outZ_{hm} + outZ_{as} + outZ_{hs} + outZ_{ps}$	mgCOD/ℓ	Total particulate COD in Effluent
$outS_{totsol} = outS_{bs} + outS_{us} + outHAc\_Ac + outH\,\mathrm{Pr}\_\,\mathrm{Pr} + outS_{sulph}$	mgCOD/ℓ	Total soluble COD in Effluent

$outFSA = \left(\frac{[NH_3]}{MW_{NH_3}} + \frac{[NH_4]}{MW_{NH_4}} \right) \times AW_N$	mgN/ℓ	Total effluent free and saline ammonia
$outGas\,\mathrm{Pr}odtot = outCH_4gas + outCO_2gas + outH_2Sgas$	ℓ/d	Total Gas production
$outH_2Saq = \frac{[H_2Saq]}{MW_{H_2S}} \times AW_S$	mgS/ℓ	Effluent sulphide concentration
$outHAc\_Ac = [HAc] \times in\_f\_HAcCOD + [Ac] \times in\_f\_HAcCOD$	mgCOD/ℓ	Total effluent acetate system
$outH\,\mathrm{Pr}\_\mathrm{Pr} = [H\,\mathrm{Pr}] \times in\_f\_H\,\mathrm{Pr}COD + [\mathrm{Pr}] \times in\_f\_H\,\mathrm{Pr}COD$	mgCOD/ℓ	Total effluent propionate system
$outNH_3 = \frac{[NH_3]}{MW_{NH_3}} \times AW_N$	mgN/ℓ	Effluent NH_3
$outPO_4 = \frac{[PO_4]}{MW_{PO_4}} \times AW_P$	mgP/ℓ	Effluent PO_4
$outPsol = \left(\frac{[H_3PO_4]}{MW_{H_3PO_4}} + \frac{[H_2PO_4]}{MW_{H_2PO_4}} + \frac{[HPO_4]}{MW_{HPO_4}} + \frac{[PO_4]}{MW_{PO_4}} \right) \times AW_P$	mgP/ℓ	Total effluent soluble phosphorus system

$outPtot = \left(\frac{[H_3PO_4]}{MW_{H_3PO_4}} + \frac{[H_2PO_4]}{MW_{H_2PO_4}} + \frac{[HPO_4]}{MW_{HPO_4}} + \frac{[PO_4]}{MW_{PO_4}} \right) \times AW_P + [S_{bp}] \times in\_f\_P\_bp$	mgP/ℓ	Total effluent phosphorus system
$outSO_4 = [SO_4]$	g/m3 or mg/ℓ	Effluent SO_4 concentration
$outTKN = \left(\frac{[NH_3]}{MW_{NH_3}} + \frac{[NH_4]}{MW_{NH_4}} + \left(\frac{[X_{hm}]}{MW_{C_5H_7O_2N}} + \frac{[X_{ae}]}{MW_{C_5H_7O_2N}} + \frac{[X_{am}]}{MW_{C_5H_7O_2N}} + \frac{[X_{ai}]}{MW_{C_5H_7O_2N}} + \frac{[X_{ps}]}{MW_{C_5H_7O_2N}} + \frac{[X_{as}]}{MW_{C_5H_7O_2N}} + \frac{[X_{hs}]}{MW_{C_5H_7O_2N}} \right) \times in\_f\_X_i \right) \times AW_N + [S_{bp}] \times in\_f\_N\_bp$	mgN/ℓ	Total dissolved nitrogen species in digester
$outVFA = \left(\frac{[HAc]}{MW_{HAc}} + \frac{[Ac]}{MW_{Ac}} + \frac{[H\,\mathrm{Pr}]}{MW_{H\,\mathrm{Pr}}} + \frac{[\mathrm{Pr}]}{MW_{\mathrm{Pr}}} \right) \times MW_{HAc}$	mg/ℓ as HAc	Effluent volatile fatty acids

$outZ_{ae} = [Z_{ae}] \times f\_C_5H_7O_2NCOD$	mgCOD/ℓ	Effluent acetogenic biomass COD
$outZ_{ai} = [Z_{ai}] \times f\_C_5H_7O_2NCOD$	mgCOD/ℓ	Effluent acidogenic biomass COD
$outZ_{am} = [Z_{am}] \times f\_C_5H_7O_2NCOD$	mgCOD/ℓ	Effluent acetoclastic methanogenic biomass COD
$outZ_{hm} = [Z_{hm}] \times f\_C_5H_7O_2NCOD$	mgCOD/ℓ	Effluent hydrogenotrophic methanogenic biomass COD
$outZ_{as} = [Z_{as}] \times f\_C_5H_7O_2NCOD$	mgCOD/ℓ	Effluent acetoclastic sulphidogenic biomass COD
$outZ_{ps} = [Z_{ps}] \times f\_C_5H_7O_2NCOD$	mgCOD/ℓ	Effluent propionate-degrading sulphidogenic biomass COD
$outZ_{hs} = [Z_{hs}] \times f\_C_5H_7O_2NCOD$	mgCOD/ℓ	Effluent hydrogenotrophic sulphidogenic biomass COD
$pCH_4 = \frac{\frac{[CH_4]}{MW_{CH_4}}}{\frac{[CH_4]}{MW_{CH_4}} + \frac{[CO_2gas]}{MW_{CO_2}} + \frac{[H_2Sgas]}{MW_{H_2S}}}$	-	Partial pressure of CH_4 gas

$pCO_2 = \frac{\frac{[CO_2]}{MW_{CH_4}}}{\frac{[CH_4]}{MW_{CH_4}} + \frac{[CO_2 gas]}{MW_{CO_2}} + \frac{[H_2 Sgas]}{MW_{H_2S}}}$	-	Partial pressure of CO_2 gas
$pH_2S = \frac{\frac{[H_2 Sgas]}{MW_{CH_4}}}{\frac{[CH_4]}{MW_{CH_4}} + \frac{[CO_2 gas]}{MW_{CO_2}} + \frac{[H_2 Sgas]}{MW_{H_2S}}}$	-	Partial pressure of H_2S gas
$pKH_{CO_2} = -\frac{2025.3}{T_k} - 0.0104 \times T_k + k_{CO_2}$	-	pK constant for the dissolution of CO_2
$pKH_{H_2S} = \frac{998.58}{T_k} - k_{H_2S}$	-	pK constant for the dissolution of H_2S
$pK_{HS} = \frac{1156.8}{T_k} + 3.1301$	-	pK constant for $H_2S \leftrightarrow HS^- + H^+$
$pK_{\mathrm{Pr}} = \frac{1170.5}{T_k} - 3.165 + 0.0134 \times T_k$	-	pK constant for $HPr \leftrightarrow Pr^- + H^+$

$pK_S = \frac{2642.7}{T_k} + 10.1363$	-	pK constant for $HS^- \leftrightarrow S^{2-} + H^+$
$pK_W = 14$	-	pK constant for dissociation of H_2O
$pK_a = \frac{1170.5}{T_k} - 3.165 + 0.0134 \times T_k$	-	pK constant for $HAc \leftrightarrow Ac^- + H^+$
$pK_{c1} = \frac{3404.7}{T_k} - 14.8435 + 0.03279 \times T_k$	-	pK constant for $H_2CO_3 \leftrightarrow HCO_3^- + H^+$
$pK_{c2} = \frac{2902.4}{T_k} - 6.498 + 0.02379 \times T_k$	-	pK constant for $HCO_3^- \leftrightarrow CO_3^{2-} + H^+$
$pK_n = \frac{2835.8}{T_k} - 0.6322 + 0.00123 \times T_k$	-	pK constant for $NH_4^+ \leftrightarrow NH_3 + H^+$
$pK_{p1} = \frac{799.3}{T_k} - 4.5535 + 0.01349 \times T_k$	-	pK constant for $H_3PO_4 \leftrightarrow H_2PO_4^- + H^+$
$pK_{p2} = \frac{1979.5}{T_k} - 5.3541 + 0.01984 \times T_k$	-	pK constant for $H_2PO_4^- \leftrightarrow HPO_4^{2-} + H^+$
$pK_{p3} = 12.023$	-	pK constant for $HPO_4^{2-} \leftrightarrow PO_4^{3-} + H^+$

APPENDIX B

INFLUENT CHARACTERISATION

Table B-1: Feed batch data for steady state experiments (Ristow, et al., 2005)

Feed batch number	pH	Alkalinity (mg/ℓ as $CaCO_3$)
F12	4.91	47.3
F13	5.73	151.6
F14	5.38	90.28
F15	5.38	90.28

Table B-2: Influent characterisation for steady state numbers 1-11

Steady state number	**1**	**2**	**3**	**4**	**5**	**6**	**7**	**8**	**9**	**10**	**11**
Feed batch number	F12	F12	F12	F12	F12	F12	F13	F13	F13	F13	F13
Reactor volume (ℓ)	16	16	20	20	20	16	16	16	16	20	20
Retention time (d)	10	8	20	15	15	10	6.67	5.71	5	15	15
Flowrate (ℓ/d)	1.6	2	1	1.33	1.33	1.6	2.40	2.80	3.2	1.33	1.33
H_20 (g/d)	1600	2000	1000	1333.33	1333.33	1600	2398.80	2802.10	3200	1333.33	1333.33
pH	4.91	4.91	4.91	4.91	4.91	4.91	5.73	5.73	5.73	5.73	5.73
H^+ (g/d)	1.98E-05	2.48E-05	1.24E-05	1.65E-05	1.65E-05	1.98E-05	4.50E-06	5.26E-06	6.01E-06	2.50E-06	2.50E-06
OH^- (g/d)	2.21E-08	2.76E-08	1.38E-08	1.84E-08	1.84E-08	2.21E-08	2.19E-07	2.56E-07	2.92E-07	1.22E-07	1.22E-07
S_{VFAi} (mg COD/ℓ)	4000	1740	1775	1900	1060	4000	1260	1250	1196	1830	2020
Ac^- (g/d)	3.53E+00	1.92E+00	9.78E-01	1.40E+00	7.79E-01	3.53E+00	2.56E+00	2.97E+00	3.25E+00	2.07E+00	2.28E+00
HAc (g/d)	2.52E+00	1.37E+00	6.99E-01	9.98E-01	5.57E-01	2.52E+00	2.77E-01	3.21E-01	3.51E-01	2.24E-01	2.47E-01
Pr^- (g/d)	0	0	0	0	0	0	0	0	0	0	0
HPr (g/d)	0	0	0	0	0	0	0	0	0	0	0
FSA (mg N/ℓ)	39	39	39	39	20	39	106	124	131	180	198
NH_3 (g/d)	3.45E-06	4.32E-06	2.16E-06	2.88E-06	1.48E-06	3.45E-06	9.29E-05	1.27E-04	1.53E-04	8.77E-05	9.65E-05
NH_4^+ (g/d)	8.04E-02	1.00E-01	5.02E-02	6.70E-02	3.43E-02	8.04E-02	3.27E-01	4.47E-01	5.40E-01	3.09E-01	3.40E-01
Alkalinity (mg/ℓ as $CaCO_3$)	47.3	47.3	47.3	47.3	47.3	47.3	151.6	151.6	151.6	151.6	151.6
CO_3^{2-} (g/d)	3.50E-07	4.38E-07	2.19E-07	2.92E-07	2.92E-07	3.50E-07	1.10E-05	1.28E-05	1.47E-05	6.11E-06	6.11E-06
HCO_3^- (g/d)	9.35E-02	1.17E-01	5.84E-02	7.79E-02	7.79E-02	9.35E-02	4.44E-01	5.18E-01	5.92E-01	2.47E-01	2.47E-01
H_2CO_3 (g/d)	2.69	3.36	1.68	2.24	2.24	2.69	1.93	2.26	2.58	1.07	1.07
Sulphate (mg/ℓ)	0	0	0	0	0	1000	0	0	0	0	0
SO_4^{2+} (g/d)	0	0	0	0	0	1.6	0	0	0	0	0
COD Fractionation											
S_{bp} (mg COD/ℓ)	14940.72	14596.72	14945.72	14624.72	7630.78	14624.72	14531.31	14107.88	13864.31	22959.25	22490.25
S_{bp} (g COD/d)	23.91	29.19	14.95	19.50	10.17	23.40	34.86	39.53	44.37	30.61	29.99
S_{up} (mg COD/ℓ)	8681.28	8681.28	8681.28	8681.28	4555.22	8681.28	8322.69	8349.12	8322.69	13309.76	13309.76
S_{up} (g COD/d)	13.89	17.36	8.68	11.58	6.07	13.89	19.96	23.40	26.63	17.75	17.75
S_{bs} (mg COD/ℓ)	1076	1253	1073	1245	668	1076	914	1149	1196	1635	1846
S_{bs} (g/d)	1.62	2.35	1.01	1.56	0.84	1.62	2.06	3.02	3.59	2.05	2.31
S_{us} (mg COD/ℓ)	178	168	179	157	97	178	200	205	301	250	299
S_{us} (g COD/d)	2.85E-01	3.36E-01	1.79E-01	2.09E-01	1.29E-01	2.85E-01	4.80E-01	5.74E-01	9.63E-01	3.33E-01	3.99E-01

Table B-3: Influent characterisation for steady state numbers 12-23

Steady state number	**12**	**13**	**14**	**15**	**17**	**18**	**19**	**20**	**21**	**22**	**23**
Feed batch number	F13	F13	F13	F13	F12	F14	F14	F14	F14	F14	F14
Reactor volume (ℓ)	20	20	20	16	20	16	16	16	20	16	20
Retention time (d)	10	10	8	8	60	8	8	8	8	8	6.67
Flowrate (ℓ/d)	2	2	2.5	2	0.33	2	2	2	2.5	2	3.00
H_20 (g/d)	2000	2000	2500	2000	333.33	2000	2000	2000	2500	2000	2998.50
pH	5.73	5.73	5.73	5.73	4.91	5.38	5.38	5.38	5.38	5.38	5.38
H^+ (g/d)	3.75E-06	3.75E-06	4.69E-06	3.75E-06	4.13E-06	8.40E-06	8.40E-06	8.40E-06	1.05E-05	8.40E-06	1.26E-05
OH^- (g/d)	1.83E-07	1.83E-07	2.28E-07	1.83E-07	4.61E-09	8.16E-08	8.16E-08	8.16E-08	1.02E-07	8.16E-08	1.22E-07
S_{VFAi} (mg COD/ℓ)	2090	533	710	710	558	116	116	116	1812	116	2096
Ac^- (g/d)	3.54E+00	9.04E-01	1.51E+00	1.20E+00	1.02E-01	1.76E-01	1.76E-01	1.76E-01	3.43E+00	1.76E-01	4.76E+00
HAc (g/d)	3.84E-01	9.78E-02	1.63E-01	1.30E-01	7.33E-02	4.26E-02	4.26E-02	4.26E-02	8.31E-01	4.26E-02	1.15E+00
Pr^- (g/d)	0	0	0	0	0	0	0	0	0	0	0
HPr (g/d)	0	0	0	0	0	0	0	0	0	0	0
FSA (mg N/ℓ)	214	59	73	72	15	7	8	8	44	10	70
NH_3 (g/d)	1.56E-04	4.31E-05	6.67E-05	5.26E-05	2.77E-07	2.29E-06	2.61E-06	2.61E-06	1.80E-05	3.27E-06	3.43E-05
NH_4^+ (g/d)	5.51E-01	1.52E-01	2.35E-01	1.85E-01	6.44E-03	1.80E-02	2.06E-02	2.06E-02	1.42E-01	2.58E-02	2.70E-01
Alkalinity (mg/ℓ as $CaCO_3$)	151.6	151.6	151.6	151.6	47.3	90.28	90.28	90.28	90.28	90.28	90.28
CO_3^{2-} (g/d)	9.16E-06	9.16E-06	1.15E-05	9.16E-06	7.30E-08	2.44E-06	2.44E-06	2.44E-06	3.05E-06	2.44E-06	3.66E-06
HCO_3^- (g/d)	3.70E-01	3.70E-01	4.62E-01	3.70E-01	1.95E-02	2.21E-01	2.21E-01	2.21E-01	2.76E-01	2.21E-01	3.31E-01
H_2CO_3 (g/d)	1.61	1.61	2.01	1.61	0.56	2.15	2.15	2.15	2.69	2.15	3.22
Sulphate (mg/ℓ)	0	0	0	9600	0	0	0	2000	0	2000	0
SO_4^{2+} (g/d)	0	0	0	19.2	0	0	0	4	0	4	0
COD Fractionation											
S_{bp} (mg COD/ℓ)	22057.56	7657.19	7306.19	7306.19	5324.56	1013.73	1013.73	1013.73	19343.38	1013.73	18773.38
S_{bp} (g COD/d)	44.12	15.31	18.27	14.61	1.77	2.03	2.03	2.03	48.36	2.03	56.29
S_{up} (mg COD/ℓ)	13316.45	4438.82	4438.82	4438.82	3281.45	652.28	652.28	652.28	11646.62	652.28	11646.62
S_{up} (g COD/d)	26.63	8.88	11.10	8.88	1.09	1.30	1.30	1.30	29.12	1.30	34.92
S_{bs} (mg COD/ℓ)	2090	533	710	710	558	116	116	116	1812	116	2096
S_{bs} (g/d)	3.92	1.00	1.67	1.33	0.17	0.22	0.22	0.22	4.25	0.22	5.90
S_{us} (mg COD/ℓ)	256	108	104	104	88	51	51	51	205	51	207
S_{us} (g COD/d)	5.12E-01	2.16E-01	2.60E-01	2.08E-01	2.93E-02	1.02E-01	1.02E-01	1.02E-01	5.13E-01	1.02E-01	6.21E-01

Table B-4: Influent characterisation for steady state numbers 24-28, 31, 36, 41, 42, 46 and 47

Steady state number	**24**	**25**	**26**	**27**	**28**	**31**	**36**	**41**	**42**	**46**	**47**
Feed batch number	F14	F14	F14	F15	F15	F15	F15	F15	F15	F15	F15
Reactor volume (ℓ)	20	20	20	16	20	20	16	20	20	20	16
Retention time (d)	6.67	10	8	8	5.71	5.71	8	16	13.3	10	8
Flowrate (ℓ/d)	3.00	2	2.5	2	3.50	3.50	2	1.25	1.50	2	2
H_20 (g/d)	2998.50	2000	2500	2000	3502.63	3502.63	2000	1250	1503.76	2000	2000
pH	5.38	5.38	5.38	5.38	5.38	5.38	5.38	5.38	5.38	5.38	5.38
H^+ (g/d)	1.26E-05	8.40E-06	1.05E-05	8.40E-06	1.47E-05	1.47E-05	8.40E-06	5.25E-06	6.32E-06	8.40E-06	8.40E-06
OH^- (g/d)	1.22E-07	8.16E-08	1.02E-07	8.16E-08	1.43E-07	1.43E-07	8.16E-08	5.10E-08	6.13E-08	8.16E-08	8.16E-08
S_{VFAi} (mg COD/ℓ)	875	111	116	104	1144	418	116	98	104	47	94
Ac^- (g/d)	1.99E+00	1.68E-01	2.20E-01	1.58E-01	3.04E+00	1.11E+00	1.76E-01	9.28E-02	1.19E-01	7.12E-02	1.42E-01
HAc (g/d)	4.82E-01	4.07E-02	5.32E-02	3.82E-02	7.35E-01	2.69E-01	4.26E-02	2.25E-02	2.87E-02	1.73E-02	3.45E-02
Pr^- (g/d)	0	0	0	0	0	0	0	0	0	0	0
HPr (g/d)	0	0	0	0	0	0	0	0	0	0	0
FSA (mg N/ℓ)	37	5	7	8	40	18	13	6	10	7	4
NH_3 (g/d)	1.81E-05	1.63E-06	2.86E-06	2.61E-06	2.29E-05	1.03E-05	4.25E-06	1.22E-06	2.46E-06	2.29E-06	1.31E-06
NH_4^+ (g/d)	1.43E-01	1.29E-02	2.25E-02	2.06E-02	1.80E-01	8.12E-02	3.35E-02	9.66E-03	1.94E-02	1.80E-02	1.03E-02
Alkalinity (mg/ℓ as $CaCO_3$)	90.28	90.28	90.28	90.28	90.28	90.28	90.28	90.28	90.28	90.28	90.28
CO_3^{2-} (g/d)	3.66E-06	2.44E-06	3.05E-06	2.44E-06	4.28E-06	4.28E-06	2.44E-06	1.53E-06	1.84E-06	2.44E-06	2.44E-06
HCO_3^- (g/d)	3.31E-01	2.21E-01	2.76E-01	2.21E-01	3.86E-01	3.86E-01	2.21E-01	1.38E-01	1.66E-01	2.21E-01	2.21E-01
H_2CO_3 (g/d)	3.22	2.15	2.69	2.15	3.76	3.76	2.15	1.34	1.62	2.15	2.15
Sulphate (mg/ℓ)	0	0	0	0	0	0	2000	2000	2000	2000	2000
SO_4^{2+} (g/d)	0	0	0	0	0	0	4	2.5	3.01	4	4
COD Fractionation											
S_{bp} (mg COD/ℓ)	7191.82	1043.73	1013.73	1118.31	24996.99	7819.28	1013.73	1127.32	1118.31	556.18	1061.45
S_{bp} (g COD/d)	21.56	2.09	2.53	2.24	87.56	27.39	2.03	1.41	1.68	1.11	2.12
S_{up} (mg COD/ℓ)	4542.18	652.28	652.28	674.69	13862.01	4410.72	652.28	672.68	674.69	330.82	635.55
S_{up} (g COD/d)	13.62	1.30	1.63	1.35	48.55	15.45	1.30	0.84	1.01	0.66	1.27
S_{bs} (mg COD/ℓ)	875	111	116	104	1144	418	116	98	104	47	94
S_{bs} (g/d)	2.46	0.21	0.27	0.20	3.76	1.37	0.22	0.11	0.15	0.09	0.18
S_{us} (mg COD/ℓ)	96	32	51	16	295	120	51	16	16	8	15
S_{us} (g COD/d)	2.88E-01	6.40E-02	1.28E-01	3.20E-02	1.03E+00	4.20E-01	1.02E-01	2.00E-02	2.41E-02	1.60E-02	3.00E-02

Table B-5: Influent characterisation of the PSS and mine water feed streams to the pilot plant

Feed Stream	**PSS**	**Mine water**
Reactor volume (ℓ)	250000	250000
Retention time (d)	18.94	1.09
Flowrate (ℓ/d)	13200	230000
H_20 (g/d)	13200000	230000000
pH	7*	7.5
H^+ (g/d)	1.33E-03	7.33E-03
OH^- (g/d)	2.24E-02	1.24
S_{VFAi} (mg COD/ℓ)	1245	0
Ac^- (g/d)	15332.51	0
HAc (g/d)	89.08	0
Pr^- (g/d)	0	0
HPr (g/d)	0	0
FSA (mg N/ℓ)	39*	0
NH_3 (g/d)	3.49	0
NH_4^+ (g/d)	659.28	0
Alkalinity (mg/ℓ as $CaCO_3$)	300*	350
CO_3^{2-} (g/d)	2.22	142.74
HCO_3^- (g/d)	4823.78	97856.93
H_2CO_3 (g/d)	1127.23	7231.32
Sulphate (mg/ℓ)	0	1300
SO_4^{2+} (g/d)	0	299000
COD Fractionation		
S_{bp} (mg COD/ℓ)	17271.00	0
S_{bp} (g COD/d)	227977.20	0
S_{up} (mg COD/ℓ)	10035.00	0
S_{up} (g COD/d)	132462.00	0
S_{bs} (mg COD/ℓ)	1245	0
S_{bs} (g/d)	15421.09	0
S_{us} (mg COD/ℓ)	204	0
S_{us} (g COD/d)	2692.80	0

* Guesstimate Value

APPENDIX C

SIMULATION RESULTS OF MODELLING STEADY STATE EXPERIMENTS

Steady State Number 1

Table C-1: Operating conditions for steady state number 1

Feed Batch Number	F12
Reactor Volume (ℓ)	16
Retention Time (d)	10
pH	steady state
Biological Groups Present	acidogenic, acetogenic and methanogenic

Table C-2: Results summary for steady state number 1

	Measured	**Model**	**Relative error (%)**
Feed Total COD (mg COD/ℓ)	25952	28876	-
Feed Soluble COD (mg COD/ℓ)	2330	5254	-
Feed TKN (mg N/ℓ)	482	482	-
Feed FSA (mg N/ℓ)	39	39	-
Effluent Total COD (mg COD/ℓ)	10849 ± 304	11079.48	2.08
Effluent Soluble COD (mg COD/ℓ)	178 ± 14	215.73	17.49
Reactor pH	7.00 ± 0.01	6.83	-2.55
Effluent VFA (mg HAc/ℓ)	24 ± 14	1.01	-2276.68
Effluent Alkalinity (mg/ℓ as $CaCO_3$)	2424 ± 127	2475.25	2.07
Sulphate Addition (mg SO4/ℓ)	0	0	-
Effluent Sulphate (mg SO4/ℓ)	0	0	-
% Sulphate Conversion	-	-	-
Methane Production (ℓ/d)	10.69	12.23	12.57

Gas Composition (% CH_4)	63.24	59.86	-5.65
Effluent FSA (mg N/ℓ)	208 ± 4	205.02	-1.45
Effluent TKN (mg N/ℓ)	518 ± 10	488.13	-6.12

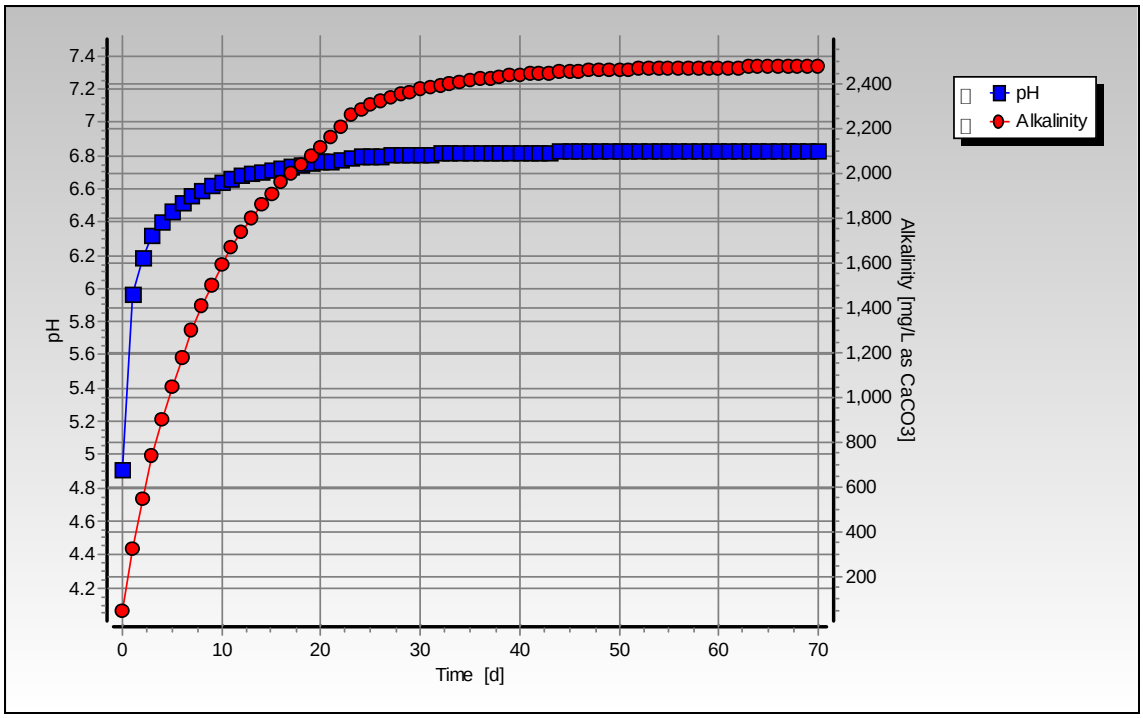

Figure C-1: Simulated pH and alkalinity profiles for steady state number 1

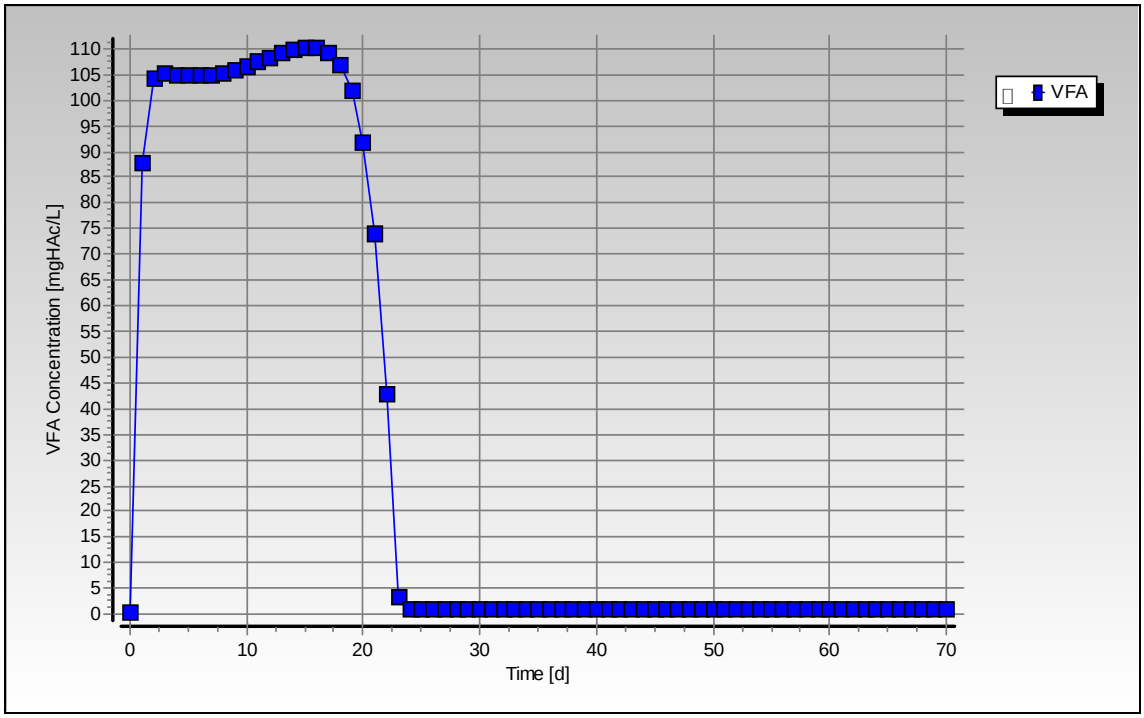

Figure C-2: Simulated VFA concentration profile for steady state number 1

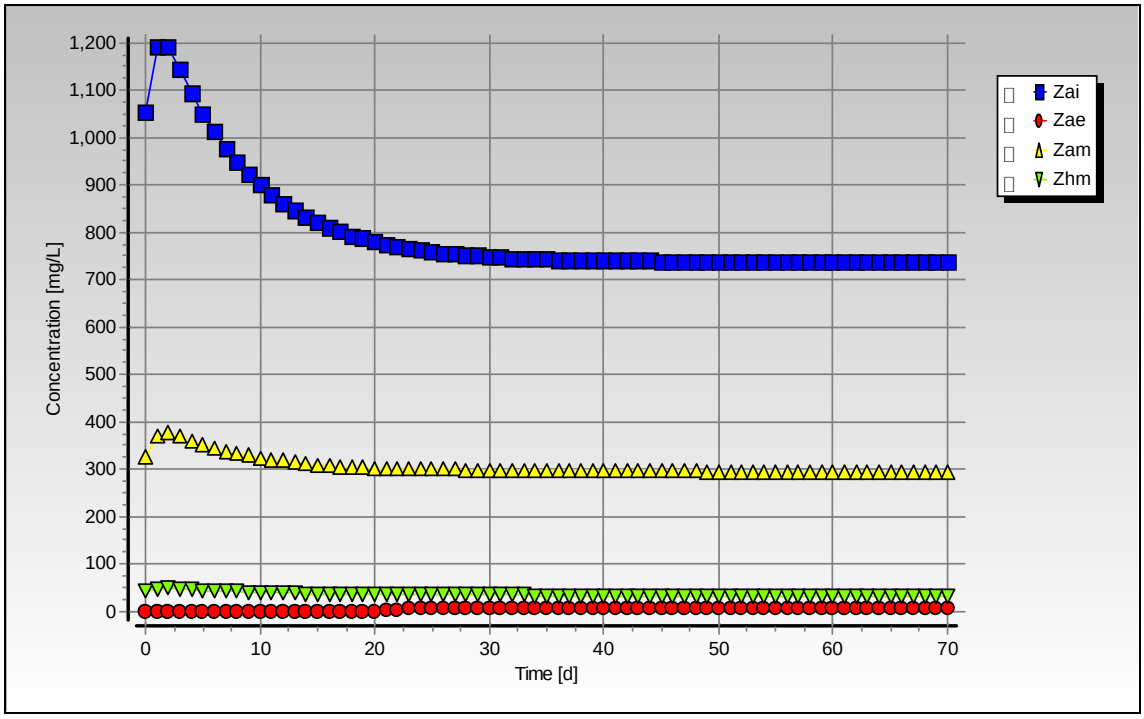

Figure C-3: Simulated biomass concentration profiles for steady state number 1

Steady State Number 2

Table C-3: Operating conditions for steady state number 2

Feed Batch Number	F12
Reactor Volume (ℓ)	16
Retention Time (d)	8
pH	steady state
Biological Groups Present	acidogenic, acetogenic and methanogenic

Table C-4: Results summary for steady state number 2

	Measured	**Model**	**Relative error (%)**
Feed Total COD (mg COD/ℓ)	25952	26439	-
Feed Soluble COD (mg COD/ℓ)	2674	3161	-
Feed TKN (mg N/ℓ)	482	482	-
Feed FSA (mg N/ℓ)	39	39	-
Effluent Total COD (mg COD/ℓ)	11299 ± 266	11223.93	-0.67
Effluent Soluble COD (mg COD/ℓ)	168 ± 4	215.60	22.08
Reactor pH	6.80 ± 0.02	6.57	-3.50
Effluent VFA (mg HAc/ℓ)	21 ± 11	1.62	-1193.62
Effluent Alkalinity (mg/ℓ as $CaCO_3$)	1394 ± 26	1407.98	0.99
Sulphate Addition (mg SO4/ℓ)	0	0	-
Effluent Sulphate (mg SO4/ℓ)	0	0	-
% Sulphate Conversion	-	-	-
Methane Production (ℓ/d)	10.94	13.19	17.05
Gas Composition (% CH_4)	63.24	58.62	-7.88
Effluent FSA (mg N/ℓ)	186 ± 9	196.21	5.20
Effluent TKN (mg N/ℓ)	543 ± 17	480.68	-12.96

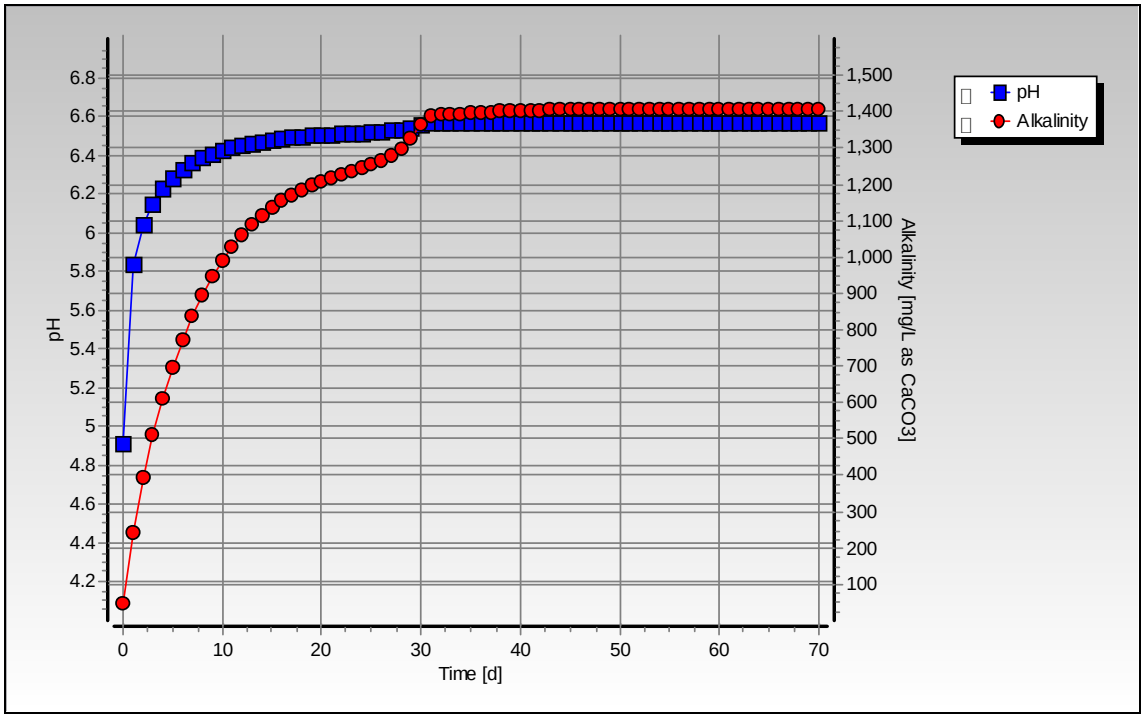

Figure C-4: Simulated pH and alkalinity profiles for steady state number 2

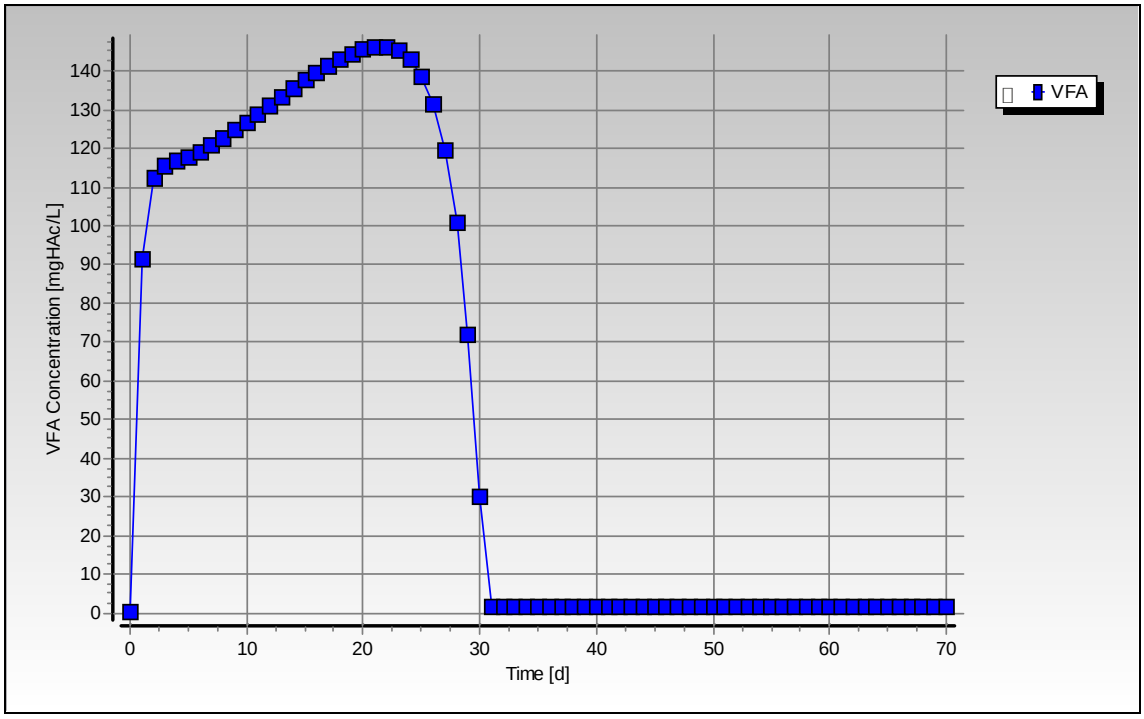

Figure C-5: Simulated VFA concentration profile for steady state number 2

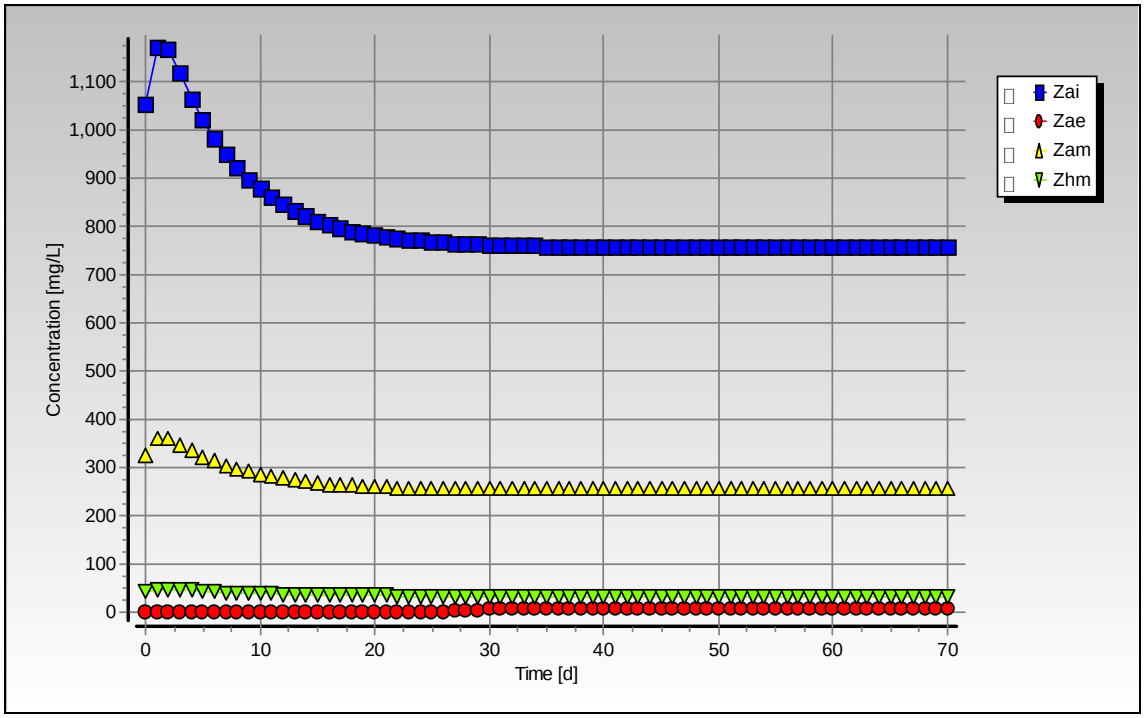

Figure C-6: Simulated biomass concentration profiles for steady state number 2

Steady State Number 3

Table C-5: Operating conditions for steady state number 3

Feed Batch Number	F12
Reactor Volume (ℓ)	20
Retention Time (d)	20
pH	steady state
Biological Groups Present	acidogenic, acetogenic and methanogenic

Table C-6: Results summary for steady state number 3

	Measured	**Model**	**Relative error (%)**
Feed Total COD (mg COD/ℓ)	25952	26654	-
Feed Soluble COD (mg COD/ℓ)	2325	3027	-
Feed TKN (mg N/ℓ)	482	482	-
Feed FSA (mg N/ℓ)	39	39	-
Effluent Total COD (mg COD/ℓ)	10525 ± 166	10402.06	-1.18
Effluent Soluble COD (mg COD/ℓ)	179 ± 8	200.76	10.84
Reactor pH	6.89 ± 0.02	6.62	-4.08
Effluent VFA (mg HAc/ℓ)	11 ± 7	0.60	-1724.48
Effluent Alkalinity (mg/ℓ as $CaCO_3$)	1577 ± 20	1576.84	-0.01
Sulphate Addition (mg SO4/ℓ)	0	0	-
Effluent Sulphate (mg SO4/ℓ)	0	0	-
% Sulphate Conversion	-	-	-
Methane Production (ℓ/d)	5.41	7.05	23.29
Gas Composition (% CH_4)	63.11	58.70	-7.52
Effluent FSA (mg N/ℓ)	231 ± 6	240.00	3.75
Effluent TKN (mg N/ℓ)	518 ± 6	516.39	-0.31

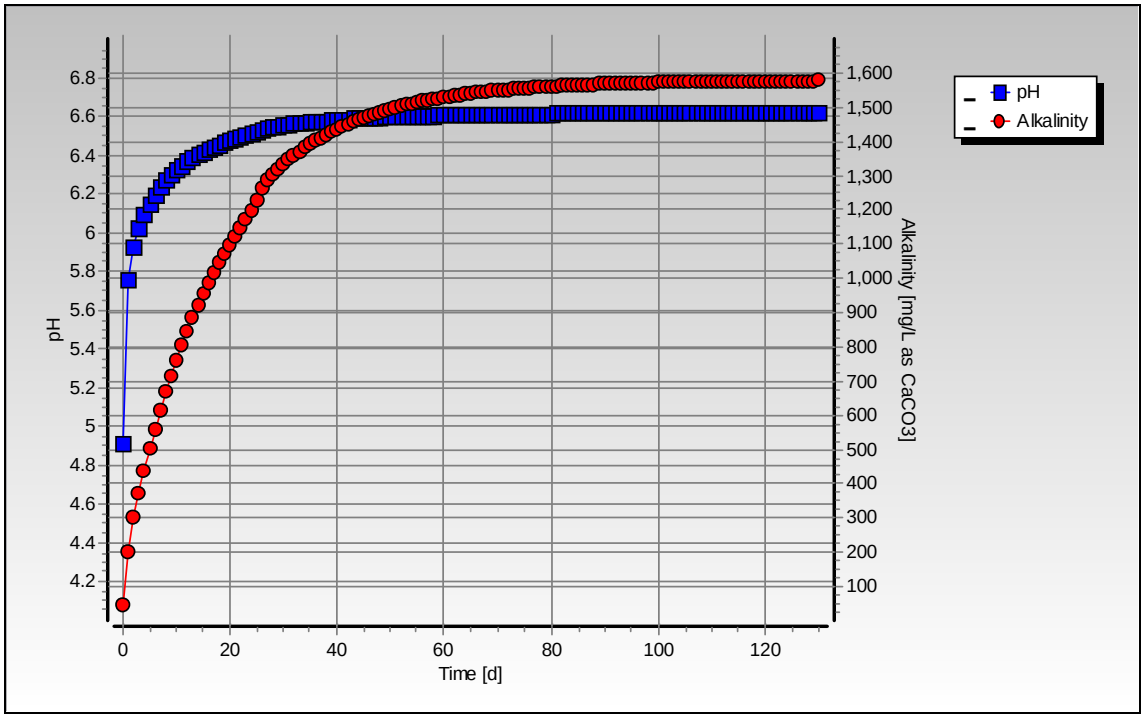

Figure C-7: Simulated pH and alkalinity profiles for steady state number 3

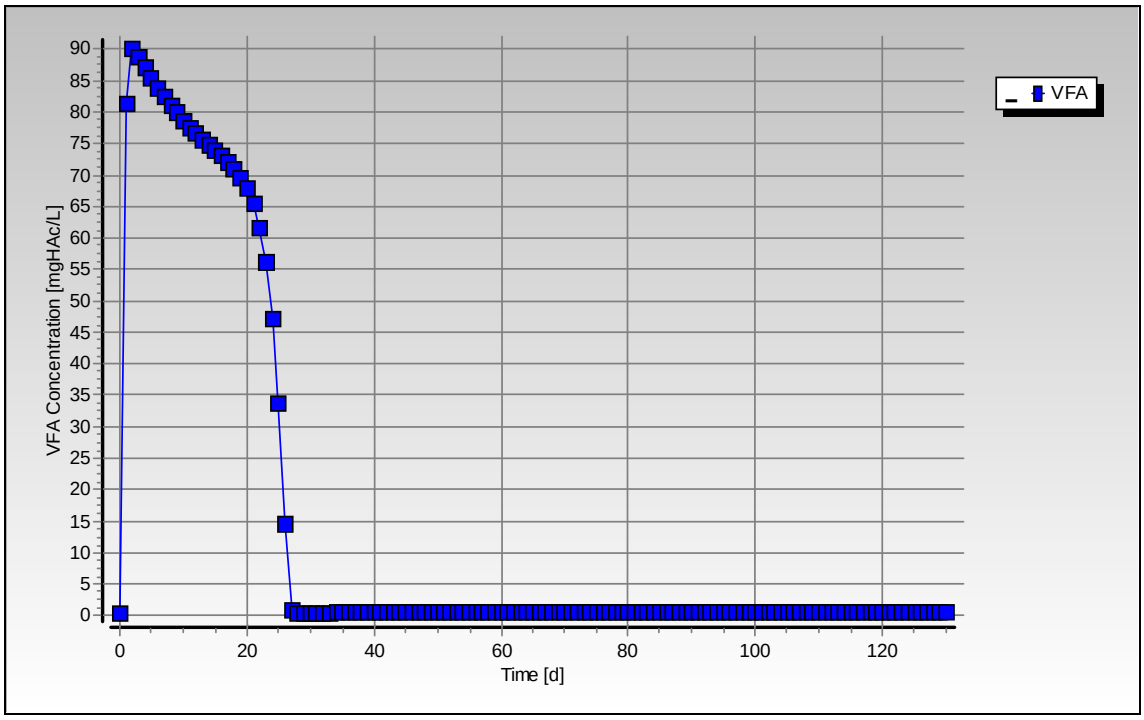

Figure C-8: Simulated VFA concentration profile for steady state number 3

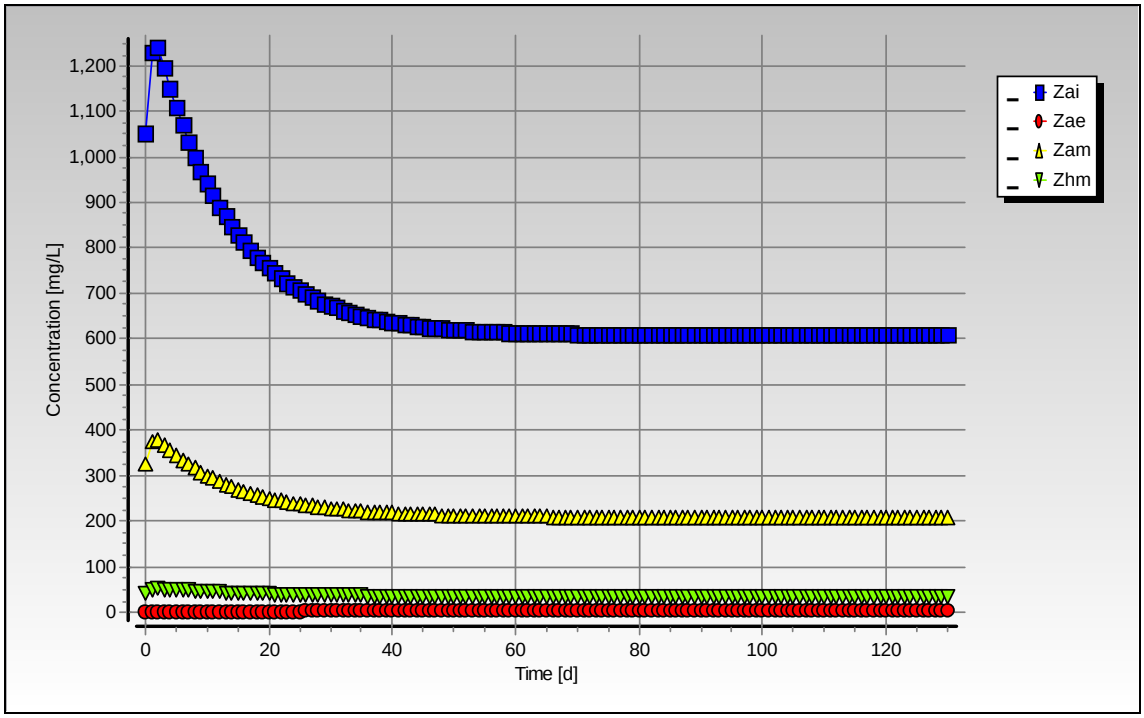

Figure C-9: Simulated biomass concentration profiles for steady state number 3

Steady State Number 4

Table C-7: Operating conditions for steady state number 4

Feed Batch Number	F12
Reactor Volume (ℓ)	20
Retention Time (d)	15
pH	steady state
Biological Groups Present	acidogenic, acetogenic and methanogenic

Table C-8: Results summary for steady state number 4

	Measured	**Model**	**Relative error (%)**
Feed Total COD (mg COD/ℓ)	25953	26608	-
Feed Soluble COD (mg COD/ℓ)	2647	3302	-
Feed TKN (mg N/ℓ)	482	482	-
Feed FSA (mg N/ℓ)	39	39	-
Effluent Total COD (mg COD/ℓ)	10212 ± 131	10370.99	1.53
Effluent Soluble COD (mg COD/ℓ)	157 ± 4	189.51	17.16
Reactor pH	6.85 ± 0.03	6.61	-3.57
Effluent VFA (mg HAc/ℓ)	17 ± 9	0.99	-1625.49
Effluent Alkalinity (mg/ℓ as $CaCO_3$)	1539 ± 40	1561.55	1.44
Sulphate Addition (mg SO4/ℓ)	0	0	-
Effluent Sulphate (mg SO4/ℓ)	0	0	-
% Sulphate Conversion	-	-	-
Methane Production (ℓ/d)	7.71	9.38	17.80
Gas Composition (% CH_4)	63.08	58.71	-7.44
Effluent FSA (mg N/ℓ)	212 ± 6	218.18	2.83
Effluent TKN (mg N/ℓ)	522 ± 6	494.35	-5.59

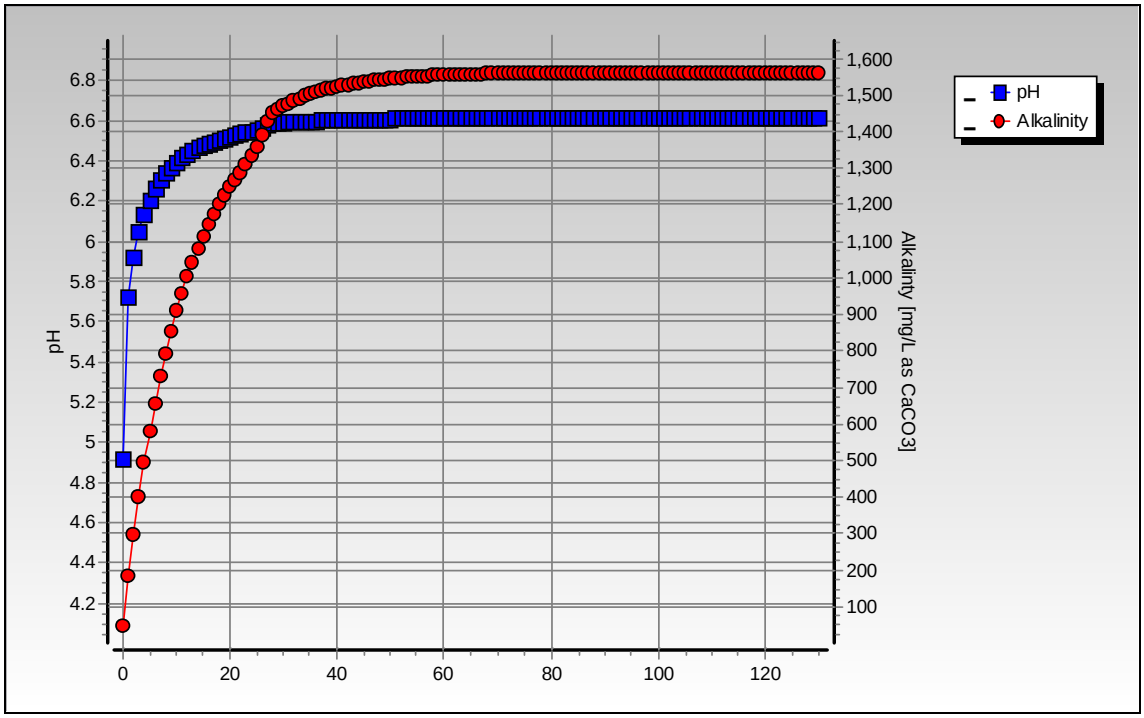

Figure C-10: Simulated pH and alkalinity profiles for steady state number 4

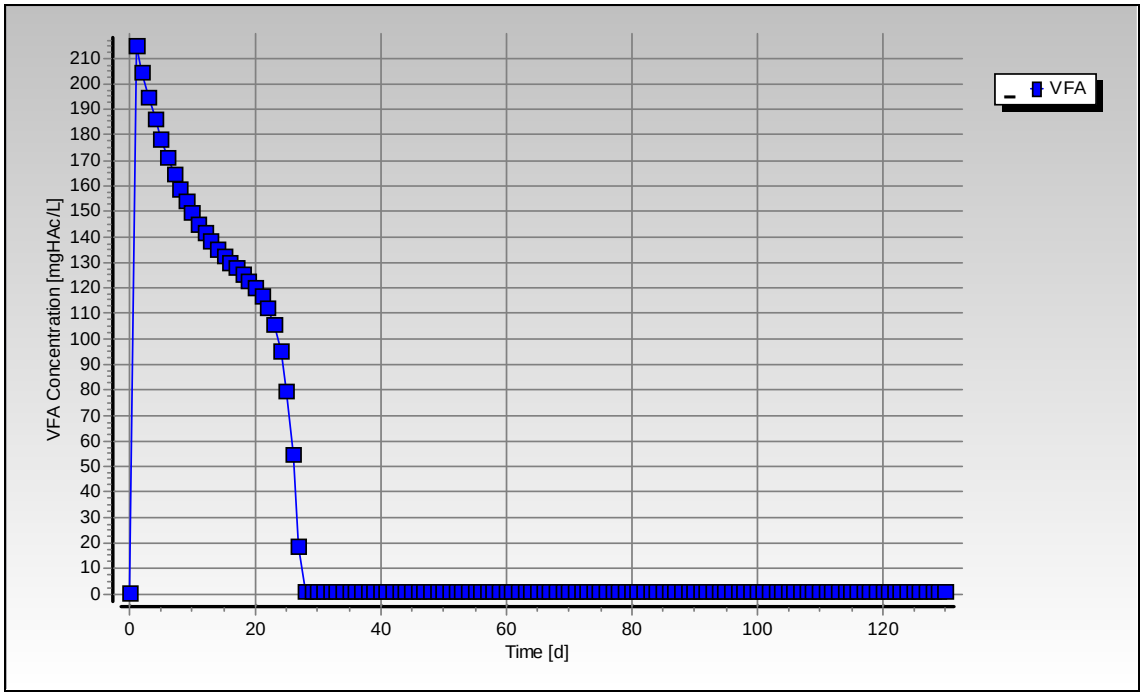

Figure C-11: Simulated VFA concentration profile for steady state number 4

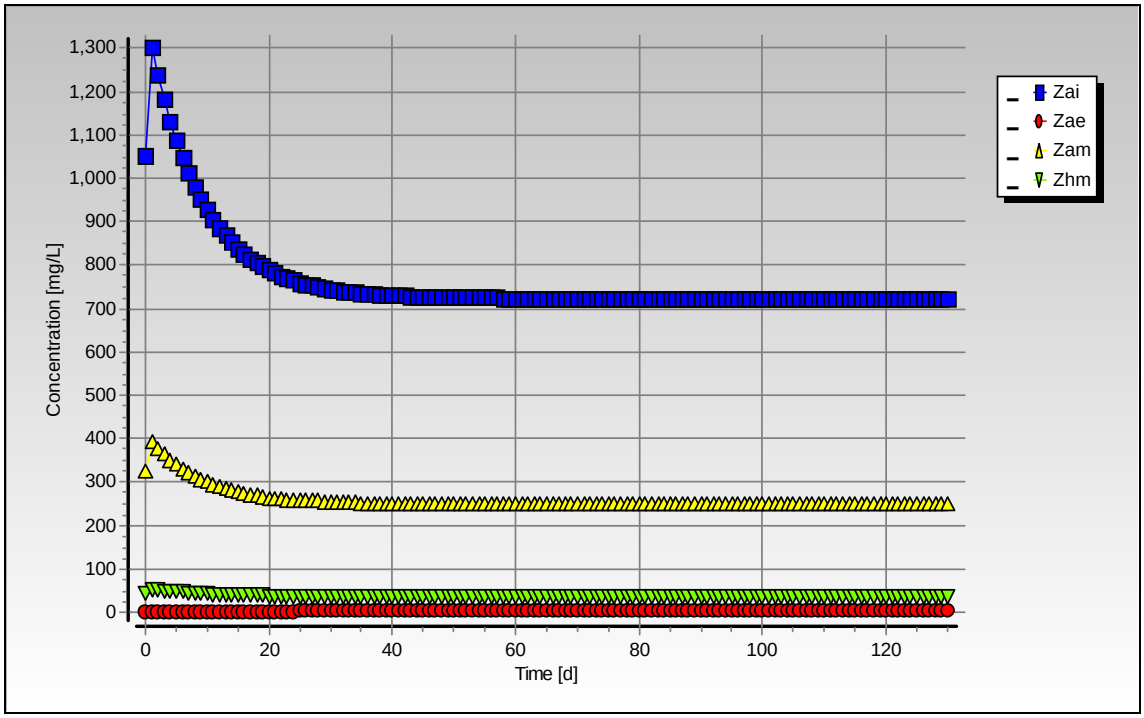

Figure C-12: Simulated biomass concentration profiles for steady state number 4

Steady State Number 5

Table C-9: Operating conditions for steady state number 5

Feed Batch Number	F12
Reactor Volume (ℓ)	20
Retention Time (d)	15
pH	steady state
Biological Groups Present	acidogenic, acetogenic and methanogenic

Table C-10: Results summary for steady state number 5

	Measured	**Model**	**Relative error (%)**
Feed Total COD (mg COD/ℓ)	13619	14011	-
Feed Soluble COD (mg COD/ℓ)	1433	1825	-
Feed TKN (mg N/ℓ)	253	253	-
Feed FSA (mg N/ℓ)	20	20	-
Effluent Total COD (mg COD/ℓ)	5751 ± 106	5711.95	-0.68
Effluent Soluble COD (mg COD/ℓ)	97 ± 3	129.93	25.34
Reactor pH	6.80 ± 0.02	6.34	-7.26
Effluent VFA (mg HAc/ℓ)	6 ± 6	1.38	-333.39
Effluent Alkalinity (mg/ℓ as $CaCO_3$)	845 ± 22	854.83	1.15
Sulphate Addition (mg SO4/ℓ)	0	0	-
Effluent Sulphate (mg SO4/ℓ)	0	0	-
% Sulphate Conversion	-	-	-
Methane Production (ℓ/d)	3.95	4.83	18.25
Gas Composition (% CH_4)	63.26	57.01	-10.96
Effluent FSA (mg N/ℓ)	114 ± 3	111.53	-2.21
Effluent TKN (mg N/ℓ)	294 ± 7	259.35	-13.36

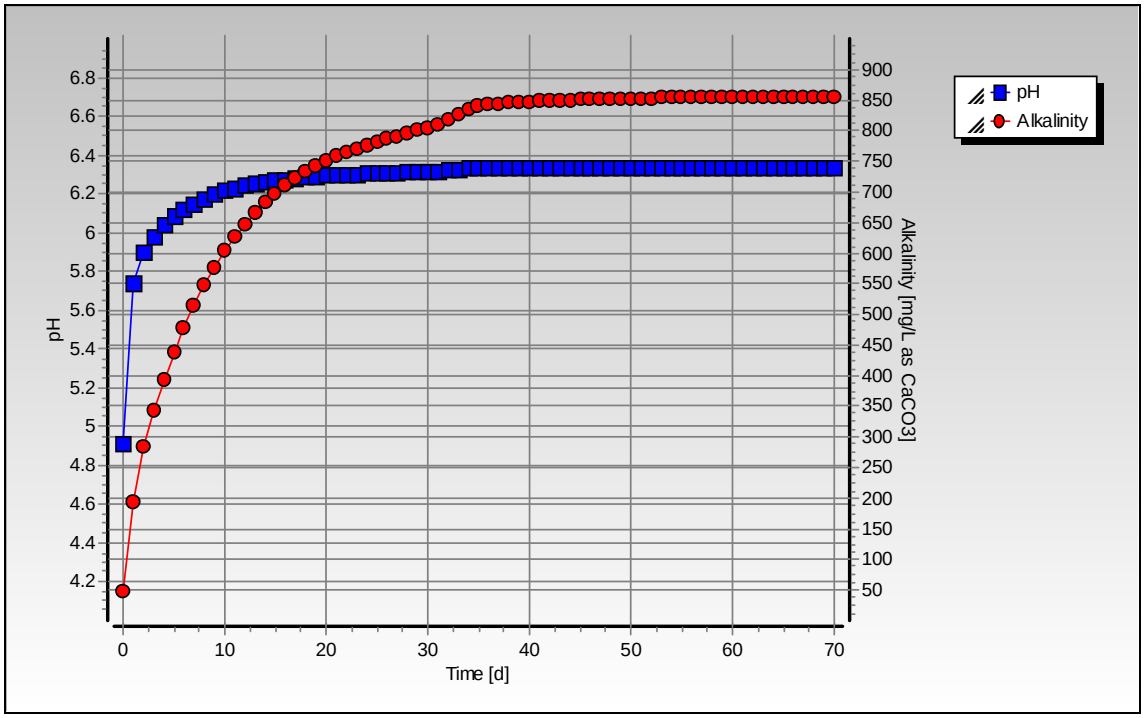

Figure C-13: Simulated pH and alkalinity profiles for steady state number 5

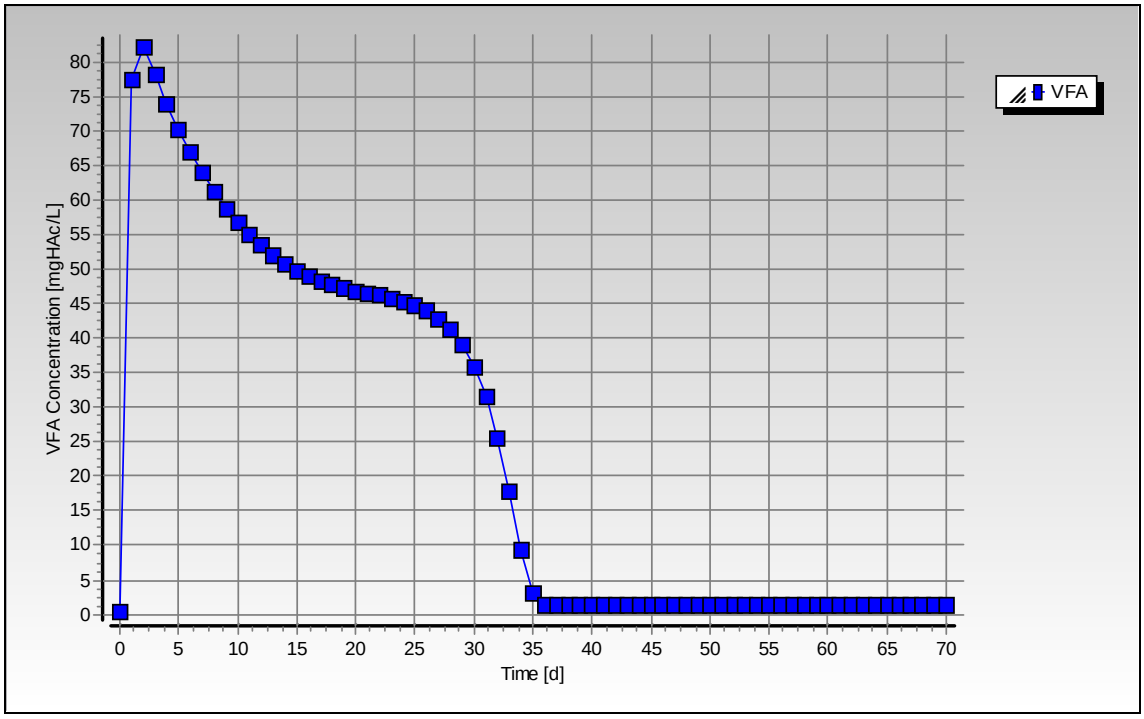

Figure C-14: Simulated VFA concentration profile for steady state number 5

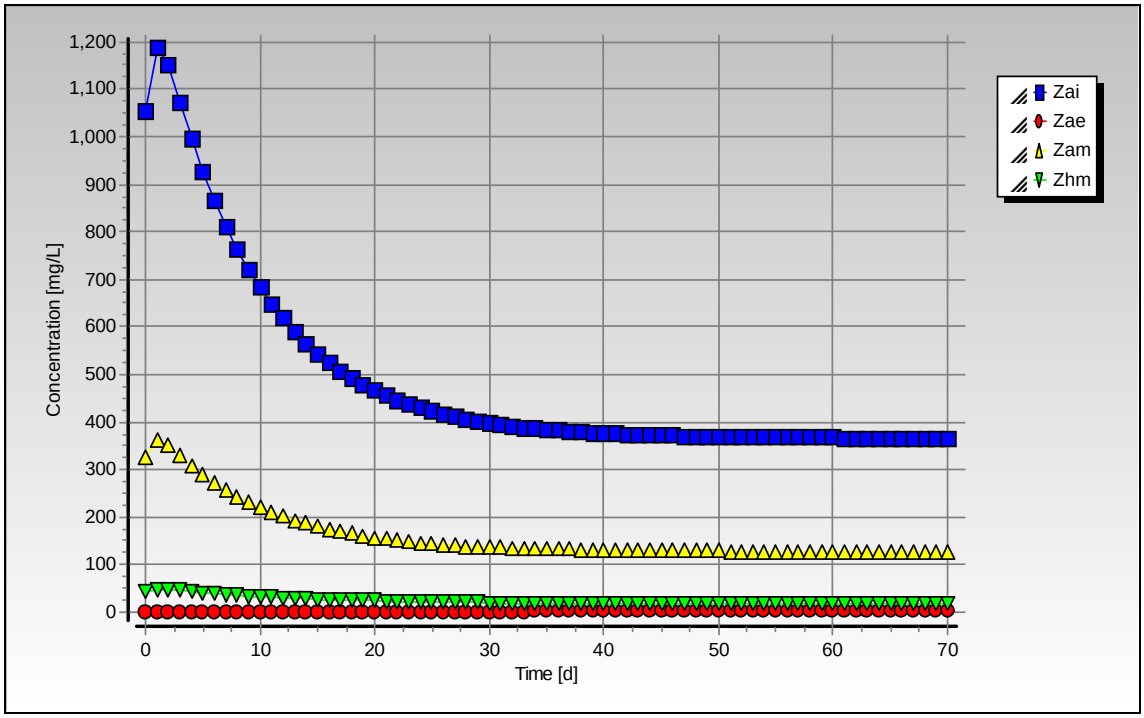

Figure C-15: Simulated biomass concentration profiles for steady state number 5

Steady State Number 6

Table C-11: Operating conditions for steady state number 6

Feed Batch Number	F12
Reactor Volume (ℓ)	16
Retention Time (d)	10
pH	steady state
Biological Groups Present	acidogenic, acetogenic, methanogenic and sulphidogenic

Table C-12: Results summary for steady state number 6

	Measured	**Model**	**Relative error (%)**
Feed Total COD (mg COD/ℓ)	25953	28876	-
Feed Soluble COD (mg COD/ℓ)	2647	5254	-
Feed TKN (mg N/ℓ)	482	482	-
Feed FSA (mg N/ℓ)	39	39	-
Effluent Total COD (mg COD/ℓ)	10684 ± 297	11109.43	4.15
Effluent Soluble COD (mg COD/ℓ)	157 ± 8	221.95	29.26
Reactor pH	7.06 ± 0.03	6.99	-1.00
Effluent VFA (mg HAc/ℓ)	37 ± 18	0.92	-3916.45
Effluent Alkalinity (mg/ℓ as $CaCO_3$)	2534 ± 62	3492.40	27.44
Sulphate Addition (mg SO4/ℓ)	1000	1000	-
Effluent Sulphate (mg SO4/ℓ)	34 ± 3	1.19	-2751.76
% Sulphate Conversion	96.60	99.88	-
Methane Production (ℓ/d)	8.88	11.80	24.74
Gas Composition (% CH_4)	64.53	58.96	-9.44
Effluent FSA (mg N/ℓ)	207 ± 6	203.05	-1.95
Effluent TKN (mg N/ℓ)	532 ± 19	486.41	-9.37

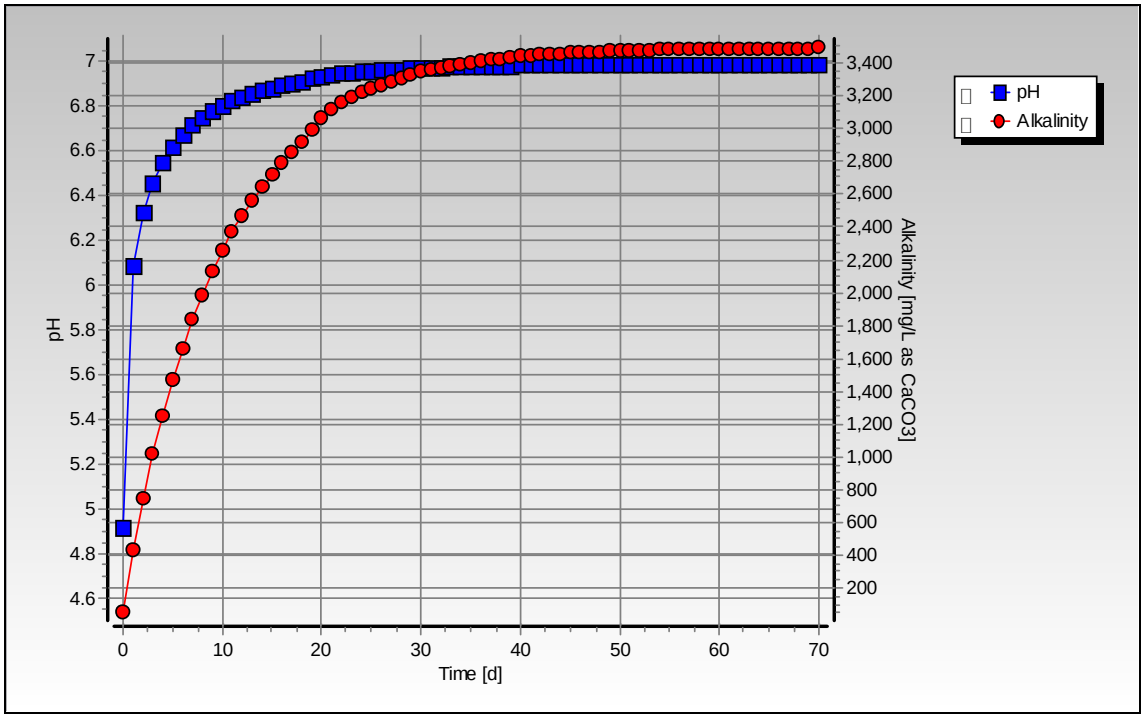

Figure C-16: Simulated pH and alkalinity profiles for steady state number 6

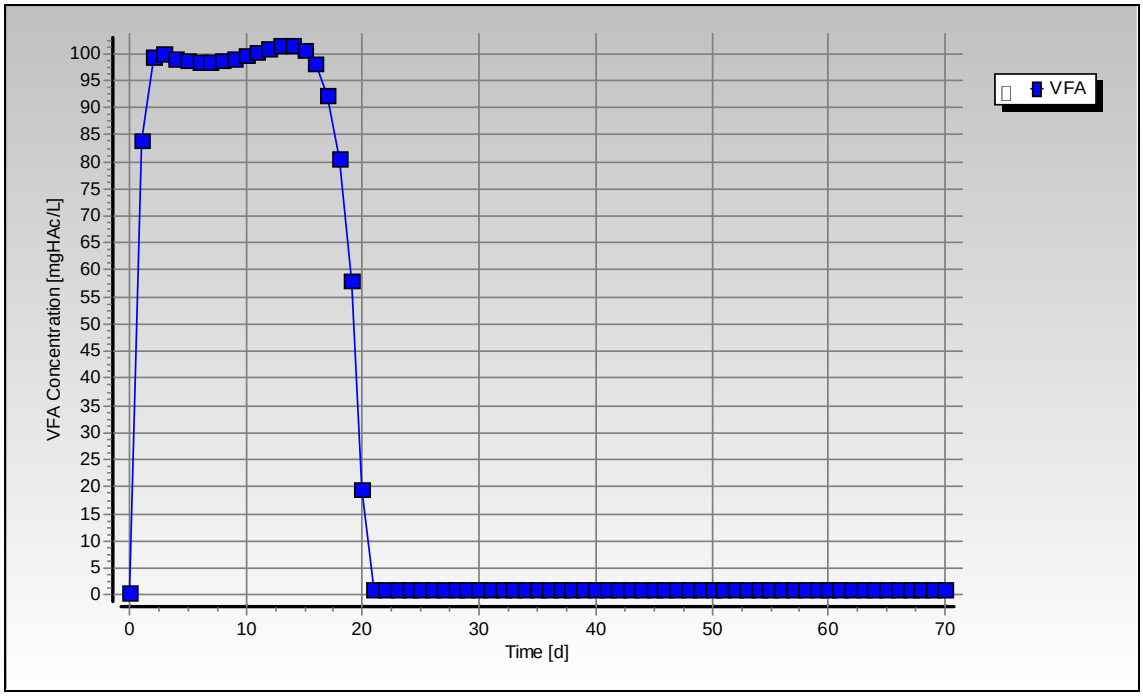

Figure C-17: Simulated VFA concentration profile for steady state number 6

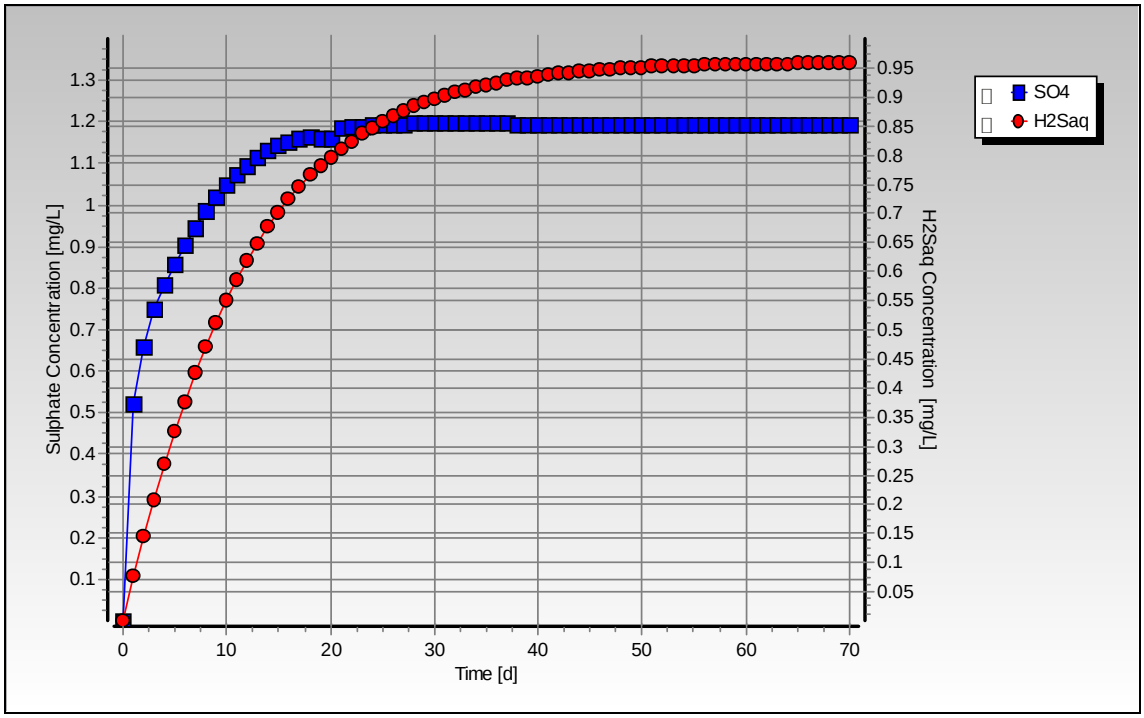

Figure C-18: Simulated sulphate and aqueous hydrogen sulphide concentration profiles for steady state number 6

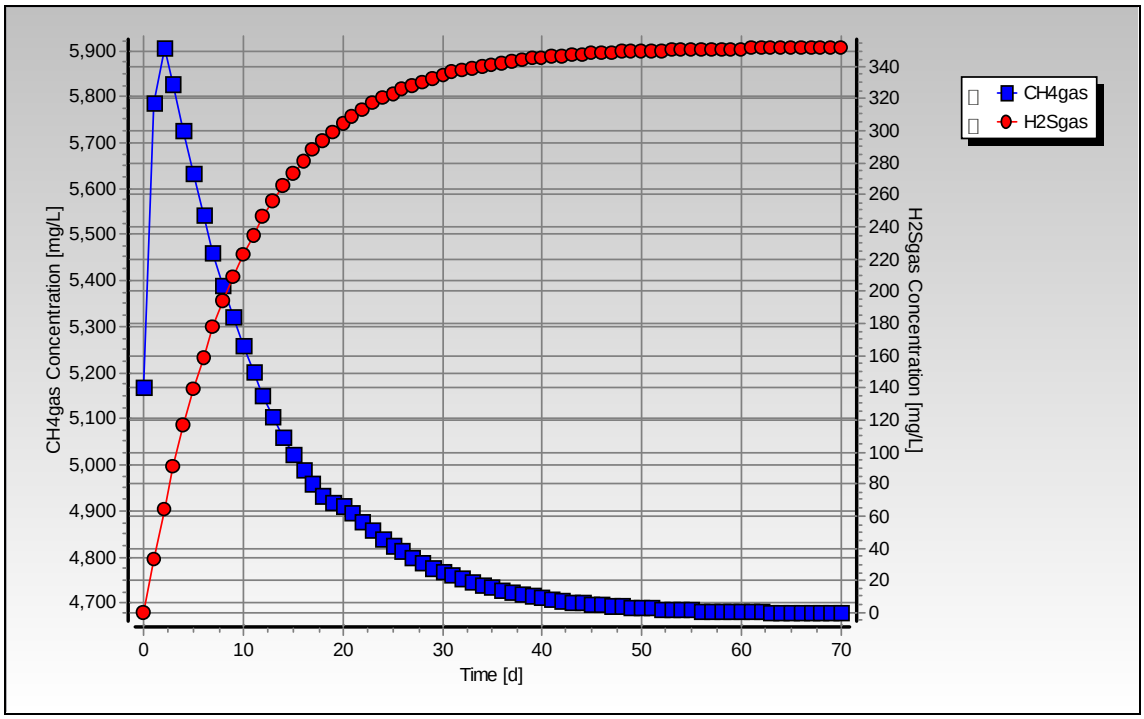

Figure C-19: Simulated methane and hydrogen sulphide gas concentration profiles for steady state number 6

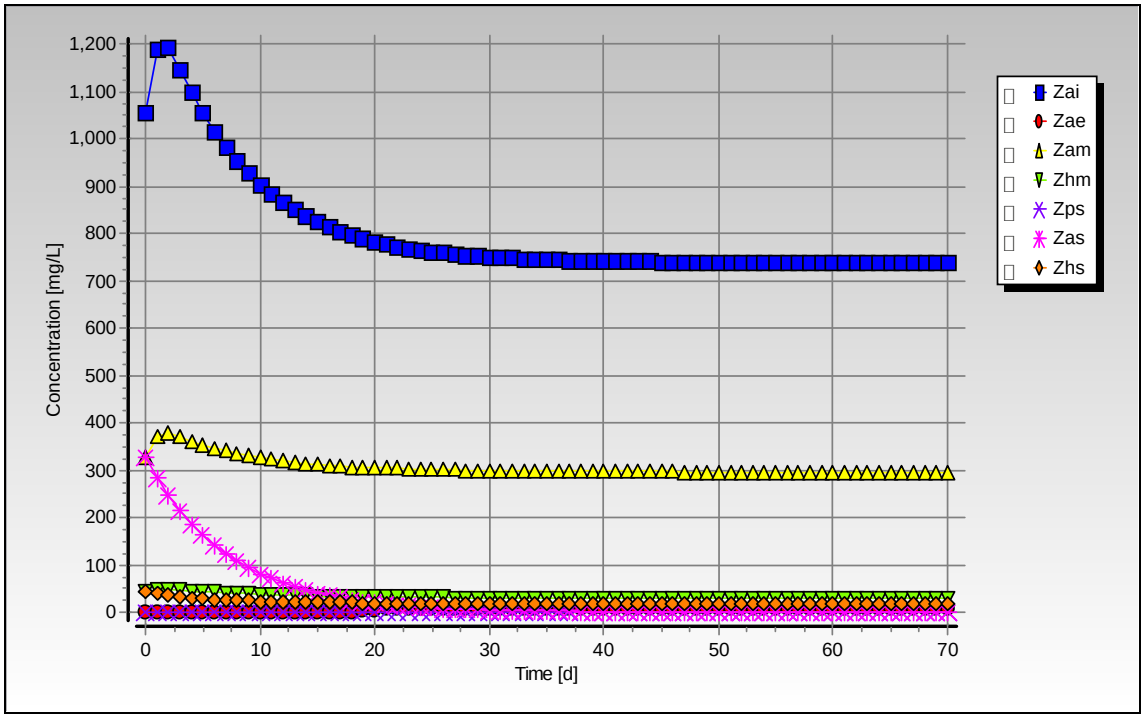

Figure C-20: Simulated biomass concentration profiles for steady state number 6

Steady State Number 7

Table C-13: Operating conditions for steady state number 7

Feed Batch Number	F13
Reactor Volume (ℓ)	16
Retention Time (d)	6.67
pH	steady state
Biological Groups Present	acidogenic, acetogenic and methanogenic

Table C-14: Results summary for steady state number 7

	Measured	**Model**	**Relative error (%)**
Feed Total COD (mg COD/ℓ)	24882	25228	-
Feed Soluble COD (mg COD/ℓ)	2028	2374	-
Feed TKN (mg N/ℓ)	614	614	-
Feed FSA (mg N/ℓ)	106	106	-
Effluent Total COD (mg COD/ℓ)	12595 ± 239	12549.55	-0.36
Effluent Soluble COD (mg COD/ℓ)	200 ± 12	257.55	22.35
Reactor pH	6.86 ± 0.05	6.63	-3.47
Effluent VFA (mg HAc/ℓ)	19 ± 13	1.90	-899.03
Effluent Alkalinity (mg/ℓ as $CaCO_3$)	1504 ± 27	1518.46	0.95
Sulphate Addition (mg SO4/ℓ)	0	0	-
Effluent Sulphate (mg SO4/ℓ)	0	0	-
% Sulphate Conversion	-	-	-
Methane Production (ℓ/d)	11.66	13.19	11.63
Gas Composition (% CH_4)	60.98	61.52	0.89
Effluent FSA (mg N/ℓ)	196 ± 2	239.92	18.30
Effluent TKN (mg N/ℓ)	581 ± 28	529.95	-9.63

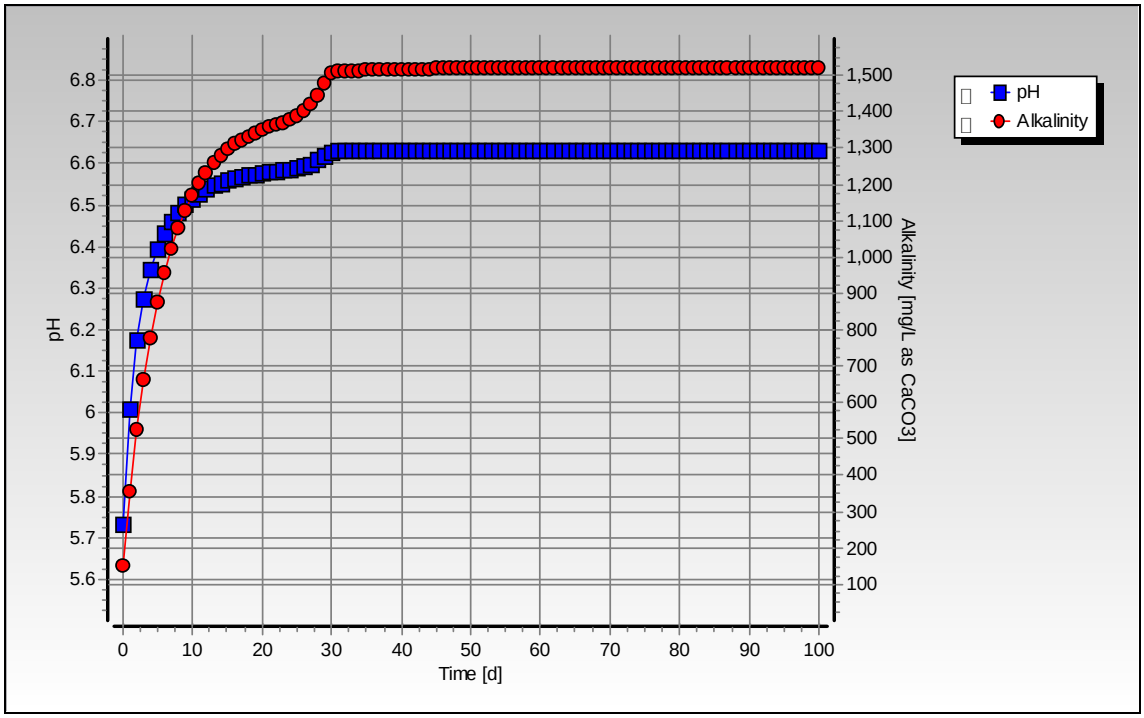

Figure C-21: Simulated pH and alkalinity profiles for steady state number 7

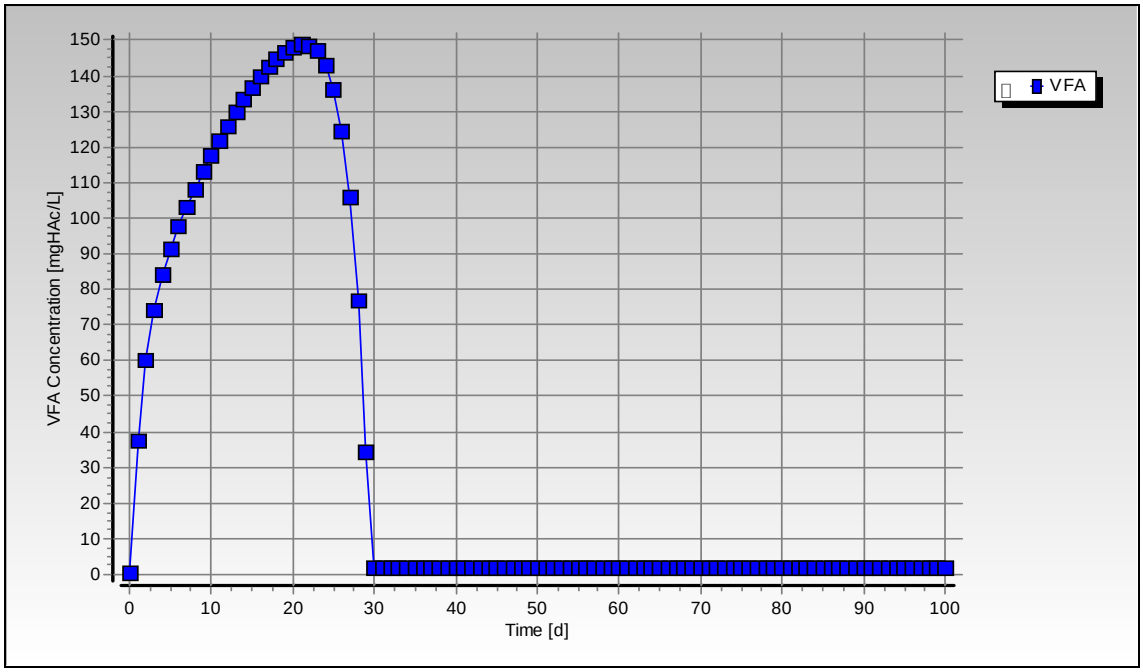

Figure C-22: Simulated VFA concentration profile for steady state number 7

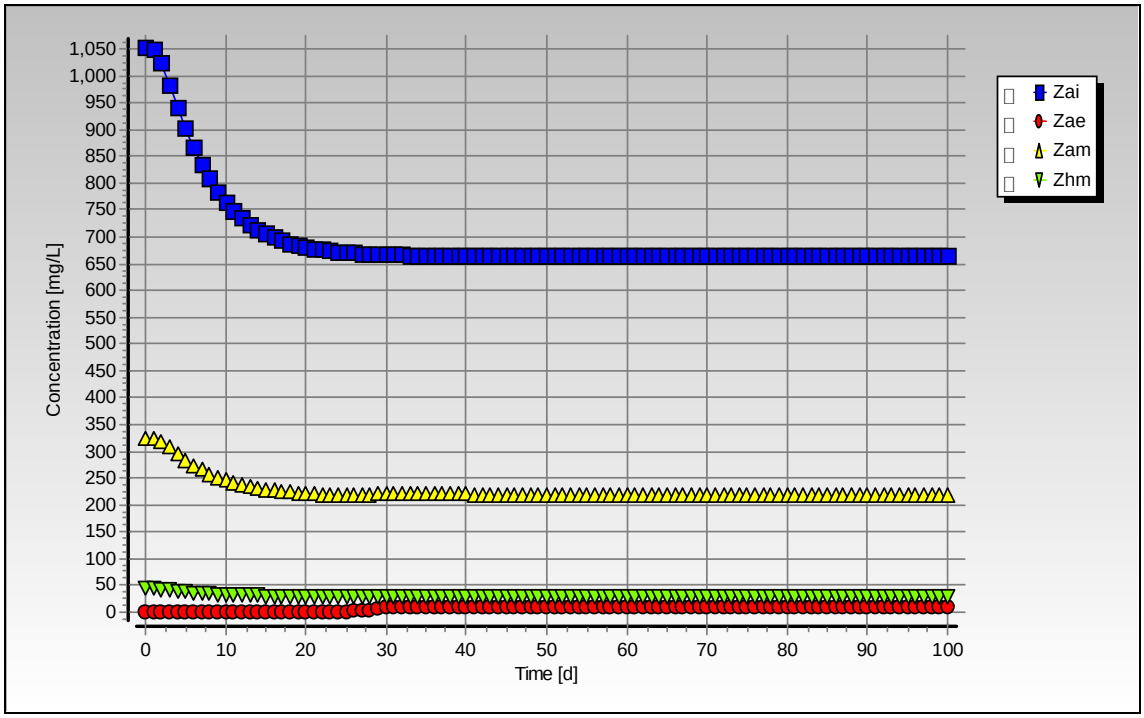

Figure C-23: Simulated biomass concentration profiles for steady state number 7

Steady State Number 8

Table C-15: Operating conditions for steady state number 8

Feed Batch Number	F13
Reactor Volume (ℓ)	16
Retention Time (d)	5.71
pH	steady state
Biological Groups Present	acidogenic, acetogenic and methanogenic

Table C-16: Results summary for steady state number 8

	Measured	**Model**	**Relative error (%)**
Feed Total COD (mg COD/ℓ)	24960	25061	-
Feed Soluble COD (mg COD/ℓ)	2503	2604	-
Feed TKN (mg N/ℓ)	616	616	-
Feed FSA (mg N/ℓ)	124	124	-
Effluent Total COD (mg COD/ℓ)	12729 ± 297	12713.84	-0.12
Effluent Soluble COD (mg COD/ℓ)	205 ± 12	273.94	25.17
Reactor pH	6.93 ± 0.01	6.62	-4.74
Effluent VFA (mg HAc/ℓ)	32 ± 10	2.38	-1242.13
Effluent Alkalinity (mg/ℓ as $CaCO_3$)	1463 ± 16	1470.85	0.53
Sulphate Addition (mg SO4/ℓ)	0	0	-
Effluent Sulphate (mg SO4/ℓ)	0	0	-
% Sulphate Conversion	-	-	-
Methane Production (ℓ/d)	13.24	15.01	11.79
Gas Composition (% CH_4)	61.67	61.37	-0.49
Effluent FSA (mg N/ℓ)	200 ± 4	246.47	18.85
Effluent TKN (mg N/ℓ)	574 ± 6	538.51	-6.59

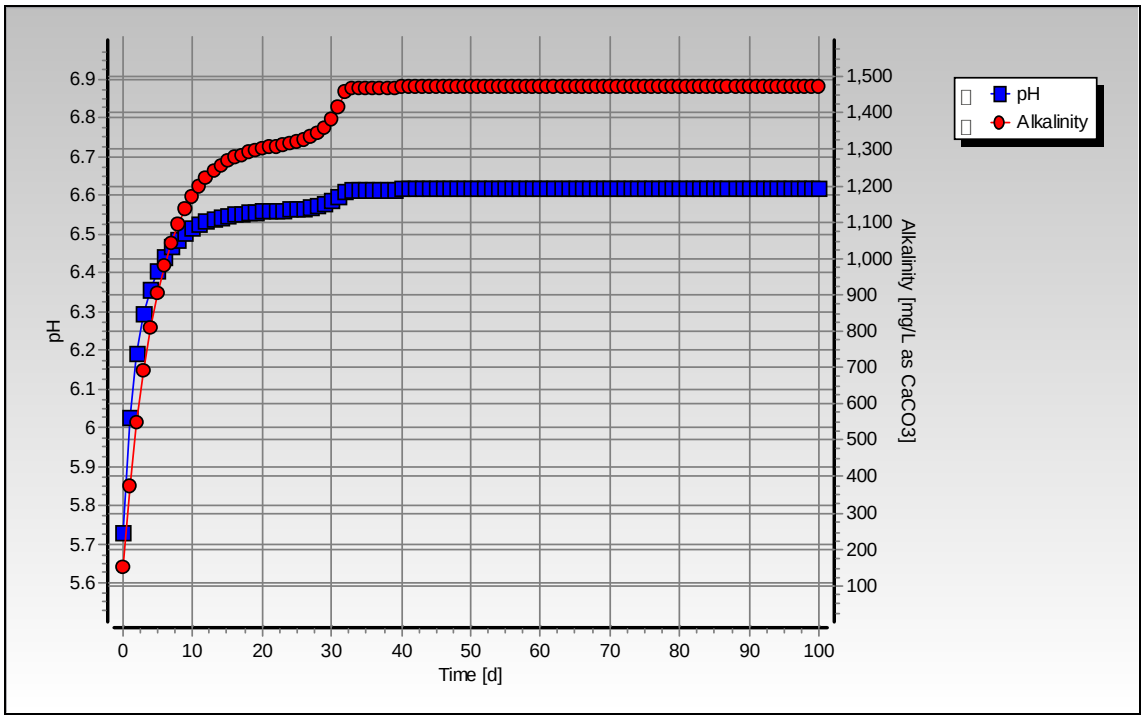

Figure C-24: Simulated pH and alkalinity profiles for steady state number 8

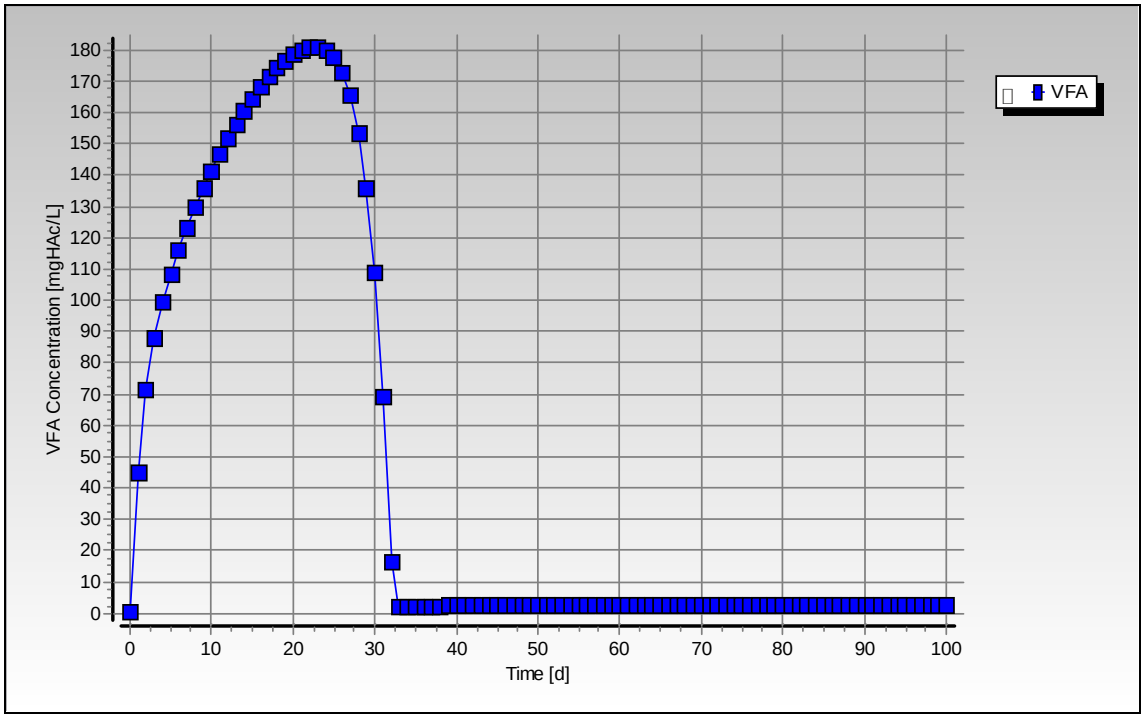

Figure C-25: Simulated VFA concentration profile for steady state number 8

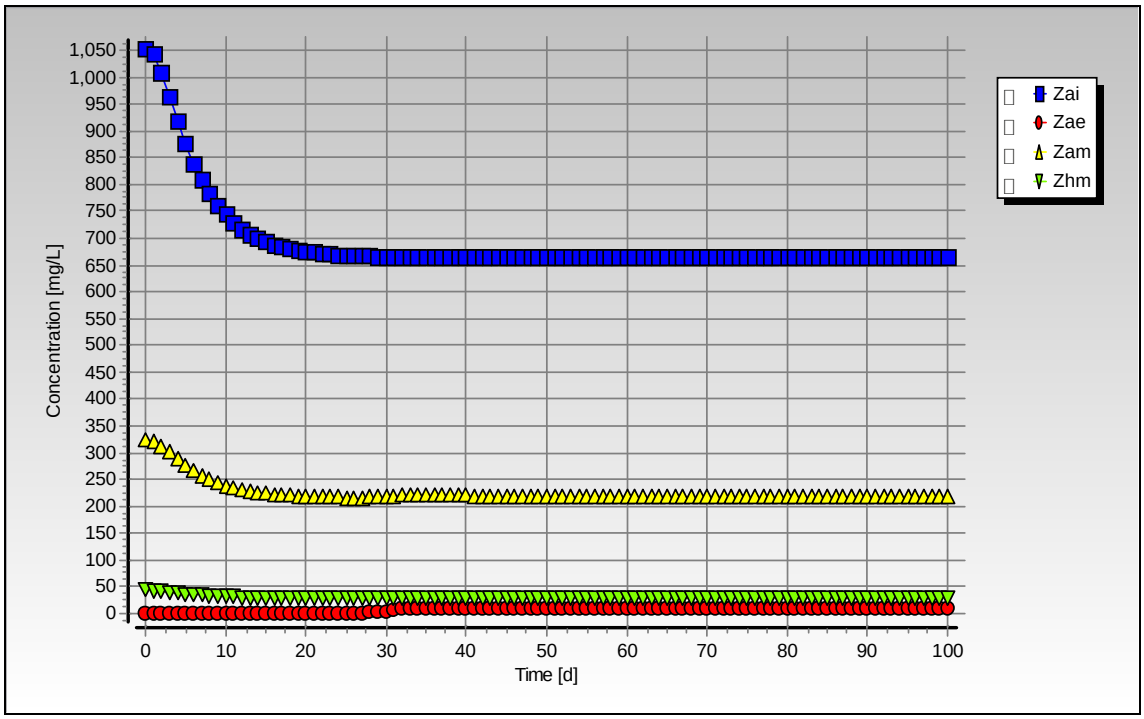

Figure C-26: Simulated biomass concentration profiles for steady state number 8

Steady State Number 9

Table C-17: Operating conditions for steady state number 9

Feed Batch Number	F13
Reactor Volume (ℓ)	16
Retention Time (d)	5
pH	steady state
Biological Groups Present	acidogenic, acetogenic and methanogenic

Table C-18: Results summary for steady state number 9

	Measured	**Model**	**Relative error (%)**
Feed Total COD (mg COD/ℓ)	24880	24880	-
Feed Soluble COD (mg COD/ℓ)	2693	2693	-
Feed TKN (mg N/ℓ)	614	614	-
Feed FSA (mg N/ℓ)	131	131	-
Effluent Total COD (mg COD/ℓ)	12610 ± 262	12847.97	1.85
Effluent Soluble COD (mg COD/ℓ)	301 ± 15	382.47	21.30
Reactor pH	6.78 ± 0.02	6.60	-2.73
Effluent VFA (mg HAc/ℓ)	87 ± 7	2.96	-2838.49
Effluent Alkalinity (mg/ℓ as $CaCO_3$)	1359 ± 18	1412.22	3.77
Sulphate Addition (mg SO4/ℓ)	0	0	-
Effluent Sulphate (mg SO4/ℓ)	0	0	-
% Sulphate Conversion	-	-	-
Methane Production (ℓ/d)	13.57	16.71	18.79
Gas Composition (% CH_4)	61.23	61.34	0.19
Effluent FSA (mg N/ℓ)	193 ± 4	247.66	22.07
Effluent TKN (mg N/ℓ)	455 ± 6	539.42	15.65

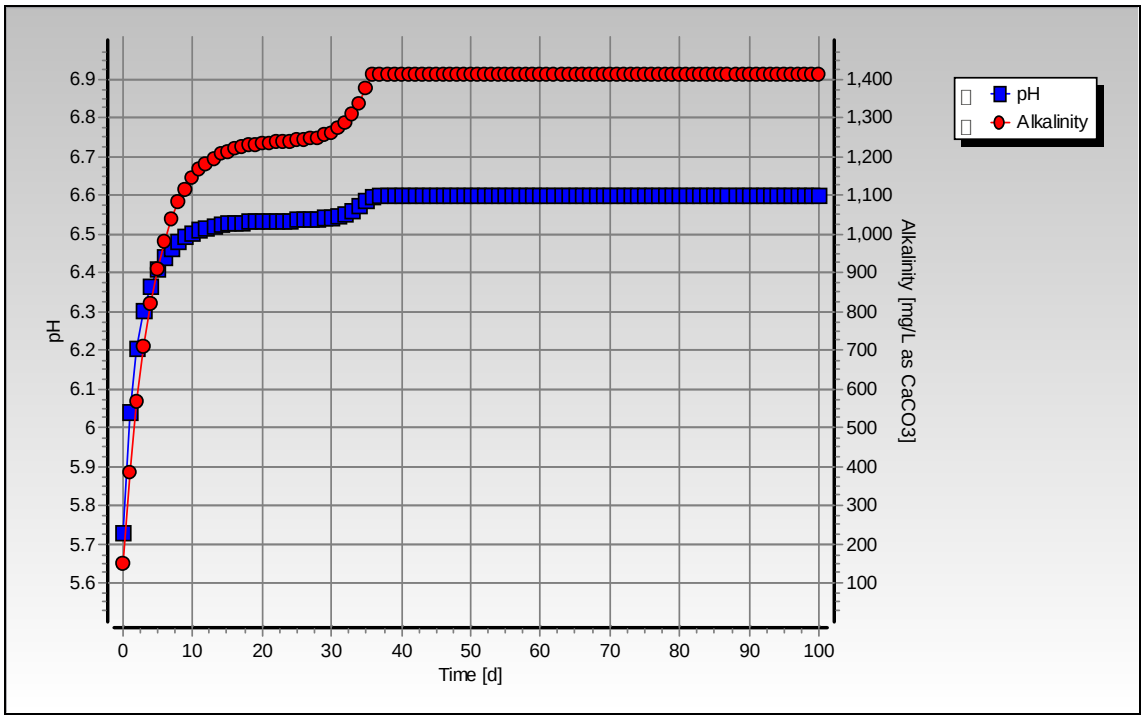

Figure C-27: Simulated pH and alkalinity profiles for steady state number 9

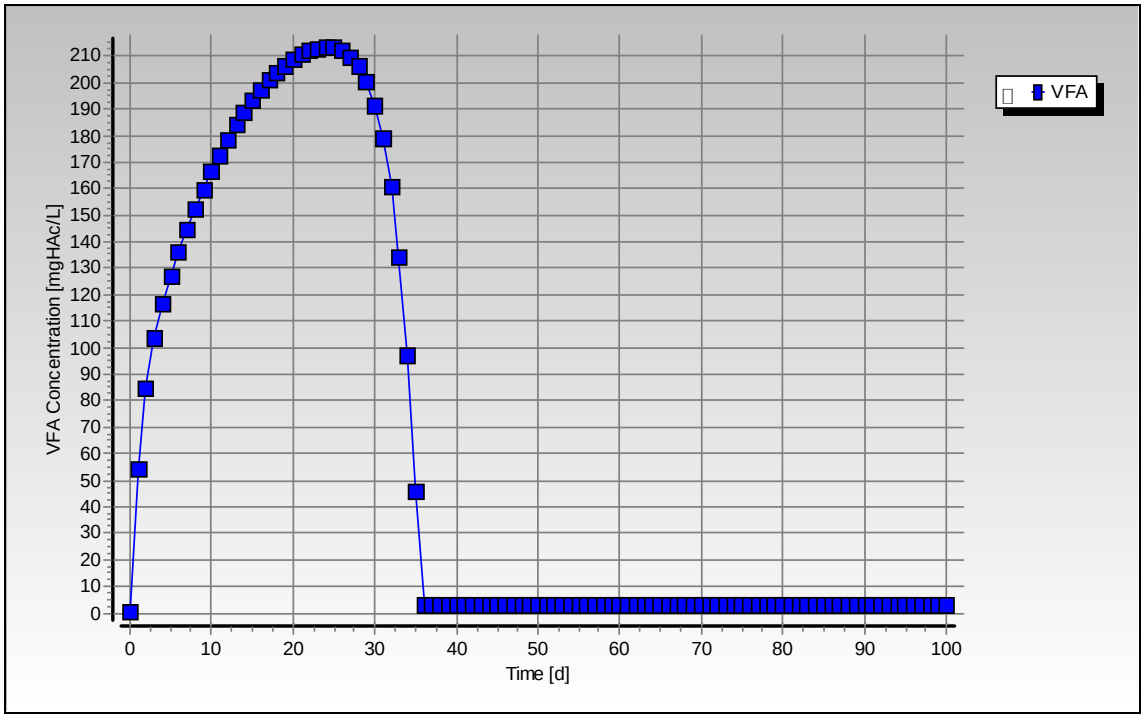

Figure C-28: Simulated VFA concentration profile for steady state number 9

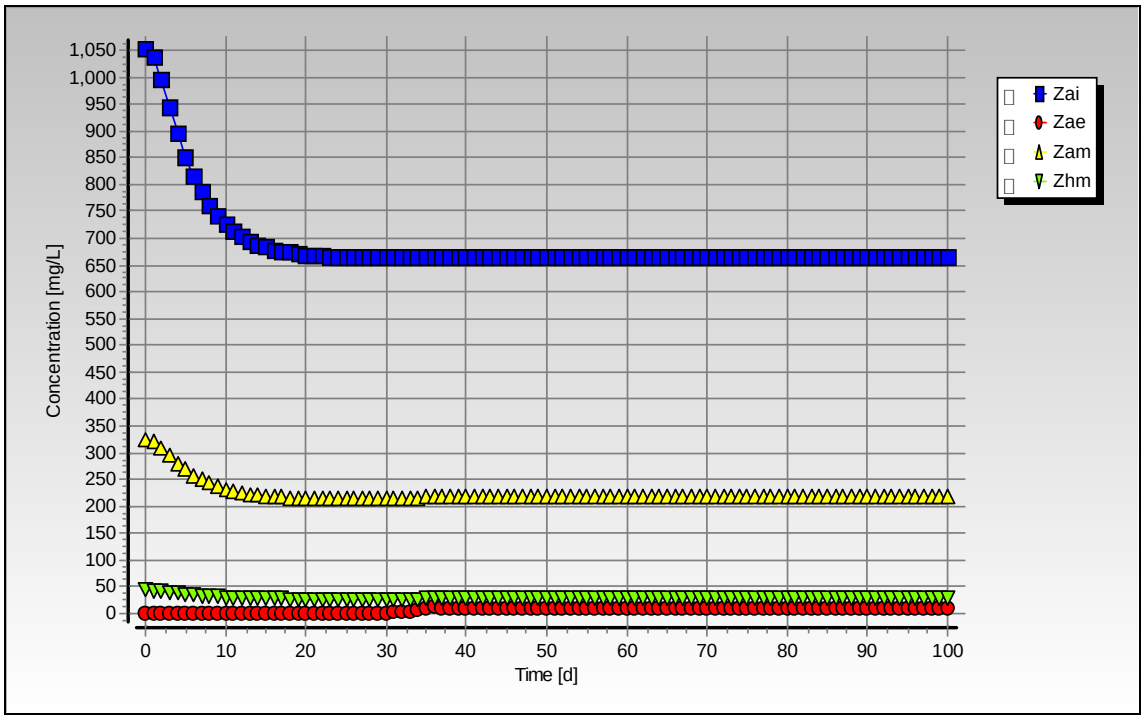

Figure C-29: Simulated biomass concentration profiles for steady state number 9

Steady State Number 10

Table C-19: Operating conditions for steady state number 10

Feed Batch Number	F13
Reactor Volume (ℓ)	20
Retention Time (d)	15
pH	steady state
Biological Groups Present	acidogenic, acetogenic and methanogenic

Table C-20: Results summary for steady state number 10

	Measured	**Model**	**Relative error (%)**
Feed Total COD (mg COD/ℓ)	39789	39984	-
Feed Soluble COD (mg COD/ℓ)	3520	3715	-
Feed TKN (mg N/ℓ)	982	982	-
Feed FSA (mg N/ℓ)	180	180	-
Effluent Total COD (mg COD/ℓ)	16972 ± 322	17033.63	0.36
Effluent Soluble COD (mg COD/ℓ)	250 ± 7	276.86	9.70
Reactor pH	6.98 ± 0.02	6.83	-2.16
Effluent VFA (mg HAc/ℓ)	28 ± 7	0.67	-4093.73
Effluent Alkalinity (mg/ℓ as $CaCO_3$)	2446 ± 25	2442.00	-0.16
Sulphate Addition (mg SO4/ℓ)	0	0	-
Effluent Sulphate (mg SO4/ℓ)	0	0	-
% Sulphate Conversion	-	-	-
Methane Production (ℓ/d)	12.12	13.30	8.86
Gas Composition (% CH_4)	61.4	61.11	-0.47
Effluent FSA (mg N/ℓ)	347 ± 8	459.10	24.42
Effluent TKN (mg N/ℓ)	854 ± 14	893.84	4.46

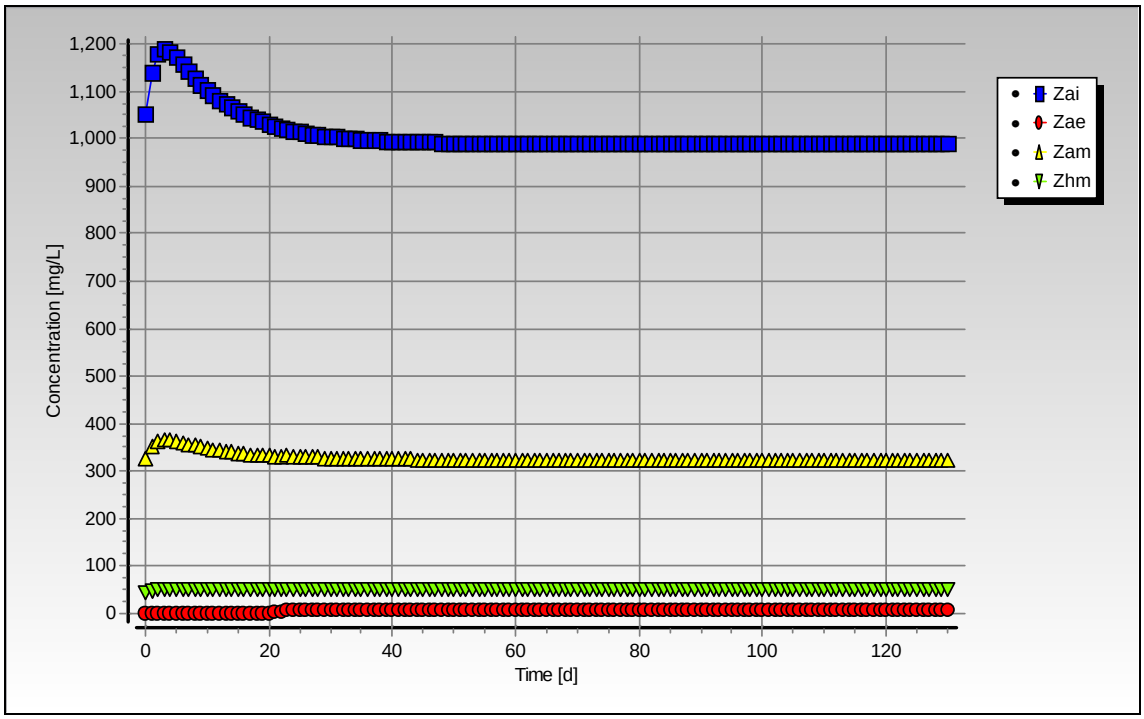

Figure C-30: Simulated pH and alkalinity profiles for steady state number 10

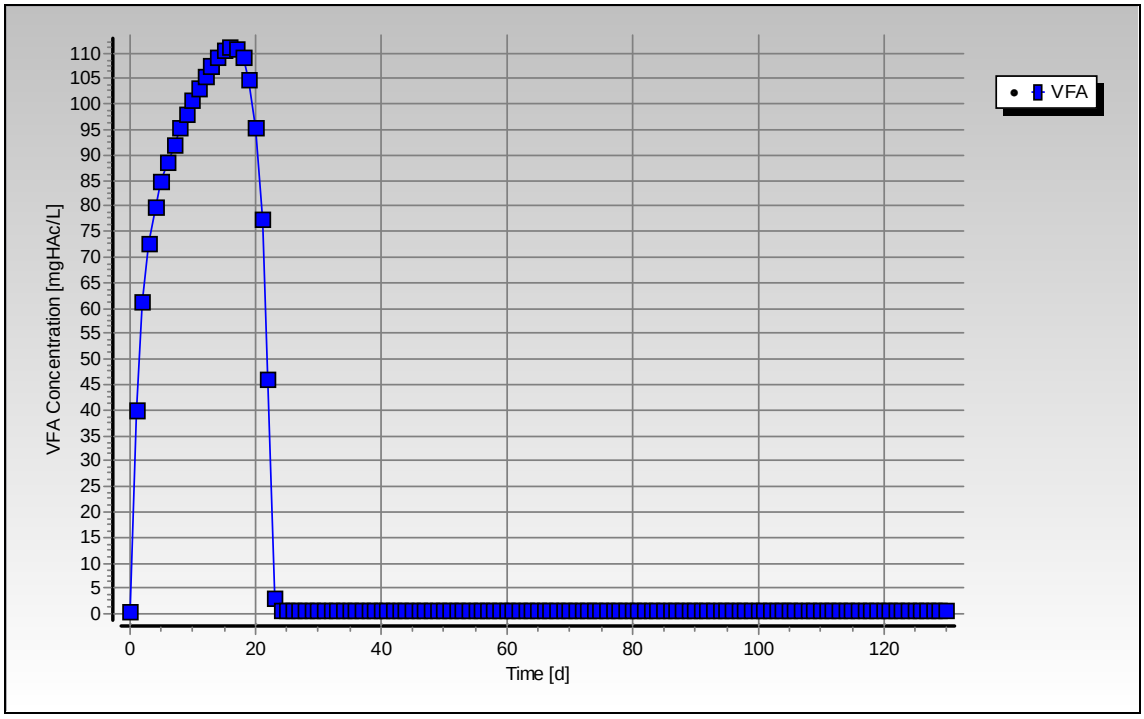

Figure C-31: Simulated VFA concentration profile for steady state number 10

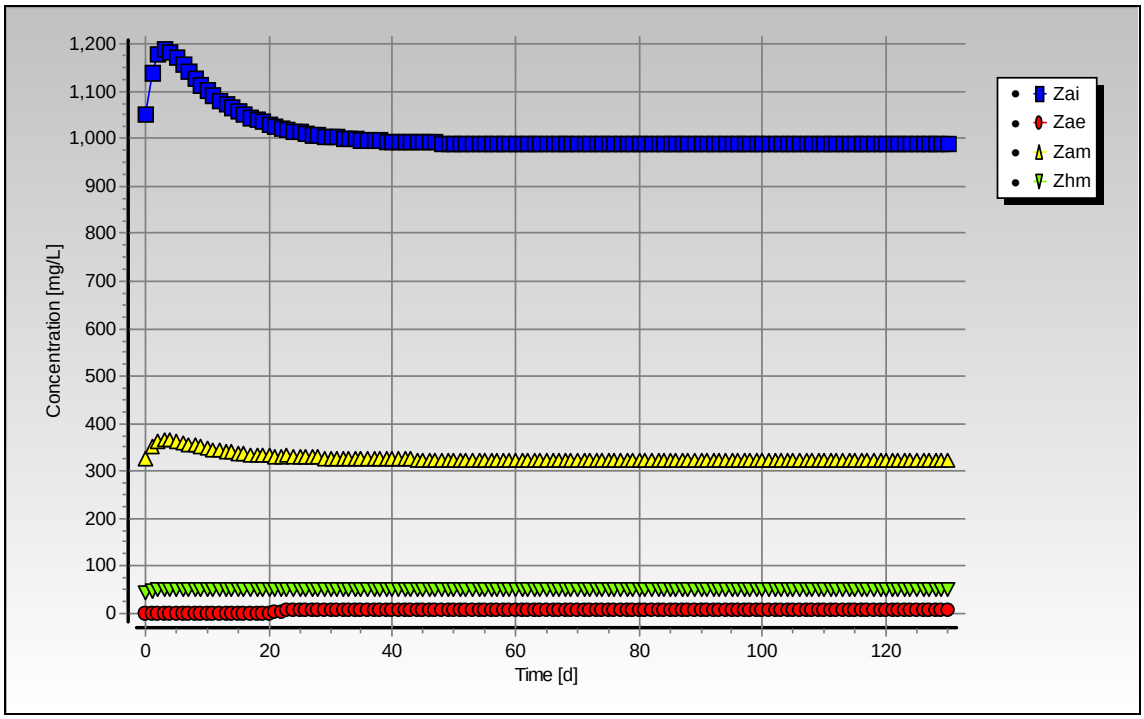

Figure C-32: Simulated biomass concentration profiles for steady state number 10

Steady State Number 11

Table C-21: Operating conditions for steady state number 11

Feed Batch Number	F13
Reactor Volume (ℓ)	20
Retention Time (d)	15
pH	steady state
Biological Groups Present	acidogenic, acetogenic and methanogenic

Table C-22: Results summary for steady state number 11

	Measured	**Model**	**Relative error (%)**
Feed Total COD (mg COD/ℓ)	39791	39965	-
Feed Soluble COD (mg COD/ℓ)	3991	4165	-
Feed TKN (mg N/ℓ)	982	982	-
Feed FSA (mg N/ℓ)	198	198	-
Effluent Total COD (mg COD/ℓ)	17167 ± 283	17214.72	0.28
Effluent Soluble COD (mg COD/ℓ)	299 ± 13	325.84	8.24
Reactor pH	7.12 ± 0.01	6.85	-3.94
Effluent VFA (mg HAc/ℓ)	35 ± 17	0.66	-5195.54
Effluent Alkalinity (mg/ℓ as $CaCO_3$)	2491 ± 73	2535.34	1.75
Sulphate Addition (mg SO4/ℓ)	0	0	-
Effluent Sulphate (mg SO4/ℓ)	0	0	-
% Sulphate Conversion	-	-	-
Methane Production (ℓ/d)	11.51	13.17	12.60
Gas Composition (% CH_4)	61.17	61.14	-0.05
Effluent FSA (mg N/ℓ)	370 ± 3	466.54	20.69
Effluent TKN (mg N/ℓ)	840 ± 12	902.59	6.93

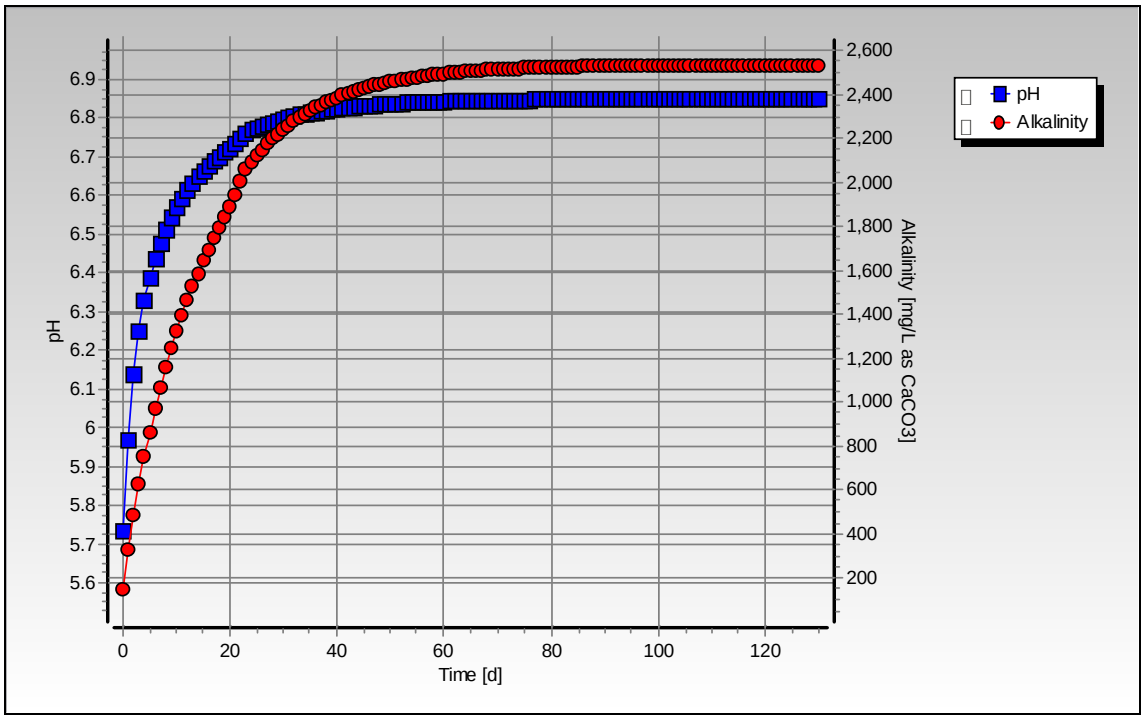

Figure C-33: Simulated pH and alkalinity profiles for steady state number 11

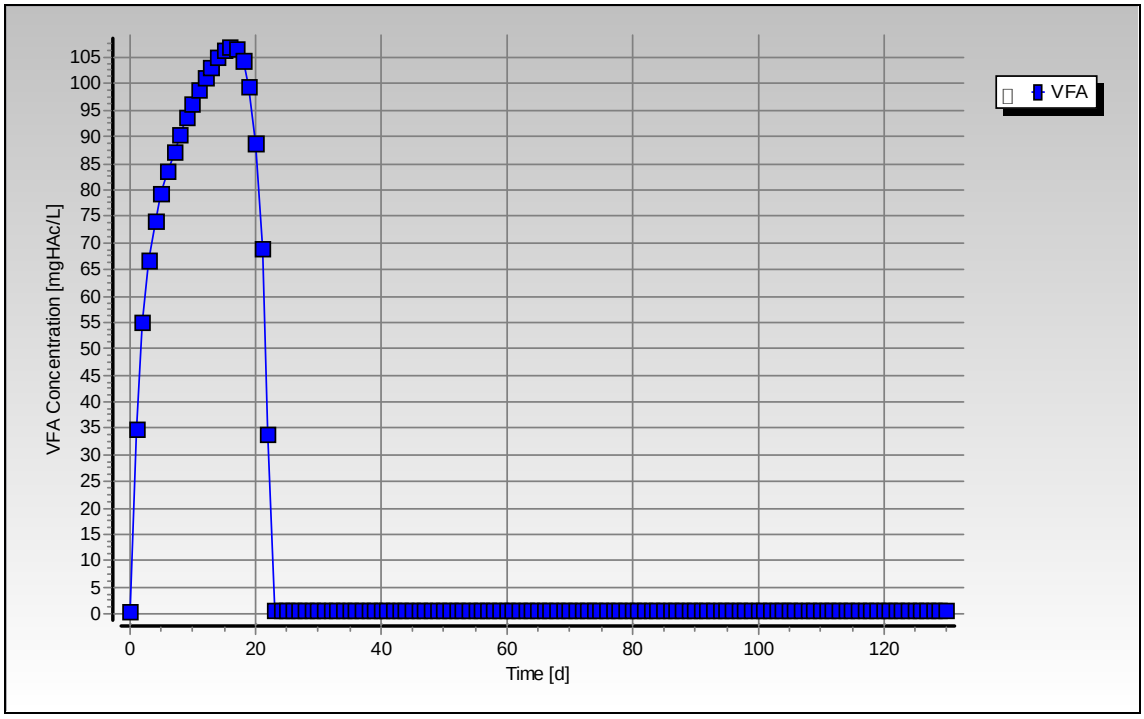

Figure C-34: Simulated VFA concentration profile for steady state number 11

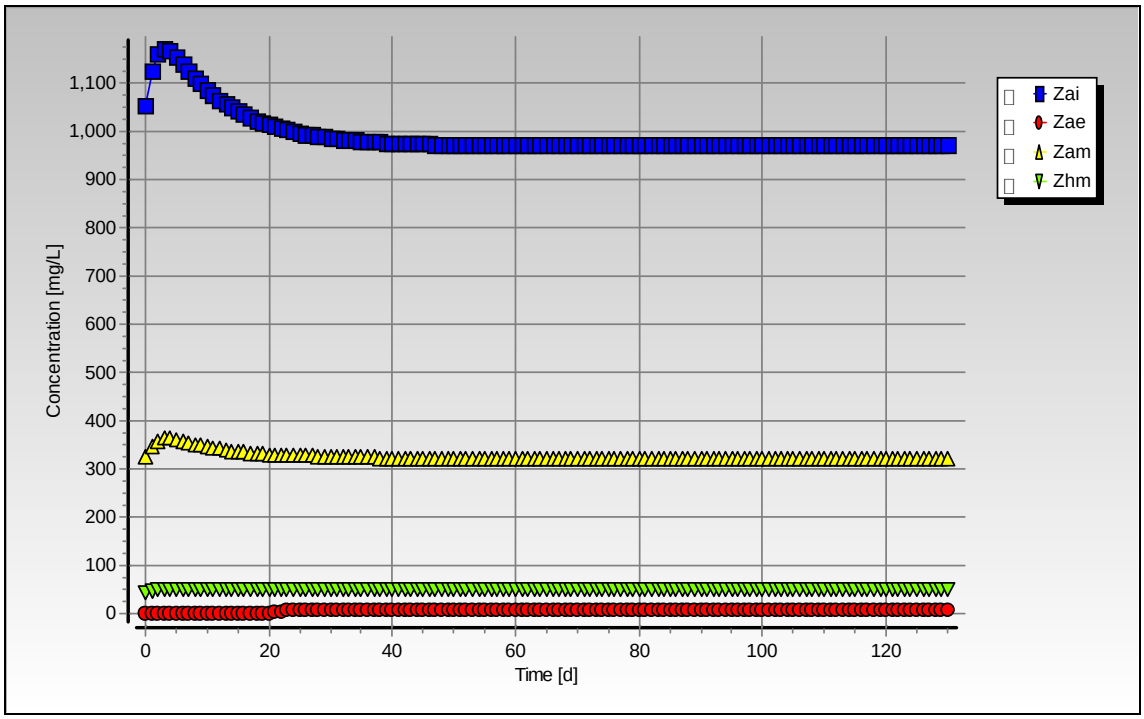

Figure C-35: Simulated biomass concentration profiles for steady state number 11

Steady State Number 12

Table C-23: Operating conditions for steady state number 12

Feed Batch Number	F13
Reactor Volume (ℓ)	20
Retention Time (d)	10
pH	steady state
Biological Groups Present	acidogenic, acetogenic and methanogenic

Table C-24: Results summary for steady state number 12

	Measured	**Model**	**Relative error (%)**
Feed Total COD (mg COD/ℓ)	39810	39810	-
Feed Soluble COD (mg COD/ℓ)	4436	4436	-
Feed TKN (mg N/ℓ)	983	983	-
Feed FSA (mg N/ℓ)	214	214	-
Effluent Total COD (mg COD/ℓ)	18085 ± 589	18629.35	2.92
Effluent Soluble COD (mg COD/ℓ)	256 ± 10	293.88	12.89
Reactor pH	6.92 ± 0.01	6.83	-1.32
Effluent VFA (mg HAc/ℓ)	27 ± 8	1.01	-2586.05
Effluent Alkalinity (mg/ℓ as $CaCO_3$)	2362 ± 25	2425.72	2.63
Sulphate Addition (mg SO4/ℓ)	0	0	-
Effluent Sulphate (mg SO4/ℓ)	0	0	-
% Sulphate Conversion	-	-	-
Methane Production (ℓ/d)	17.33	18.38	5.70
Gas Composition (% CH_4)	62.73	61.17	-2.55
Effluent FSA (mg N/ℓ)	260 ± 22	437.82	40.61
Effluent TKN (mg N/ℓ)	770 ± 14	888.51	13.34

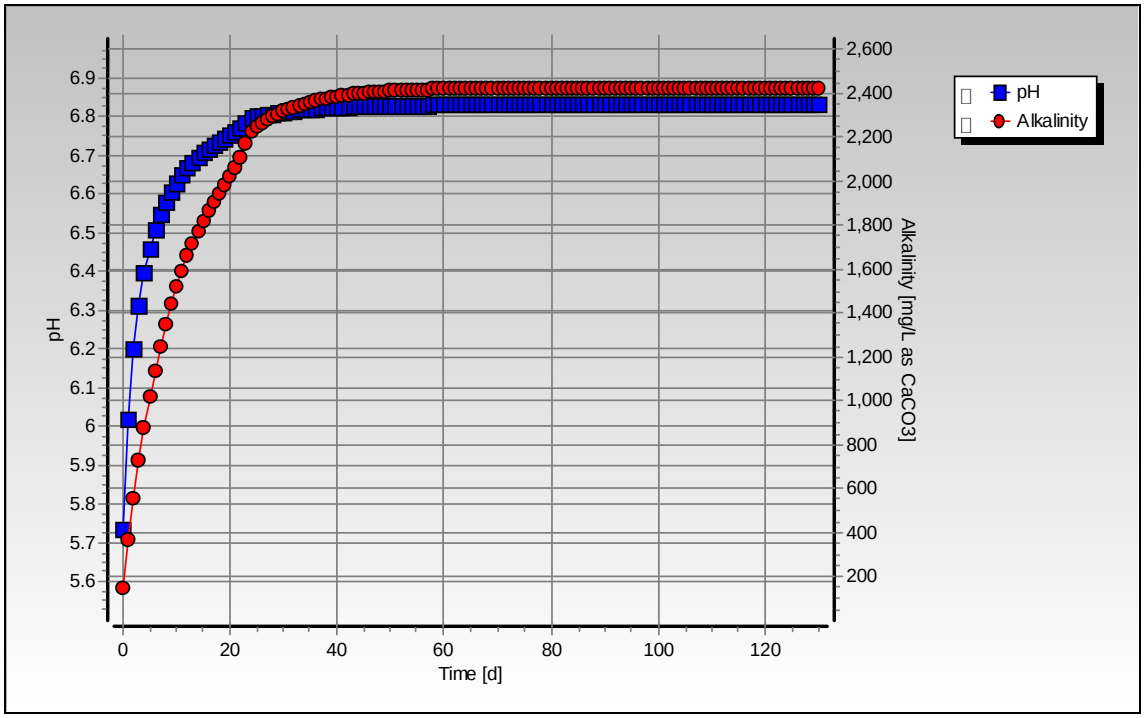

Figure C-36: Simulated pH and alkalinity profiles for steady state number 12

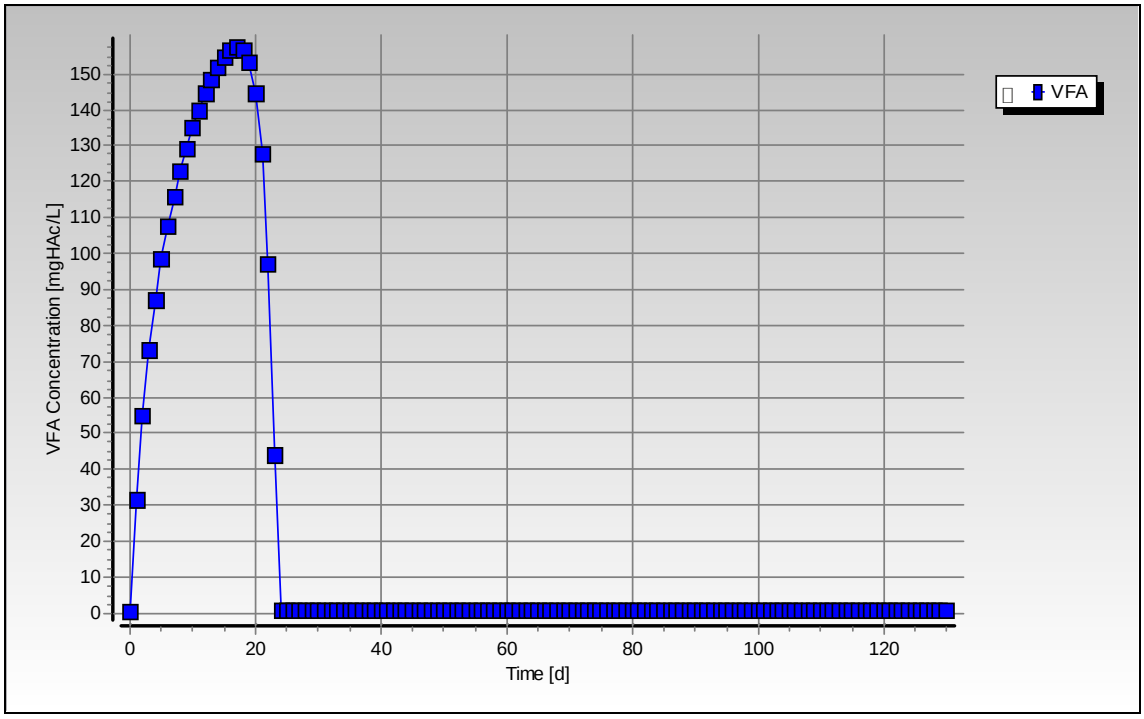

Figure C-37: Simulated VFA concentration profile for steady state number 12

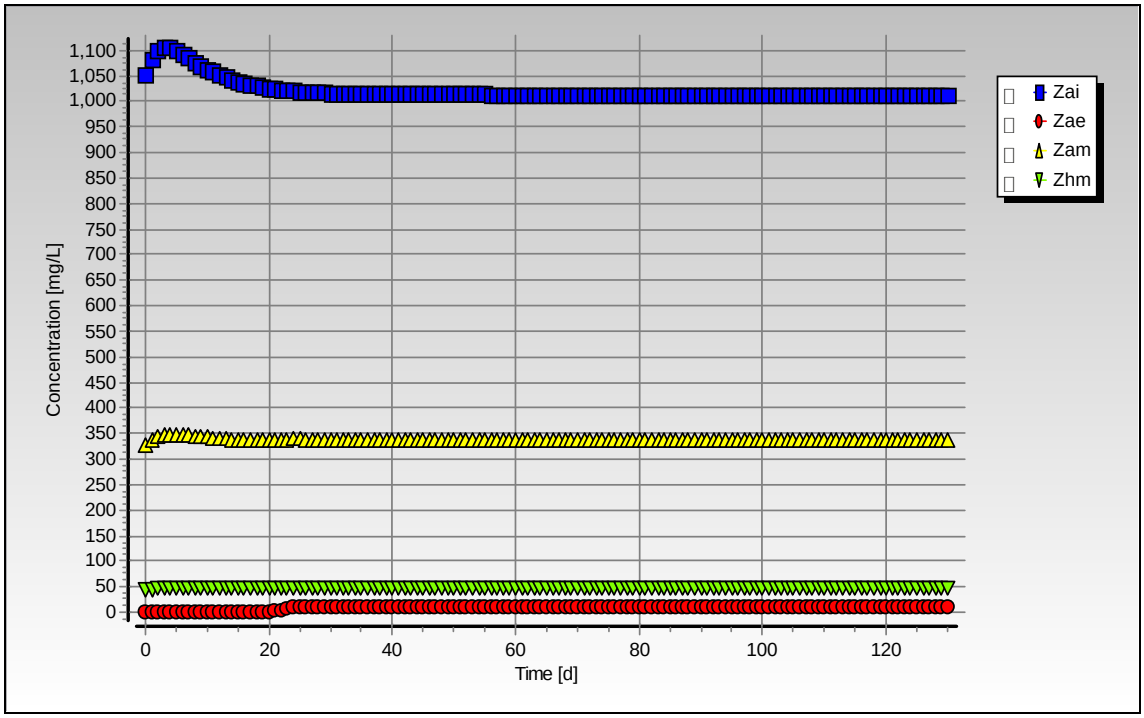

Figure C-38: Simulated biomass concentration profiles for steady state number 12

Steady State Number 13

Table C-25: Operating conditions for steady state number 13

Feed Batch Number	F13
Reactor Volume (ℓ)	20
Retention Time (d)	10
pH	steady state
Biological Groups Present	acidogenic, acetogenic and methanogenic

Table C-26: Results summary for steady state number 13

	Measured	**Model**	**Relative error (%)**
Feed Total COD (mg COD/ℓ)	13270	13270	-
Feed Soluble COD (mg COD/ℓ)	1174	1174	-
Feed TKN (mg N/ℓ)	328	328	-
Feed FSA (mg N/ℓ)	59	59	-
Effluent Total COD (mg COD/ℓ)	6249 ± 109	6147.25	-1.66
Effluent Soluble COD (mg COD/ℓ)	108 ± 5	147.03	26.55
Reactor pH	6.69 ± 0.01	6.35	-5.28
Effluent VFA (mg HAc/ℓ)	8 ± 3	1.63	-389.62
Effluent Alkalinity (mg/ℓ as $CaCO_3$)	854 ± 9	820.53	-4.08
Sulphate Addition (mg SO4/ℓ)	0	0	-
Effluent Sulphate (mg SO4/ℓ)	0	0	-
% Sulphate Conversion	-	-	-
Methane Production (ℓ/d)	5.00	6.19	19.27
Gas Composition (% CH_4)	60.98	60.56	-0.69
Effluent FSA (mg N/ℓ)	127 ± 2	141.18	10.04
Effluent TKN (mg N/ℓ)	302 ± 11	292.55	290.30

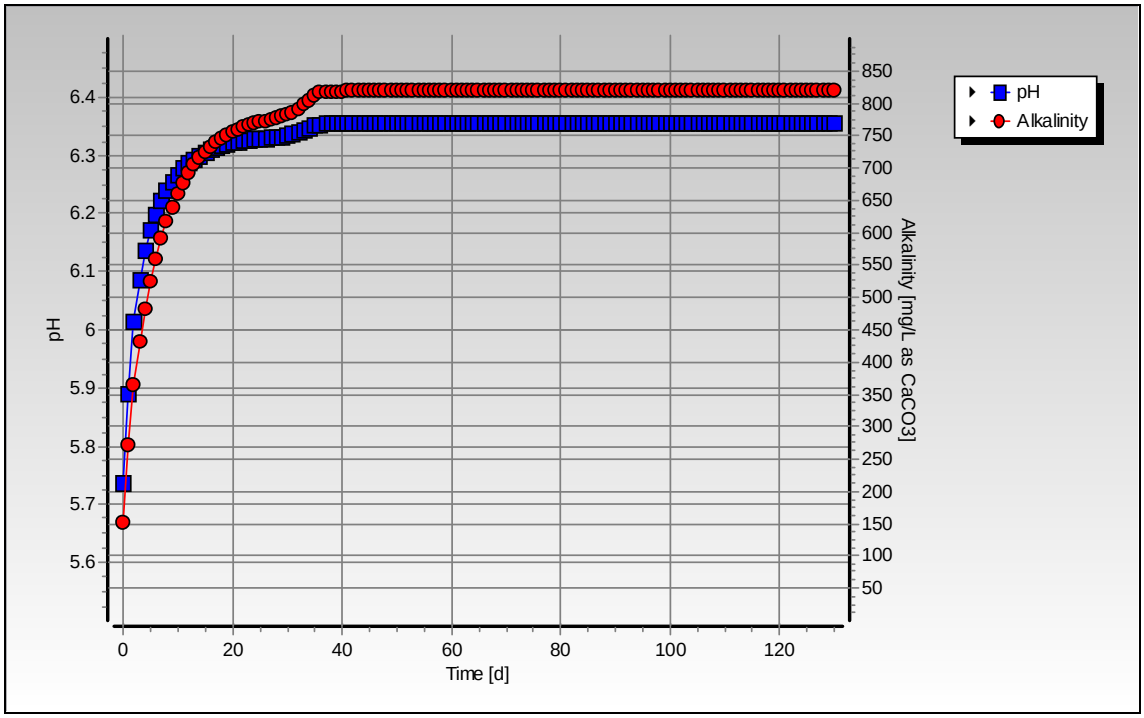

Figure C-39: Simulated pH and alkalinity profiles for steady state number 13

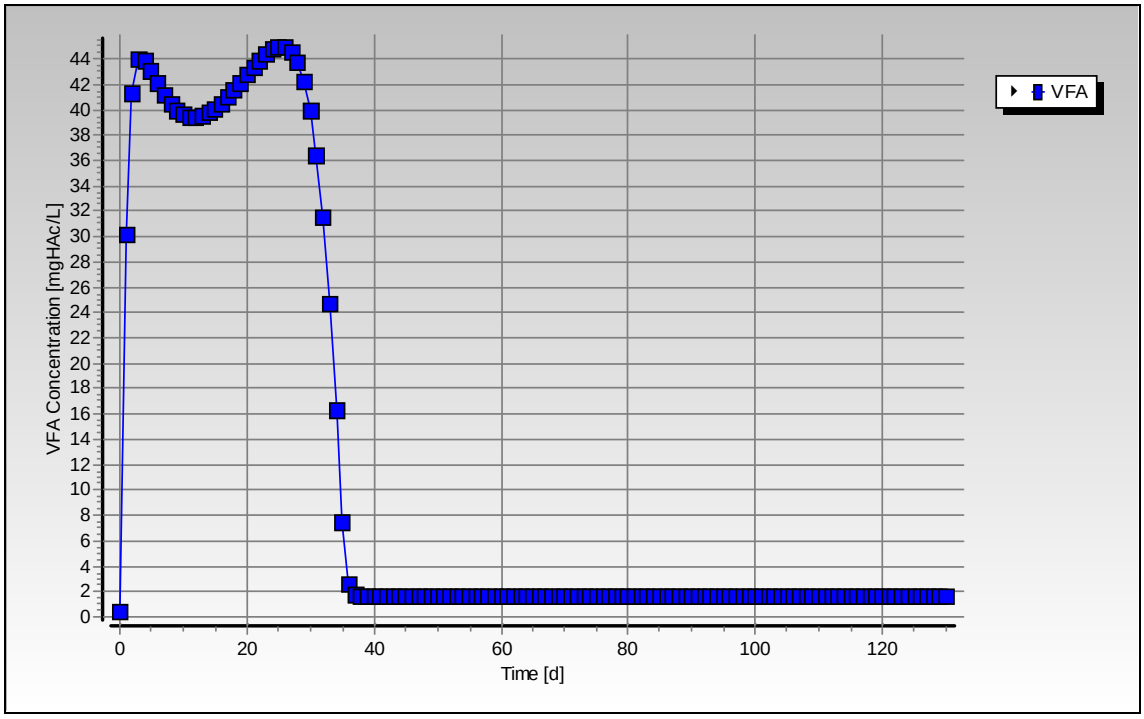

Figure C-40: Simulated VFA concentration profile for steady state number 13

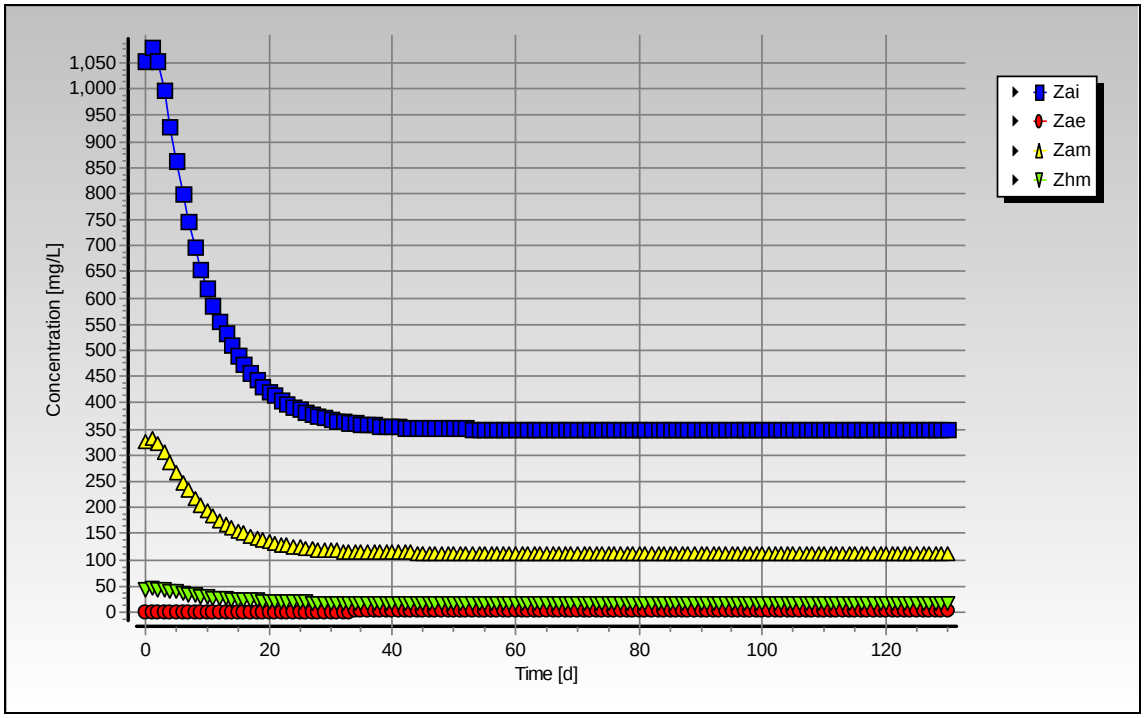

Figure C-41: Simulated biomass concentration profiles for steady state number 13

Steady State Number 14

Table C-27: Operating conditions for steady state number 14

Feed Batch Number	F13
Reactor Volume (ℓ)	20
Retention Time (d)	8
pH	steady state
Biological Groups Present	acidogenic, acetogenic and methanogenic

Table C-28: Results summary for steady state number 14

	Measured	**Model**	**Relative error (%)**
Feed Total COD (mg COD/ℓ)	13269	13269	-
Feed Soluble COD (mg COD/ℓ)	1524	1524	-
Feed TKN (mg N/ℓ)	328	328	-
Feed FSA (mg N/ℓ)	73	73	-
Effluent Total COD (mg COD/ℓ)	6299 ± 86	6384.39	1.34
Effluent Soluble COD (mg COD/ℓ)	104 ± 4	152.34	31.73
Reactor pH	6.78 ± 0.01	6.40	-5.96
Effluent VFA (mg HAc/ℓ)	7 ± 6	2.01	-247.56
Effluent Alkalinity (mg/ℓ as $CaCO_3$)	863 ± 7	903.30	4.46
Sulphate Addition (mg SO4/ℓ)	0	0	-
Effluent Sulphate (mg SO4/ℓ)	0	0	-
% Sulphate Conversion	-	-	-
Methane Production (ℓ/d)	6.4	7.47	14.29
Gas Composition (% CH_4)	63.06	60.76	-3.78
Effluent FSA (mg N/ℓ)	112 ± 3	143.00	21.68
Effluent TKN (mg N/ℓ)	143 ± 28	295.88	51.67

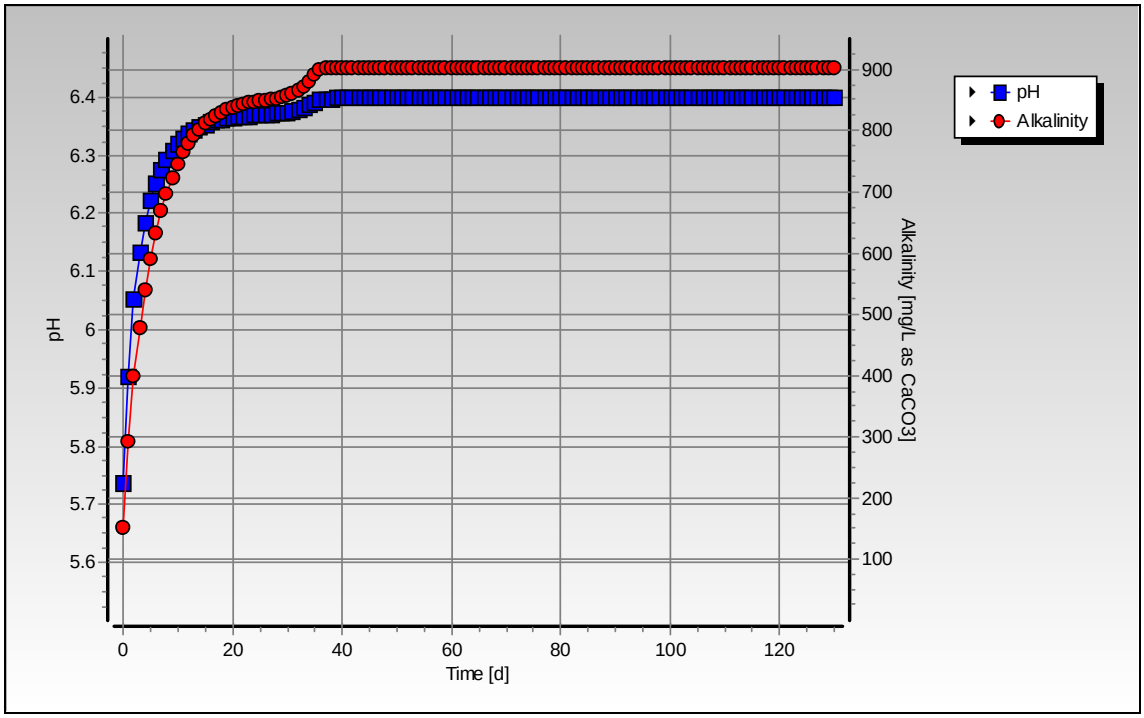

Figure C-42: Simulated pH and alkalinity profiles for steady state number 14

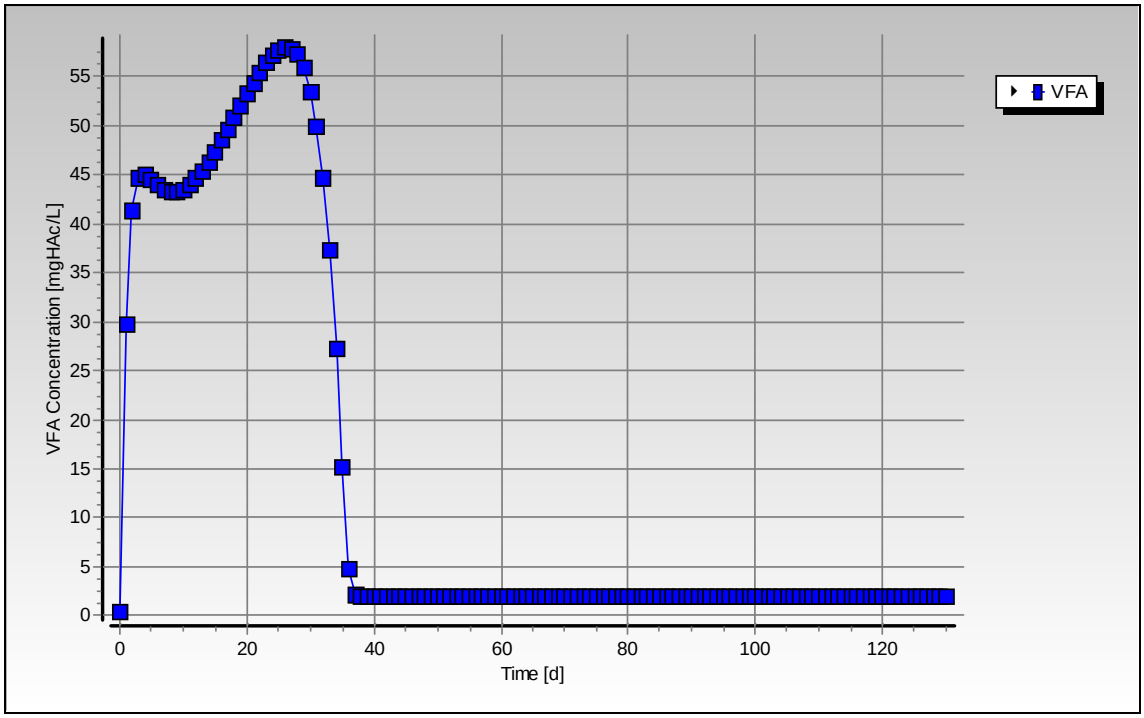

Figure C-43: Simulated VFA concentration profile for steady state number 14

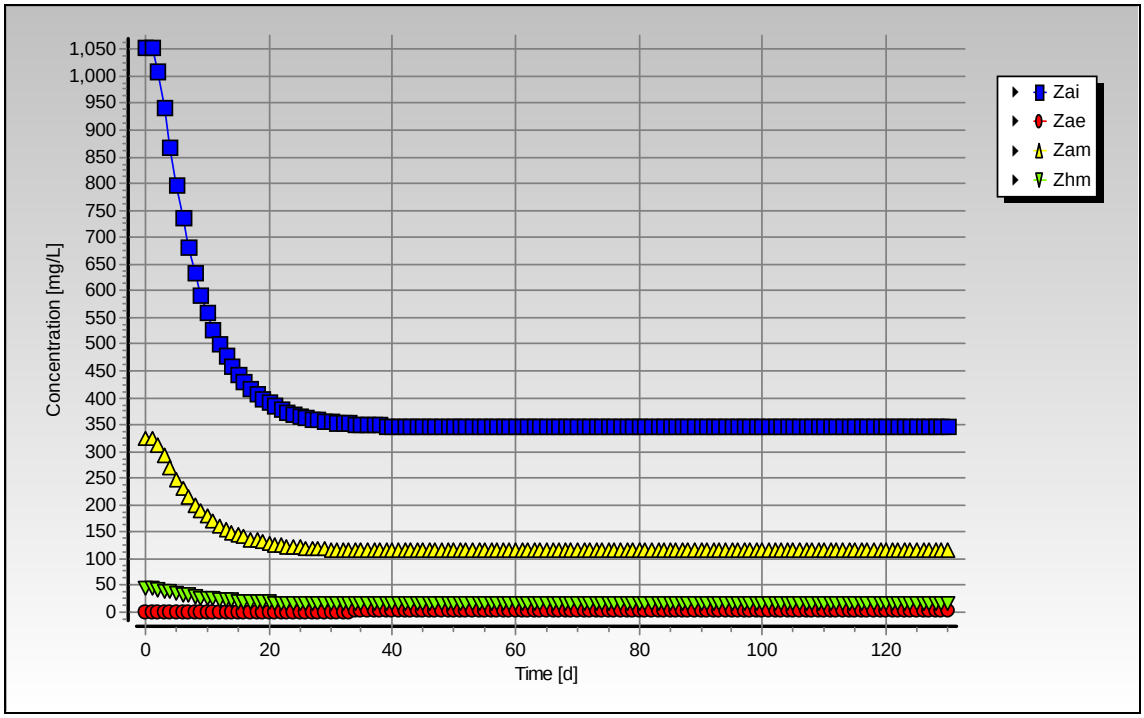

Figure C-44: Simulated biomass concentration profiles for steady state number 14

Steady State Number 15

Table C-29: Operating conditions for steady state number 15

Feed Batch number	F13
Reactor Volume (ℓ)	16
Retention Time (d)	8
pH	Controlled to ~ 6.8
Biological Groups Present	acidogenic, acetogenic, methanogenic and sulphidogenic

Table C-30: Results summary for steady state number 15

	Measured	**Model**	**Relative error (%)**
Feed Total COD (mg COD/ℓ)	13269	13269	-
Feed Soluble COD (mg COD/ℓ)	1524	1524	-
Feed TKN (mg N/ℓ)	328	328	-
Feed FSA (mg N/ℓ)	72	72	-
Effluent Total COD (mg COD/ℓ)	13001 ± 457	5969.54	-117.79
Effluent Soluble COD (mg COD/ℓ)	197 ± 19	192.45	-2.37
Reactor pH	6.87	6.87	-
Effluent VFA (mg HAc/ℓ)	6 ± 6	0.98	-511.75
Effluent Alkalinity (mg/ℓ as $CaCO_3$)	2894 ± 54	2483.95	-16.51
Sulphate Addition (mg SO4/ℓ)	9600	9600	-
Effluent Sulphate (mg SO4/ℓ)	733 ± 35	5953	87.69
% Sulphate Conversion	92.36	37.99	-
Methane Production (ℓ/d)	0.02	3.59	99.44
Gas Composition (% CH_4)	0.53	41.35	98.72
Effluent FSA (mg N/ℓ)	69 ± 5	141.72	51.31
Effluent TKN (mg N/ℓ)	270 ± 24	288.68	6.47

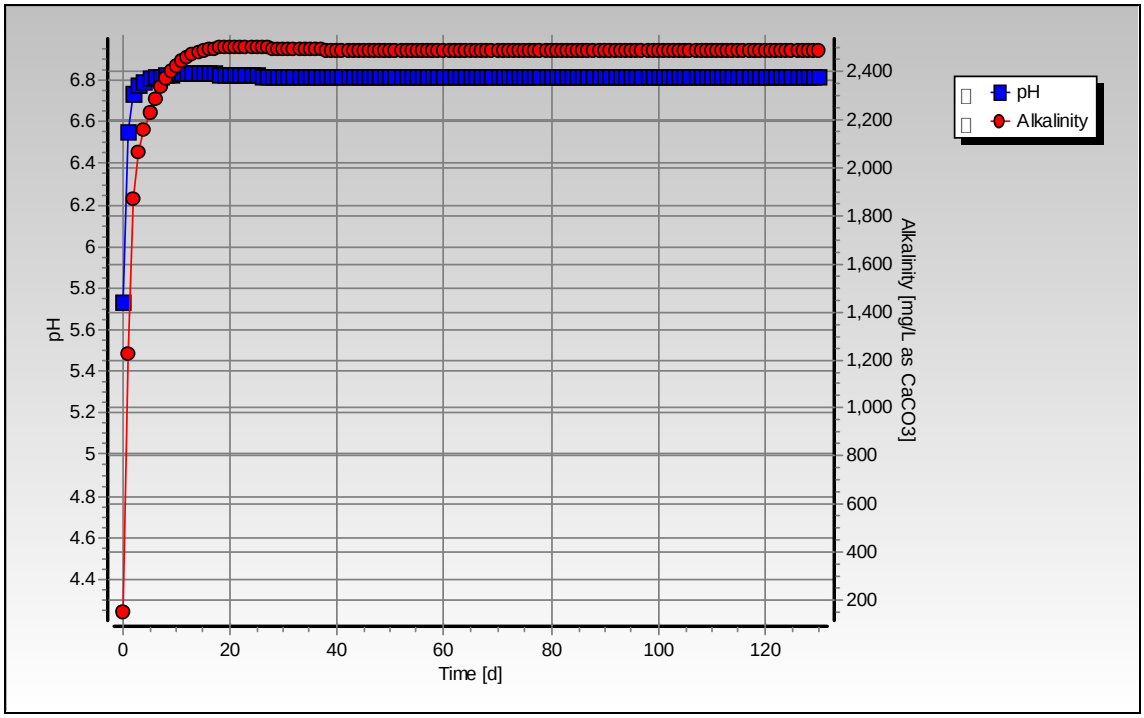

Figure C-45: Simulated pH and alkalinity profiles for steady state number 15

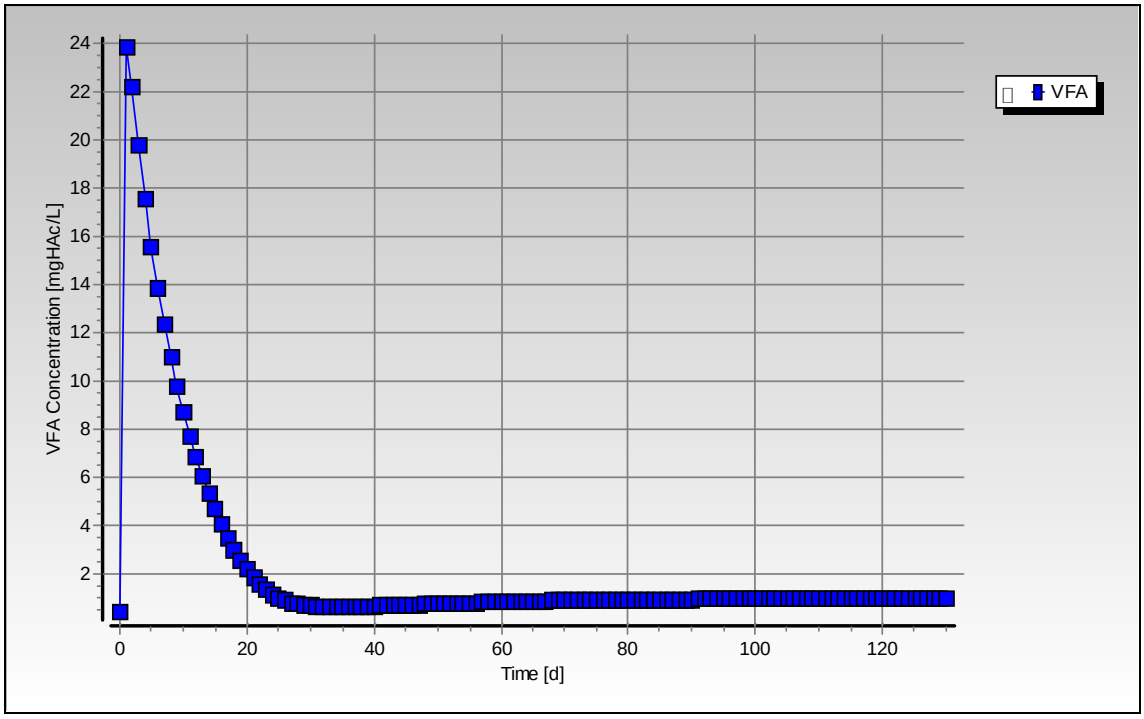

Figure C-46: Simulated VFA concentration profile for steady state number 15

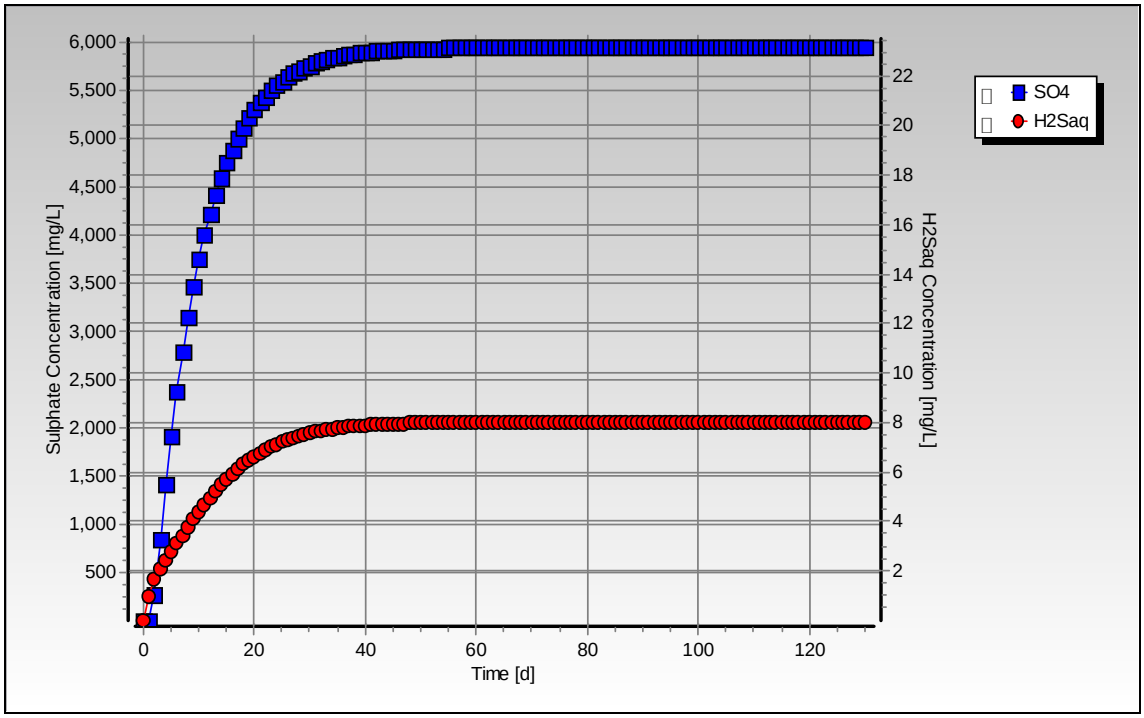

Figure C-47: Simulated sulphate and aqueous hydrogen sulphide concentration profiles for steady state number 15

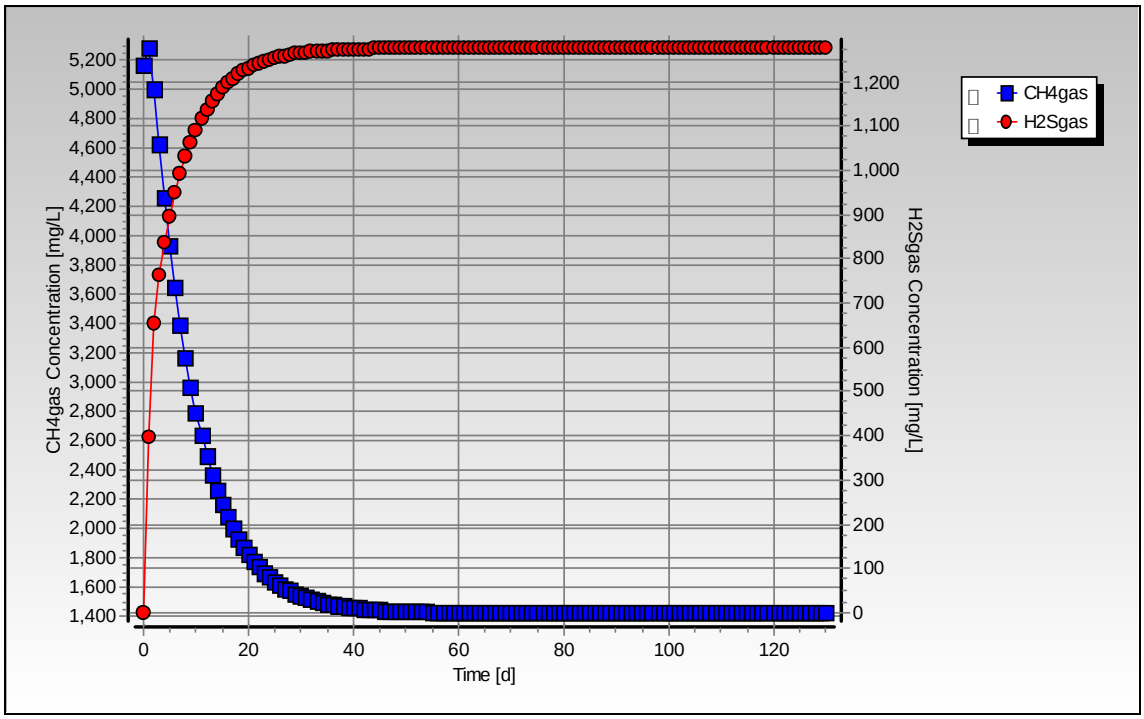

Figure C-48: Simulated methane and hydrogen sulphide gas concentration profiles for steady state number 15

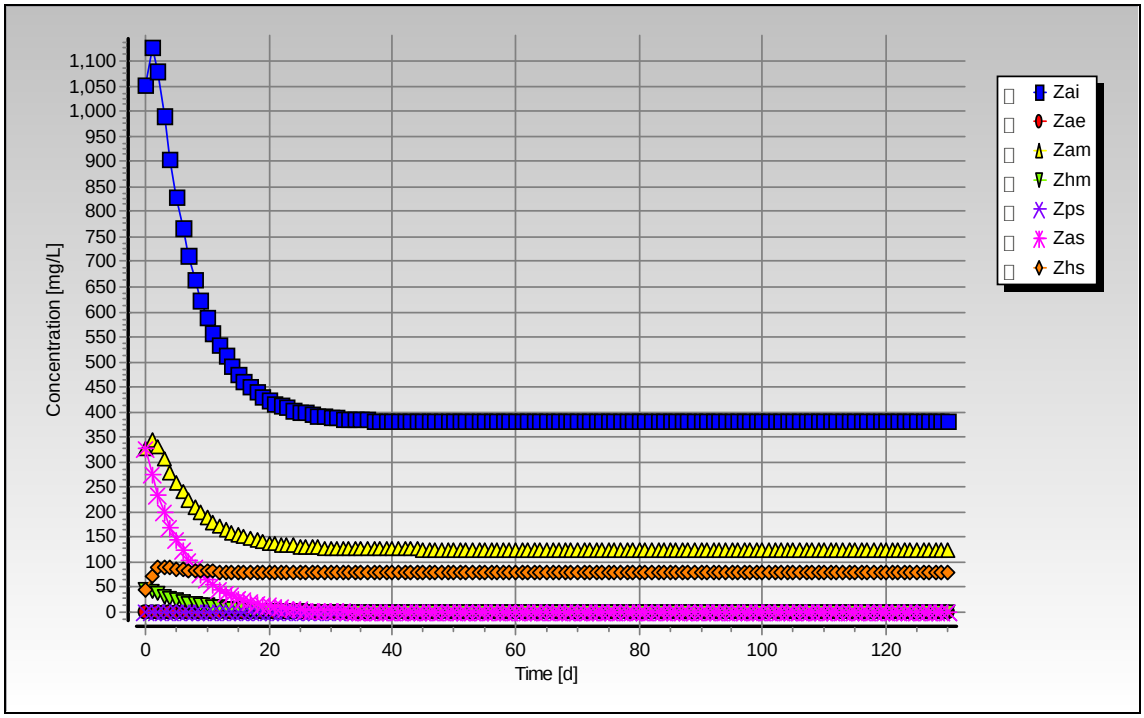

Figure C-49: Simulated biomass concentration profiles for steady state number 15

Steady State Number 17

Table C-31: Operating conditions for steady state number 17

Feed Batch Number	F12
Reactor Volume (ℓ)	20
Retention Time (d)	60
pH	steady state
Biological Groups Present	acidogenic, acetogenic and methanogenic

Table C-32: Results summary for steady state number 17

	Measured	**Model**	**Relative error (%)**
Feed Total COD (mg COD/ℓ)	9810	9810	-
Feed Soluble COD (mg COD/ℓ)	1204	1204	-
Feed TKN (mg N/ℓ)	182	182	-
Feed FSA (mg N/ℓ)	15	15	-
Effluent Total COD (mg COD/ℓ)	3590 ± 119	3657.88	1.86
Effluent Soluble COD (mg COD/ℓ)	88 ± 7	100.84	12.73
Reactor pH	6.74 ± 0.03	6.18	-9.06
Effluent VFA (mg HAc/ℓ)	5 ± 2	0.44	-1030.80
Effluent Alkalinity (mg/ℓ as $CaCO_3$)	775 ± 13	619.27	-25.15
Sulphate Addition (mg SO4/ℓ)	0	0	-
Effluent Sulphate (mg SO4/ℓ)	0	0	-
% Sulphate Conversion	-	-	-
Methane Production (ℓ/d)	0.78	0.90	12.90
Gas Composition (% CH_4)	66.51	55.38	-20.09
Effluent FSA (mg N/ℓ)	101 ± 14	104.38	3.23
Effluent TKN (mg N/ℓ)	189 ± 29	205.97	8.24

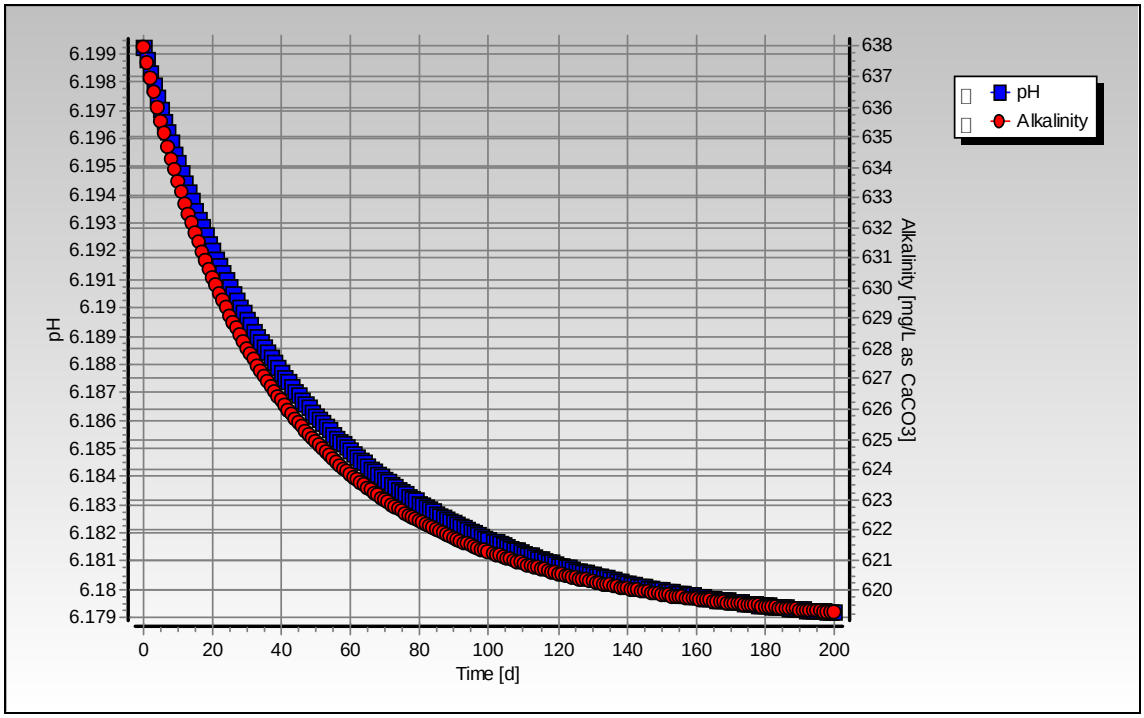

Figure C-50: Simulated pH and alkalinity profiles for steady state number 17

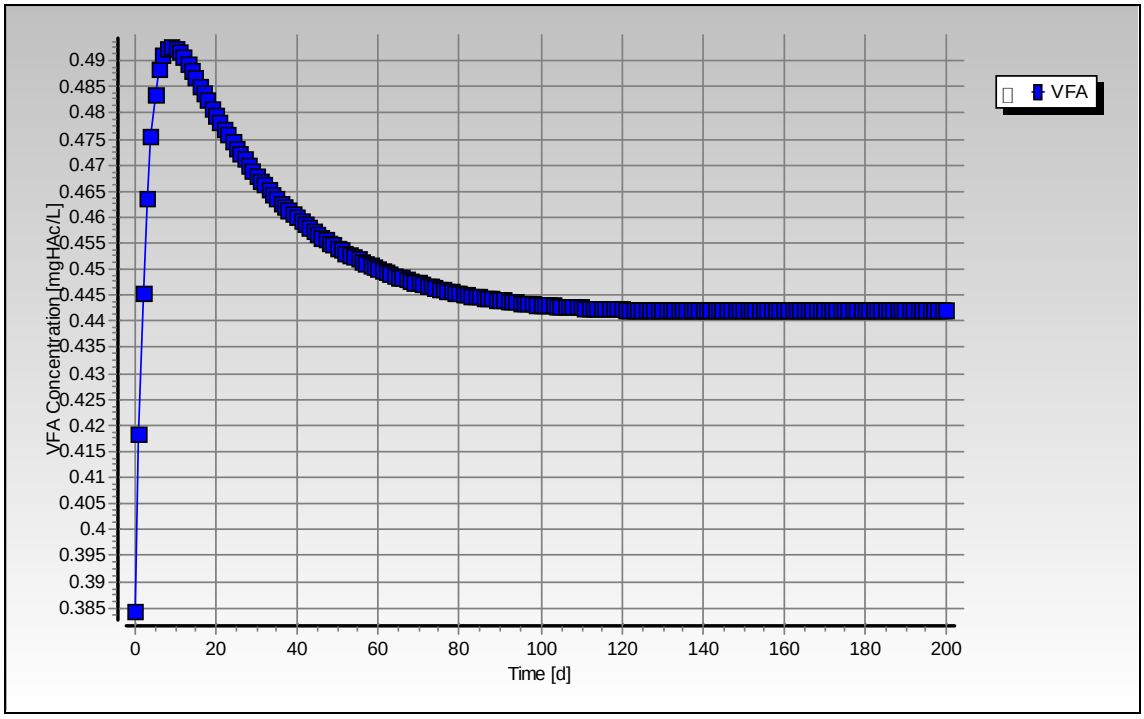

Figure C-51: Simulated VFA concentration profile for steady state number 17

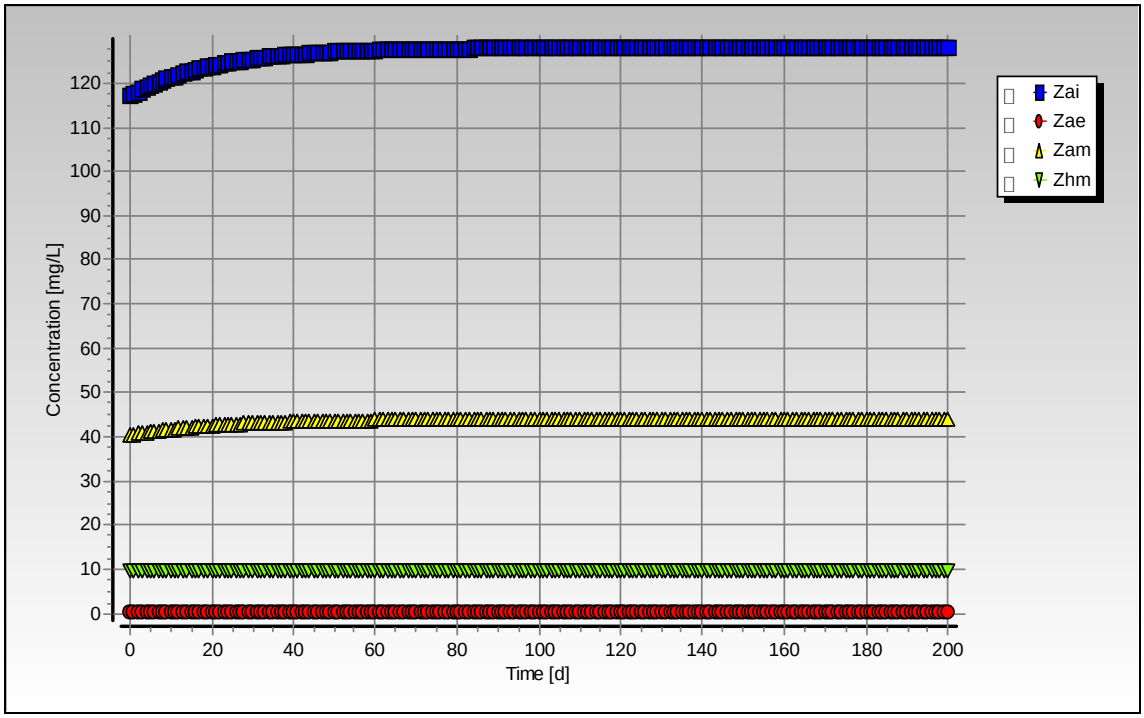

Figure C-52: Simulated biomass concentration profiles for steady state number 17

Steady State Number 18

Table C-33: Operating conditions for steady state number 18

Feed Batch Number	F14
Reactor Volume (ℓ)	16
Retention Time (d)	8
pH	Controlled to ~ 7.5
Biological Groups Present	acidogenic, acetogenic and methanogenic

Table C-34: Results summary for steady state number 18

	Measured	**Model**	**Relative error (%)**
Feed Total COD (mg COD/ℓ)	1949	1949	-
Feed Soluble COD (mg COD/ℓ)	283	283	-
Feed TKN (mg N/ℓ)	43	43	-
Feed FSA (mg N/ℓ)	7	7	-
Effluent Total COD (mg COD/ℓ)	827 ± 29	864.43	4.33
Effluent Soluble COD (mg COD/ℓ)	43 ± 6	97.48	55.89
Reactor pH	7.48 ± 0.02	7.50	0.23
Effluent VFA (mg HAc/ℓ)	0	1.00	100.00
Effluent Alkalinity (mg/ℓ as $CaCO_3$)	571 ± 13	1536.15	62.83
Sulphate Addition (mg SO4/ℓ)	0	0	-
Effluent Sulphate (mg SO4/ℓ)	0	0	-
% Sulphate Conversion	-	-	-
Methane Production (ℓ/d)	0.84	0.94	10.69
Gas Composition (% CH_4)	84.69	94.72	10.59
Effluent FSA (mg N/ℓ)	18 ± 2	18.67	3.61
Effluent TKN (mg N/ℓ)	17 ± 1	39.44	56.90

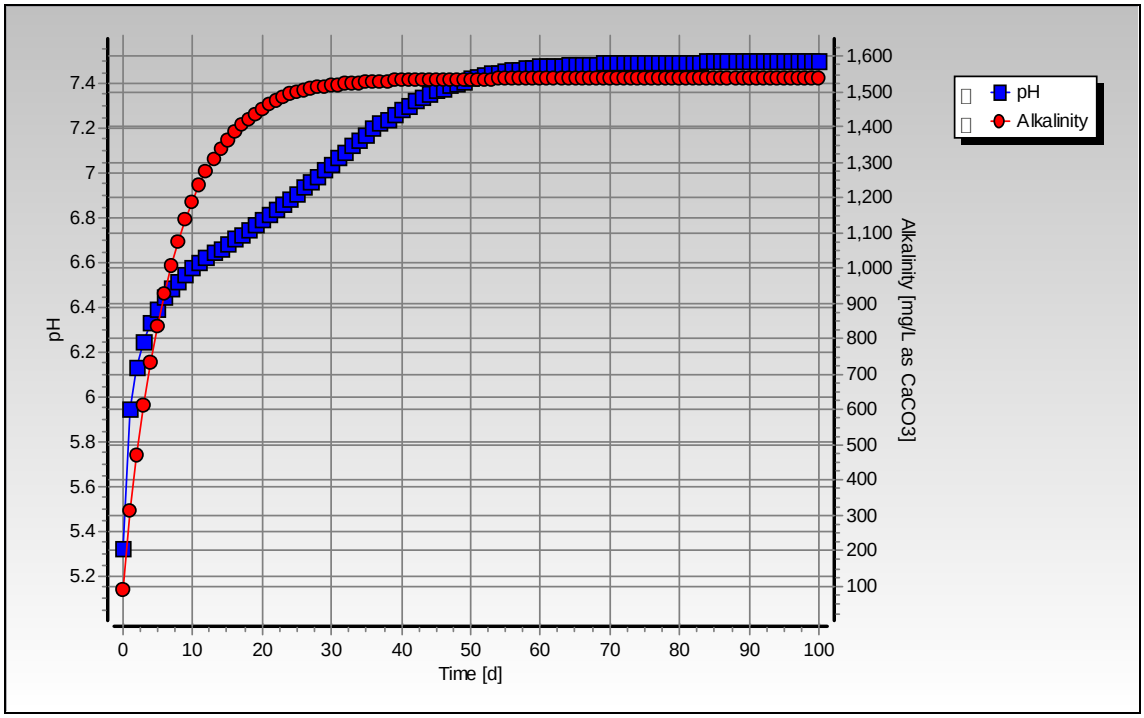

Figure C-53: Simulated pH and alkalinity profiles for steady state number 18

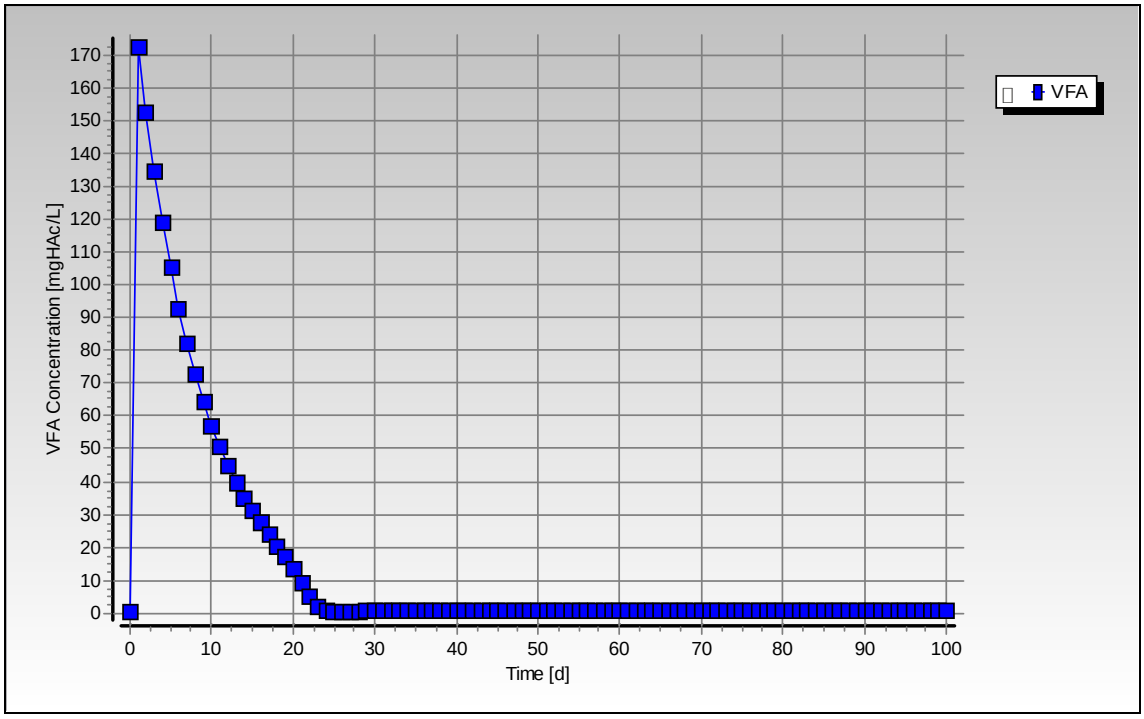

Figure C-54: Simulated VFA concentration profile for steady state number 18

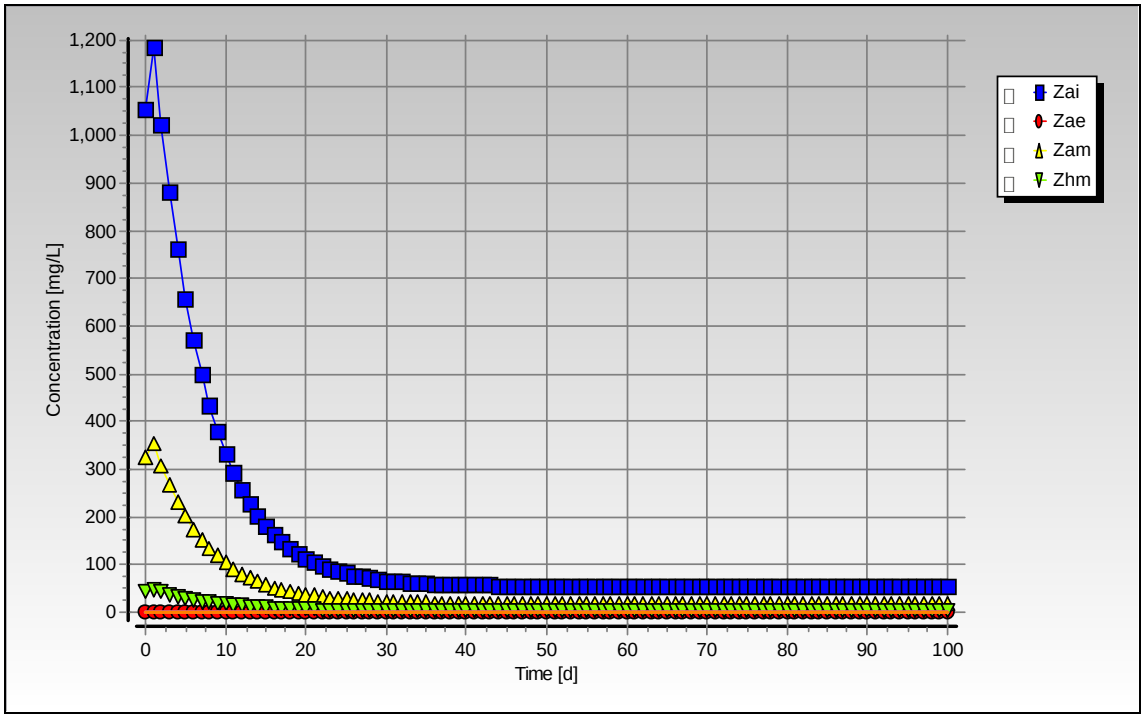

Figure C-55: Simulated biomass concentration profiles for steady state number 18

Steady State Number 19

Table C-35: Operating conditions for steady state number 19

Feed Batch Number	F14
Reactor Volume (ℓ)	16
Retention Time (d)	8
pH	Controlled to ~ 7.0
Biological Groups Present	acidogenic, acetogenic and methanogenic

Table C-36: Results summary for steady state number 19

	Measured	**Model**	**Relative error (%)**
Feed Total COD (mg COD/ℓ)	1949	1949	-
Feed Soluble COD (mg COD/ℓ)	283	283	-
Feed TKN (mg N/ℓ)	43	43	-
Feed FSA (mg N/ℓ)	8	8	-
Effluent Total COD (mg COD/ℓ)	815 ± 25	864.69	5.75
Effluent Soluble COD (mg COD/ℓ)	35 ± 7	97.76	64.20
Reactor pH	7.02 ± 0.02	7.02	-
Effluent VFA (mg HAc/ℓ)	0 ± 1	1.15	100.00
Effluent Alkalinity (mg/ℓ as $CaCO_3$)	323 ± 21	1328.49	75.69
Sulphate Addition (mg SO4/ℓ)	0	0	-
Effluent Sulphate (mg SO4/ℓ)	0	0	-
% Sulphate Conversion	-	-	-
Methane Production (ℓ/d)	0.78	0.94	17.05
Gas Composition (% CH_4)	72.2	86.40	16.44
Effluent FSA (mg N/ℓ)	23 ± 1	19.69	-16.84
Effluent TKN (mg N/ℓ)	20 ± 3	40.46	50.56

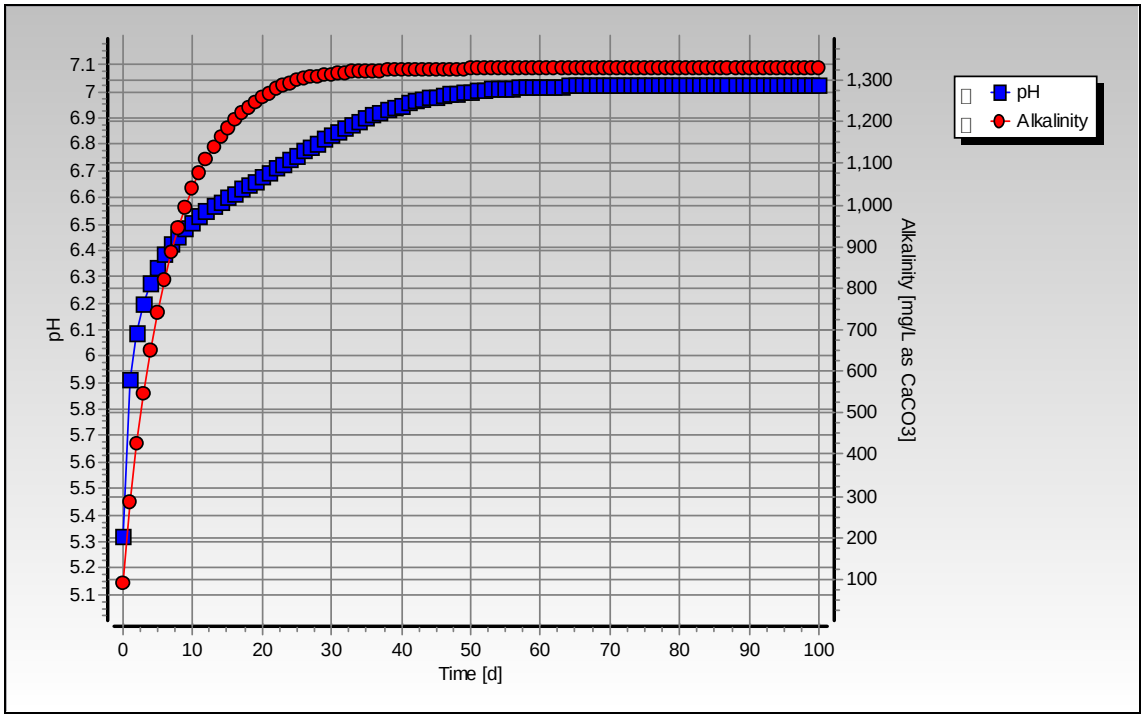

Figure C-56: Simulated pH and alkalinity profiles for steady state number 19

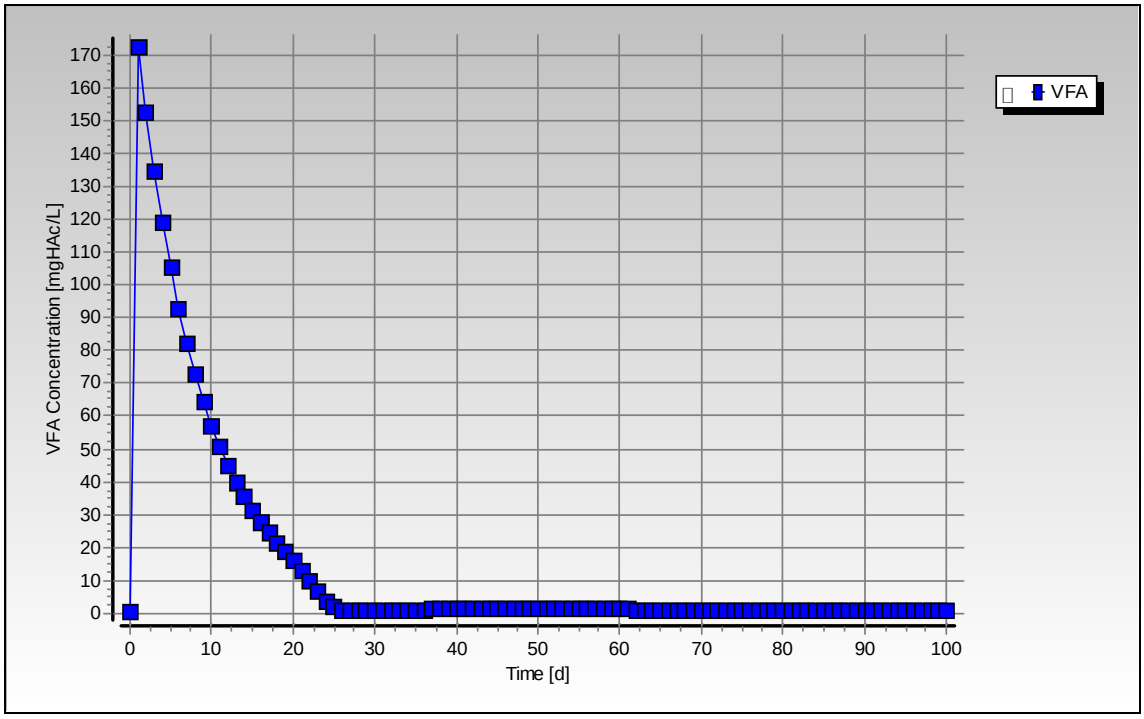

Figure C-57: Simulated VFA concentration profile for steady state number 19

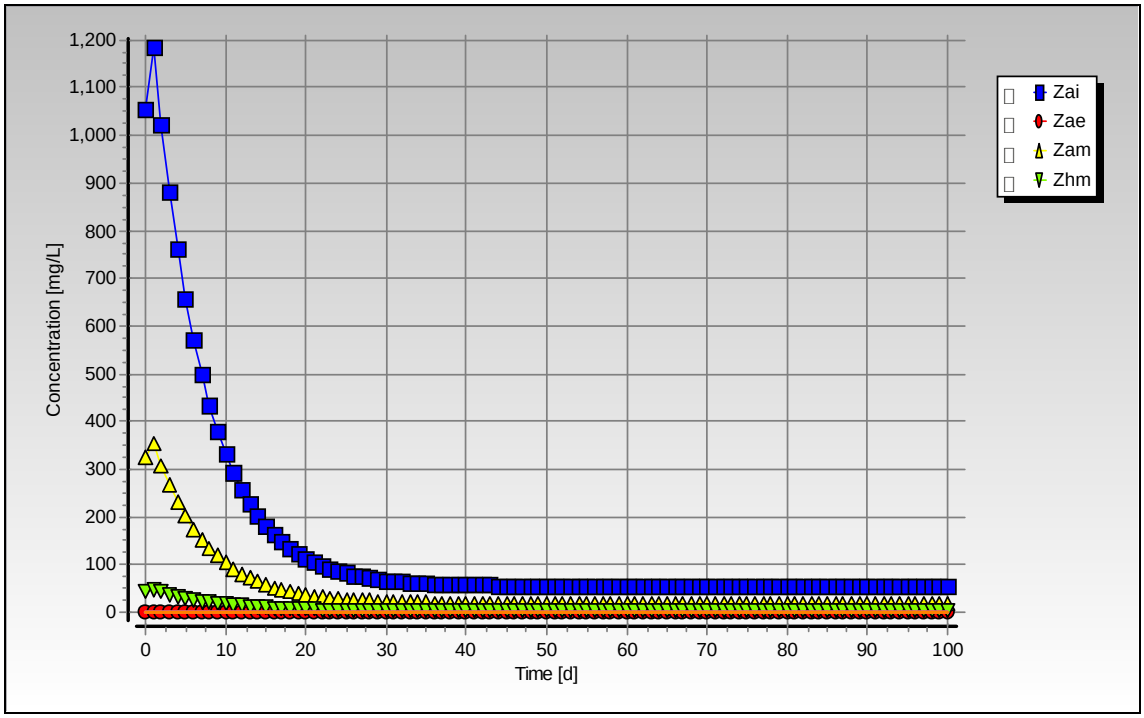

Figure C-58: Simulated biomass concentration profiles for steady state number 19

Steady State Number 20

Table C-37: Operating conditions for steady state number 20

Feed Batch Number	F14
Reactor Volume (ℓ)	16
Retention Time (d)	8
pH	Controlled to ~ 7.5
Biological Groups Present	acidogenic, acetogenic, methanogenic and sulphidogenic

Table C-38: Results summary for steady state number 20

	Measured	**Model**	**Relative error (%)**
Feed Total COD (mg COD/ℓ)	1949	1949	-
Feed Soluble COD (mg COD/ℓ)	283	283	-
Feed TKN (mg N/ℓ)	43	43	-
Feed FSA (mg N/ℓ)	8	8	-
Effluent Total COD (mg COD/ℓ)	1532 ± 58	1117.75	-37.06
Effluent Soluble COD (mg COD/ℓ)	790 ± 40	247.63	-219.03
Reactor pH	7.52 ± 0.03	7.52	-
Effluent VFA (mg HAc/ℓ)	0	0.16	100
Effluent Alkalinity (mg/ℓ as $CaCO_3$)	1386 ± 36	1812.58	23.53
Sulphate Addition (mg SO4/ℓ)	2000	2000	-
Effluent Sulphate (mg SO4/ℓ)	530 ± 26	1523	65.19
% Sulphate Conversion	73.50	23.87	-
Methane Production (ℓ/d)	0	0.48	100
Gas Composition (% CH_4)	0	75.11	100
Effluent FSA (mg N/ℓ)	18 ± 1	17.41	-3.41
Effluent TKN (mg N/ℓ)	44 ± 1	39.21	-12.22

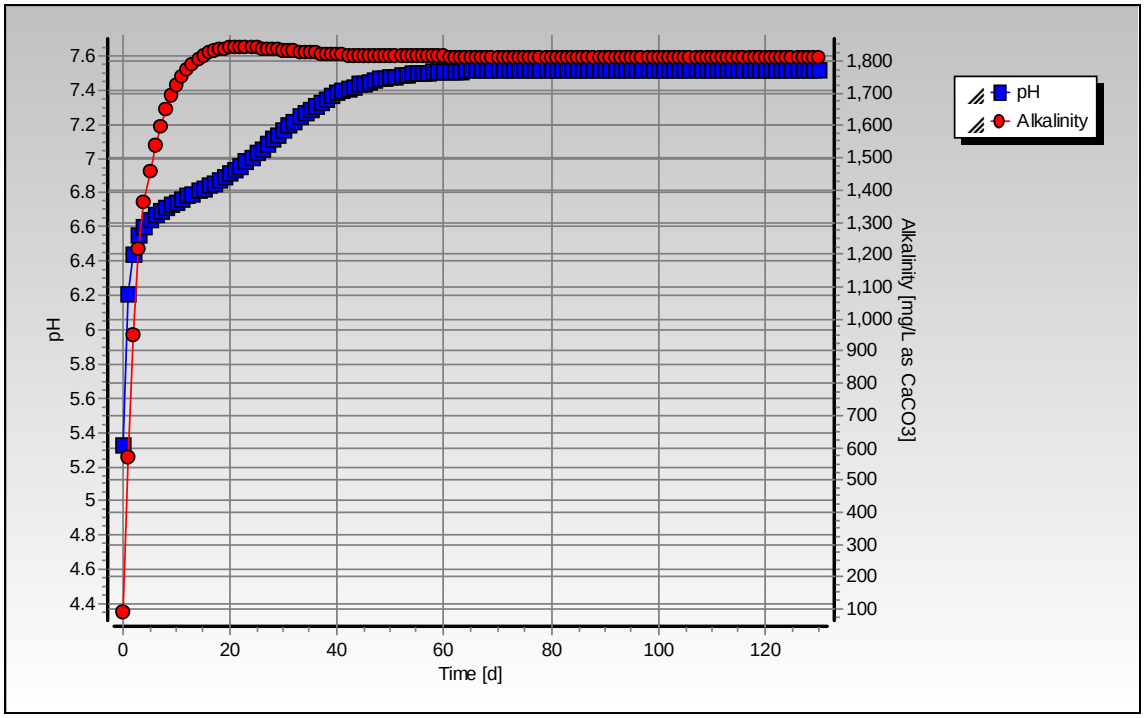

Figure C-59: Simulated pH and alkalinity profiles for steady state number 20

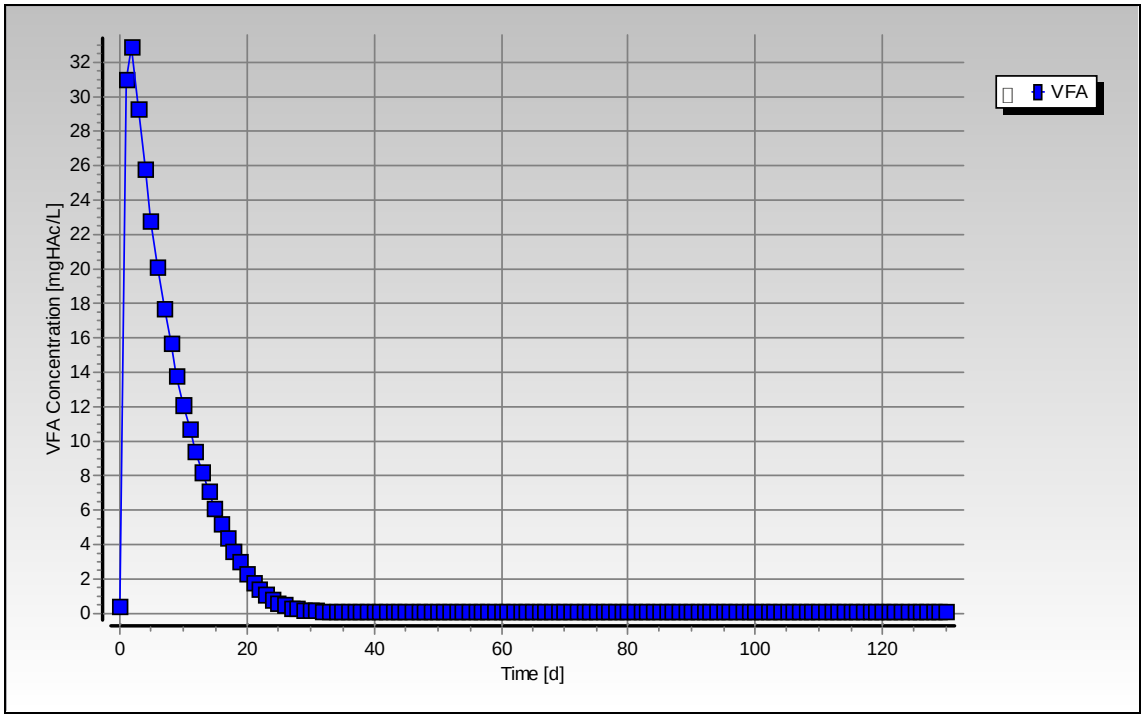

Figure C-60: Simulated VFA concentration profile for steady state number 20

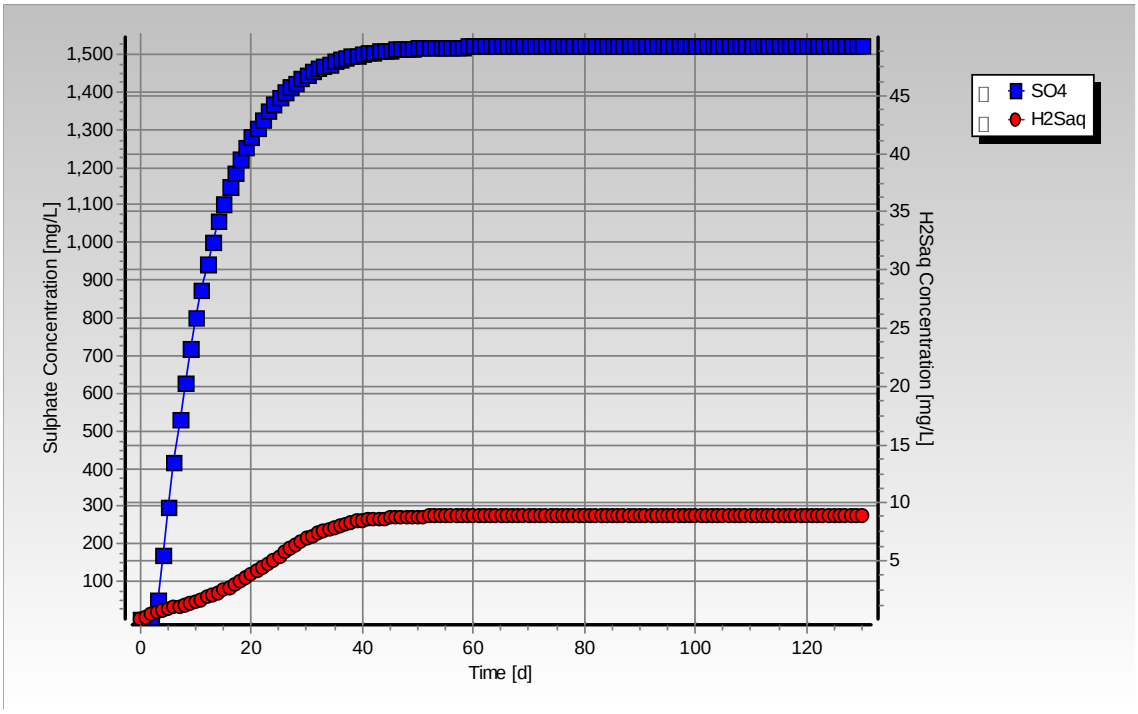

Figure C-61: Simulated sulphate and aqueous hydrogen sulphide concentration profiles for steady state number 20

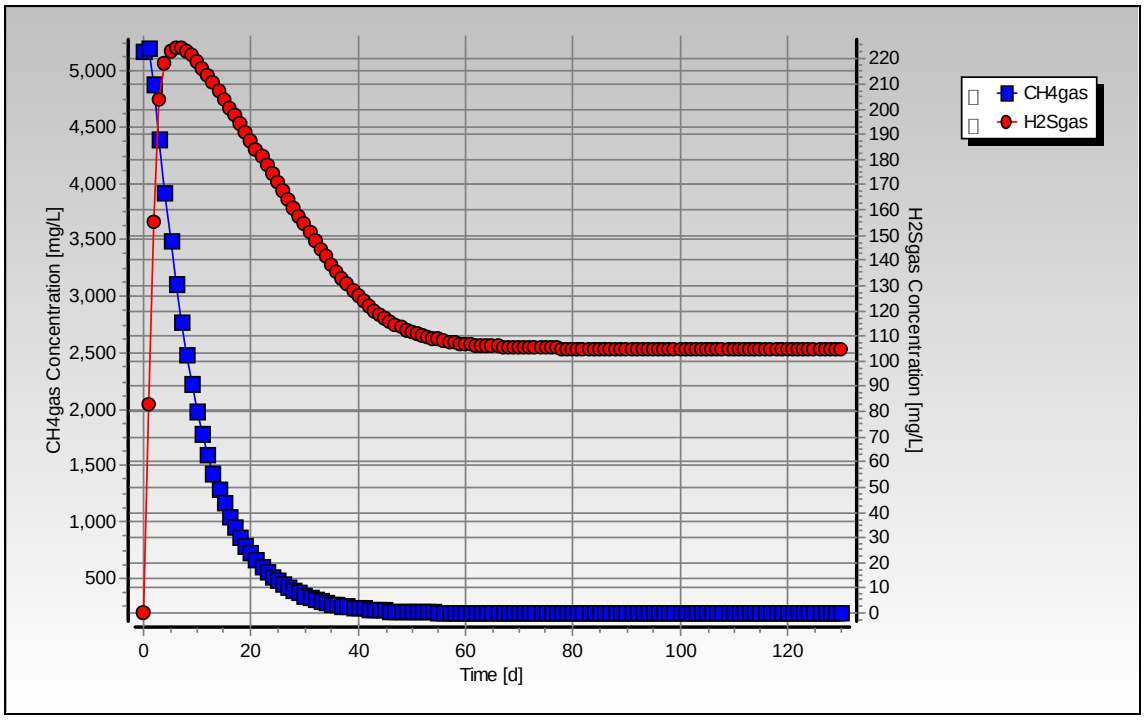

Figure C-62: Simulated methane and hydrogen sulphide gas concentration profiles for steady state number 20

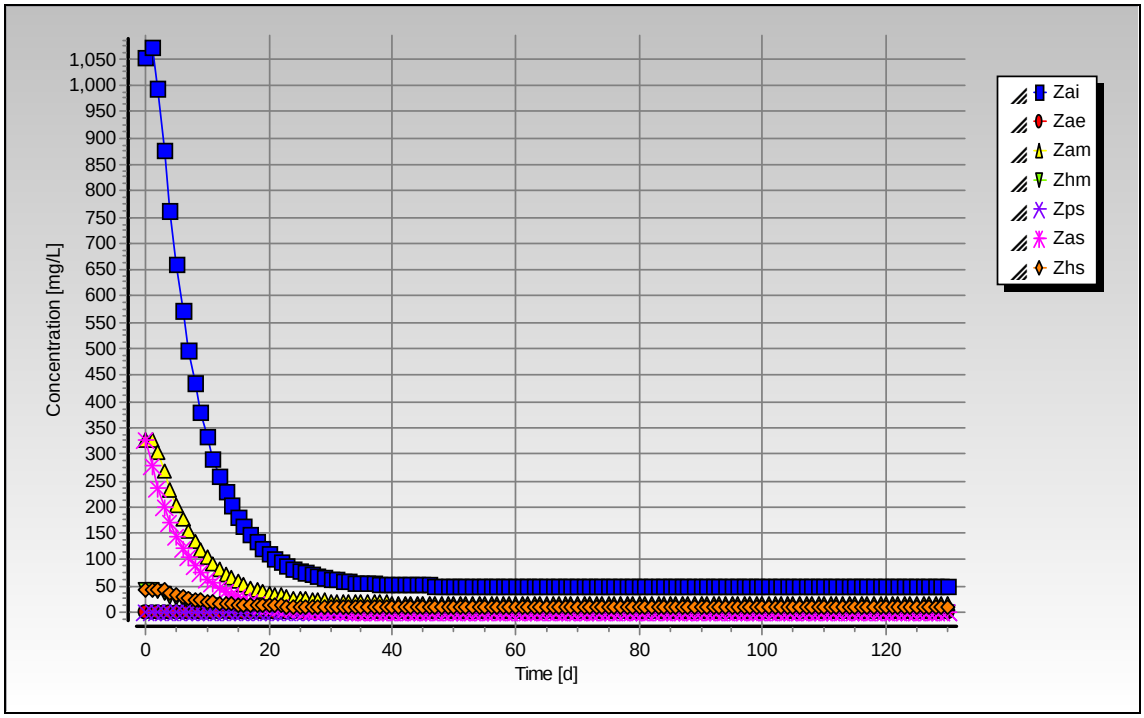

Figure C-63: Simulated biomass concentration profiles for steady state number 20

Steady State Number 21

Table C-39: Operating conditions for steady state number 21

Feed Batch Number	F14
Reactor Volume (ℓ)	20
Retention Time (d)	8
pH	steady state
Biological Groups Present	acidogenic, acetogenic and methanogenic

Table C-40: Results summary for steady state number 21

	Measured	**Model**	**Relative error (%)**
Feed Total COD (mg COD/ℓ)	34819	34819	-
Feed Soluble COD (mg COD/ℓ)	3829	3829	-
Feed TKN (mg N/ℓ)	770	770	-
Feed FSA (mg N/ℓ)	44	44	-
Effluent Total COD (mg COD/ℓ)	15094 ± 493	15490.07	2.56
Effluent Soluble COD (mg COD/ℓ)	205 ± 8	252.20	18.71
Reactor pH	6.90 ± 0.01	6.73	-2.53
Effluent VFA (mg HAc/ℓ)	22 ± 10	1.39	-1482.43
Effluent Alkalinity (mg/ℓ as $CaCO_3$)	1868 ± 74	1952.11	4.31
Sulphate Addition (mg SO4/ℓ)	0	0	-
Effluent Sulphate (mg SO4/ℓ)	0	0	-
% Sulphate Conversion	-	-	-
Methane Production (ℓ/d)	19.39	20.97	7.55
Gas Composition (% CH_4)	58.85	60.45	2.64
Effluent FSA (mg N/ℓ)	258 ± 10	245.52	-5.08
Effluent TKN (mg N/ℓ)	651 ± 14	631.80	-3.04

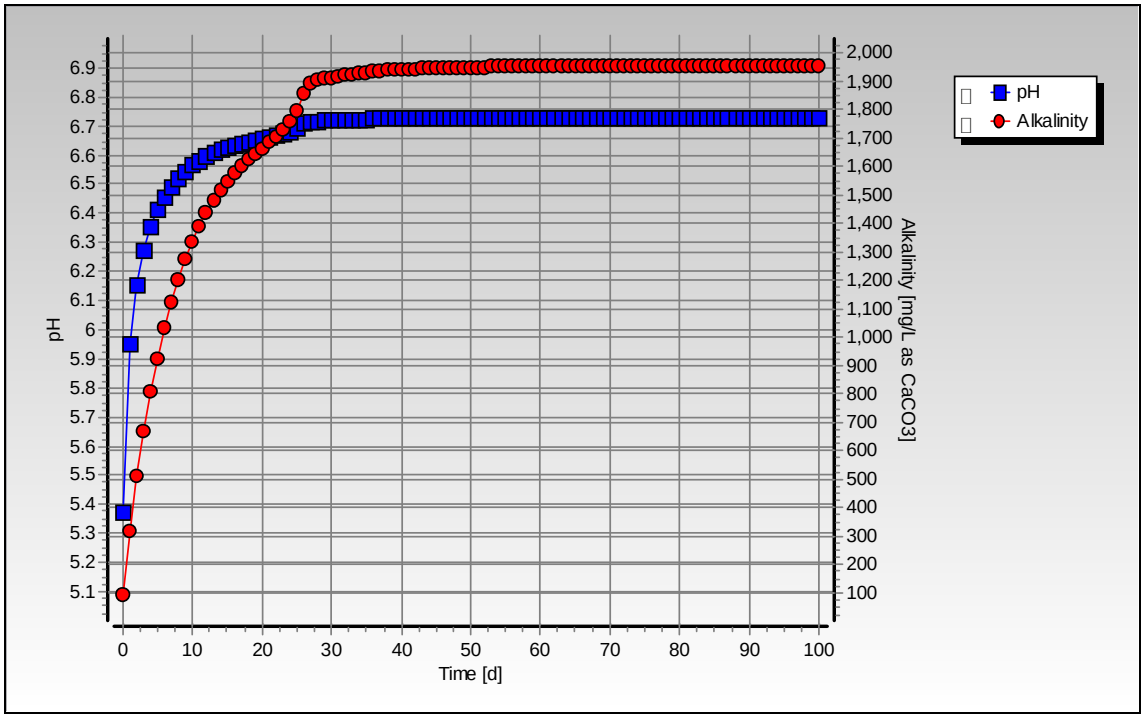

Figure C-64: Simulated pH and alkalinity profiles for steady state number 21

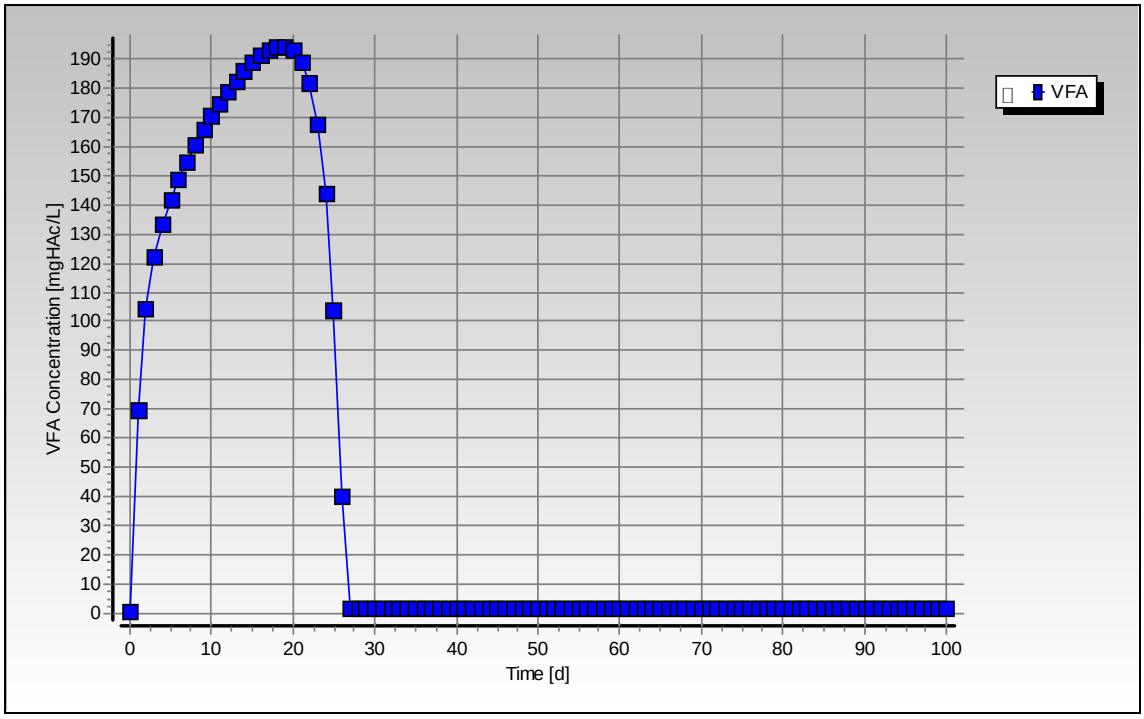

Figure C-65: Simulated VFA concentration profile for steady state number 21

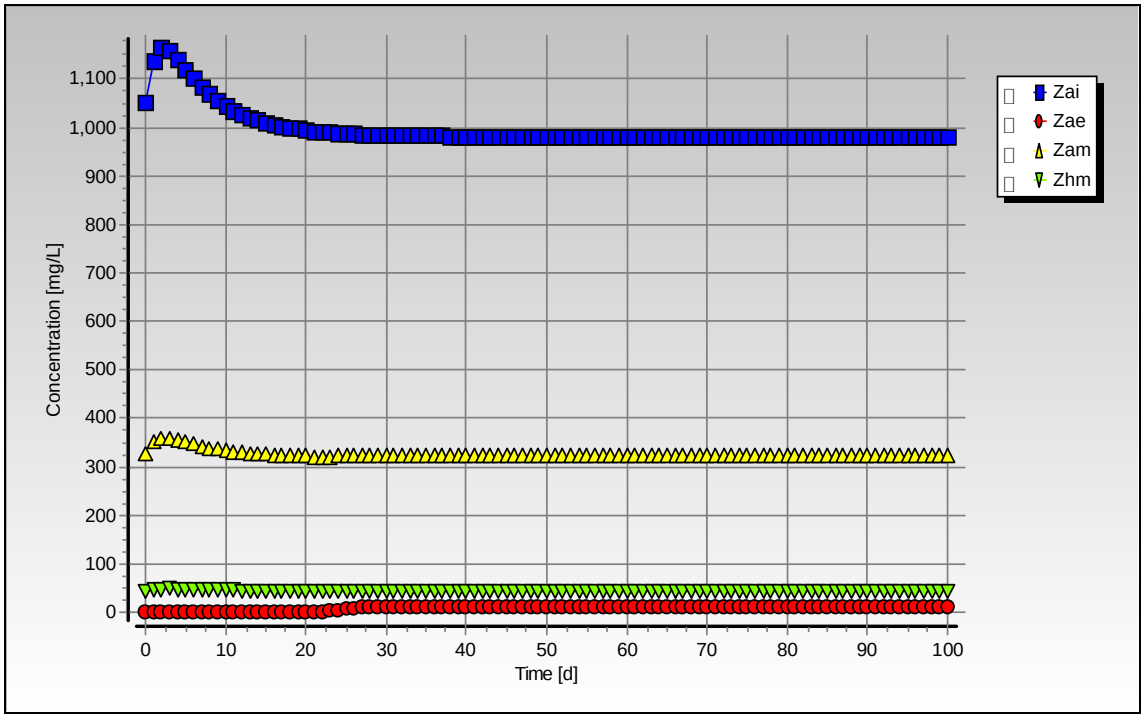

Figure C-66: Simulated biomass concentration profiles for steady state number 21

Steady State Number 22

Table C-41: Operating conditions for steady state number 22

Feed Batch Number	F14
Reactor Volume (ℓ)	16
Retention Time (d)	8
pH	Controlled to ~ 7.0
Biological Groups Present	acidogenic, acetogenic, methanogenic and sulphidogenic

Table C-42: Results summary for steady state number 22

	Measured	**Model**	**Relative error (%)**
Feed Total COD (mg COD/ℓ)	1949	1949	-
Feed Soluble COD (mg COD/ℓ)	283	283	-
Feed TKN (mg N/ℓ)	43	43	-
Feed FSA (mg N/ℓ)	10	10	-
Effluent Total COD (mg COD/ℓ)	1406 ± 17	994.07	-15.89
Effluent Soluble COD (mg COD/ℓ)	655 ± 37	123.95	-93.62
Reactor pH	6.99 ± 0.02	6.41	-9.12
Effluent VFA (mg HAc/ℓ)	63 ± 8	0.17	-36174.76
Effluent Alkalinity (mg/ℓ as $CaCO_3$)	782 ± 21	873.92	10.52
Sulphate Addition (mg SO4/ℓ)	2000	2000	-
Effluent Sulphate (mg SO4/ℓ)	770 ± 138	1523	49.43
% Sulphate Conversion	61.50	23.87	-
Methane Production (ℓ/d)	0	0.61	100
Gas Composition (% CH_4)	0	45.35	100
Effluent FSA (mg N/ℓ)	11 ± 1	19.43	43.37
Effluent TKN (mg N/ℓ)	48 ± 1	41.23	-16.43

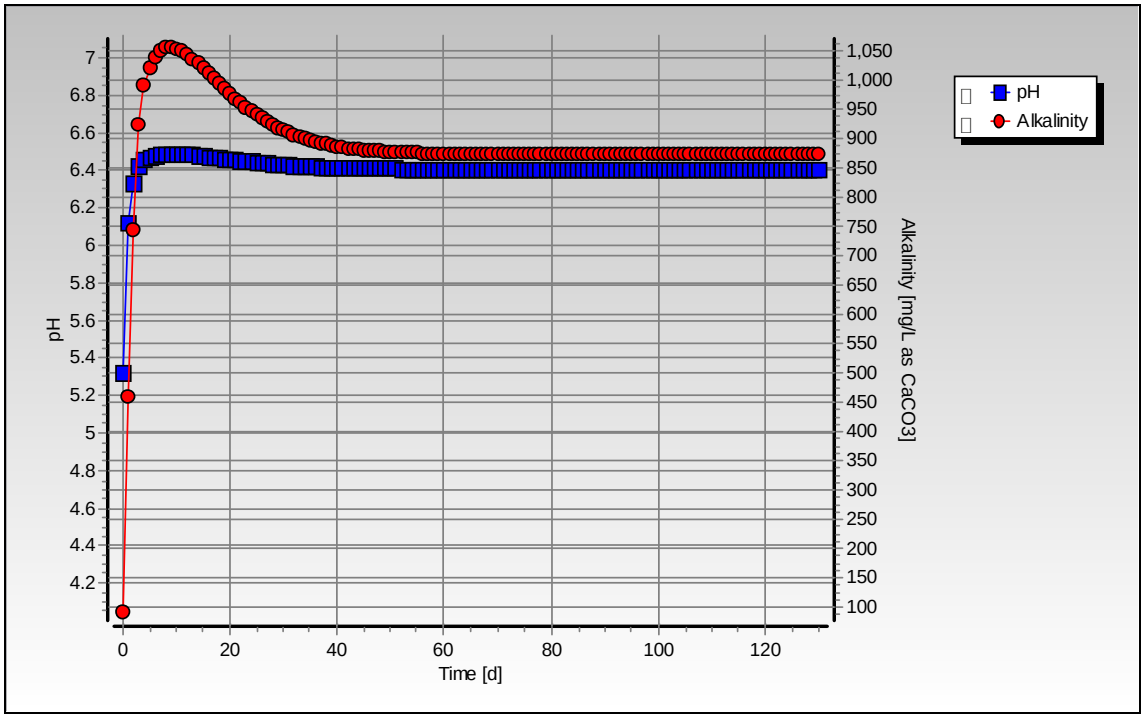

Figure C-67: Simulated pH and alkalinity profiles for steady state number 22

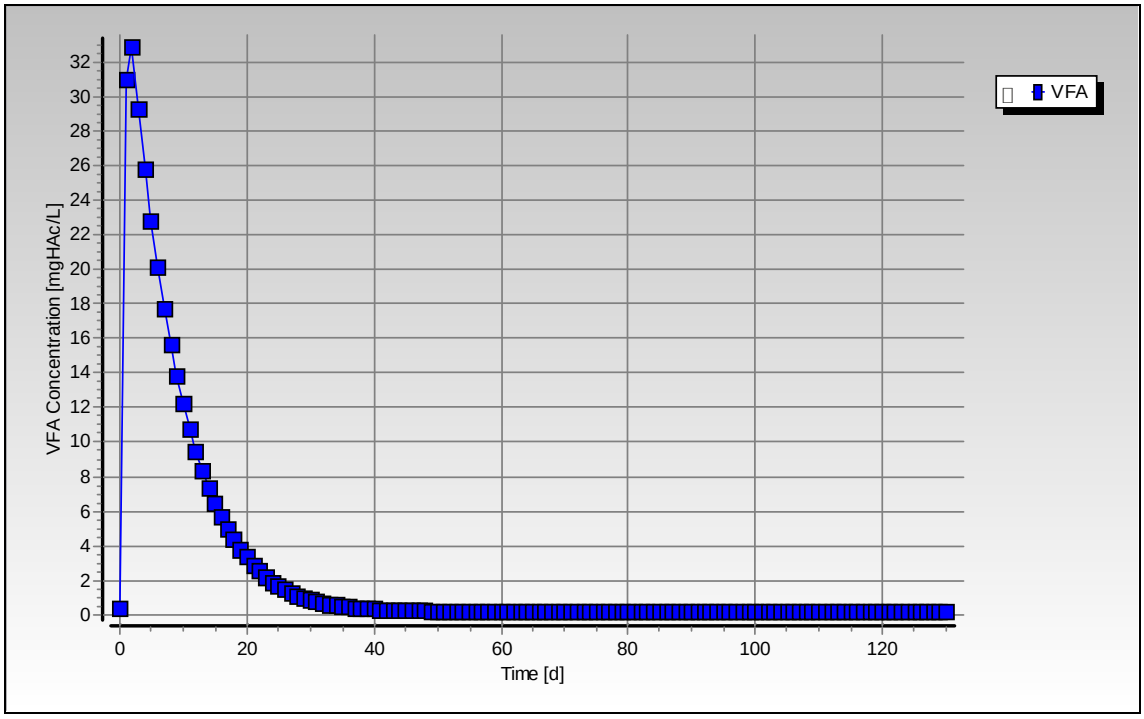

Figure C-68: Simulated VFA concentration profile for steady state number 22

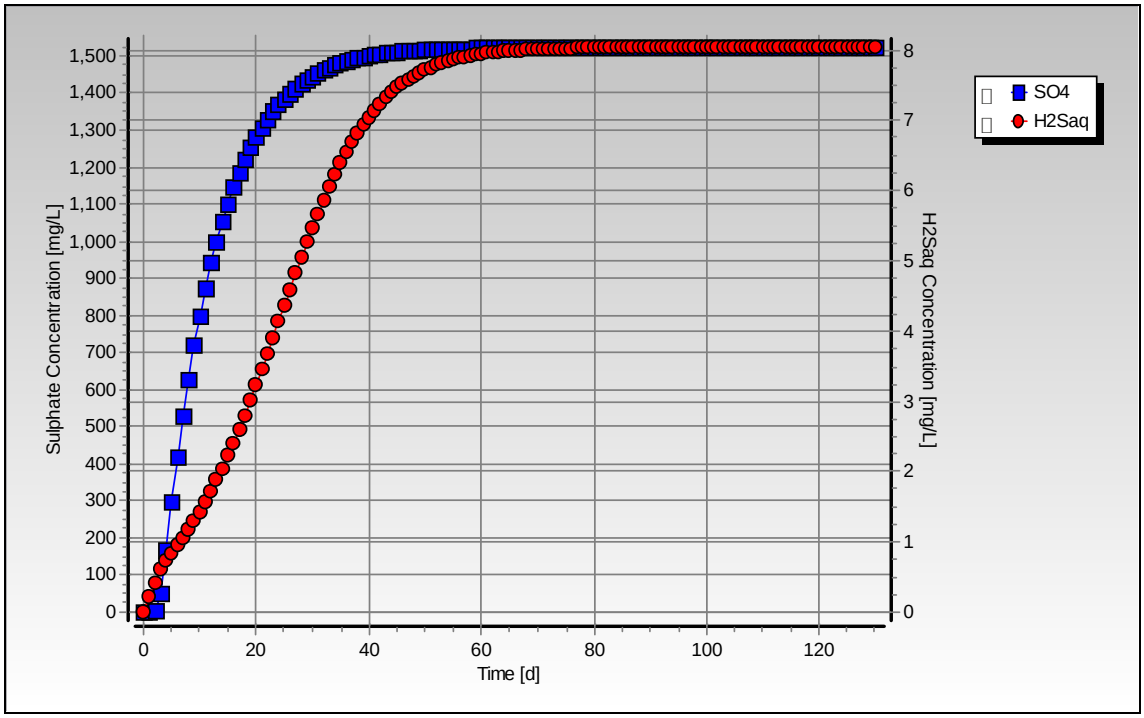

Figure C-69: Simulated sulphate and aqueous hydrogen sulphide concentration profiles for steady state number 22

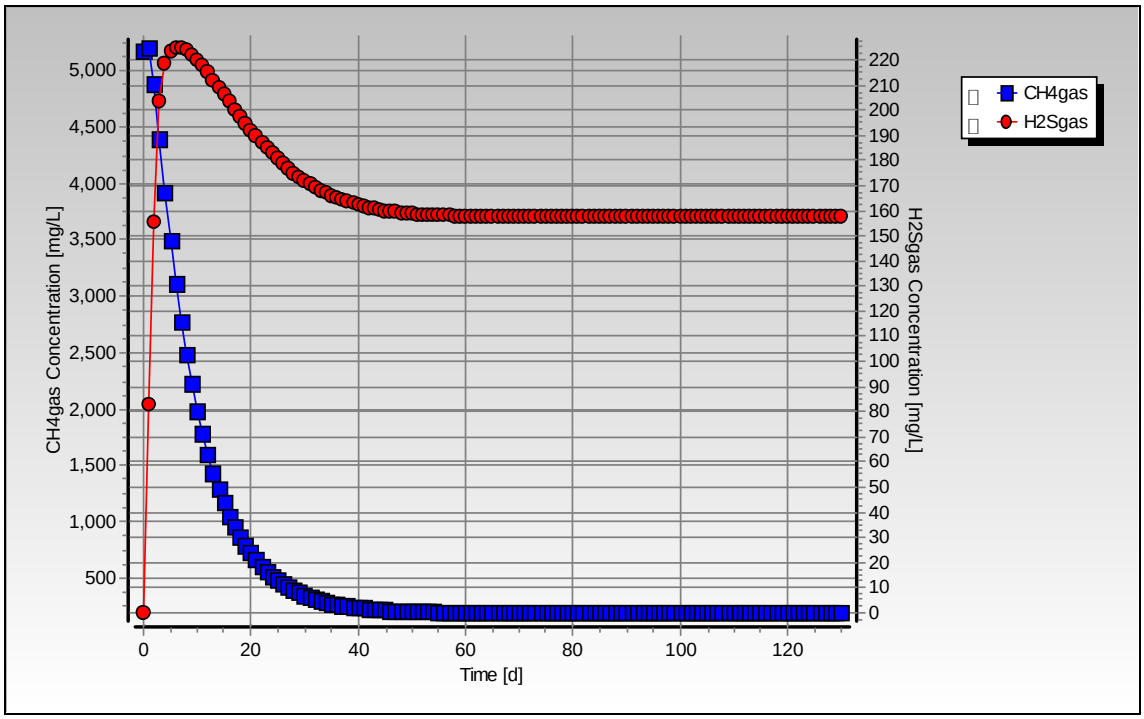

Figure C-70: Simulated methane and hydrogen sulphide gas concentration profiles for steady state number 22

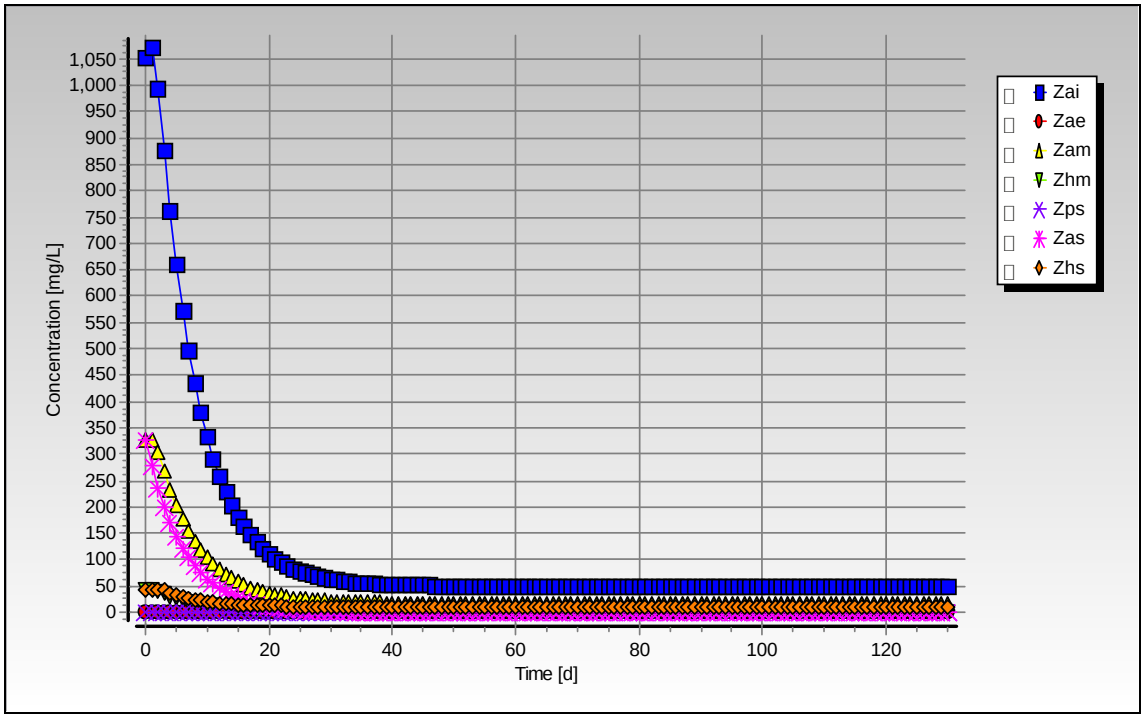

Figure C-71: Simulated biomass concentration profiles for steady state number 22

Steady State Number 23

Table C-43: Operating conditions for steady state number 23

Feed Batch Number	F14
Reactor Volume (ℓ)	20
Retention Time (d)	6.67
pH	steady state
Biological Groups Present	acidogenic, acetogenic and methanogenic

Table C-44: Results summary for steady state number 23

	Measured	**Model**	**Relative error (%)**
Feed Total COD (mg COD/ℓ)	34819	34819	-
Feed Soluble COD (mg COD/ℓ)	4399	4399	-
Feed TKN (mg N/ℓ)	770	770	-
Feed FSA (mg N/ℓ)	70	70	-
Effluent Total COD (mg COD/ℓ)	14984 ± 431	15405.23	2.73
Effluent Soluble COD (mg COD/ℓ)	207 ± 10	264.17	21.64
Reactor pH	6.83 ± 0.01	6.76	-1.04
Effluent VFA (mg HAc/ℓ)	12 ± 9	1.69	-609.49
Effluent Alkalinity (mg/ℓ as $CaCO_3$)	1821 ± 24	2081.30	12.51
Sulphate Addition (mg SO4/ℓ)	0	0	-
Effluent Sulphate (mg SO4/ℓ)	0	0	-
% Sulphate Conversion	-	-	-
Methane Production (ℓ/d)	22.71	25.24	10.01
Gas Composition (% CH_4)	59.32	60.56	2.05
Effluent FSA (mg N/ℓ)	255 ± 4	257.31	0.90
Effluent TKN (mg N/ℓ)	578 ± 65	642.65	10.06

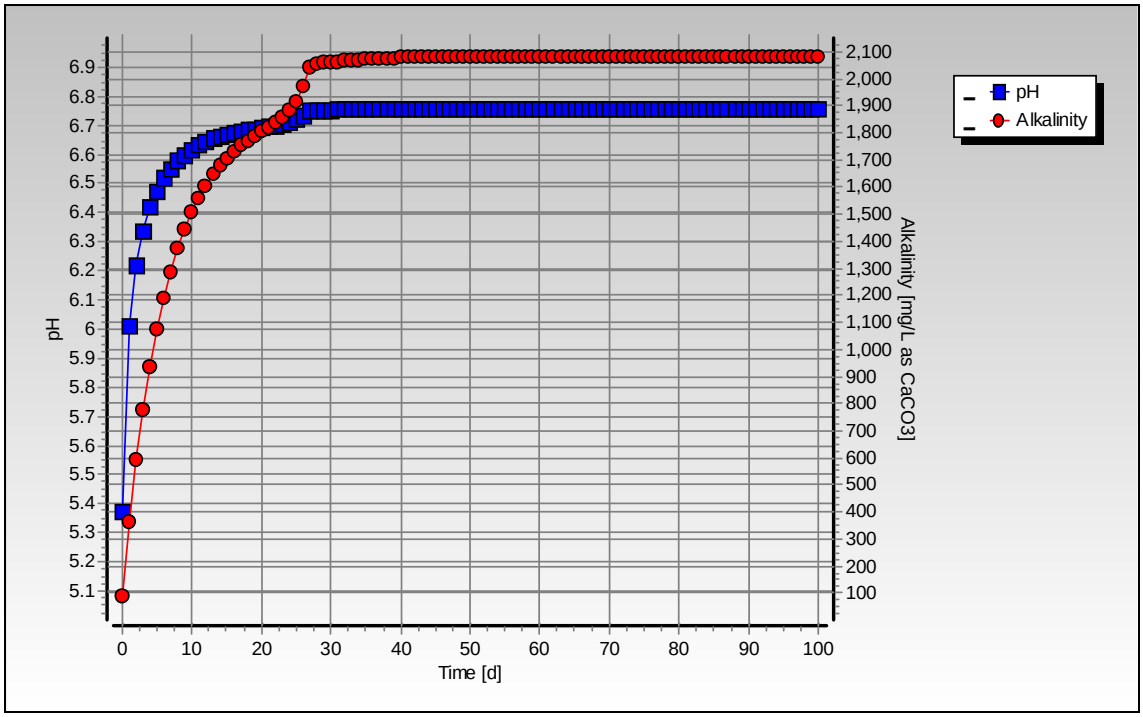

Figure C-72: Simulated pH and alkalinity profiles for steady state number 23

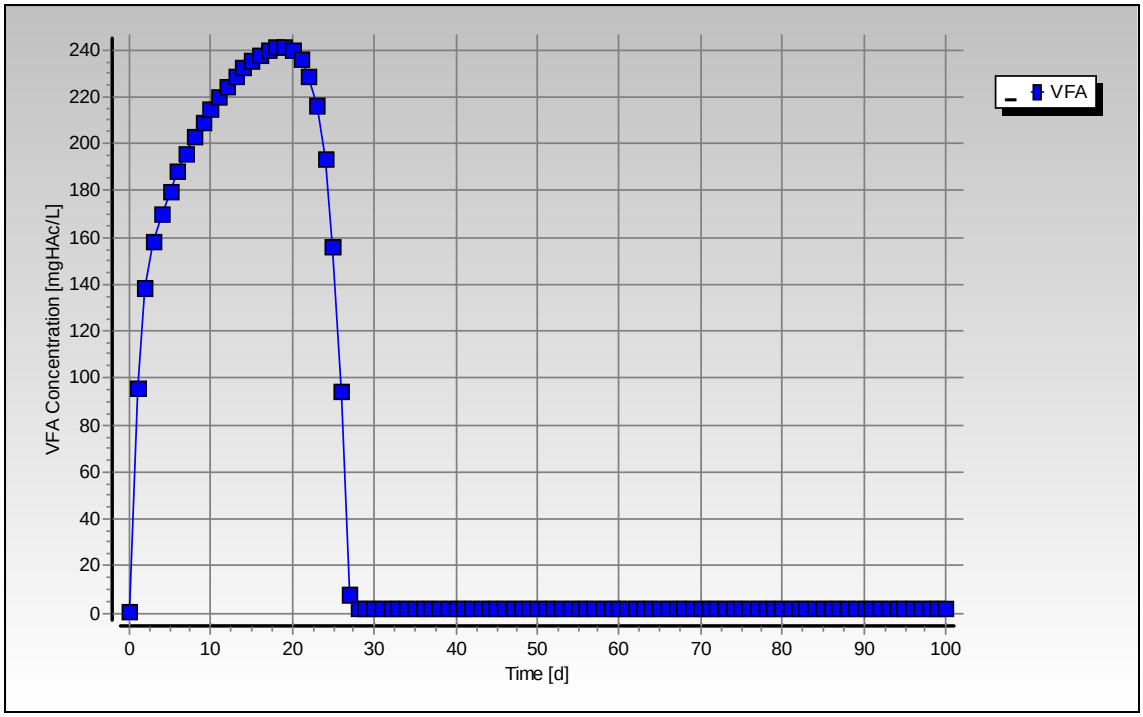

Figure C-73: Simulated VFA concentration profile for steady state number 23

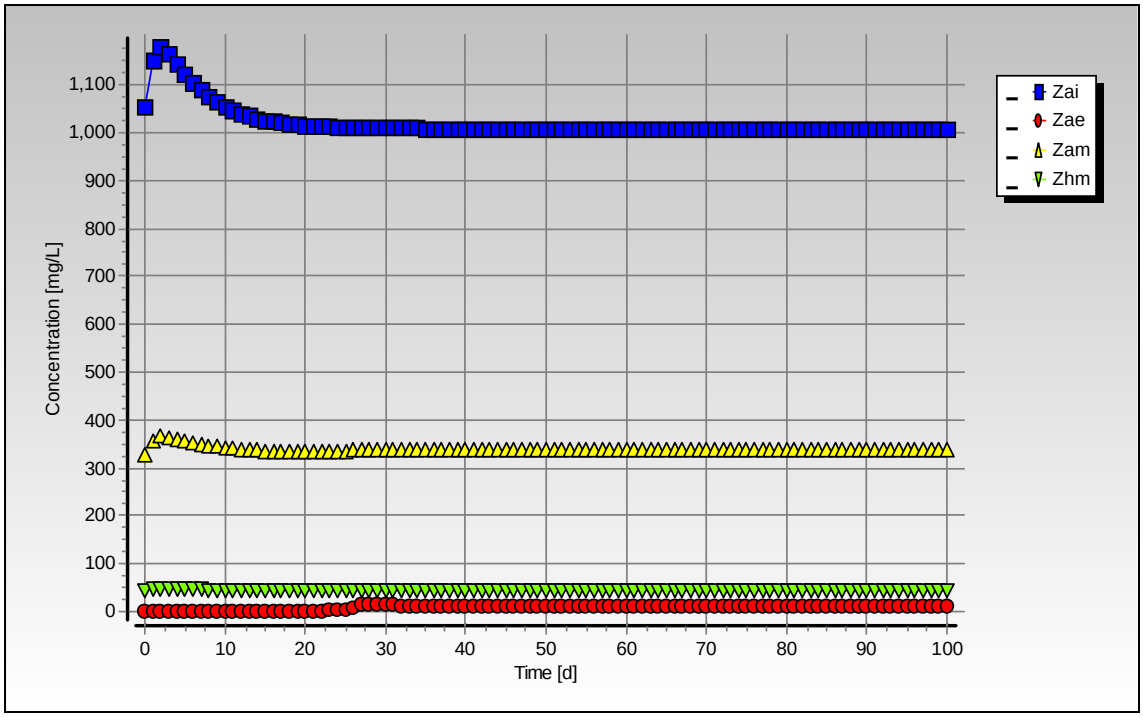

Figure C-74: Simulated biomass concentration profiles for steady state number 23

Steady State Number 24

Table C-45: Operating conditions for steady state number 24

Feed Batch Number	F14
Reactor Volume (ℓ)	20
Retention Time (d)	6.67
pH	steady state
Biological Groups Present	acidogenic, acetogenic and methanogenic

Table C-46: Results summary for steady state number 24

	Measured	**Model**	**Relative error (%)**
Feed Total COD (mg COD/ℓ)	13580	13580	-
Feed Soluble COD (mg COD/ℓ)	1846	1846	-
Feed TKN (mg N/ℓ)	300	300	-
Feed FSA (mg N/ℓ)	37	37	-
Effluent Total COD (mg COD/ℓ)	5944 ± 140	6094.14	2.46
Effluent Soluble COD (mg COD/ℓ)	96 ± 14	154.92	38.03
Reactor pH	6.57 ± 0.01	6.38	-2.98
Effluent VFA (mg HAc/ℓ)	5 ± 3	2.65	-88.86
Effluent Alkalinity (mg/ℓ as $CaCO_3$)	789 ± 11	893.28	11.67
Sulphate Addition (mg SO4/ℓ)	0	0	-
Effluent Sulphate (mg SO4/ℓ)	0	0	-
% Sulphate Conversion	-	-	-
Methane Production (ℓ/d)	8.74	9.73	10.13
Gas Composition (% CH_4)	60.95	59.48	-2.47
Effluent FSA (mg N/ℓ)	104 ± 3	107.58	3.33
Effluent TKN (mg N/ℓ)	246 ± 1	258.20	4.73

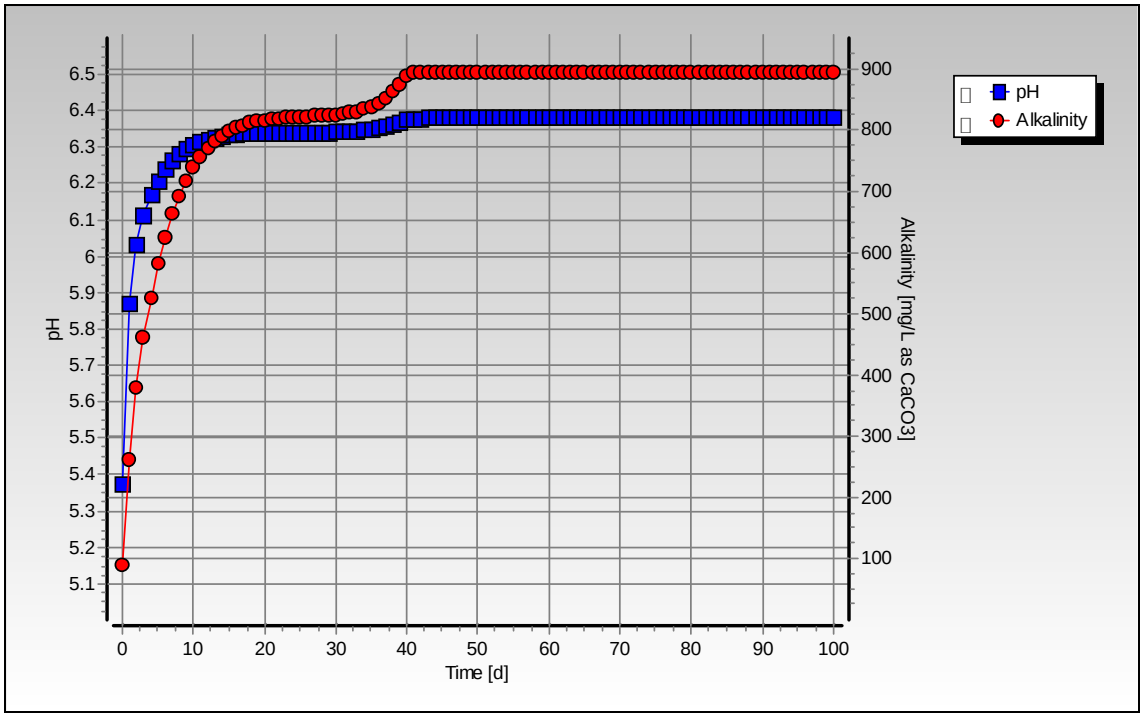

Figure C-75: Simulated pH and alkalinity profiles for steady state number 24

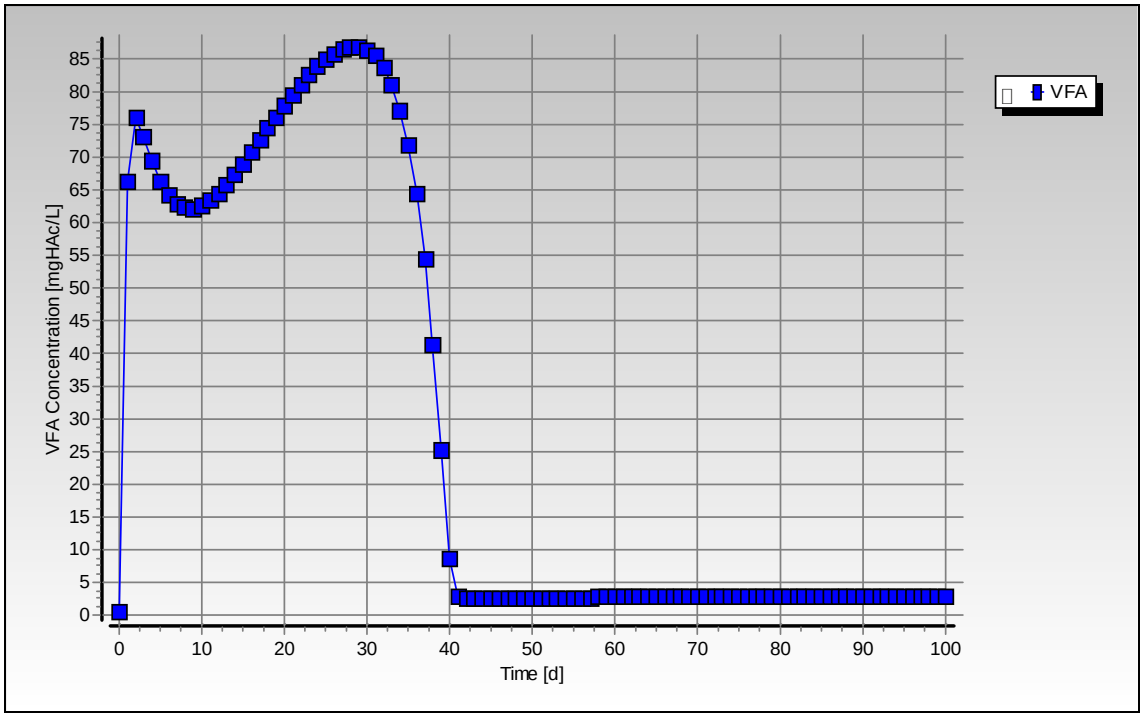

Figure C-76: Simulated VFA concentration profile for steady state number 24

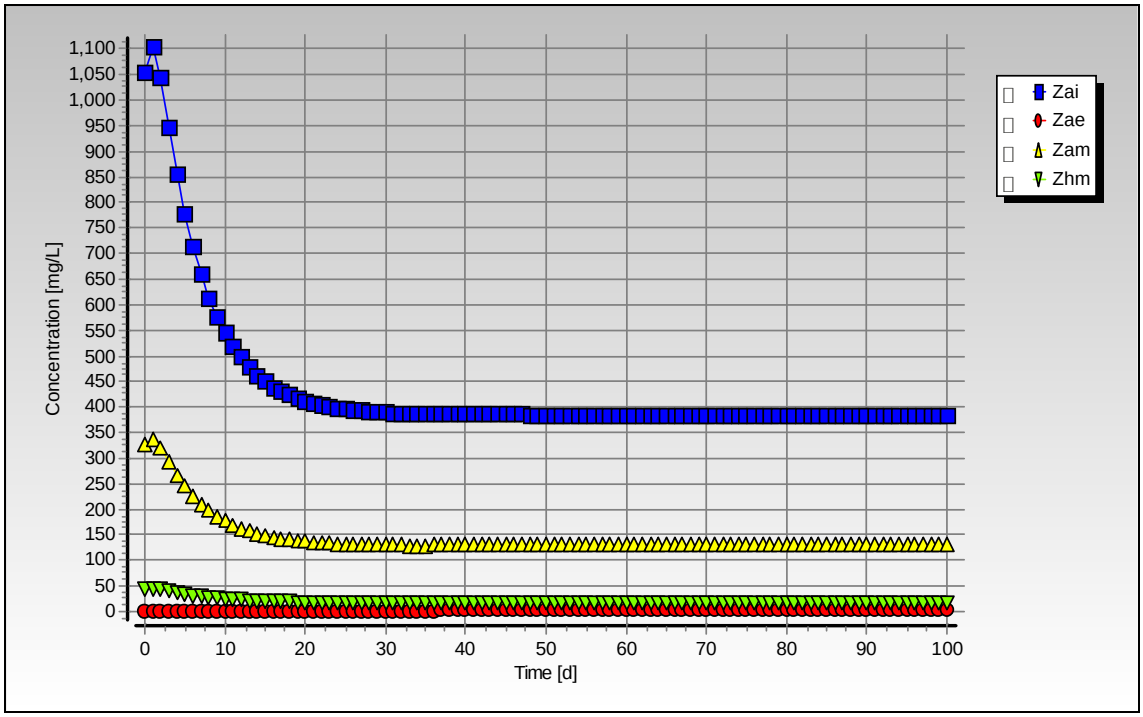

Figure C-77: Simulated biomass concentration profiles for steady state number 24

Steady State Number 25

Table C-47: Operating conditions for steady state number 25

Feed Batch Number	F14
Reactor Volume (ℓ)	20
Retention Time (d)	10
pH	steady state
Biological Groups Present	acidogenic, acetogenic and methanogenic

Table C-48: Results summary for steady state number 25

	Measured	**Model**	**Relative error (%)**
Feed Total COD (mg COD/ℓ)	1950	1950	-
Feed Soluble COD (mg COD/ℓ)	254	254	-
Feed TKN (mg N/ℓ)	43	43	-
Feed FSA (mg N/ℓ)	5	5	-
Effluent Total COD (mg COD/ℓ)	905 ± 31	935.25	3.23
Effluent Soluble COD (mg COD/ℓ)	32 ± 2	85.15	62.42
Reactor pH	6.59 ± 0.07	5.65	-16.64
Effluent VFA (mg HAc/ℓ)	0 ± 1	9.36	100
Effluent Alkalinity (mg/ℓ as $CaCO_3$)	170 ± 7	193.85	12.30
Sulphate Addition (mg SO4/ℓ)	0	0	-
Effluent Sulphate (mg SO4/ℓ)	0	0	-
% Sulphate Conversion	-	-	-
Methane Production (ℓ/d)	0.62	0.88	29.58
Gas Composition (% CH_4)	53.2	52.20	-1.91
Effluent FSA (mg N/ℓ)	19 ± 1	16.36	-16.15
Effluent TKN (mg N/ℓ)	40 ± 1	37.95	-5.39

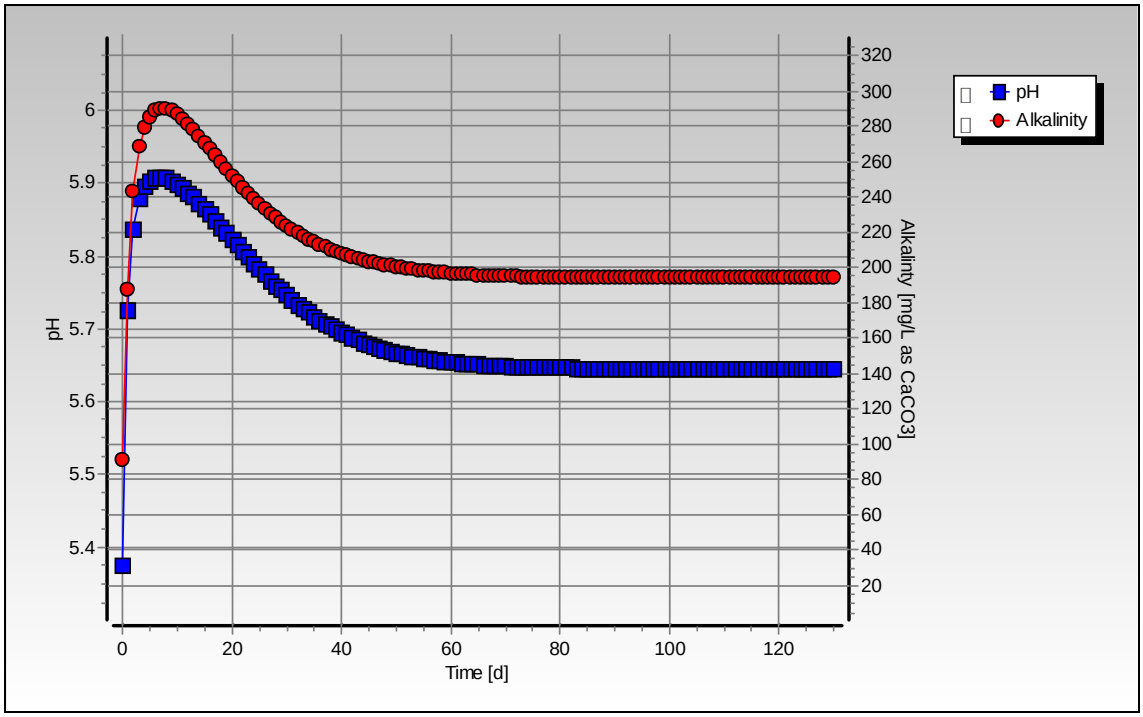

Figure C-78: Simulated pH and alkalinity profiles for steady state number 25

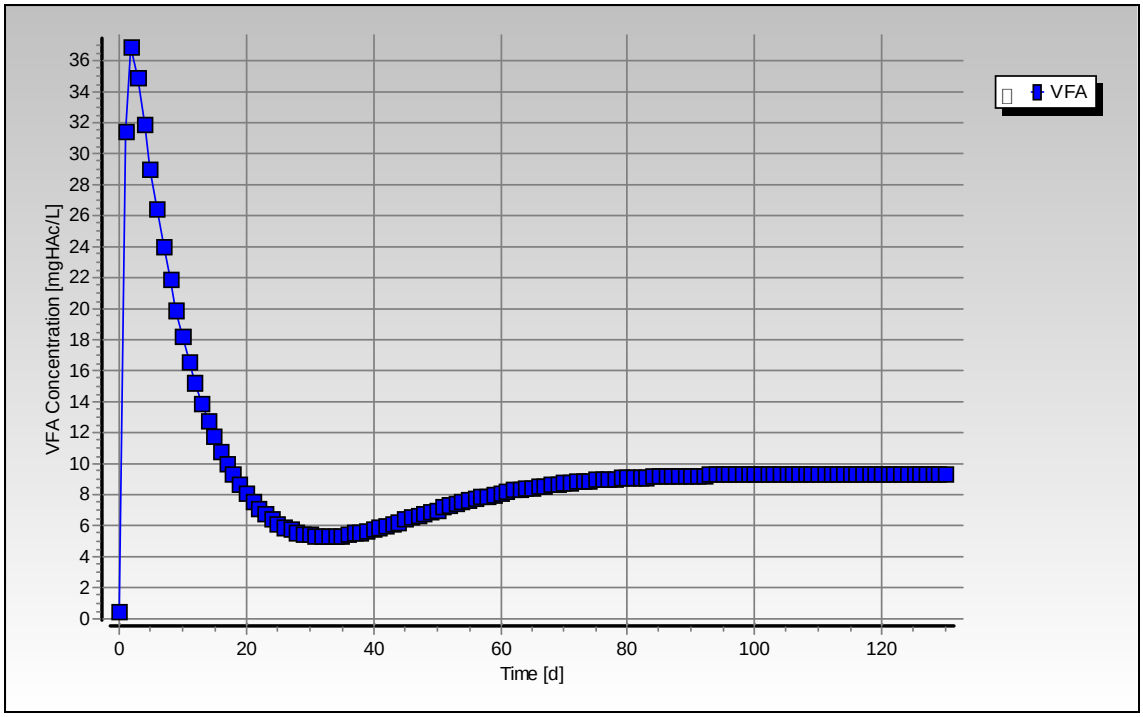

Figure C-79: Simulated VFA concentration profile for steady state number 25

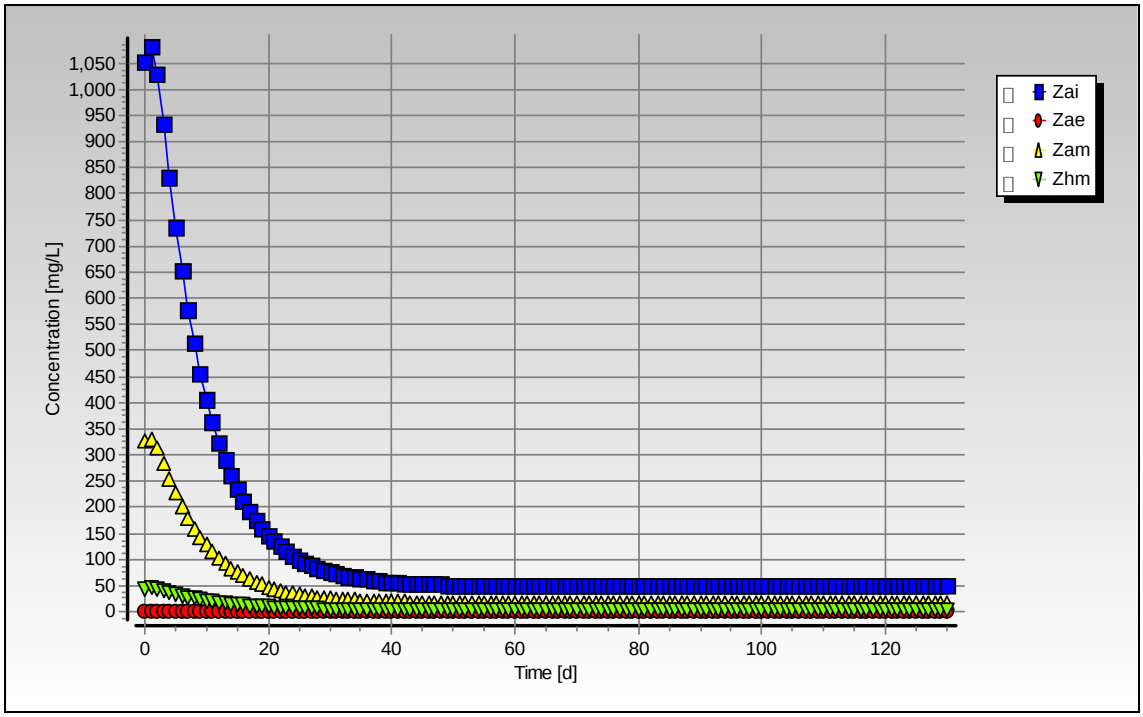

Figure C-80: Simulated biomass concentration profiles for steady state number 25

Steady State Number 26

Table C-49: Operating conditions for steady state number 26

Feed Batch Number	F14
Reactor Volume (ℓ)	20
Retention Time (d)	8
pH	steady state
Biological Groups Present	acidogenic, acetogenic and methanogenic

Table C-50: Results summary for steady state number 26

	Measured	**Model**	**Relative error (%)**
Feed Total COD (mg COD/ℓ)	1949	1949	-
Feed Soluble COD (mg COD/ℓ)	283	283	-
Feed TKN (mg N/ℓ)	43	43	-
Feed FSA (mg N/ℓ)	7	7	-
Effluent Total COD (mg COD/ℓ)	892 ± 21	921.82	3.24
Effluent Soluble COD (mg COD/ℓ)	51 ± 8	117.40	56.56
Reactor pH	6.38 ± 0.02	5.65	-12.92
Effluent VFA (mg HAc/ℓ)	10 ± 3	11.89	15.90
Effluent Alkalinity (mg/ℓ as $CaCO_3$)	144 ± 1	194.80	26.08
Sulphate Addition (mg SO4/ℓ)	0	0	-
Effluent Sulphate (mg SO4/ℓ)	0	0	-
% Sulphate Conversion	-	-	-
Methane Production (ℓ/d)	0.84	1.11	24.60
Gas Composition (% CH_4)	59.3	-13.34	-13.34
Effluent FSA (mg N/ℓ)	15 ± 1	18.24	17.75
Effluent TKN (mg N/ℓ)	36 ± 1	39.38	8.58

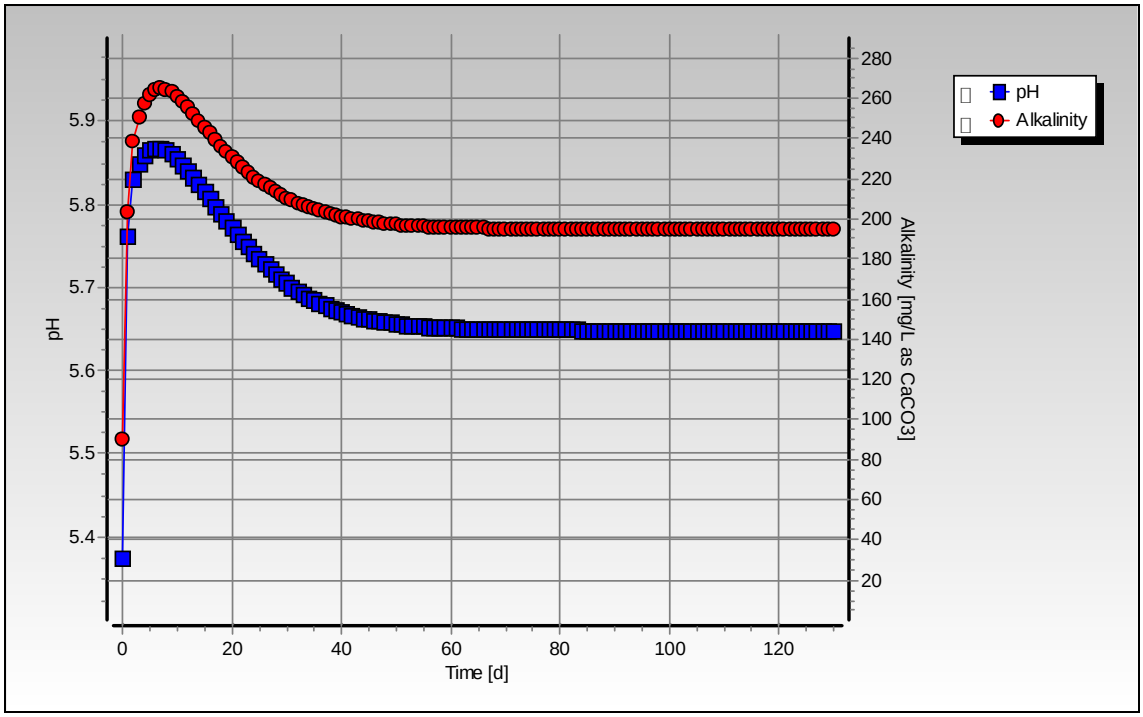

Figure C-81: Simulated pH and alkalinity profiles for steady state number 26

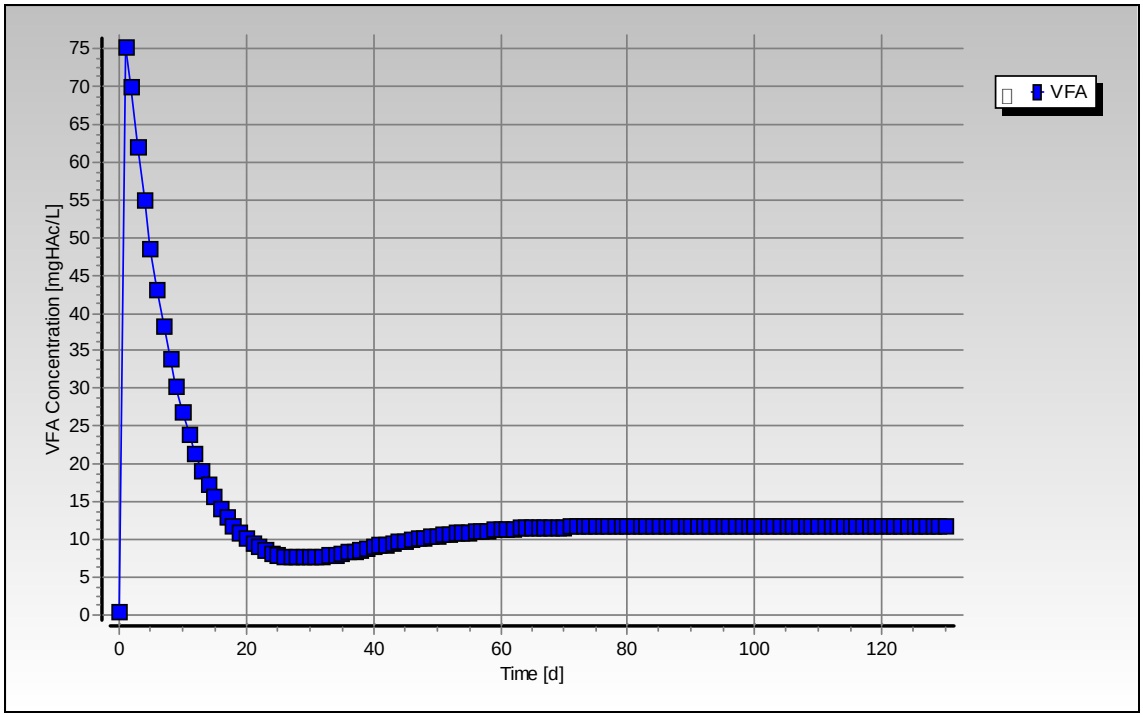

Figure C-82: Simulated VFA concentration profile for steady state number 26

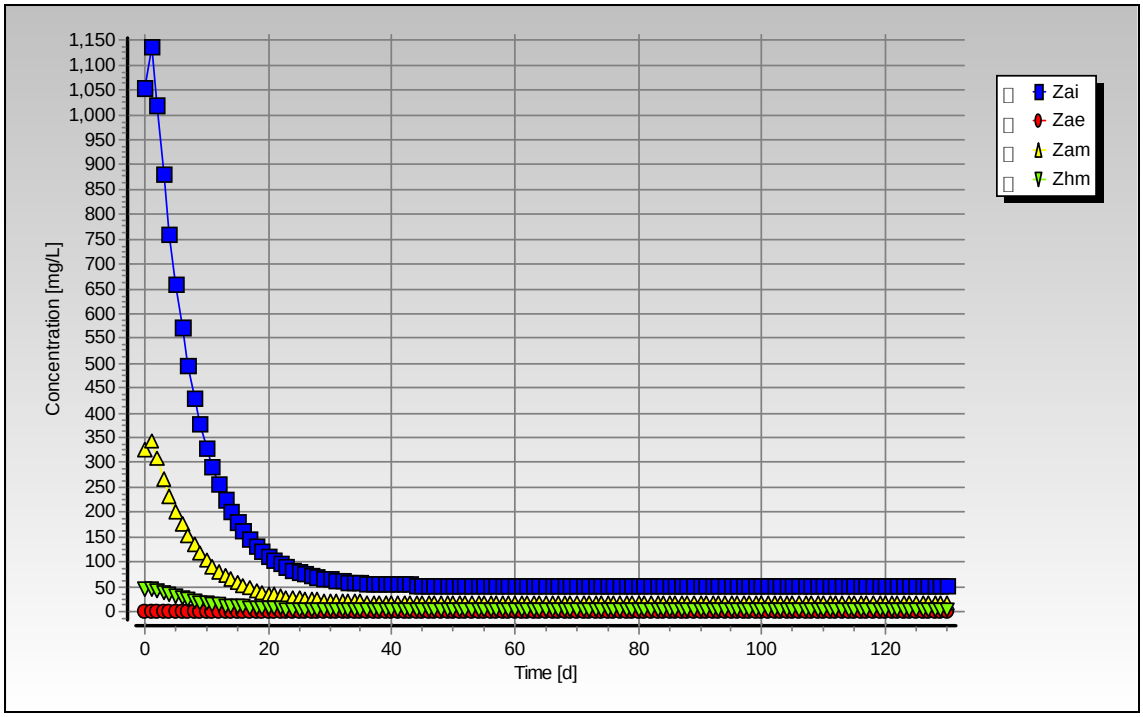

Figure C-83: Simulated biomass concentration profiles for steady state number 26

Steady State Number 27

Table C-51: Operating conditions for steady state number 27

Feed Batch Number	F15
Reactor Volume (ℓ)	16
Retention Time (d)	8
pH	controlled to ~ 6.5
Biological Groups Present	acidogenic, acetogenic and methanogenic

Table C-52: Results summary for steady state number 27

	Measured	**Model**	**Relative error (%)**
Feed Total COD (mg COD/ℓ)	2017	2017	-
Feed Soluble COD (mg COD/ℓ)	224	224	-
Feed TKN (mg N/ℓ)	39	39	-
Feed FSA (mg N/ℓ)	8	8	-
Effluent Total COD (mg COD/ℓ)	913 ± 17	920.30	0.79
Effluent Soluble COD (mg COD/ℓ)	27 ± 3	63.58	57.54
Reactor pH	6.58 ± 0.01	6.58	-
Effluent VFA (mg HAc/ℓ)	1 ± 1	1.60	37.54
Effluent Alkalinity (mg/ℓ as $CaCO_3$)	127 ± 3	949.28	86.62
Sulphate Addition (mg SO4/ℓ)	0	0	-
Effluent Sulphate (mg SO4/ℓ)	0	0	-
% Sulphate Conversion	-	-	-
Methane Production (ℓ/d)	0.70	0.95	26.48
Gas Composition (% CH_4)	58.46	72.85	19.75
Effluent FSA (mg N/ℓ)	15 ± 1	20.31	26.16
Effluent TKN (mg N/ℓ)	36 ± 1	42.43	15.15

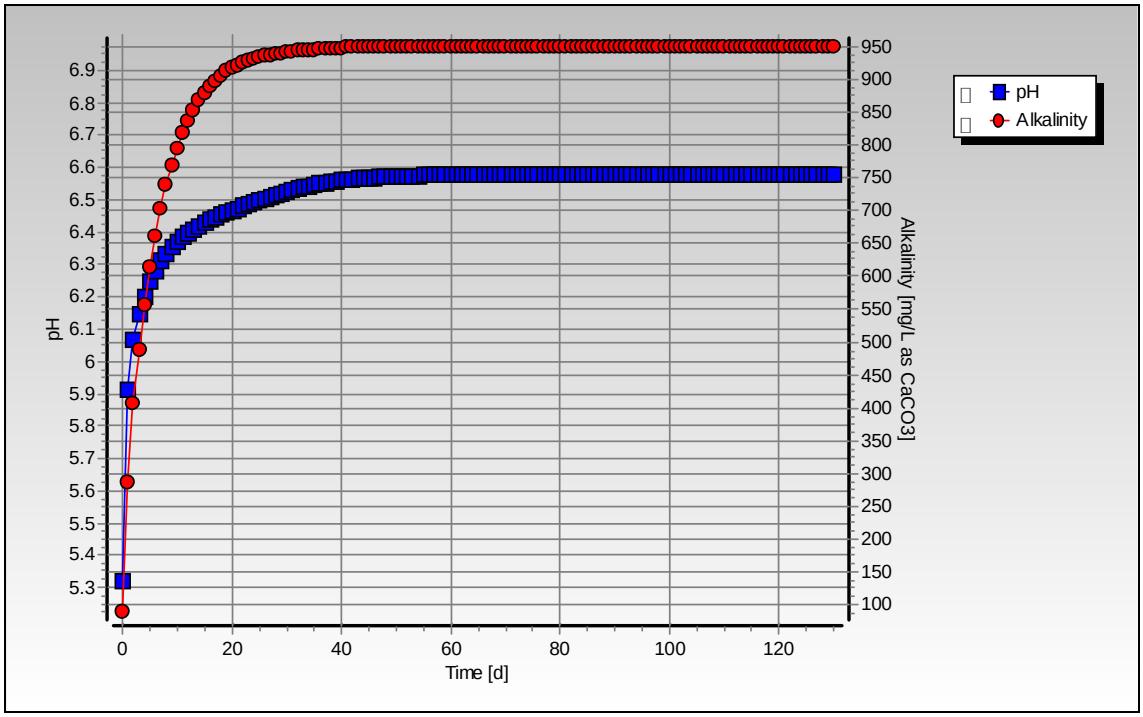

Figure C-84: Simulated pH and alkalinity profiles for steady state number 27

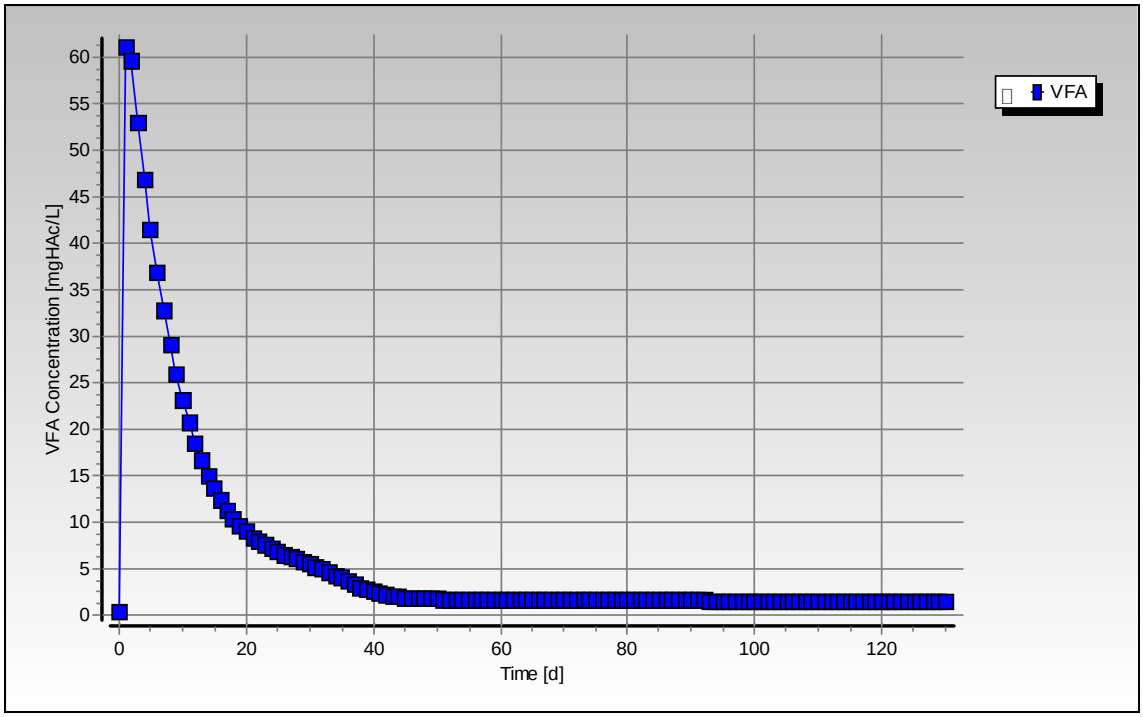

Figure C-85: Simulated VFA concentration profile for steady state number 27

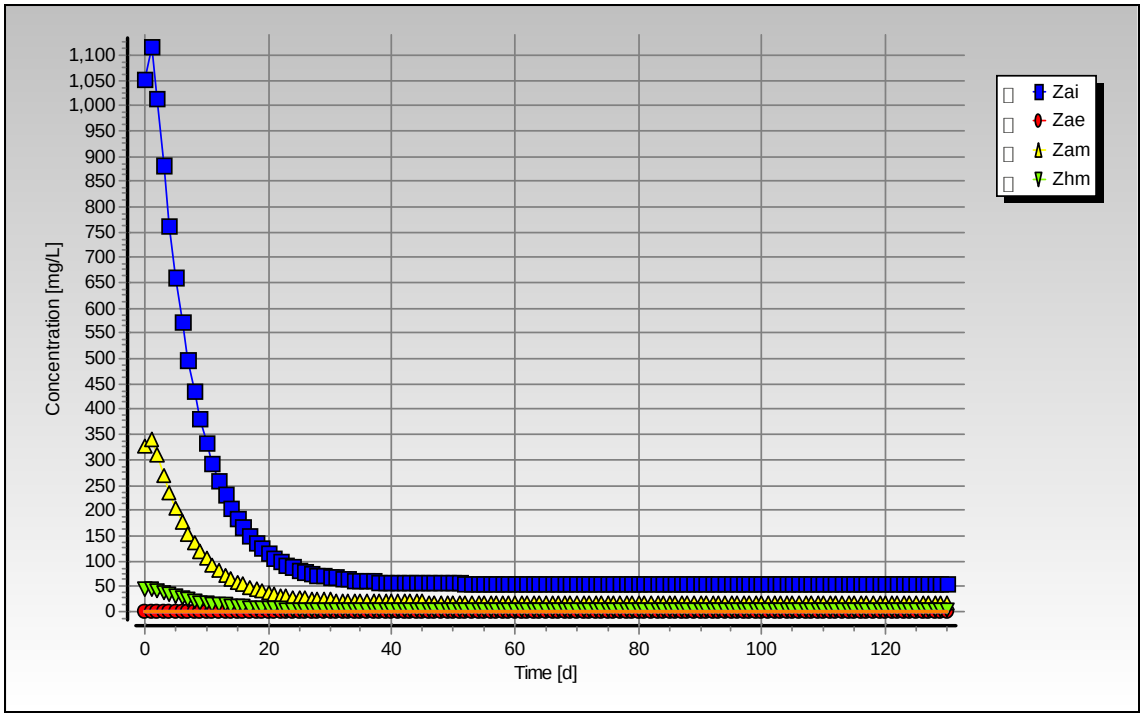

Figure C-86: Simulated biomass concentration profiles for steady state number 27

Steady State Number 28

Table C-53: Operating conditions for steady state number 28

Feed Batch Number	F15
Reactor Volume (ℓ)	20
Retention Time (d)	5.71
pH	steady state
Biological Groups Present	acidogenic, acetogenic and methanogenic

Table C-54: Results summary for steady state number 28

	Measured	**Model**	**Relative error (%)**
Feed Total COD (mg COD/ℓ)	41442	41442	-
Feed Soluble COD (mg COD/ℓ)	2583	2583	-
Feed TKN (mg N/ℓ)	792	792	-
Feed FSA (mg N/ℓ)	40	40	-
Effluent Total COD (mg COD/ℓ)	19737 ± 732	20388.97	3.20
Effluent Soluble COD (mg COD/ℓ)	295 ± 36	363.72	18.89
Reactor pH	6.75 ± 0.01	6.66	-1.30
Effluent VFA (mg HAc/ℓ)	26 ± 16	2.27	-1047.88
Effluent Alkalinity (mg/ℓ as $CaCO_3$)	1612 ± 25	1671.18	3.54
Sulphate Addition (mg SO4/ℓ)	0	0	-
Effluent Sulphate (mg SO4/ℓ)	0	0	-
% Sulphate Conversion	-	-	-
Methane Production (ℓ/d)	30.32	32.13	5.62
Gas Composition (% CH_4)	63.76	60.63	-5.16
Effluent FSA (mg N/ℓ)	183 ± 5	280.51	34.76
Effluent TKN (mg N/ℓ)	648 ± 22	759.16	14.64

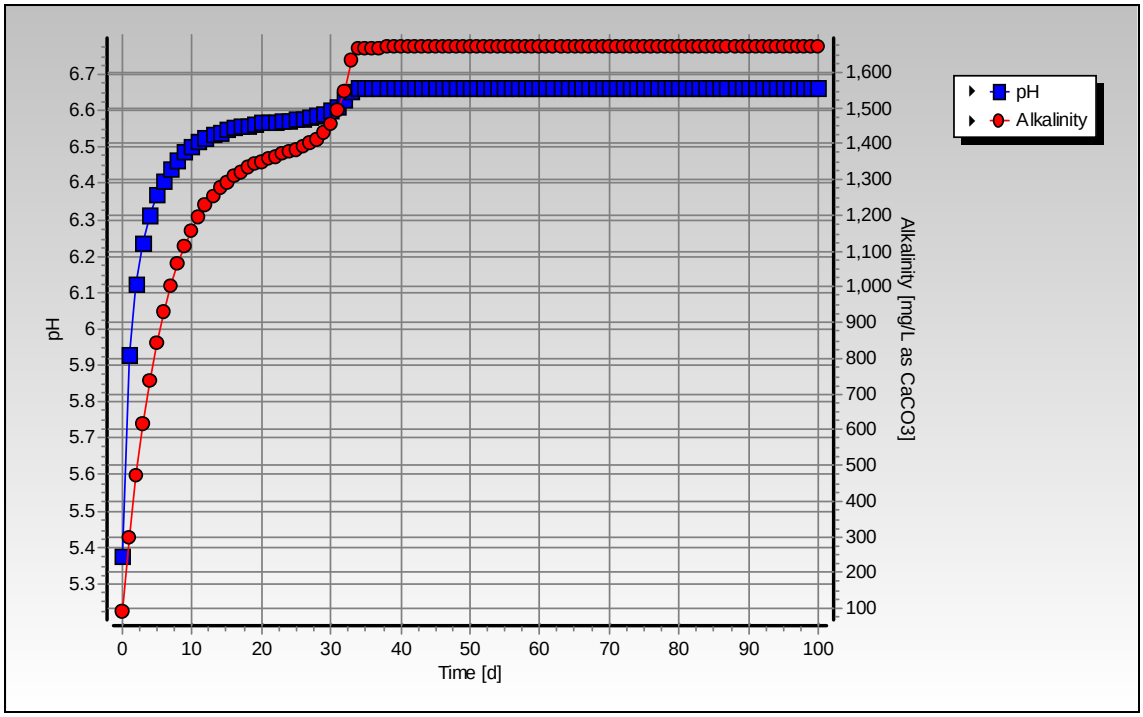

Figure C-87: Simulated pH and alkalinity profiles for steady state number 28

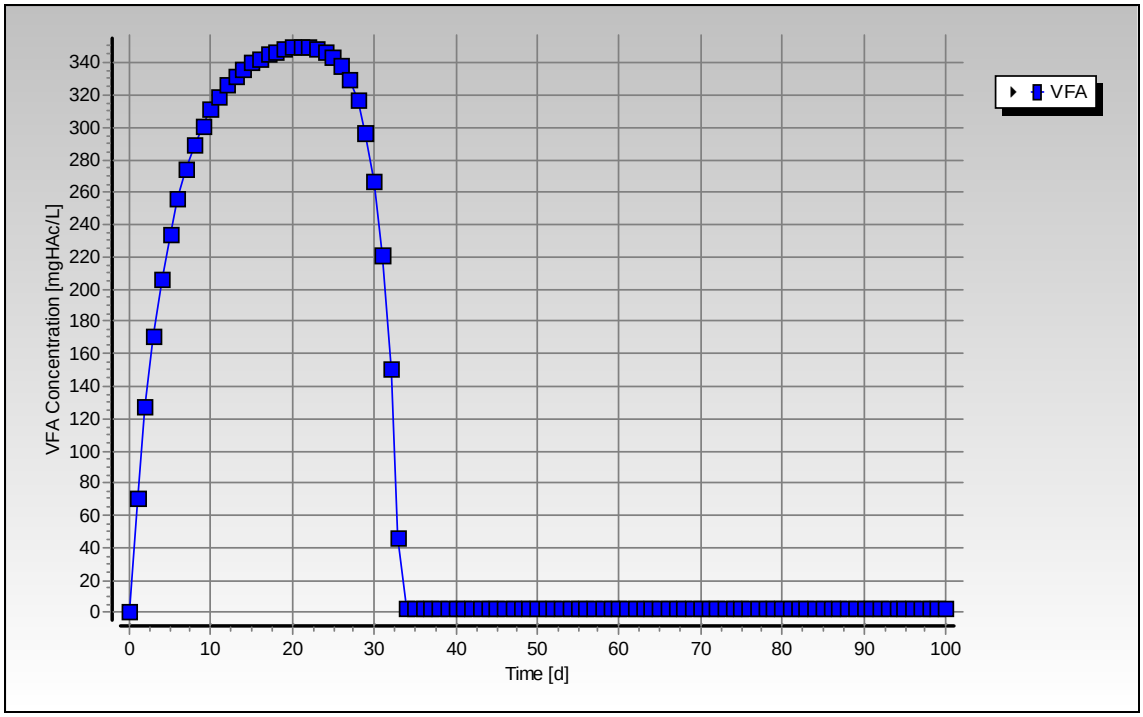

Figure C-88: Simulated VFA concentration profile for steady state number 28

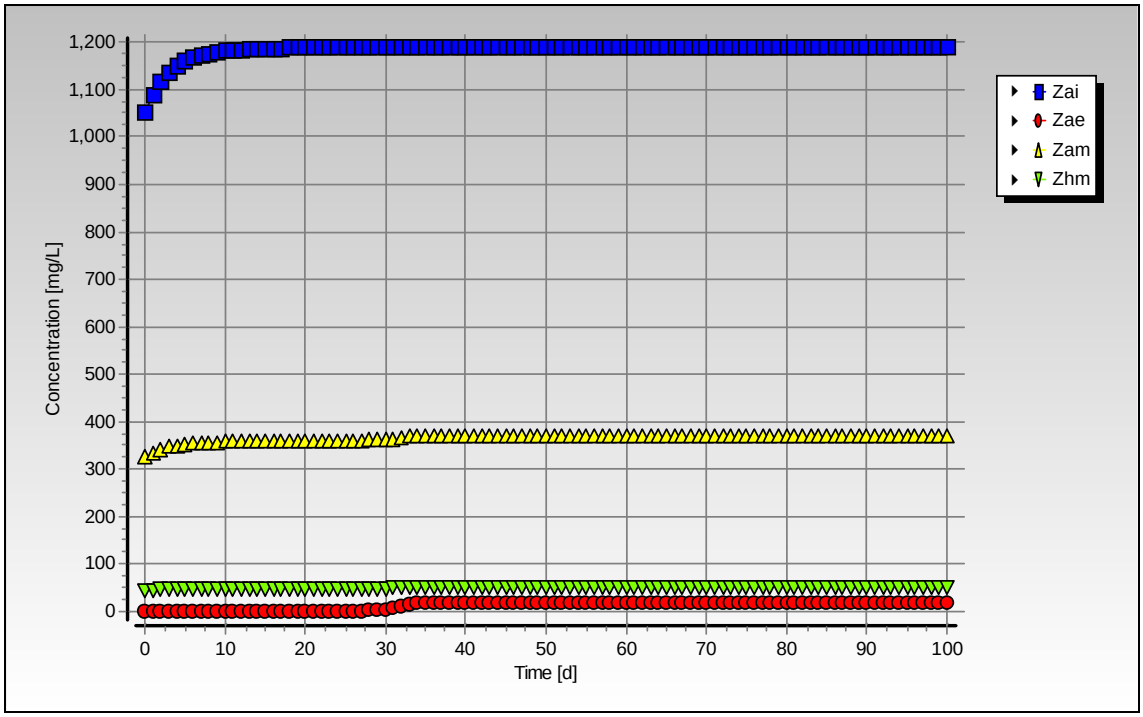

Figure C-89: Simulated biomass concentration profiles for steady state number 28

Steady State Number 31

Table C-55: Operating conditions for steady state number 31

Feed Batch Number	F15
Reactor Volume (ℓ)	20
Retention Time (d)	5.71
pH	steady state
Biological Groups Present	acidogenic, acetogenic and methanogenic

Table C-56: Results summary for steady state number 31

	Measured	**Model**	**Relative error (%)**
Feed Total COD (mg COD/ℓ)	13186	13186	-
Feed Soluble COD (mg COD/ℓ)	956	956	-
Feed TKN (mg N/ℓ)	252	252	-
Feed FSA (mg N/ℓ)	18	18	-
Effluent Total COD (mg COD/ℓ)	6757 ± 265	7007.94	3.58
Effluent Soluble COD (mg COD/ℓ)	120 ± 10	193.50	37.98
Reactor pH	6.45 ± 0.01	6.20	-4.03
Effluent VFA (mg HAc/ℓ)	19 ± 2	4.88	-289.61
Effluent Alkalinity (mg/ℓ as $CaCO_3$)	564 ± 6	595.68	5.32
Sulphate Addition (mg SO4/ℓ)	0	0	-
Effluent Sulphate (mg SO4/ℓ)	0	0	-
% Sulphate Conversion	-	-	-
Methane Production (ℓ/d)	9.23	9.42	1.98
Gas Composition (% CH_4)	65.7	59.16	-11.06
Effluent FSA (mg N/ℓ)	63 ± 1	86.68	27.32
Effluent TKN (mg N/ℓ)	206 ± 2	243.37	15.36

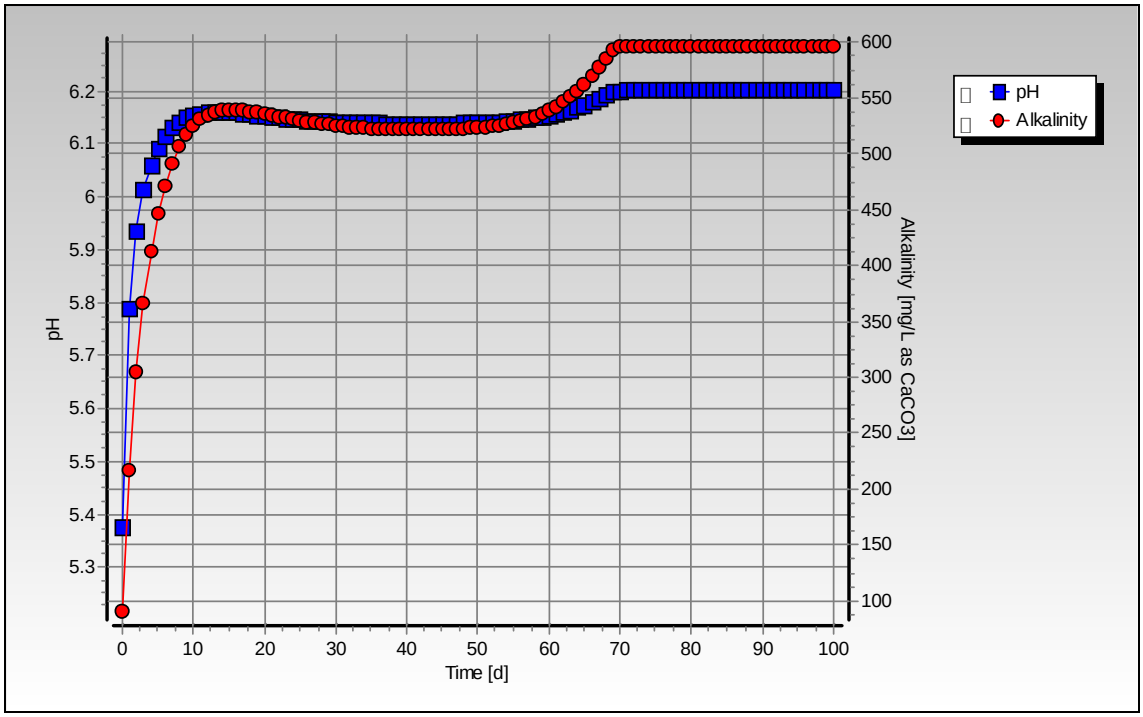

Figure C-90: Simulated pH and alkalinity profiles for steady state number 31

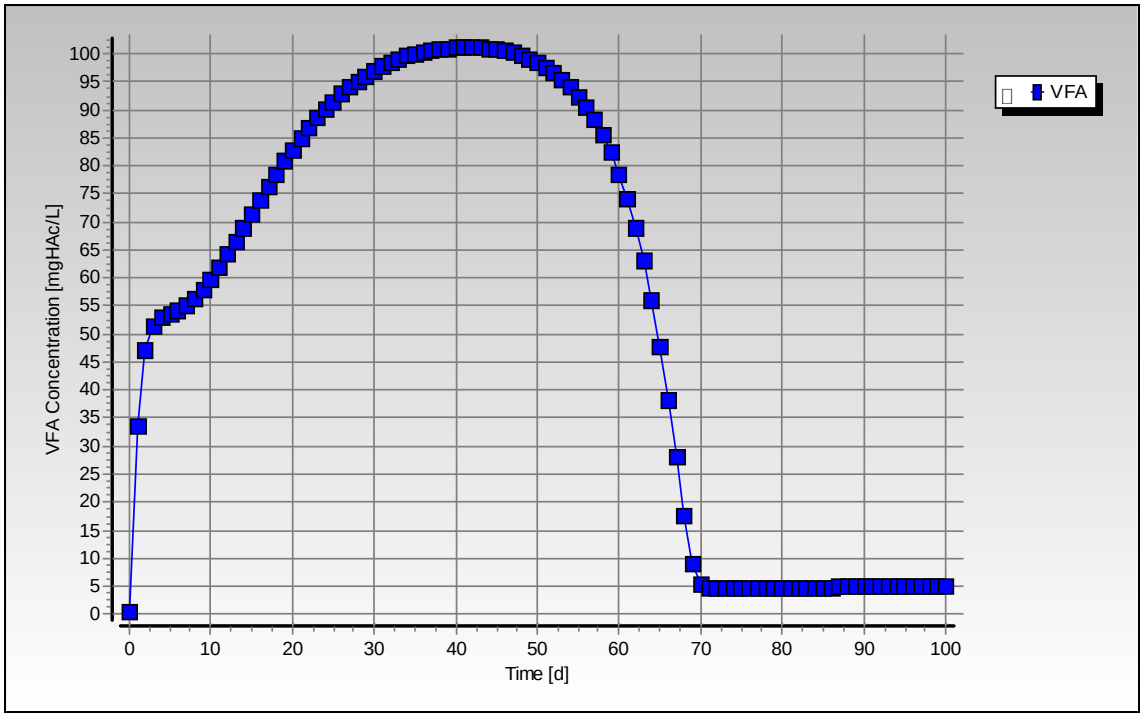

Figure C-91: Simulated VFA concentration profile for steady state number 31

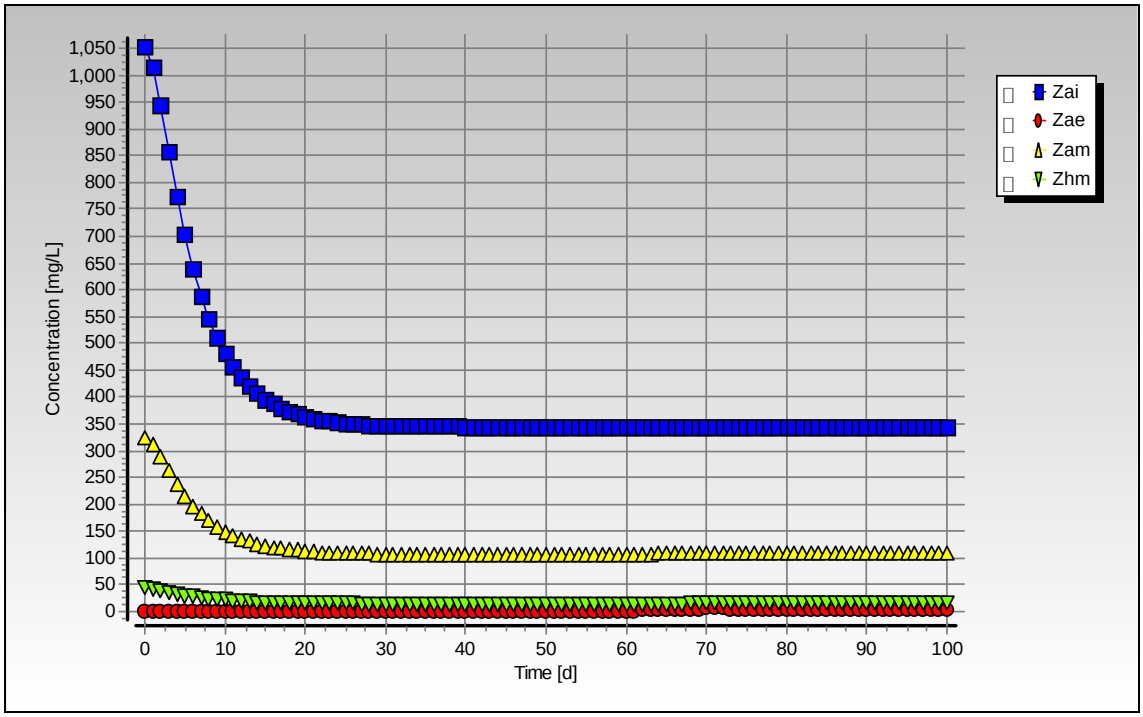

Figure C-92: Simulated biomass concentration profiles for steady state number 31

Steady State Number 36

Table C-57: Operating conditions for steady state number 36

Feed Batch Number	F15
Reactor Volume (ℓ)	16
Retention Time (d)	8
pH	Controlled to ~ 6.5
Biological Groups Present	acidogenic, acetogenic, methanogenic and sulphidogenic

Table C-58: Results summary for steady state number 36

	Measured	**Model**	**Relative error (%)**
Feed Total COD (mg COD/ℓ)	1949	1949	-
Feed Soluble COD (mg COD/ℓ)	283	283	-
Feed TKN (mg N/ℓ)	43	43	-
Feed FSA (mg N/ℓ)	13	13	-
Effluent Total COD (mg COD/ℓ)	1304 ± 48	996.00	-30.92
Effluent Soluble COD (mg COD/ℓ)	521 ± 24	125.87	-313.91
Reactor pH	6.47 ± 0.01	6.46	-0.15
Effluent VFA (mg HAc/ℓ)	0 ± 1	0.17	100
Effluent Alkalinity (mg/ℓ as $CaCO_3$)	354 ± 10	937.84	62.25
Sulphate Addition (mg SO4/ℓ)	2000	2000	-
Effluent Sulphate (mg SO4/ℓ)	436 ± 20	1523	71.37
% Sulphate Conversion	78.20	23.87	-
Methane Production (ℓ/d)	0	0.61	100
Gas Composition (% CH_4)	0	46.76	100
Effluent FSA (mg N/ℓ)	16 ± 3	22.42	28.62
Effluent TKN (mg N/ℓ)	46 ± 1	44.22	-4.03

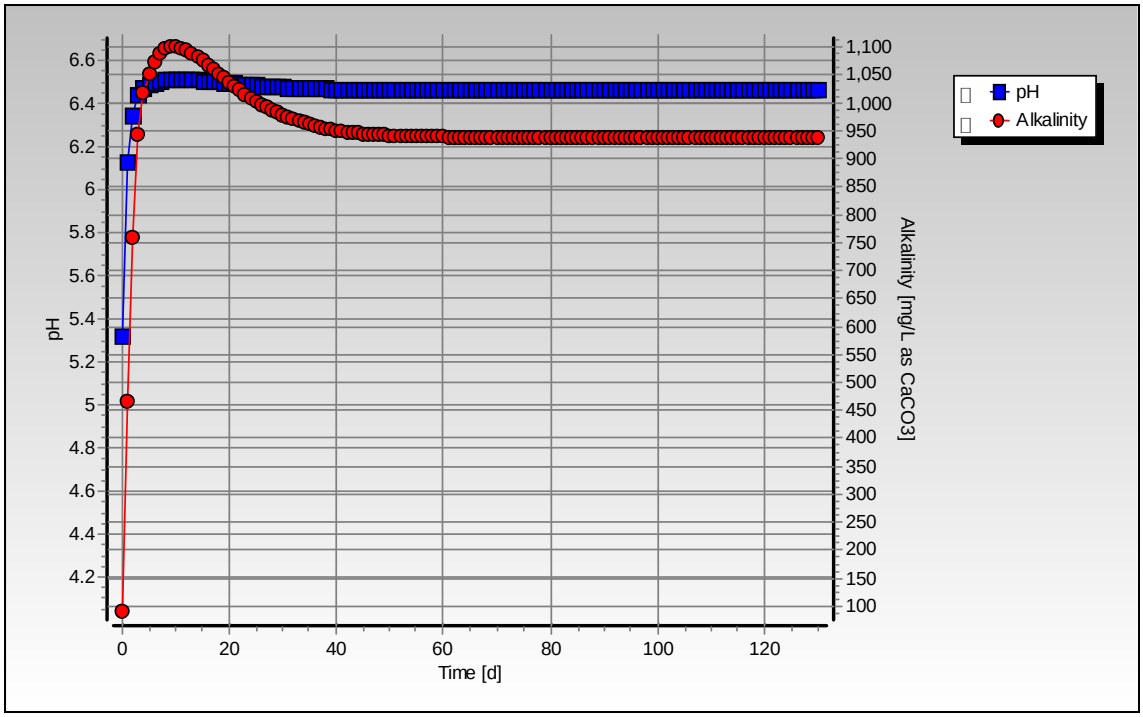

Figure C-93: Simulated pH and alkalinity profiles for steady state number 36

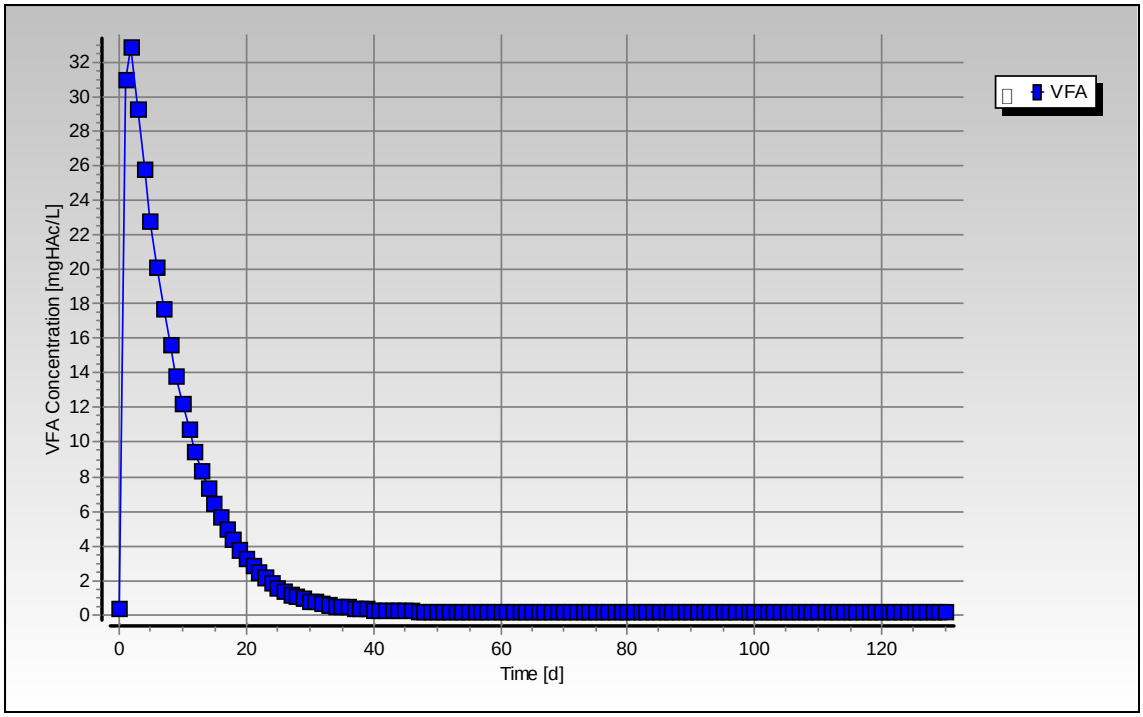

Figure C-94: Simulated VFA concentration profile for steady state number 36

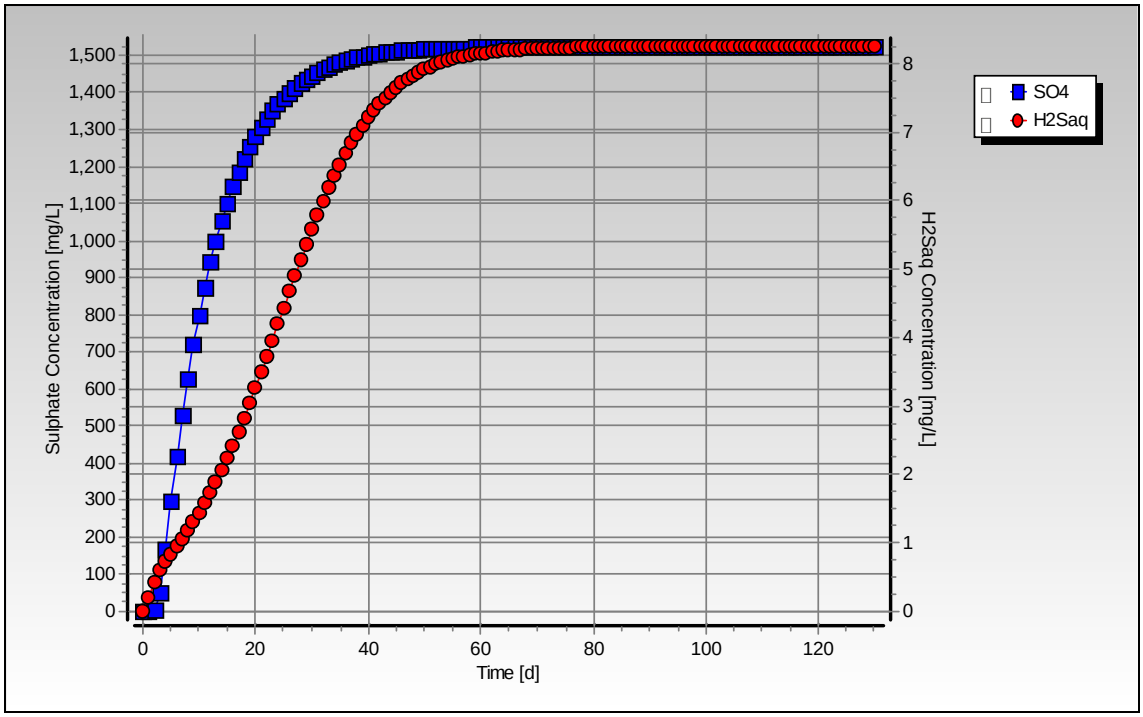

Figure C-95: Simulated sulphate and aqueous hydrogen sulphide concentration profiles for steady state number 36

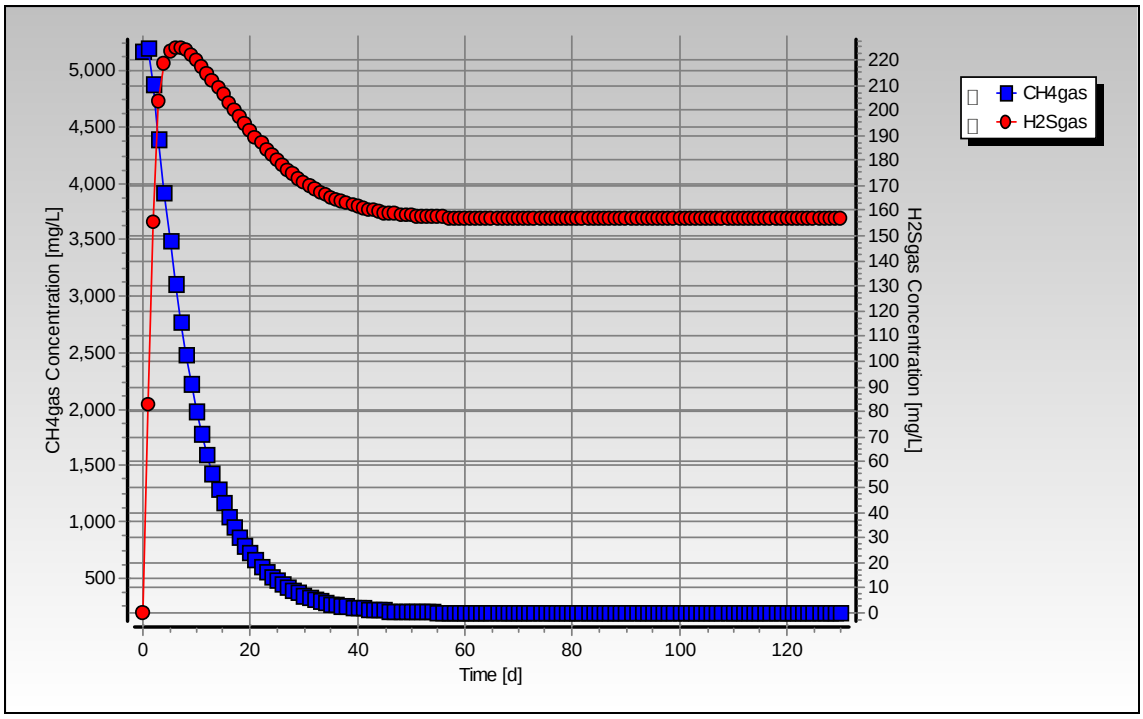

Figure C-96: Simulated methane and hydrogen sulphide gas concentration profiles for steady state number 36

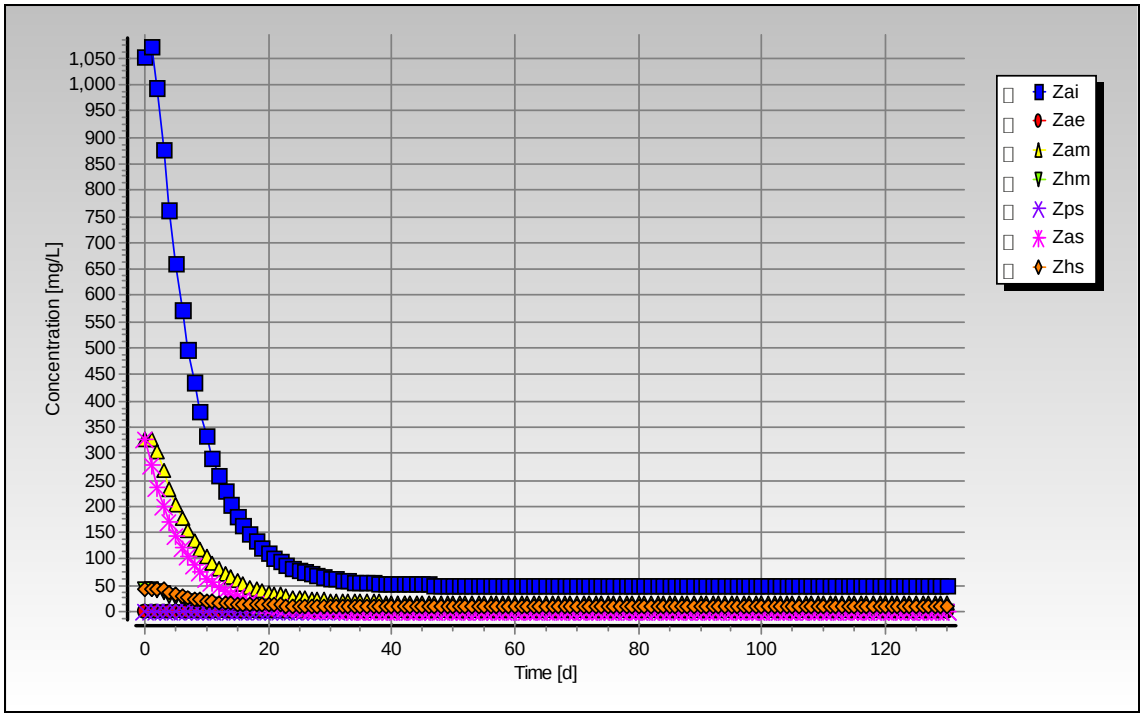

Figure C-97: Simulated biomass concentration profiles for steady state number 36

Steady State Number 41

Table C-59: Operating conditions for steady state number 41

Feed Batch Number	F15
Reactor Volume (ℓ)	20
Retention Time (d)	16
pH	steady state
Biological Groups Present	acidogenic, acetogenic, methanogenic and sulphidogenic

Table C-60: Results summary for steady state number 41

	Measured	**Model**	**Relative error (%)**
Feed Total COD (mg COD/ℓ)	2012	2012	-
Feed Soluble COD (mg COD/ℓ)	212	212	-
Feed TKN (mg N/ℓ)	39	39	-
Feed FSA (mg N/ℓ)	6	6	-
Effluent Total COD (mg COD/ℓ)	1697 ± 41	898.94	-54.67
Effluent Soluble COD (mg COD/ℓ)	897 ± 41	66.44	-241.19
Reactor pH	7.64 ± 0.01	6.32	-20.88
Effluent VFA (mg HAc/ℓ)	0 ± 1	0.13	100
Effluent Alkalinity (mg/ℓ as $CaCO_3$)	1633 ± 41	789.57	-106.82
Sulphate Addition (mg SO4/ℓ)	2000	2000	-
Effluent Sulphate (mg SO4/ℓ)	-	1425	-
% Sulphate Conversion	-	28.75	-
Methane Production (ℓ/d)	0	0.44	100
Gas Composition (% CH_4)	0	42.00	100
Effluent FSA (mg N/ℓ)	11 ± 1	19.55	43.74
Effluent TKN (mg N/ℓ)	45 ± 1	41.46	-8.54

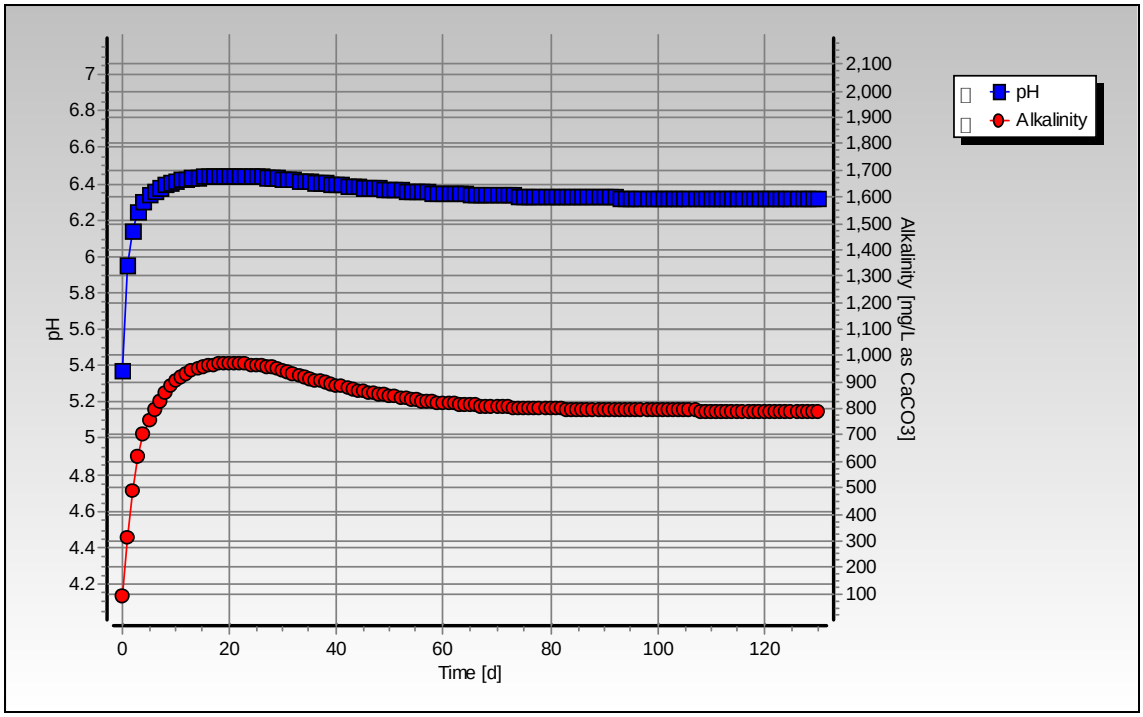

Figure C-98: Simulated pH and alkalinity profiles for steady state number 41

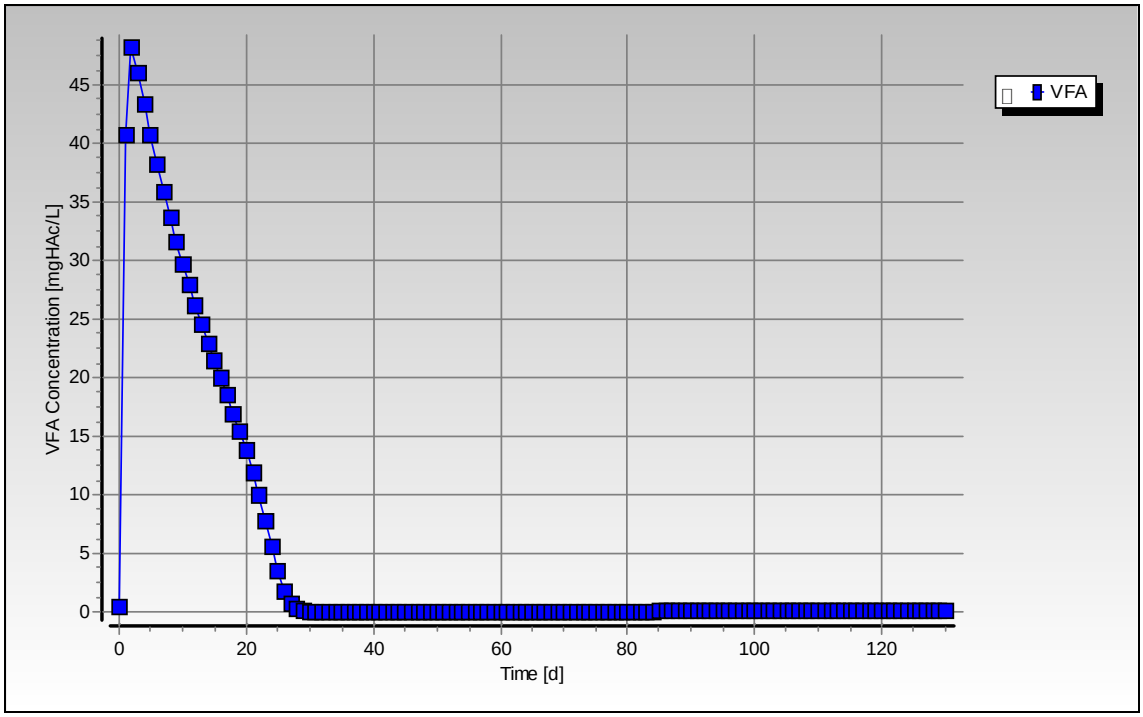

Figure C-99: Simulated VFA concentration profile for steady state number 41

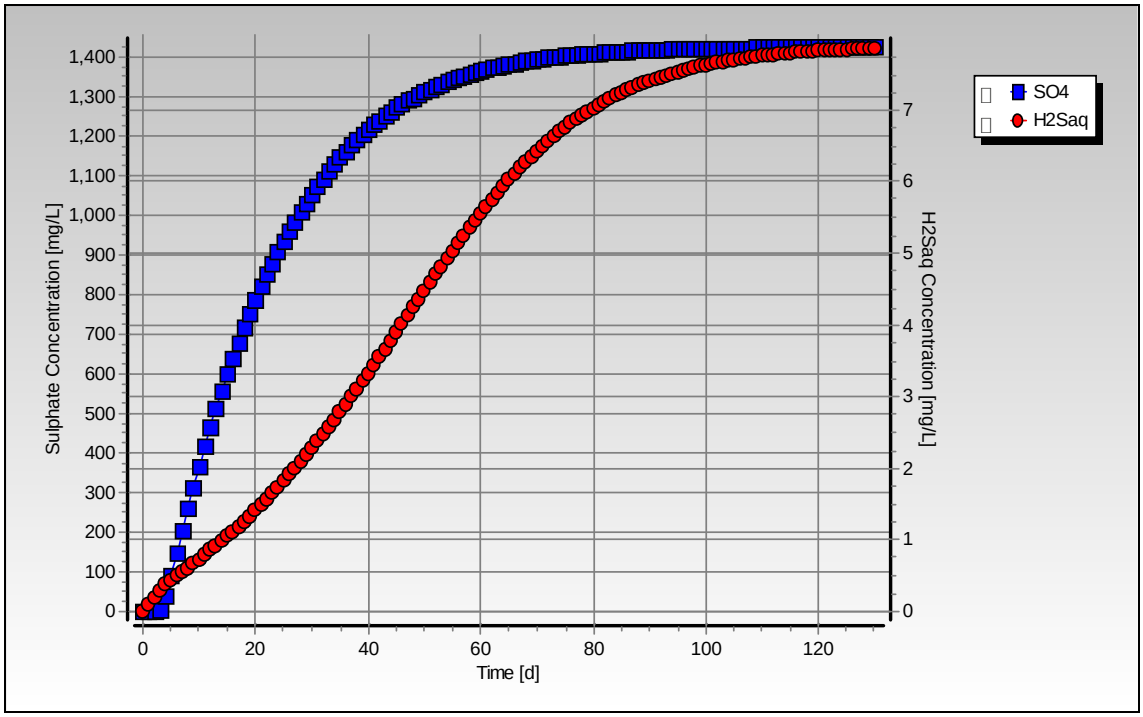

Figure C-100: Simulated sulphate and aqueous hydrogen sulphide concentration profiles for steady state number 41

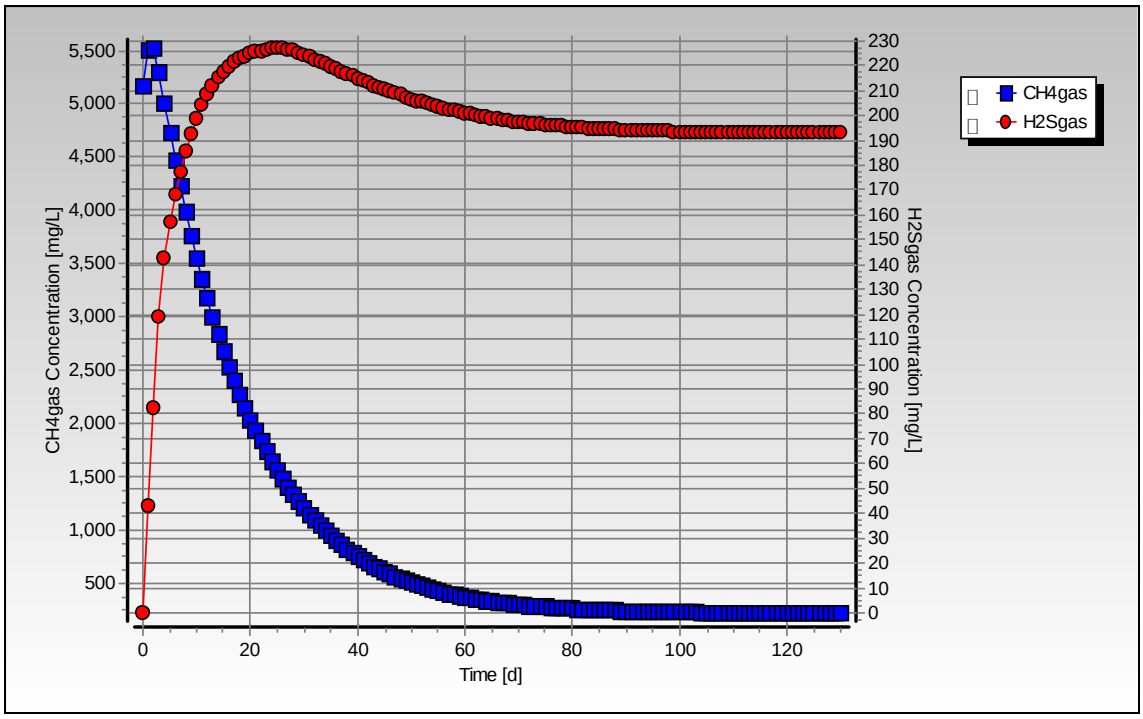

Figure C-101: Simulated methane and hydrogen sulphide gas concentration profiles for steady state number 41

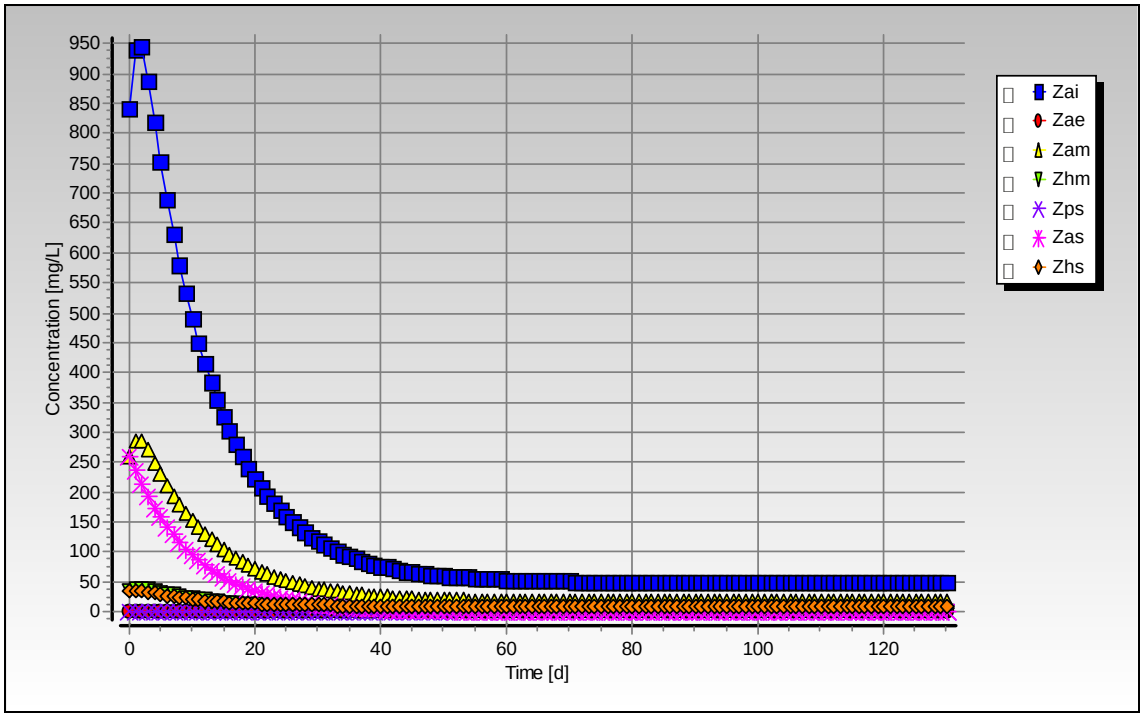

Figure C-102: Simulated biomass concentration profiles for steady state number 41

Steady State Number 42

Table C-61: Operating conditions for steady state number 42

Feed Batch Number	F15
Reactor Volume (ℓ)	20
Retention Time (d)	13.3
pH	steady state
Biological Groups Present	acidogenic, acetogenic, methanogenic and sulphidogenic

Table C-62: Results summary for steady state number 42

	Measured	**Model**	**Relative error (%)**
Feed Total COD (mg COD/ℓ)	2017	2017	-
Feed Soluble COD (mg COD/ℓ)	224	224	-
Feed TKN (mg N/ℓ)	38	38	-
Feed FSA (mg N/ℓ)	10	10	-
Effluent Total COD (mg COD/ℓ)	1749 ± 34	918.44	-90.43
Effluent Soluble COD (mg COD/ℓ)	964 ± 63	69.90	-1279.16
Reactor pH	7.75 ± 0.01	6.31	-22.81
Effluent VFA (mg HAc/ℓ)	57 ± 16	0.14	-39417.78
Effluent Alkalinity (mg/ℓ as $CaCO_3$)	1573 ± 41	776.91	-102.47
Sulphate Addition (mg SO4/ℓ)	2000	2000	-
Effluent Sulphate (mg SO4/ℓ)	147 ± 39	1439	89.78
% Sulphate Conversion	92.65	28.07	-
Methane Production (ℓ/d)	0	0.52	100
Gas Composition (% CH_4)	0	41.86	100
Effluent FSA (mg N/ℓ)	19 ± 1	22.54	15.71
Effluent TKN (mg N/ℓ)	127 ± 3	44.59	-184.82

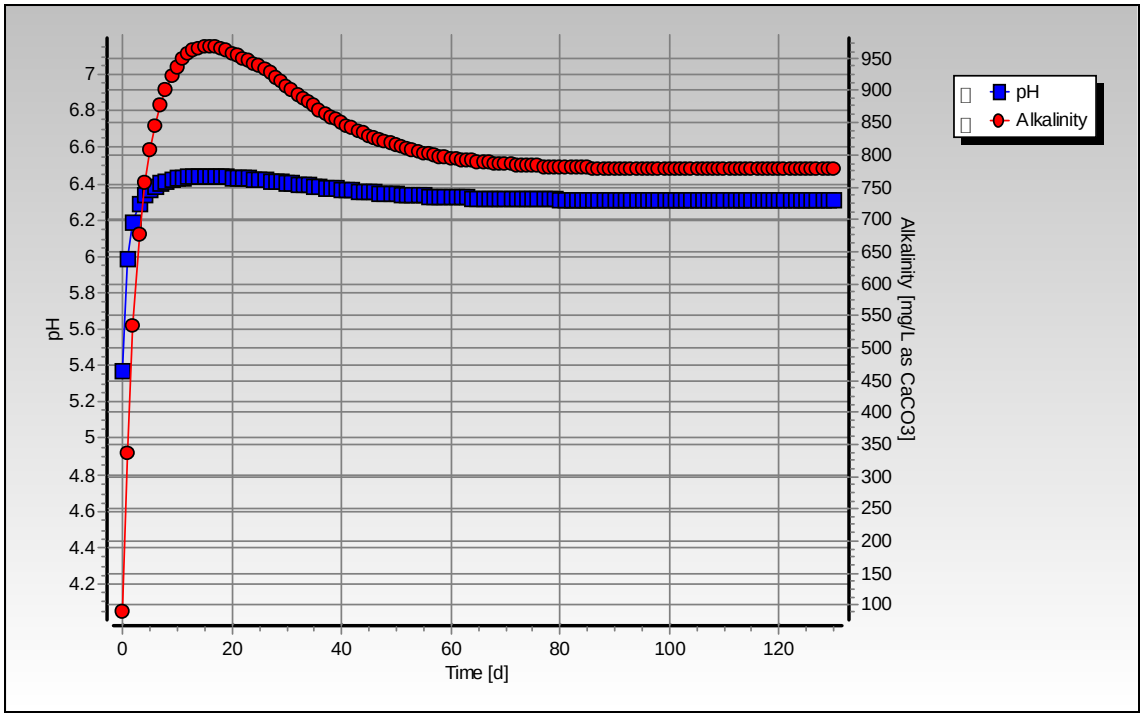

Figure C-103: Simulated pH and alkalinity profiles for steady state number 42

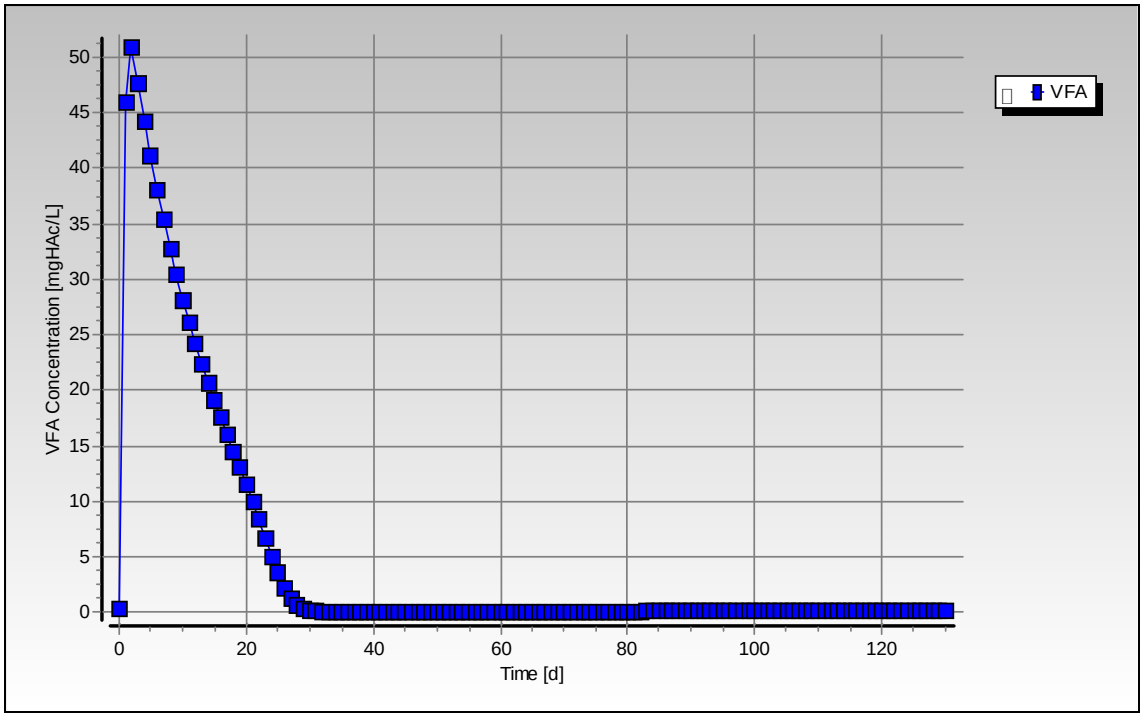

Figure C-104: Simulated VFA concentration profile for steady state number 42

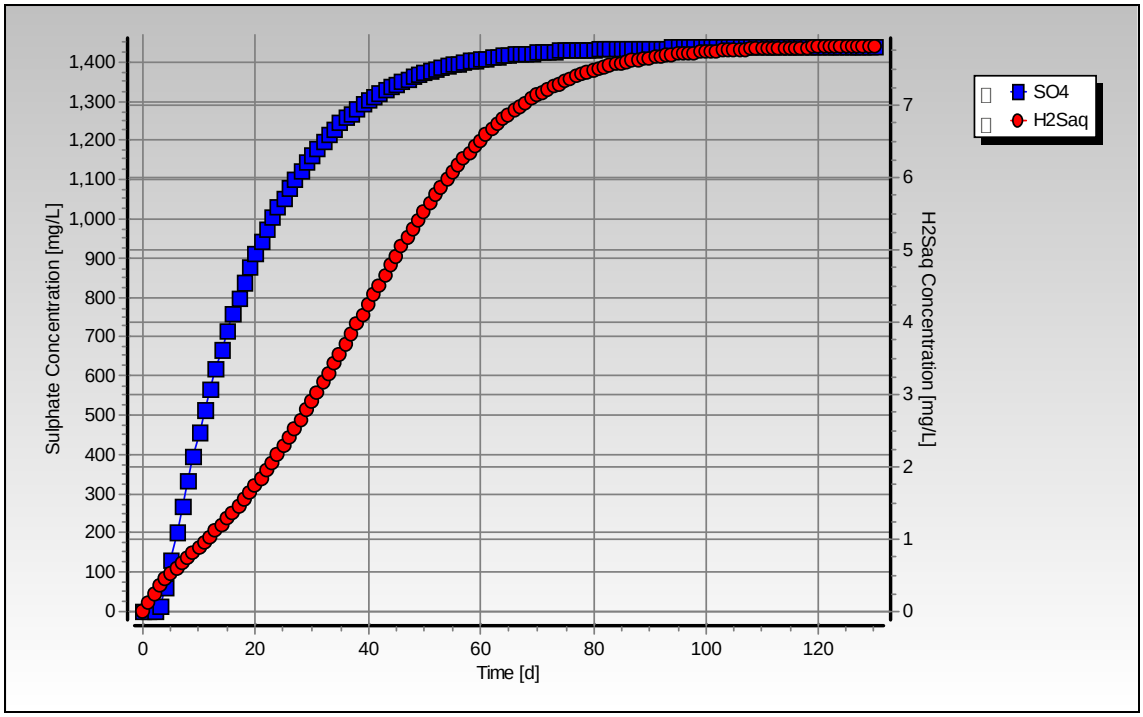

Figure C-105: Simulated sulphate and aqueous hydrogen sulphide concentration profiles for steady state number 42

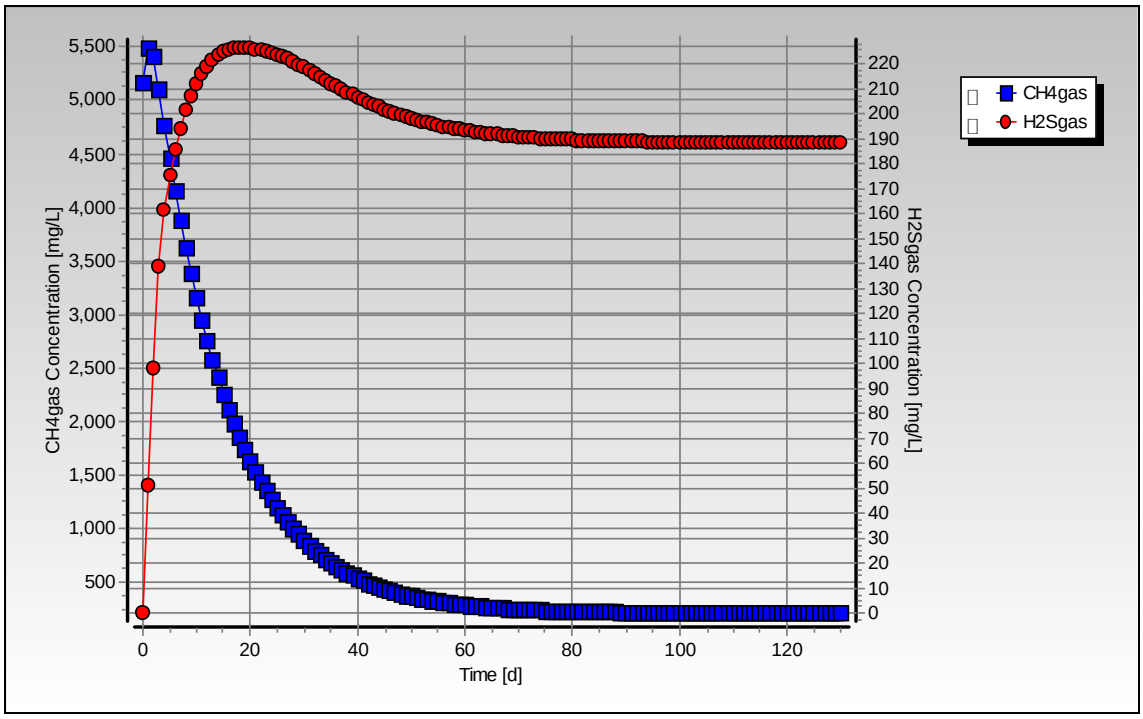

Figure C-106: Simulated methane and hydrogen sulphide gas concentration profiles for steady state number 42

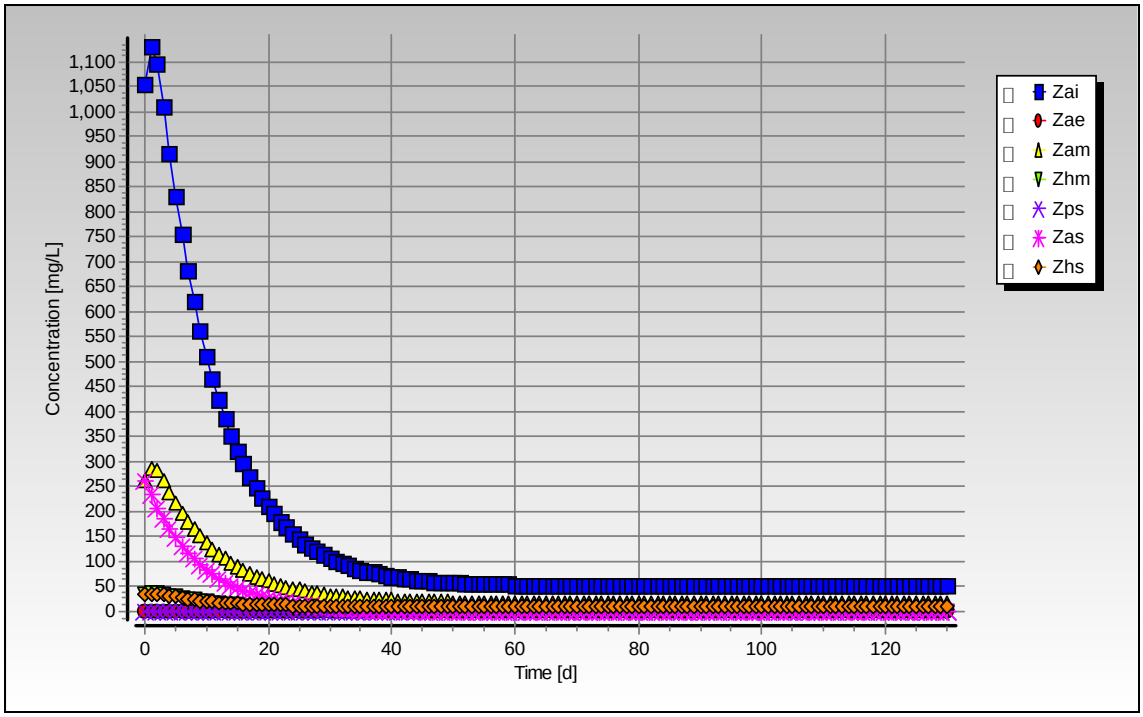

Figure C-107: Simulated biomass concentration profiles for steady state number 42

Steady State Number 46

Table C-63: Operating conditions for steady state number 46

Feed Batch Number	F15
Reactor Volume (ℓ)	20
Retention Time (d)	10
pH	steady state
Biological Groups Present	acidogenic, acetogenic, methanogenic and sulphidogenic

Table C-64: Results summary for steady state number 46

	Measured	**Model**	**Relative error (%)**
Feed Total COD (mg COD/ℓ)	989	989	-
Feed Soluble COD (mg COD/ℓ)	102	102	-
Feed TKN (mg N/ℓ)	19	19	-
Feed FSA (mg N/ℓ)	7	7	-
Effluent Total COD (mg COD/ℓ)	897 ± 25	477.42	-87.88
Effluent Soluble COD (mg COD/ℓ)	466 ± 18	71.89	-548.20
Reactor pH	7.92 ± 0.04	5.98	-32.49
Effluent VFA (mg HAc/ℓ)	3 ± 6	0.14	-2046.72
Effluent Alkalinity (mg/ℓ as $CaCO_3$)	1025 ± 26	414.56	-147.25
Sulphate Addition (mg SO4/ℓ)	1000	1000	-
Effluent Sulphate (mg SO4/ℓ)	51 ± 9	734	79.98
% Sulphate Conversion	94.90	26.59	-
Methane Production (ℓ/d)	0	0.32	100
Gas Composition (% CH_4)	0	37.74	100
Effluent FSA (mg N/ℓ)	-	13.06	-
Effluent TKN (mg N/ℓ)	-	23.76	-

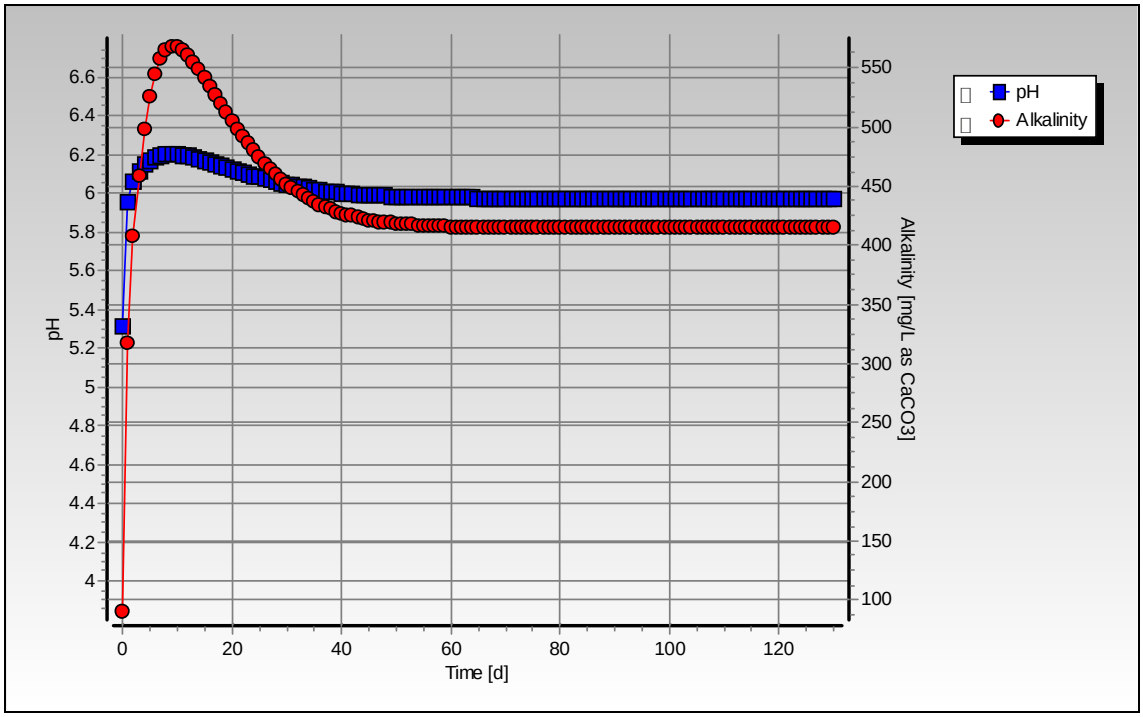

Figure C-108: Simulated pH and alkalinity profiles for steady state number 46

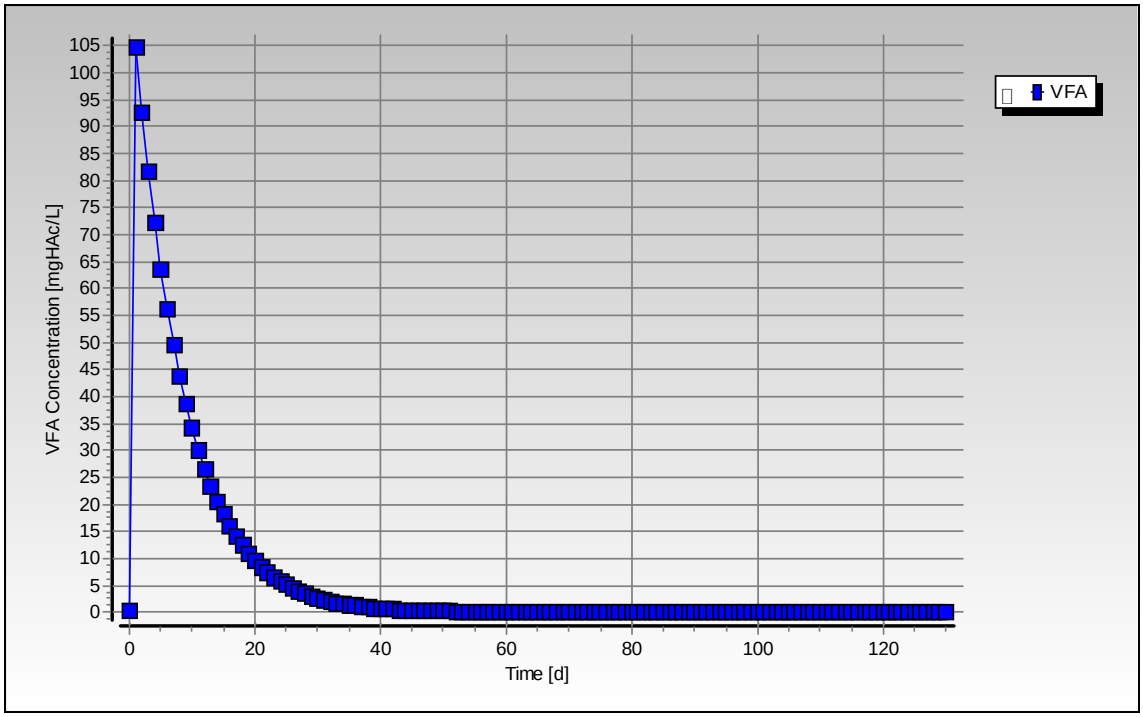

Figure C-109: Simulated VFA concentration profile for steady state number 46

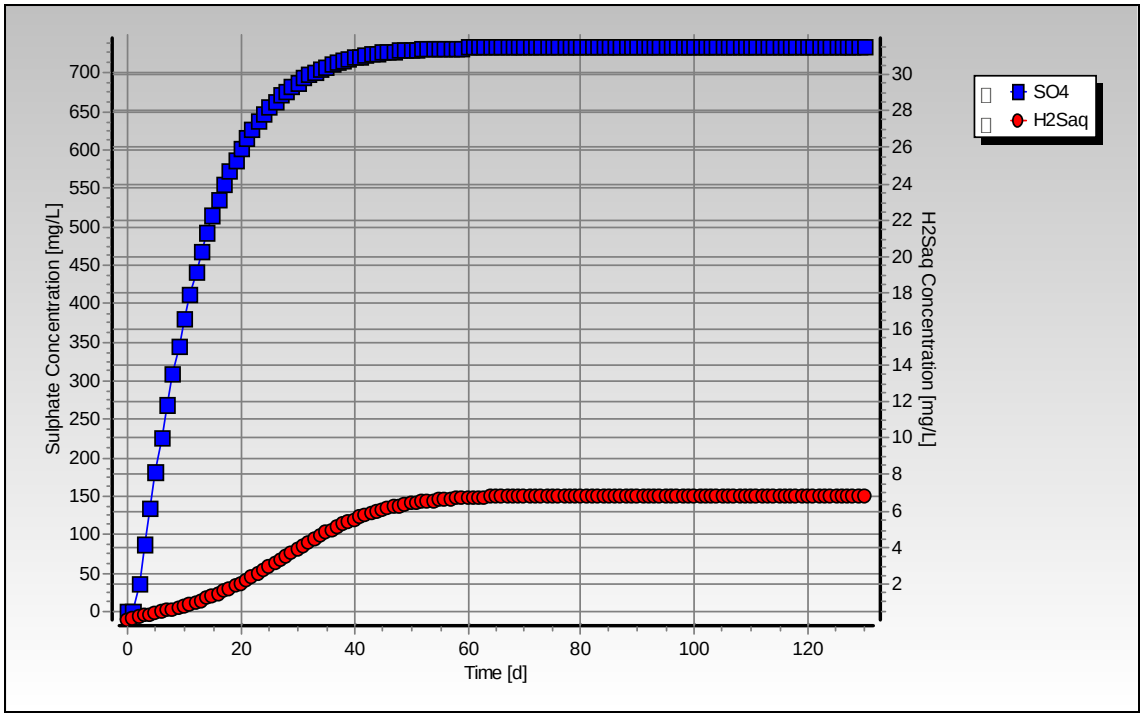

Figure C-110: Simulated sulphate and aqueous hydrogen sulphide concentration profiles for steady state number 46

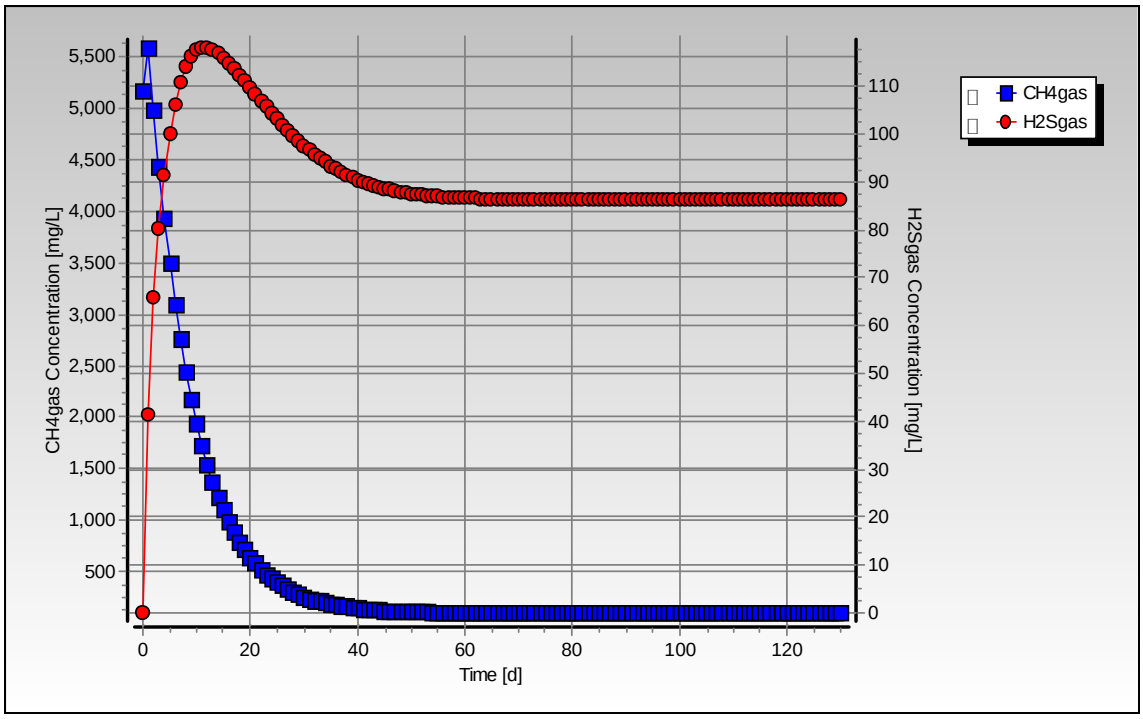

Figure C-111: Simulated methane and hydrogen sulphide gas concentration profiles for steady state number 46

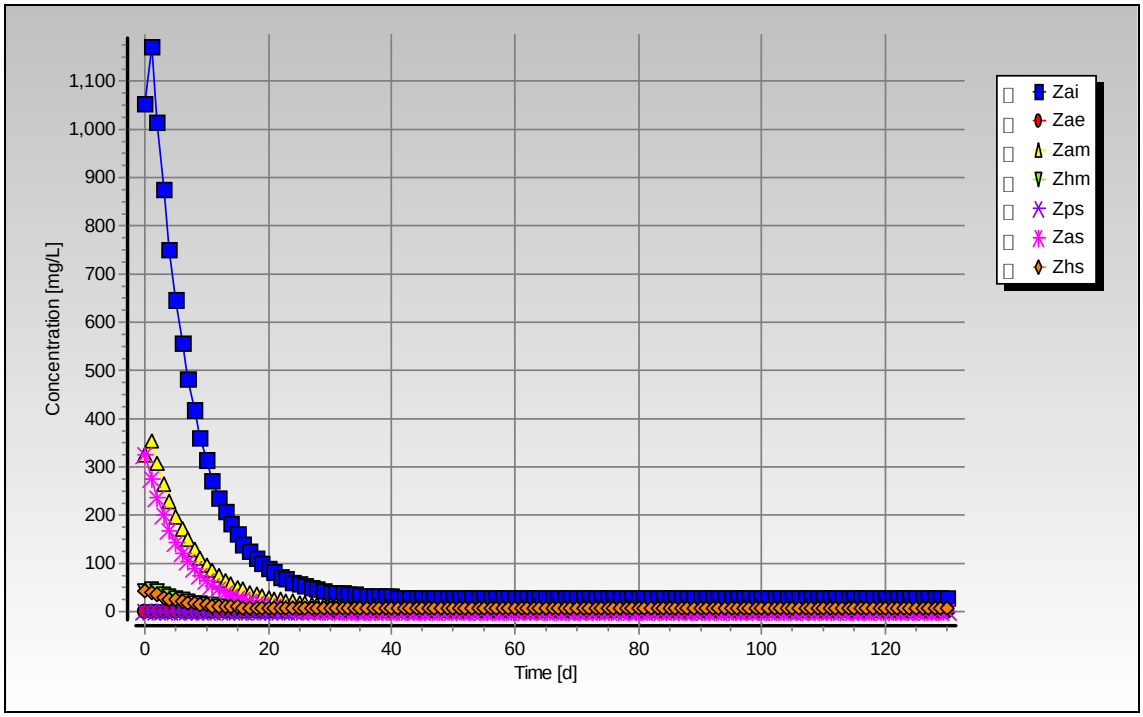

Figure C-112: Simulated biomass concentration profiles for steady state number 46

Steady State Number 47

Table C-65: Operating conditions for steady state number 47

Feed Batch Number	F15
Reactor Volume (ℓ)	16
Retention Time (d)	8
pH	controlled to ~ 8.3
Biological Groups Present	acidogenic, acetogenic, methanogenic and sulphidogenic

Table C-66: Results summary for steady state number 47

	Measured	**Model**	**Relative error (%)**
Feed Total COD (mg COD/ℓ)	1900	1900	-
Feed Soluble COD (mg COD/ℓ)	203	203	-
Feed TKN (mg N/ℓ)	46	46	-
Feed FSA (mg N/ℓ)	4	4	-
Effluent Total COD (mg COD/ℓ)	2020 ± 43	1206.19	-67.47
Effluent Soluble COD (mg COD/ℓ)	926 ± 47	392.69	-135.81
Reactor pH	8.27 ± 0.04	8.27	-
Effluent VFA (mg HAc/ℓ)	34 ± 14	0.17	-19809.77
Effluent Alkalinity (mg/ℓ as $CaCO_3$)	1950 ± 50	2104.80	7.35
Sulphate Addition (mg SO4/ℓ)	2000	2000	-
Effluent Sulphate (mg SO4/ℓ)	47 ± 52	1487	96.84
% Sulphate Conversion	97.65	25.64	-
Methane Production (ℓ/d)	0	0.63	100
Gas Composition (% CH_4)	0	90.33	100
Effluent FSA (mg N/ℓ)	-	14.76	-
Effluent TKN (mg N/ℓ)	-	35.67	-

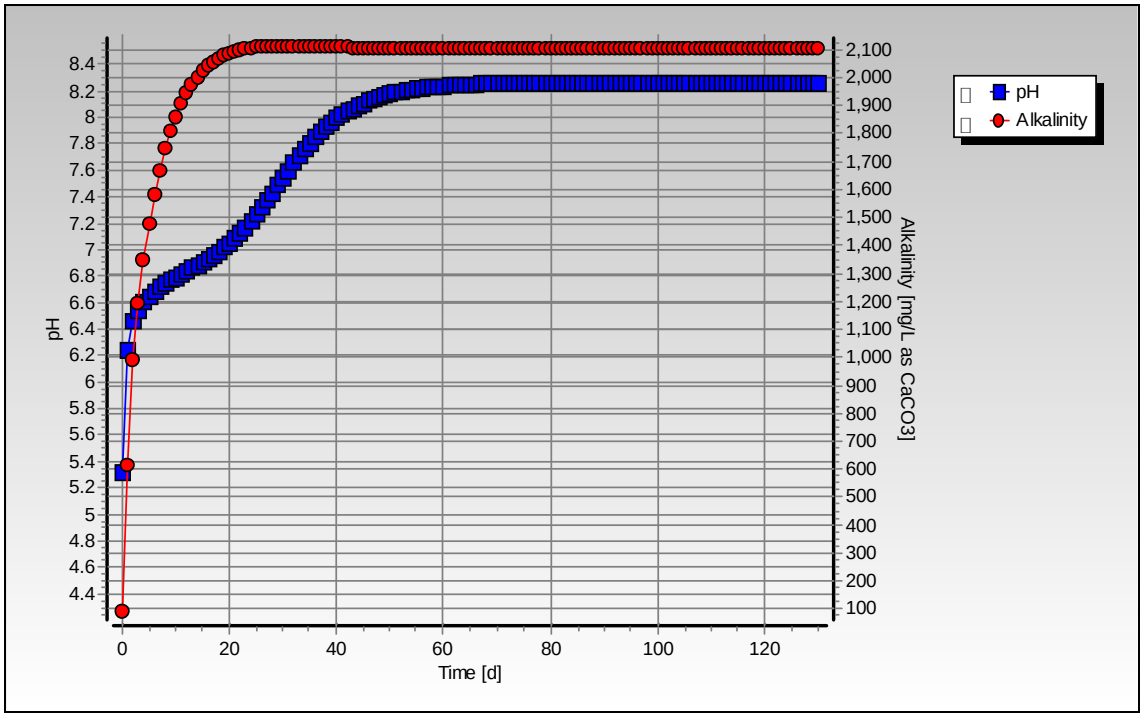

Figure C-113: Simulated pH and alkalinity profiles for steady state number 47

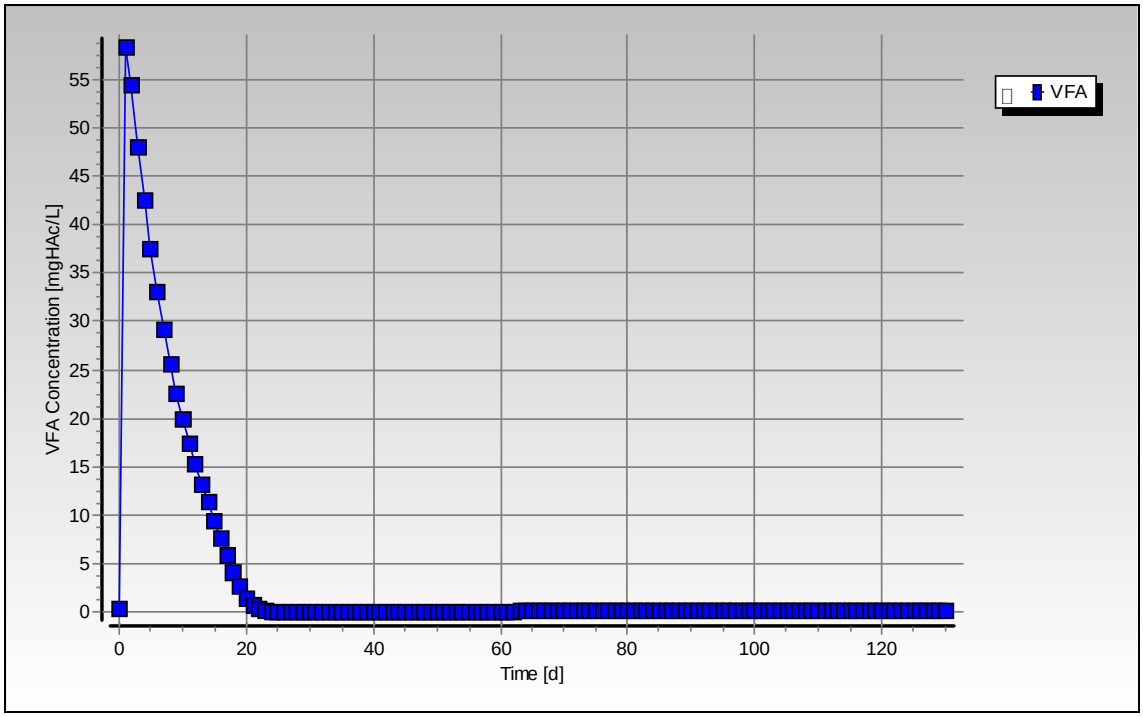

Figure C-114: Simulated VFA concentration profile for steady state number 47

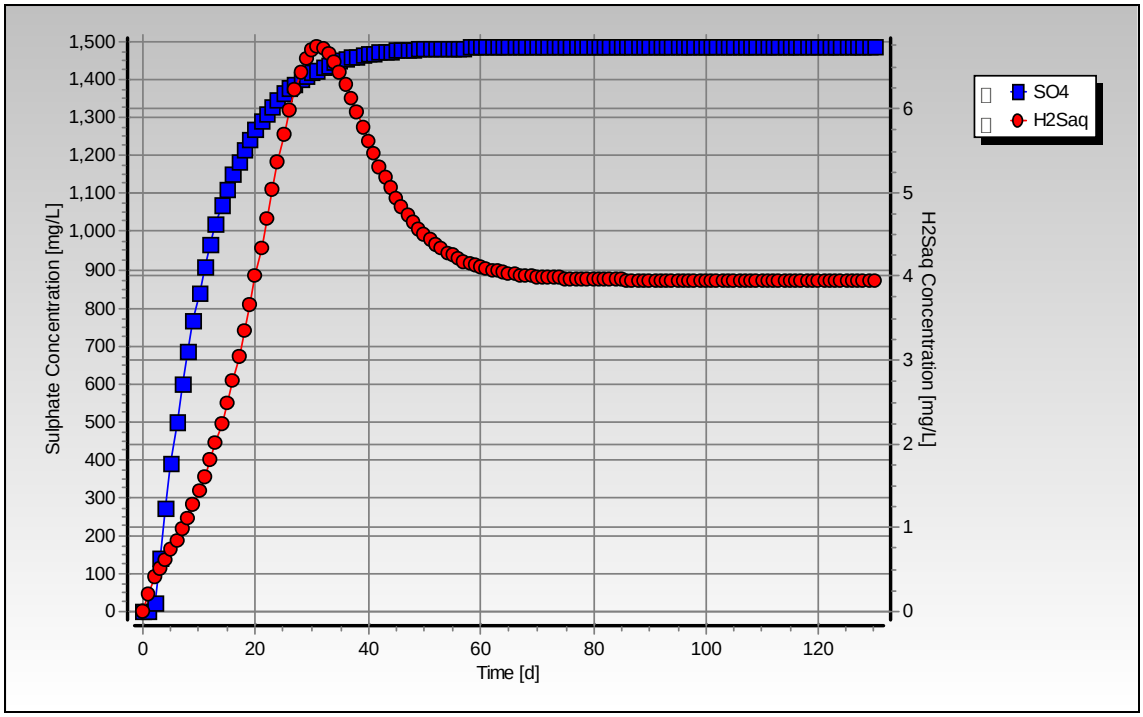

Figure C-115: Simulated sulphate and aqueous hydrogen sulphide concentration profiles for steady state number 47

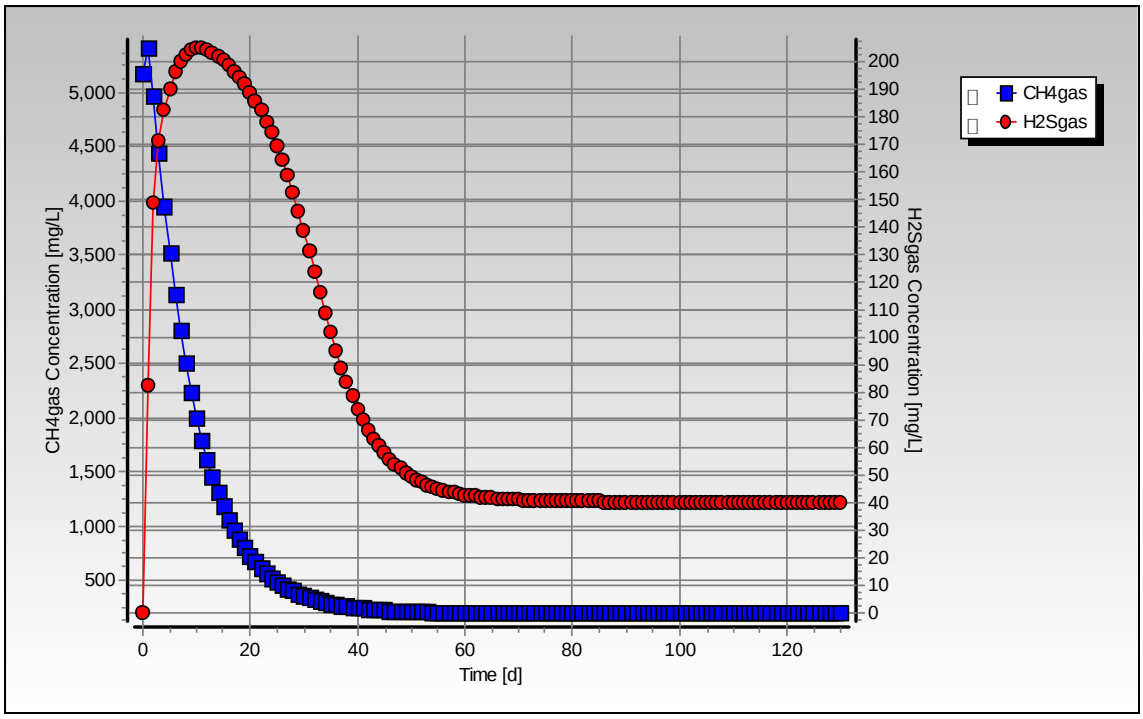

Figure C-116: Simulated methane and hydrogen sulphide gas concentration profiles for steady state number 47

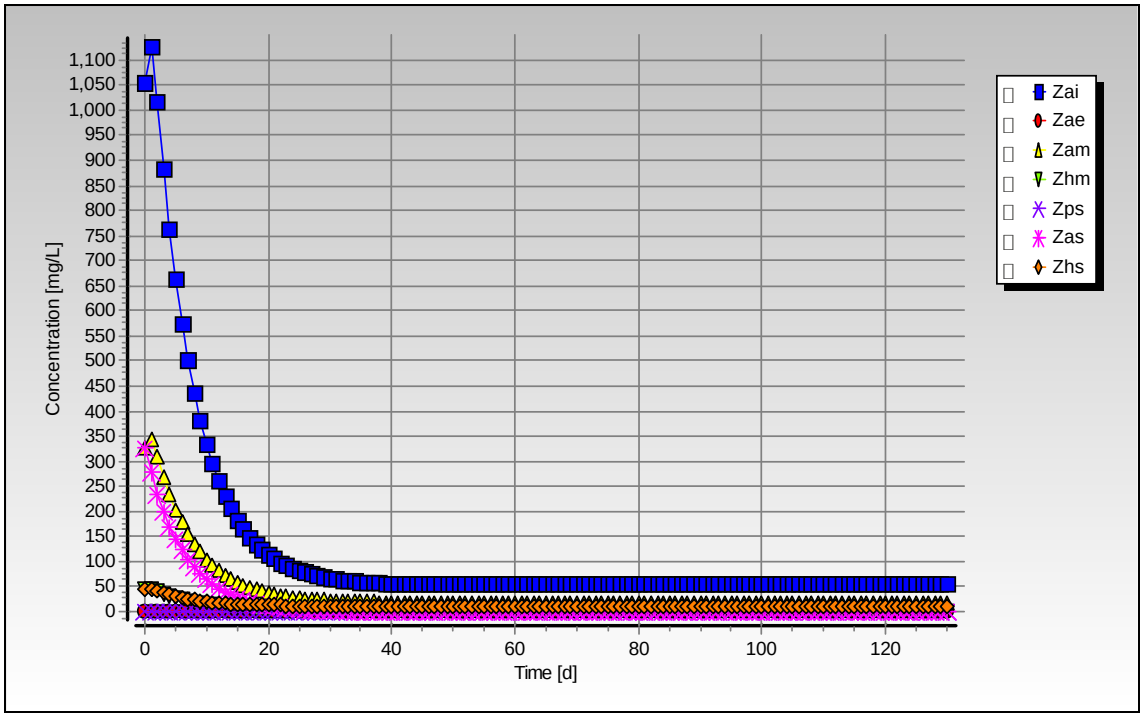

Figure C-118: Simulated biomass concentration profiles for steady state number 47

APPENDIX D

SIMULATION RESULTS OF PILOT PLANT MODELLING

Table D-1: PSS feed stream specifications

Temperature (^oC)	23 ^oC
pH	7
Alkalinity (mg/ℓ as $CaCO_3$)	300
COD (mg/ℓ)	~ 30 000
Flowrate (ℓ/d)	13 200

Table D-2: Mine water feed stream specifications

Temperature (^oC)	23 ^oC
pH	7.5
Alkalinity (mg/ℓ as $CaCO_3$)	350
Sulphate (mg SO_4/ℓ)	1300
Flowrate (ℓ/d)	230 000

Table D-3: Results summary for pilot plant

	Measured	Model
Feed Total COD (mg COD/ℓ)	30 000	30 000
Feed Soluble COD (mg COD/ℓ)	-	2694
Effluent Total COD (mg COD/ℓ)	-	8681.34
Effluent Soluble COD (mg COD/ℓ)	-	37.92
Reactor pH	~ 7.7	7.18
Effluent VFA (mg HAc/ℓ)	< 50	0.07
Effluent Alkalinity (mg/ℓ as $CaCO_3$)	1500	1001.45
Sulphate Addition (mg SO_4/ℓ)	1300	1300
Effluent Sulphate (mg SO_4/ℓ)	< 200	702.07
% Sulphate Conversion	-	45.99
Methane Production (ℓ/d)	-	72.77
Gas Composition (% CH_4)	-	15.58
Total Gas Production (ℓ/d)	-	130.43
Effluent FSA (mg N/ℓ)	-	19.02
Effluent TKN (mg N/ℓ)	-	119.90

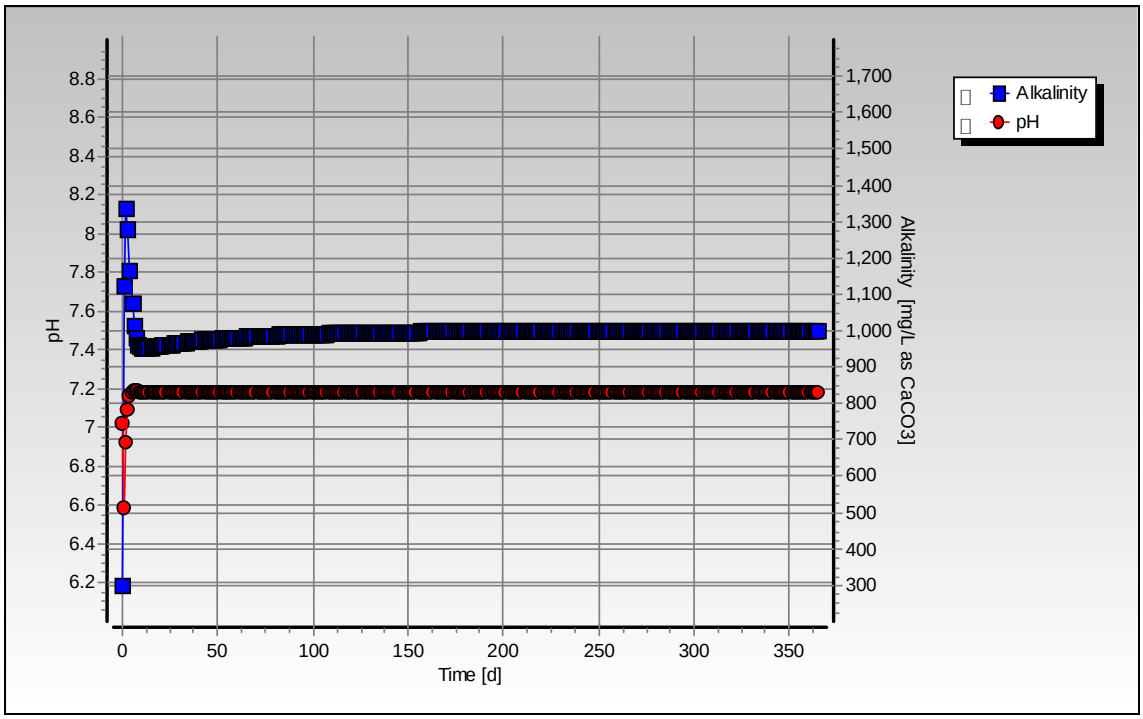

Figure D-1: Simulated pH and alkalinity profiles for pilot plant

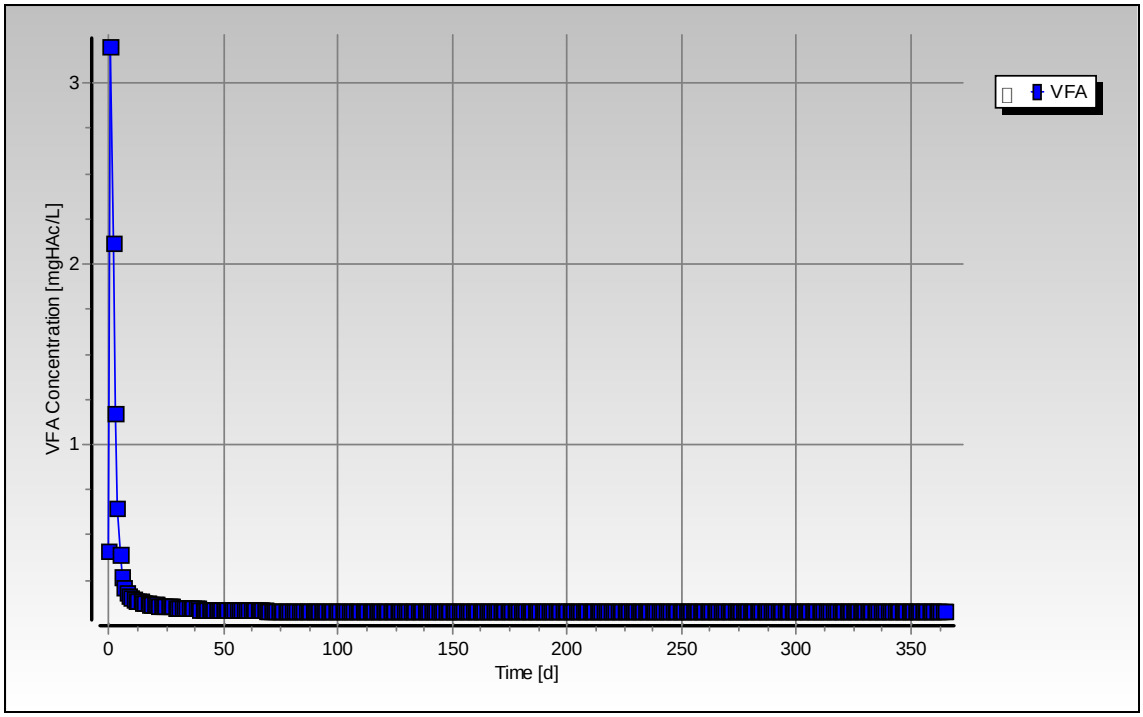

Figure D-2: Simulated VFA concentration profile for pilot plant

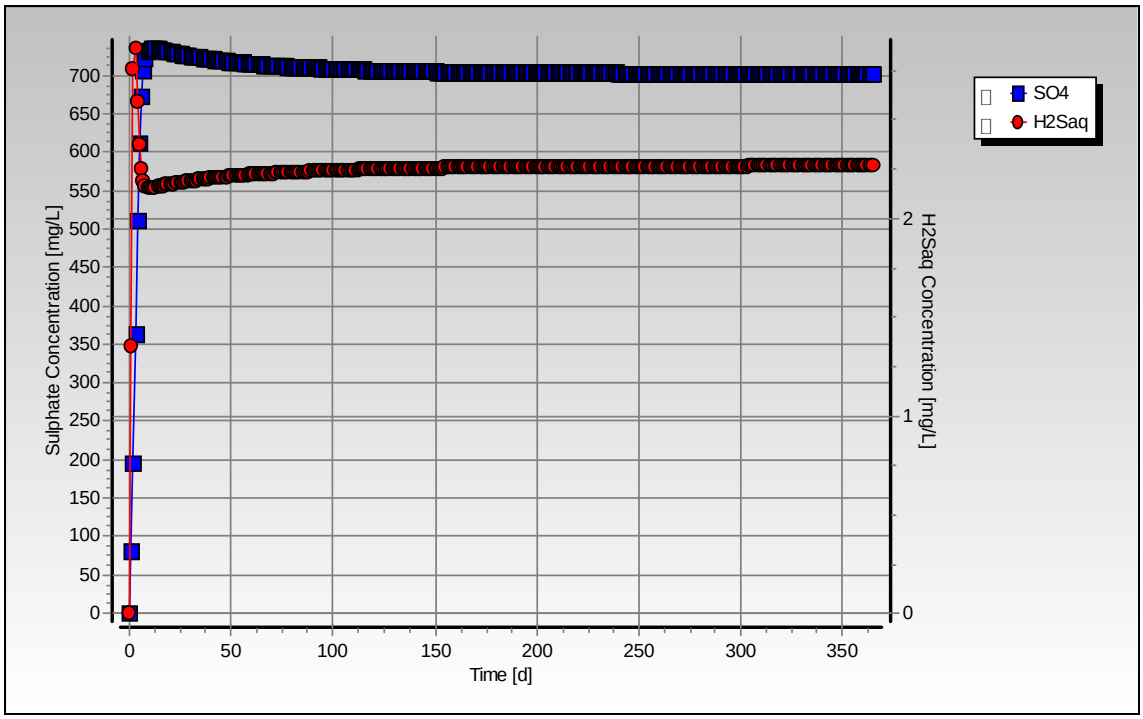

Figure D-3: Simulated sulphate and aqueous hydrogen sulphide concentration profiles for pilot plant

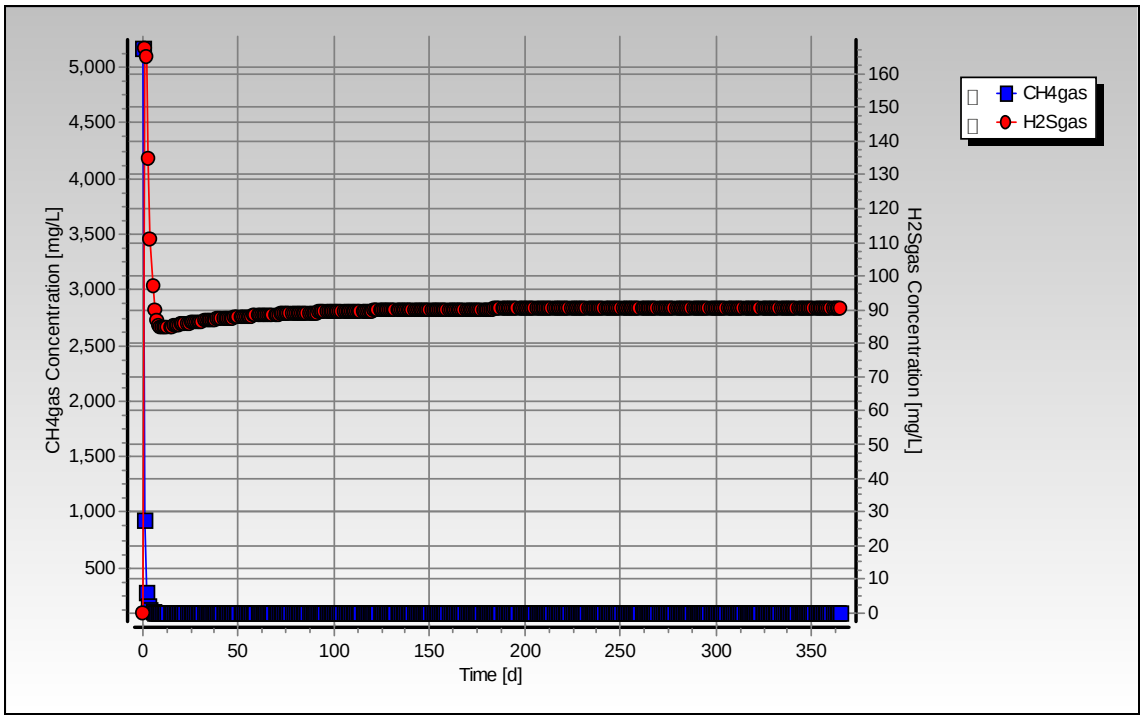

Figure D-4: Simulated methane and hydrogen sulphide gas concentration profiles for pilot plant

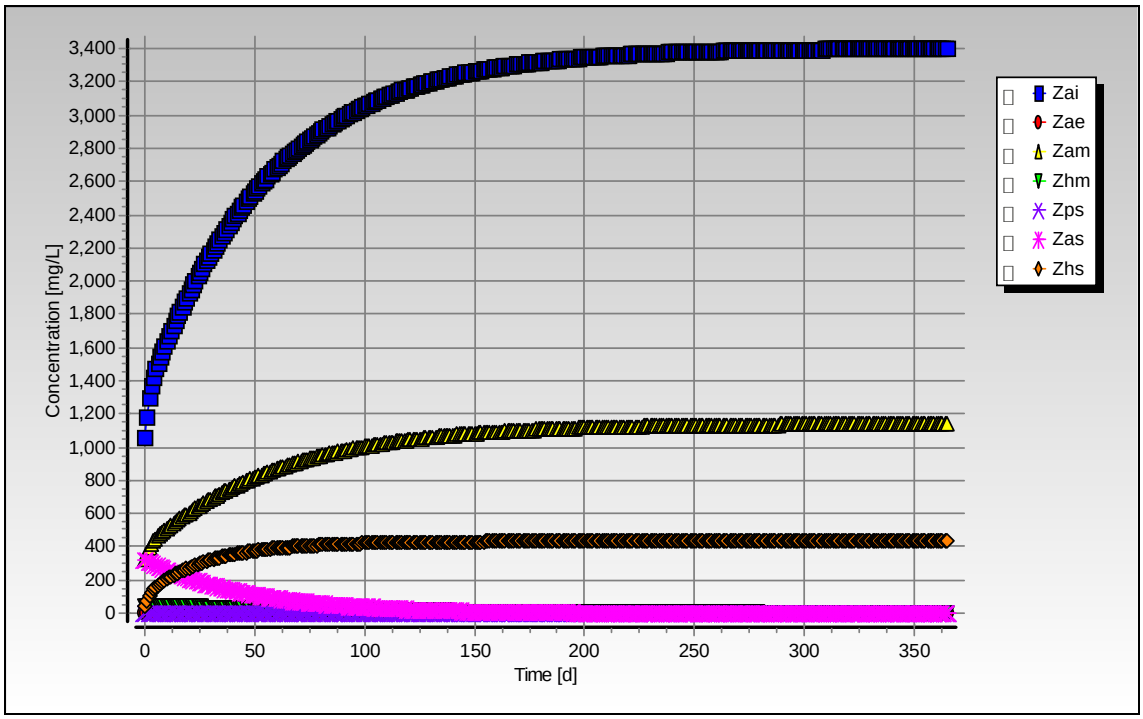

Figure D-5: Simulated biomass concentration profiles for pilot plant